frontiers | Research Topics

Aquatic microorganism and their response to environment: Virulence and antimicrobial resistance

Edited by
Yiqin Deng, Jie Huang, Songzhe Fu, Learn-Han Lee and Juan Feng

Published in
Frontiers in Marine Science

ISSN 1664-8714
ISBN 978-2-8325-2950-8
DOI 10.3389/978-2-8325-2950-8

About Frontiers

Frontiers is more than just an open access publisher of scholarly articles: it is a pioneering approach to the world of academia, radically improving the way scholarly research is managed. The grand vision of Frontiers is a world where all people have an equal opportunity to seek, share and generate knowledge. Frontiers provides immediate and permanent online open access to all its publications, but this alone is not enough to realize our grand goals.

Frontiers journal series

The Frontiers journal series is a multi-tier and interdisciplinary set of open-access, online journals, promising a paradigm shift from the current review, selection and dissemination processes in academic publishing. All Frontiers journals are driven by researchers for researchers; therefore, they constitute a service to the scholarly community. At the same time, the *Frontiers journal series* operates on a revolutionary invention, the tiered publishing system, initially addressing specific communities of scholars, and gradually climbing up to broader public understanding, thus serving the interests of the lay society, too.

Dedication to quality

Each Frontiers article is a landmark of the highest quality, thanks to genuinely collaborative interactions between authors and review editors, who include some of the world's best academicians. Research must be certified by peers before entering a stream of knowledge that may eventually reach the public - and shape society; therefore, Frontiers only applies the most rigorous and unbiased reviews. Frontiers revolutionizes research publishing by freely delivering the most outstanding research, evaluated with no bias from both the academic and social point of view. By applying the most advanced information technologies, Frontiers is catapulting scholarly publishing into a new generation.

What are Frontiers Research Topics?

Frontiers Research Topics are very popular trademarks of the *Frontiers journals series*: they are collections of at least ten articles, all centered on a particular subject. With their unique mix of varied contributions from Original Research to Review Articles, Frontiers Research Topics unify the most influential researchers, the latest key findings and historical advances in a hot research area.

Find out more on how to host your own Frontiers Research Topic or contribute to one as an author by contacting the Frontiers editorial office: frontiersin.org/about/contact

Aquatic microorganism and their response to environment: Virulence and antimicrobial resistance

Topic editors

Yiqin Deng — South China Sea Fisheries Research Institute, Chinese Academy of Fishery Sciences (CAFS), China

Jie Huang — Network of Aquaculture Centres in Asia-Pacific, Thailand

Songzhe Fu — Dalian Ocean University, China

Learn-Han Lee — Sunway University, Malaysia

Juan Feng — Chinese Academy of Fishery Sciences (CAFS), China

Citation

Deng, Y., Huang, J., Fu, S., Lee, L.-H., Feng, J., eds. (2023). *Aquatic microorganism and their response to environment: Virulence and antimicrobial resistance*. Lausanne: Frontiers Media SA. doi: 10.3389/978-2-8325-2950-8

Table of contents

frontiers | Frontiers in Marine Science

TYPE Editorial
PUBLISHED 23 June 2023
DOI 10.3389/fmars.2023.1230258

OPEN ACCESS

EDITED AND REVIEWED BY
Stephen J Newman,
Department of Primary Industries and Regional Development of Western Australia (DPIRD), Australia

*CORRESPONDENCE
Yiqin Deng
yiqindd@126.com

RECEIVED 28 May 2023
ACCEPTED 16 June 2023
PUBLISHED 23 June 2023

CITATION
Deng Y, Fu S, Lee L-H, Feng J and Huang J (2023) Editorial: Aquatic microorganism and their response to environment virulence and antimicrobial resistance. *Front. Mar. Sci.* 10:1230258. doi: 10.3389/fmars.2023.1230258

Editorial: Aquatic microorganism and their response to environment virulence and antimicrobial resistance

Yiqin Deng[1]*, Songzhe Fu[2,3], Learn-Han Lee[4,5], Juan Feng[1] and Jie Huang[6]

[1]Key Laboratory of South China Sea Fishery Resources Exploitation & Utilization, Ministry of Agriculture and Rural Affairs, South China Sea Fisheries Research Institute, Chinese Academy of Fishery Sciences, Guangzhou, China, [2]College of Marine Science and Environment, Dalian Ocean University, Dalian, China, [3]Key Laboratory of Environment Controlled Aquaculture (KLECA), Ministry of Education, Dalian Ocean University, Dalian, China, [4]Novel Bacteria and Drug Discovery Research Group (NBDD), Microbiome and Bioresource Research Strength (MBRS), Jeffrey Cheah School of Medicine and Health Sciences, Monash University Malaysia, Bandar Sunway, Selangor Darul Ehsan, Malaysia, [5]Sunway Microbiomics Centre, School of Medical and Life Sciences, Sunway University, Kuala Lumpur, Malaysia, [6]Network of Aquaculture Centres in Asia-Pacific (NACA), Bangkok, Thailand

KEYWORDS

aquatic microorganism, bacterial virulence, antimicrobial resistance (AMR), environmental changes, prevention and control

Editorial on the Research Topic
Aquatic microorganism and their response to environment: virulence and antimicrobial resistance

Overloaded or poorly managed farming systems, in synergy with emissions from intensive human activities and unstable climate systems arising from global climate change, can lead to environmental degradation, create imbalances in microecosystems, and result in pathogen blooms. These issues can significantly impact aquaculture and human health, leading to frequent outbreaks of bacterial infections and greatly increasing the risk of antibiotic resistance. Therefore, ensuring the health of aquatic animals and humans requires maintaining an early detection system for diseases, constantly monitoring the usage of antimicrobial agents (AMU), establishing national surveillance programs for antimicrobial resistance (AMR), and providing guidance for their application and prudent use, and actively promoting environment/ecosystem friendly strategies for disease management.

This Research Topic of Frontiers in Marine Science contains articles that investigate the aquatic microbial community, environmental changes, bacterial virulence, AMR, and their relationships. The main objective is to establish ecological prevention and control systems based on environmental factors and inputs, aiming to mitigate the occurrence and transmission of diseases.

Huang et al., Lin et al., Han et al., and Su et al. conducted investigative studies. Huang et al. examined the Liaohe estuary to explore the distribution and coexistence of potentially pathogenic bacteria. They found that Vibrio was the most potentially pathogenic bacteria in the estuary, with spatial factors having a more significant influence than environmental

ones. Huang et al. also showed that potential opportunistic pathogens could increase the risk of multiple infections due to their significant co-occurring relationship. Lin et al., Han et al., and Su et al. investigated the microbiological community and/or specific pathogens, such as Vibrio and their respective antibiotic and/or heavy metal resistance profiles in different aquatic systems. They investigated the driving factors of antibiotic and/or heavy metal resistance among bacterial communities, mobile genetic elements and selected environmental factors. Their studies suggest that resistance levels, microbiota, and environmental factors should be routinely monitored to assess risk levels and ensure human and aquatic animal health.

Su et al., Jiang et al. and Deng et al. conducted independent studies exploring the pathogenic mechanisms and/or horizontal gene transfer (HGT) driving factors of Vibrio strains. Su et al. discovered that various physicochemical factors, including pH, temperature, and salts, affect the expression of leucine-responsive regulatory protein (Lrp), which negatively controls the virulence of V. alginolyticus in zebrafish. Jiang et al. observed that after four weeks of cultivation, marked changes occurred in the morphology and physiological activity of V. mimicus. Moreover, well known virulence-related genes were significantly downregulated. Deng et al. reported a breakthrough in improving the conjugation efficiency of V. harveyi through appropriate treatments, which could contribute to the horizontal transmission of bacterial virulence and drug resistance. From the perspective of virulent (regulatory) gene expression (endogenetic) or HGT (externally acquired) regulation, Su et al., Jiang et al., and Deng et al. suggest that environmental changes, including physicochemical factors and nutrition, regulate the virulence and/or resistance of aquatic pathogenic Vibrio bacteria.

Liu et al. and Zhang et al. focused on different methods to control pathogenic bacteria. Liu et al. reported their findings on the potential of seagrass canopy structures in coastal areas to mediate the removal of putative bacterial pathogens. They observed that the density and height of seagrass patches influenced their ability to remove different kinds of pathogens. Liu et al. suggested that fragmented seagrass meadows might hinder their potential to remove bacterial pathogens, emphasizing the importance of seaweed meadow protection and restoration for human and marine organism health. Zhang et al.'s research explored the efficacy of UVC-LEDs as a novel light source to inactivate pathogenic bacteria. They investigated the effects of UVC-LED dose, light conditions, and temperature on bacterial reactivation and found that a higher UVC-LED fluorescence led to an increased inactivation rate. Pathogens were revived after UVC-LED disinfection, with photoreactivation significantly higher than dark reactivation. Based on their findings, Zhang et al. suggested that sufficient UVC-LED irradiation and avoidance of visible light after UVC-LED disinfection can effectively inhibit bacterial reactivation, providing reference information for designing and operating UV disinfection systems in aquaculture.

In summary, this Research Topic includes articles investigating the virulence and AMR of aquatic systems in estuaries and coastal zones affected by human activities. These studies explore the regulatory mechanism of a single bacterial organism's virulence and AMR and offer strategies for controlling pathogenic bacteria through biological and physical methods. The authors also examine the effects of various biological and physicochemical factors on virulence and AMR. Overall, these findings provide valuable insights into virulence and AMR control measures that can contribute to ensuring the health of aquatic animals and humans.

Author contributions

YD, SF, L-HL, JF, and JH worked collaboratively in designing the Research Topic, inviting authors, editing manuscripts, and editorial monitoring. It is also commendable that all authors contributed to the article and approved the submitted version. Collaborative efforts among researchers can lead to high-quality research outcomes and publications.

Conflict of interest

The authors declare that the research was conducted in the absence of any commercial or financial relationships that could be construed as a potential conflict of interest.

Publisher's note

frontiers | Frontiers in Marine Science

TYPE Original Research
PUBLISHED 15 September 2022
DOI 10.3389/fmars.2022.976438

OPEN ACCESS

EDITED BY
Songzhe Fu,
Dalian Ocean University, China

REVIEWED BY
Ilunga Kamika,
University of South Africa, South Africa
Jingfeng Fan,
National Marine Environmental Monitoring Center, China

*CORRESPONDENCE
Ying Han
hanying@ysu.edu.cn

SPECIALTY SECTION
This article was submitted to Marine Fisheries, Aquaculture and Living Resources, a section of the journal Frontiers in Marine Science

RECEIVED 23 June 2022
ACCEPTED 24 August 2022
PUBLISHED 15 September 2022

CITATION
Han Y, Hu Y, Wen H, Wu J, Liu Y, Zhang Y and Wu H (2022) Occurrence and driving mechanism of antibiotic resistance genes in marine recreational water around Qinhuangdao, China.
Front. Mar. Sci. 9:976438.
doi: 10.3389/fmars.2022.976438

Occurrence and driving mechanism of antibiotic resistance genes in marine recreational water around Qinhuangdao, China

Ying Han[1,2]*, Yikai Hu[1], Hexin Wen[1], Jiayue Wu[1,2], Yuanwang Liu[1,2], Yingchao Zhang[1,2] and Hao Wu[1,2]

[1]School of Environmental and Chemical Engineering, Yanshan University, Qinhuangdao, China, [2]Hebei Province Key Laboratory of Deep Remediation of Heavy Metals in Water and Resource Utilization, Yanshan University, Qinhuangdao, China

Rapid urbanization and other human activities have exacerbated the global human health risks associated with antibiotic resistance genes (ARGs). Swimming in contaminated waters is one of important pathways by which humans can be exposed to ARGs. However, little is currently known about the overall levels of ARGs in recreational waters and the forces driving their occurrence. In this study, we analyzed the ARGs and bacterial communities in water samples taken from five recreational coastal waters (RCWs) and their adjacent estuaries in the Qinhuangdao area of Bohai Bay, China, using high-throughput quantitative PCR and 16S rRNA gene amplicon sequencing technique. The relative abundances of ARGs in RCWs varied greatly, and occurred at levels close to, or even higher than, those in the neighboring estuaries, ranging from 9.4×10^{-2} to 2.5 copies/16S rRNA gene. A total of 159 different ARGs able to express resistance to almost all antibiotics were detected in all of the water samples. β-lactamase resistance genes (*bla*TEM gene) were the most abundance of all ARGs. Patterns of ARG occurrence were significantly correlated with those of bacterial communities (Mantel test, $P < 0.05$). A partial redundancy analysis showed that differences in bacterial communities accounted for 50.3% of the total ARG variations, which was much higher than the sum of the contribution of mobile genetic elements (18.1%) and the other selected environmental factors (8.3%). Principal coordinate analysis based on Bray-Curtis distance revealed the similarities between ARG profiles in the RCWs and in their adjacent estuaries. To our knowledge, this is the first study to report the ARG profiles in RCWs using high throughput qPCR technology. These results implied that it is necessary to develop proper regulations and monitoring strategies of RCWs for reducing risks of ARGs on human health.

KEYWORDS

antibiotic resistance genes (ARGs), mobile genetic elements (MGEs), bacterial community, recreational coastal water, human public health

Introduction

The overuse of antibiotics has accelerated the emergence and spread of antibiotic resistance genes (ARGs) in the environment (Wen et al., 2015) . ARGs have been found in a wide variety of environments including agricultural soils (Sun et al., 2020), urban wastewater treatment plants (Freeman et al., 2018), lakes (Y. Q. Wang et al., 2021), rivers (Pruden et al., 2006) and aquacultural facilities (P. Gao et al., 2012). Microorganisms in the environment can contribute to, or acquire, ARGs from human pathogenic bacteria, as demonstrated by the significant similarities in their sequences (Tomova et al., 2015; Jing Yang et al., 2013). Increased levels of ARGs in the environment have led to growing concerns about an impending global public health crisis (Pruden et al., 2006). It has been estimated that the number of deaths arising from antibiotic resistant pathogens may exceed 10 million by the end of 2050 (O' Neil, 2014), and that ARGs will surpass cancer as the most serious risk factor for human health. As emerging contaminants (A. Pruden et al., 2006), ARGs replicate not only through bacterial growth but also can be transferred between different bacterial species mediated by mobile genetic elements (MGEs) (von Wintersdorff et al., 2016). The amount of ARGs can increase and spread if they are selected by antibiotic pollutions or are co-selected by ecologically favorable determinant present in the same MGEs (Blahova et al., 1999). Therefore, identifying environmental reservoirs of ARGs and exploring their routes of transmission are critical for the prevention of ARG related infections.

Estuaries occur at the boundary between terrestrial/freshwater and coastal ecosystems (Stewart et al., 2008; Marti et al., 2014). Approximately half of the world's population lives within 100 kilometers of the coastline (Culliton, 1998). Generally, estuaries receive mass discharges of waste from industry and other human activities (Wright et al., 2008), such as wastewater treatment plants (WWTP) (Wu et al., 2018; Bi Weihong et al., 2022), medical wastewater (Rodriguez-Mozaz et al., 2015), livestock rearing, aquaculture and agricultural wastewater (Jang et al., 2018). Traditional WWTPs are not generally effective in removing ARGs and the ARG abundance in the effluent can be as high as 3.13×106 copies/mL (H. Chen & Zhang, 2013; H. W. Huang et al., 2019). Terrigenous pollutants, including heavy metals, antibiotics, ARGs and drug-resistant bacteria, are also washed into rivers and then into estuaries. Surface waters also receive wastewater and municipal sewage from nearby factories and cities. It has been shown that rivers in China generally contain various ARGs, including the Yangtze, Yellow, Haihe and Huaihe Rivers (Zhuang et al., 2021). Moreover, the specificity of the water quality environment and the increasing development of tourism can also affect the evolution of microbial resistance (Su et al., 2022). The resistant bacteria will be brought into the coastal tourist area near the shore with the rain, tide, and currents. Swimming in recreational coastal waters (RCWs) is an important route by which humans are exposed to pollutants in the coastal environment. Many studies have reported various pollutants in RCWs, including heavy metals (Bigus et al., 2016), nitrogen, phosphorus, viruses (Wei et al., 2020), microplastics (F. L. Gao et al., 2021), and pollutants resulting in elevated chemical oxygen demands, which may facilitate the spread of ARGs (Stepanauskas et al., 2006; Tandukar et al., 2013; Forsberg et al., 2014). However, the overall profiles, influent factors, and driving mechanisms of ARGs in RCWs are still not fully understood.

The dynamics of ARG occurrence are far more complex than the selective pressure of antibiotics (Tamminen et al., 2011). A growing number of studies have reported that shifts in bacterial communities are the main driver of ARG accumulation in the environment (Zhang et al., 1800; Su et al., 2015). Horizontal gene transfer (HGT) mediated by MGEs is also an important mechanism of ARG propagation (K. Zhang et al., 2021). Environmental microorganism, particularly pathogenic bacteria, can acquire ARGs from different species of bacteria via HGT to express antibiotic resistant and even become the "superbugs" endangering public health (von Wintersdorff et al., 2016). Environmental factors, such as nitrogen and phosphorus concentrations (Ali et al., 2016), pH (H. N. Huang et al., 2017), salinity (Y.-J. Zhang et al., 2019), and temperature (J. Yang et al., 2020), may also be predominant factors governing the distribution patterns of environmental ARGs. Therefore, it is necessary to explore the overall ARG profiles in RCWs as well as all of the possible factors affecting their occurrence to discover the predominant drivers and to control their propagation and thus reduce potential health risks.

The Bohai Sea has a coastline of about 3,800 kilometers and is fed by large number of rivers. Qinhuangdao, located in the north part of the Bohai Sea, is one of the most important tourist cities in northern China, and is greatly impacted by human activities (L. H. Zhu et al., 2014). The "Qinhuangdao Recreational Coastal Water Management Regulations" stipulate the minimum straight-line distance between RCWs and the nearest estuary, fishing port, tourist wharf, fishing boat berth and shallow sea aquacultural area to avoid the spread of pollutants (Qinhuangdao Municipal People's Government, 2019). However, it is unclear whether the above provisions can prevent the ARG impacts of estuaries on RCWs. In this study, water samples were collected from the estuaries of typical rivers and their adjacent RCWs around Qinhuangdao: (1) to investigate the ARG profiles and bacterial communities in estuaries and their RCWs; (2) to determine the influencing factors and driving mechanisms of ARG occurrence in estuaries and their adjacent RCWs; and (3) to explore the potential antibiotic resistance risks to human health under current regulations.

Methods and materials

Sample collection, water chemistry and DNA extraction

Water samples were collected from the estuaries and their adjacent RCWs around Qinhuangdao City, located on the north coast of Bohai Bay, China. Detailed descriptions of the sampling sites are shown in Figure S1. Water samples (~5L) were taken during December 2020 on three consecutive days without rainfalls during the preceding week. All water samples were stored on ice in sterile containers and brought back to the laboratory within six hours for further treatment.

The bacteria cells in each water sample were collected by filtering through 0.22 mm mixed cellulose esters filters (Millipore, USA) and stored at -20°C for subsequent total extraction of genomic DNA using a QIAGEN Extraction Kit (Qiagen Instruments, USA), following the manufacturer's instructions. The purity and integrity of the extracted DNA were assessed using a Nano Drop spectrophotometer (Thermo Fisher Scientific, USA) and agar gel electrophoresis, respectively. The extracted DNA was stored at -20°C. Temperature, pH and salinity were measured in situ using a multiparameter water quality analyzer (Hydrolab DS5, Hach Company, Loveland, USA). Ammonia-nitrogen (NH4+-N), nitrate nitrogen (NO3+-N) (Rider and Mellon, 1946), nitrite nitrogen (NO2–N) (J. Yang et al., 2020), and phosphate (PO4–P) were measure according to standard methods (B. Wu et al., 2014).

High-throughput quantitative PCR of ARGs

HT-qPCR was performed using a Warfergen SmartChip Real-time PCR System (Anhui Microanaly Gene Technologies Co., Ltd, China) to detect and quantify ARGs, as described previously (Ouyang et al., 2015). Quality assurance/quality control was conducted following the standard protocols provided by Wafergen Biosystems. A total of 296 primers sets were used targeting at 285 ARGs, eight transposases, three integrons and one 16S rRNA gene. Detailed information on the primers is listed in Table S1. The 285 ARGs could express antibiotic resistance to almost all antibiotics by 4 mechanisms. HT-qPCR assay was performed in a 100 nL reaction system consisting of a 1 × LightCycler 480 SYBR Green I Master mix, 0.1 mg/mL albumin from bovine serum, 500 nM of each primer and 2 ng/μL DNA template. A non-template control was included on each chip for each primer set. The qPCR reaction mixture was first added to a microarray using nanoscale multi-sample point sampling instrument, and then qPCR reaction was performed using a cycler with the thermal cycles: 95°C for 10 min, 40 cycles of 95°C for 30 s, and 60°C for 30 s, ending with a melting curve analysis auto-generated by the Wafergen program.

The HT-qPCR results were analyzed using SmartChip qPCR (v 2.7.0.1) software to remove the results with multi-peak melting curve and with amplification efficiencies beyond the range of 1.8-2.2. A threshold cycle (CT) value of 31 was used as the detection limit. All qPCR reactions were conducted in triplicate, and if more than two were amplified, the result was regarded as positive. Relative copy numbers of ARGs was calculated according to the following equation:

Gene copy number = 10 ^[(31-CT)/(10/3)]

Relative ARG copy number = ARG copy number/16S rRNA gene copy number

Where, CT is the cycle threshold.

The result of the primer sets targeting at the same gene were combines. For example, blaOXA10-01 and blaOXA10-02 both target at the blaOXA10 gene according to their nomenclature (Jacoby, 2006).

Bacterial 16S rRNA gene sequencing and data processing

Bacterial communities were investigated using a 16S rRNA gene amplicon sequencing technology (Anhui Microanaly Gene Technologies Co., Limited, China). The V3-V4 region of the 16S rRNA gene was amplified using barcodes and the primer sets 341F (5'-CCTACGGGNGGCWGCAG-3') and 765R (5'-GACTACNVGGGTATCTAAT-3'). The genomic DNA was used as templates to conduct PCR using Taq DNA Polymerase (Vazyme, Nanjing, China). PCR products were purified using a QIAquick Gel Extraction Kit (QIAGEN, USA) and pooled in equimolar for sequencing using an Illumina MiSeq PE300 platform. Paired-end sequences were joined after the barcode and primers were removed using FLASH (Magoc and Salzberg, 2011). FLASH software was also used to remove short reads, chimeras and ambiguous N (Magoc and Salzberg, 2011). The sequences were clustered into Operational Taxonomic Units (OTUs) with a threshold of 97% similarity using the VSEARCH method (Rognes et al, 2016). Representative sequences were selected for further OTU annotation using a default method involving assignment to the Greengenes Database taxonomy (Wang et al., 2007). Species diversity and α-diversity of the bacterial communities were estimated with the observed species, Chao1, Shannon, Simpson and PD_whole_tree index, which were calculated using a script in QIIME software. Bacterial communities in different groups (β-diversity) were compared using the unweighted pair group method with arithmetic mean (UPGMA), principal coordinate analysis (PCoA) based on Bray-Curtis distances, and the Adonis test.

Network analysis

The co-occurrence patterns among ARGs, MGEs and bacterial communities were revealed by network analysis using Cytoscape (3.8.2) with the CoNet plug-in (Sarkar and Chang, 1997). Pairwise correlations were calculated by the Mutual information, Spearman's correlation, Pearson's correlation, Bray-Curtis dissimilarity and Kullback-Leibler dissimilarity tests. Correlations with a P value above 0.9 and a significance level below 0.05 were considered significant. ARGs or bacterial taxa detected in less than three samples were discarded in correlation calculations. Correlation efficiencies and P values were analyzed using the Simes method implemented with the CoNet plug-in to avoid false-positive correlations (Sarkar and Chang, 1997). The network topology was visualized in Gephi (0.9.2) with the Frucherman Reingold algorithm (Dalcin and Jackson, 2018).

Statistical analyses

Averages and standard deviations of all data were determined using Microsoft Excel 2010 (Microsoft Office 2010, Microsoft, U.S.A.). The normalized ARG abundances were plotted with OriginPro 2017 (OriginLab, U.S.A.). Heat maps analyzing the ARGs data of water samples were generated with using the Pheatmap package in R (Version 4.1.2). Mantel test, PcoAs based on Bray-Curtis distance, Redundancy analyses (RDA) and partial RDAs were performed using R4.1.2 with the vegan package. Aggregated boosted tree (ABT) analysis was performed using R2.7.0 with the gbmplus package. Significant differences between estuaries and RCWs were tested using the Student–Newman–Keuls (S–N–K) test (SPSS V20, IBM, U.S.A.). Pearson's correlation coefficients among ARG and MGE abundances were calculated using SPSS.

Result

Abundance and diversity of ARGs

A total of 159 ARGs and 5 MGEs were detected in the 10 water samples from RCWs and estuaries in Qinhuangdao, China. An average of 114 ARGs were detected in the estuaries and 94 in the RCWs. However, there were not necessarily fewer ARGs in the RCWs than in their adjacent estuaries, such as the Nandai and Yang Rivers (Figure S2). Aminoglycoside and β-Lactamase were the most dominant types of resistant genes, followed by Macrolide-Lincosamide-Streptogramin B (MLSB) and tetracycline resistant genes, accounted for 30.8%-83.9% of the total ARGs in each sample (Figure S2). ARGs potentially conferring resistance to vancomycin were widely distributed among the estuaries and RCWs, with occurrence ranging from 2.34%-6.94%. It should be noted that vancomycin is critically important for human medicine and is considered the last line of treatment for bacterial infections. In the 159 ARGs, antibiotic deactivation, efflux pump, and cellular protection are the most predominant resistance mechanisms (Figure S2).

The relative abundances of ARGs in water samples from the Tang and Xinkai Rivers are significantly higher than those in other samples ($P < 0.01$), as shown in Figure 1A. In contrast to the other estuaries, the most abundant type of ARG in the Tang River was aminoglycoside (17.3%). The relative abundance of ARGs in water samples from the Tang and Xinkai Rivers ranged from 1.3-2.5 copies/16S rRNA copies, about 20 times higher than those of the other samples (0.21~0.29copies/16S rRNA gene). A total of 10 MGEs were detected, including eight transposases and two integrases with relative abundances ranging from 2.7%-28.5%. As shown in Figure 1B, the relative abundance of MGEs in all RCWs and estuaries ranged from 5.6×10-3 -8.5×10-1 copies/16S rRNA genes. The normalized copy number of transposases and integrases was significantly different among sampling sites. For example, integrase accounted for 96.0% of MGEs in the RCW adjacent to the Nandai River estuary, but only transposase genes were detected in the RCW close to estuary of the Tang River (0.11copies/16S rRNA genes).

There were significant differences in the overall structure of ARGs in the different water samples (Adonis test, $P < 0.05$). PCoA based on Bray-Curtis distance (Figure 2A) showed that water samples from the Nandai, Yang and Shi Rivers clustered together and separated from the other samples. The first two PCs explained a total of 68.1% of the variance in ARGs, with PC1 explaining more than half (50.5%) of the variation. Samples from different locations were generally separated along the first PC, and samples from the same estuary and its adjacent RCW were separated along PC2, which explained 17.6% of the variation, indicating the minor differences between ARG profiles of an estuary and its adjacent RCWs. Hierarchical clustering analysis further verified such variances in ARG profiles (Figure 3). The estuary samples from the Tang and Xinkai Rivers were separated from the other water samples, which clustered together. As shown in Figure 3, all of the ARGs detected could be divided into three subgroups: (A) ARGs with high relative abundance in all water samples, such as the blaTEM、folA、blaOXA10 and aadA5 genes; (B) ARGs with high relative abundance in the estuaries of Tang and Xinkai Rivers, such as the strB and aadA genes; and (C) ARGs with high relative abundance in other sampling sites, such as the VanC and mphA genes. A detailed table of ARG abundance with names can be found in the Supplementary Materials (Table S2).

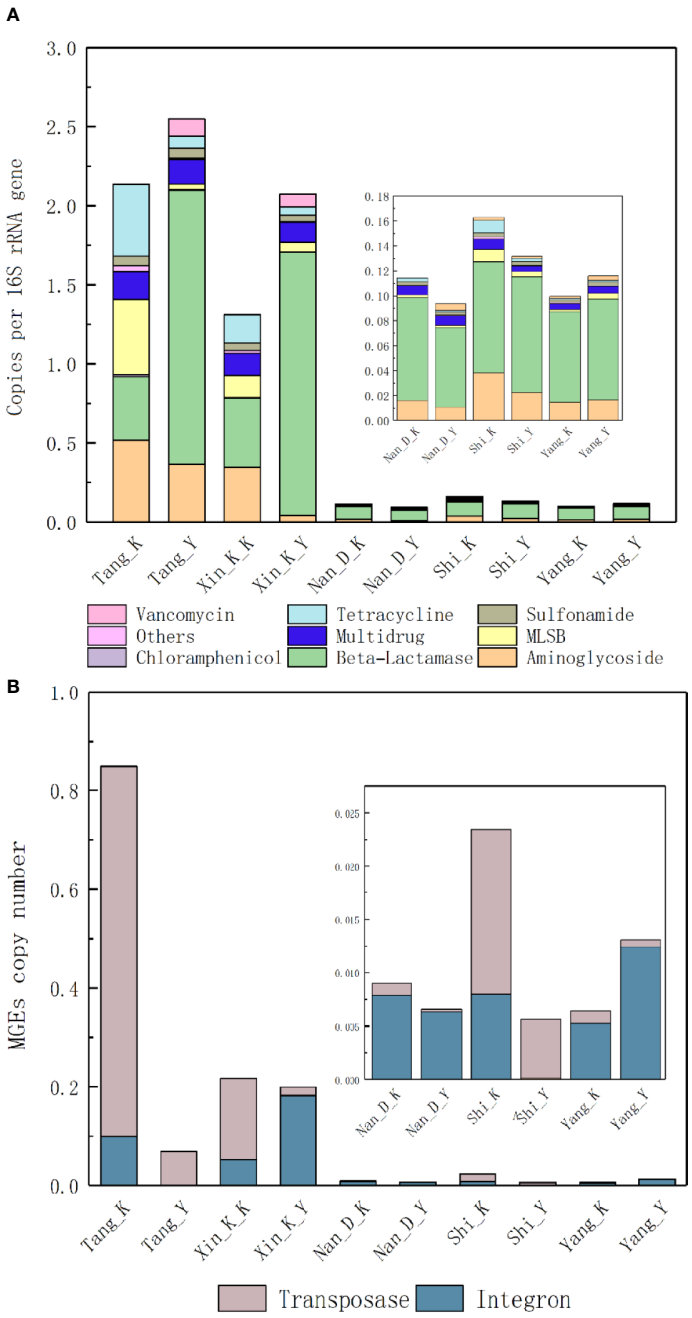

FIGURE 1
Normalized abundance of **(A)** ARGs and **(B)** MGEs in sediment of estuaries and recreational coastal waters. Normalized copy number of ARGs presented as number of ARGs per 16S rRNA genes. Multidrug resistance genes are defined as the resistance to multiple antibiotics with different structures and antimicrobial mechanisms.

Characteristics of microbial community structure

After assembling and quality filtering, a total of 640,000 high-quality sequences were obtained from 10 samples, ranging from 45,663-95,376 sequences per sample. These sequences were assigned to 8,675 OTUs at the 97% similarity level, with the number of OTUs in each single sample ranging from 638-1,112. Species accumulation curves and rank abundance curves indicated that the bacteria species in the estuarine samples were generally higher than those in the adjacent RCWs (Figure S3), Proteobacteria and Bacteriodetes were the

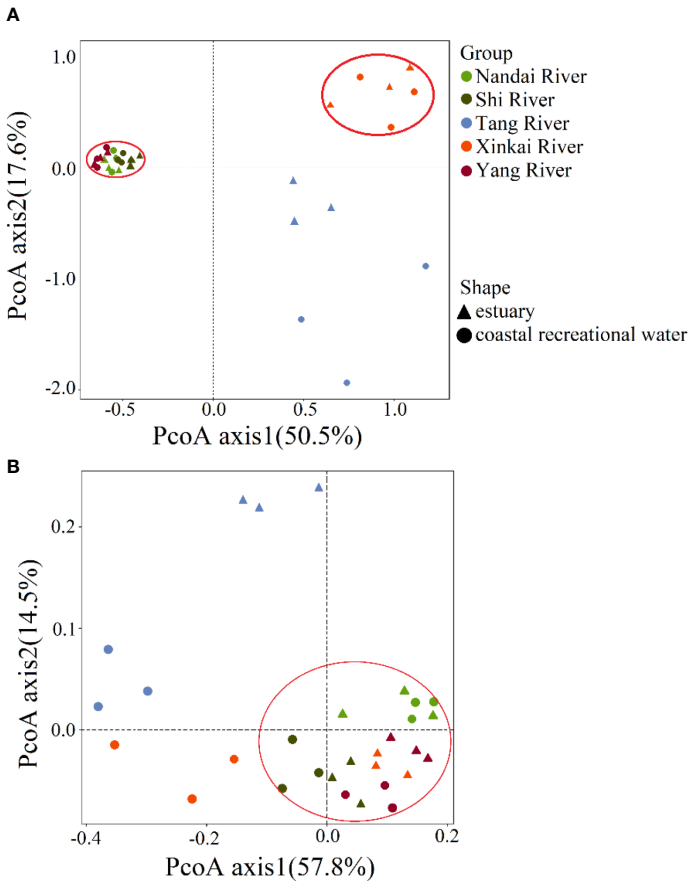

FIGURE 2
Principal coordinates analysis based on Bray-Curtis distance showing the overall distribution pattern of **(A)** ARGs and **(B)** microbial communities in water samples of estuaries and recreational coastal.

dominant phyla in all samples, accounting for 57.1-83.5% of the bacterial communities. Gammaproteobacteria and Alphaproteobacteria were the major classes of Proteobacteria, while Flavobacteriia was the major class of Bacteroidetes. The compositions of the bacterial communities at different levels are shown in Figure S4. PCoA analysis based on Bray-Curtis distance showed that estuarine bacterial communities and their corresponding RCWs were relatively similar except in the Tang and Xinkai Rivers. As shown in Figure 2B, the first two PCs explained 57.8% and 14.5% of the differences in bacterial community composition, respectively. The genus-level UPGMA hierarchical analysis confirmed that the bacterial communities in the Shi and Yang River regions were similar at the genus level (Figure S5). Psychrobacer, Litoreibacter, Sulfitobacter, Planktomarina and Loktanella were the most dominant bacteria, accounting for 29.5-49.6% of the total genera. Interestingly, the bacterial communities in samples from the Shi and Yang Rivers were similar even though they are not geographically adjacent, indicating that bacterial communities in coastal environments were affected by more complex factors than mere diffusion between. No significant differences were observed between bacterial communities from estuaries and their adjacent RCW (Anosim, $P > 0.05$), but certain bacterial species were only observed in estuaries or in RCWs. For example, Campylobacteraceae and Arcobacter were prevalent in estuariesbut rarely detected in RCWs. Whether they can be used as biomarkers to distinguish estuarine samples from RCWs requires further research. It is worth noticing that Arcobacter, a potential human pathogen, was widely distributed in estuaries. Even though its detection limit in RCWs was low in this study, its dissemination and fate in coastal environments requires further surveillance and attention.

Correlations between ARGs, MGEs and microbial community structure

Significant correlations were detected among the all classes of ARGs (Pearson's correlation), indicating that the spread of various ARGs may share the same dissemination mechanism.

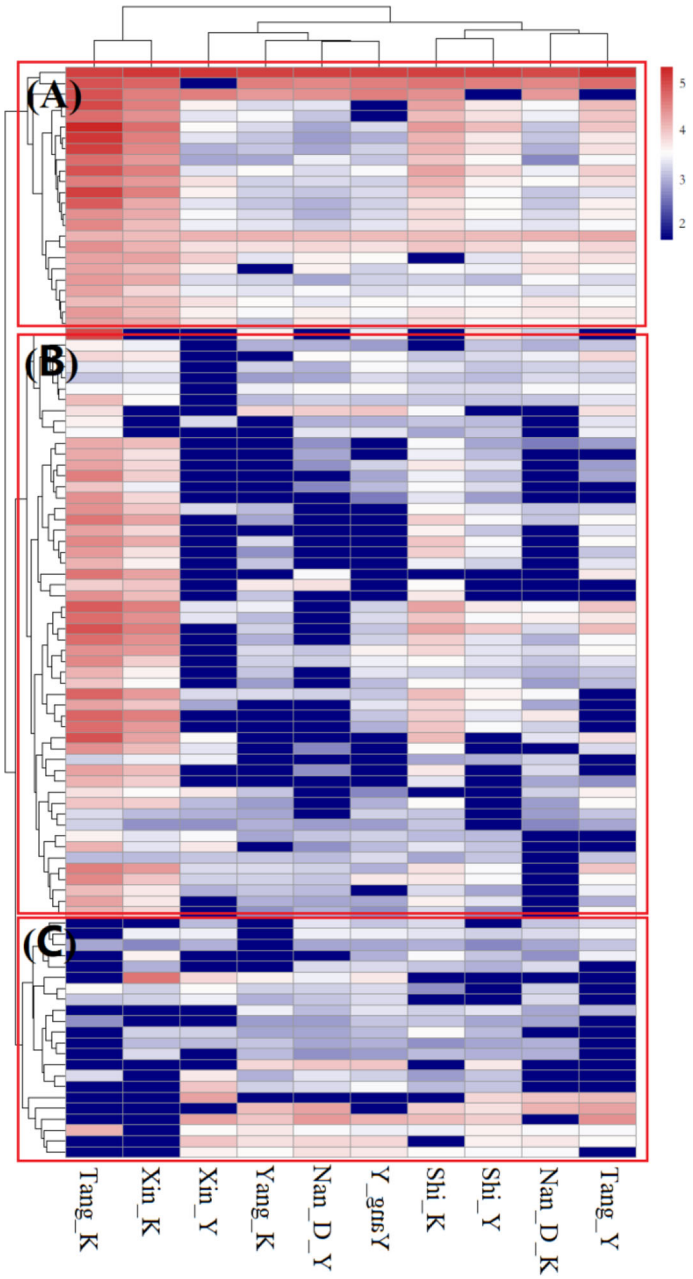

FIGURE 3
ARG profiles in sediment of estuaries and recreational coastal waters. Each column is labeled with a sample name. K represents water samples from estuaries and Y represents water samples from recreational coastal water. Plotted values are the logarithm-transformed relative abundance of each ARGs. Columns and rows were clustered based on Bray-Curtis distance. **(A)** ARGs with high relative abundance in all of the water samples; **(B)** ARGs with high relative abundance in estuaries of Tang and Xinkai Rivers; **(C)** ARGs with high relative abundance at the other sampling sites.

The abundance of integrons was not correlated with any particular class of ARG, but the total abundance of transposases genes were significantly correlated with almost all classes of ARG, except for β-Lactamase, sulfonamide, and vancomycin resistance genes, indicating that transposons played an important role in ARG propagation in coastal environment. Several ARGs (blaTEM, strB, blaVEB, sulI genes), generally embedded in transposons, were detected with the highest normalized copy number, indicating that transposons were the most common carrier of ARGs in coastal waters. With the exception of β-Lactamase and vancomycin resistant genes, the normalized abundance of ARGs were

correlated with those of MGEs, with correlation coefficients ranging from 0.67-0.99 (Table 1, Person's correlation, P < 0.05), indicating that ARGs may be readily transferred within bacterial communities. These correlations were based on the normalized abundances of ARGs and MGEs, suggesting that MGEs mediated HGT, contribute to the propagation of ARGs in coastal waters and lead to the enrichment of those ARGs in bacterial communities.

The patterns of co-occurrence among ARGs and MGEs were analyzed using co-occurrence network analysis (Figure 4) based on the strong and significant correlation between ARGs and MGEs. The network structure consists of 25 nodes and 20 edges, which could be divided into nine modules with a module degree of 0.72. The line in the Figure 4 shows a strong and significant correlation between two nodes (r > 0.9). The most densely connected node was defined as a "hub" in the module. For example, the aadA2 gene is the hub in its module and is significantly correlated with the blaOXA10, catB3, qacEdelta1 and tetM genes. The hubs can be used as indicators for all ARGs in a module to predict dynamic changes of other ARGs in the same module. Most modules contained different types of ARGs or MGEs. For example, module IV includes the aminoglycoside resistant genes (aadA2 gene) and the tetracycline resistance genes (tetR gene), and module VIII includes the vgbB gene and aadD gene, which belong to MLSB and aminoglycoside resistance genes. The correlation between transposon (tnpA gene) and aminoglycoside resistant gene (aac(6')-Ib(aka aacA4)) further indicated that transposons could contribute to the propagation of ARGs in coastal environments. The correlations between different ARGs suggested that they are carried by the same bacteria or located in the same MGE. We further analyzed the patterns of co-occurrence among ARGs, MGEs and bacterial communities at the genus level. We hypothesized that a strong nonrandom, significant correlation between microorganisms and ARGs (R2 > 0.9, P < 0.05) could indicate the identity of the host of an ARG. For instance, Acinetobacter may be the host cell of an aminoglycoside gene (aac(6')-Ib(aka aacA4)), and the β-lactamase resistance gene (blaVEB) was probably carried by the genus Phycisphaera.

We also studied the differences between the abundances of bacteria that directly correlated with ARGs in RCWs and estuaries. The bacteria which could be recognized as hosts of ARGs were detected with relatively high abundance in estuaries but low abundance in RCWs, and were perhaps present at levels below the limits of detection. The abundance of Succinispira, which is correlated with the trimethoprim resistant gene (dfrA) ranged from 0- 8.3×10-5 in estuaries, but was rarely detected in RCWs. Acinetobacter is a potential human pathogen, and was strongly and significantly associated with aminoglycoside resistant gene (aac(6')-Ib(aka aacA4)). This potentially resistant pathogen was detected in all of the water samples except for the RCWs adjacent to the Nandai River. Together, these results suggested that environmental bacteria and pathogens had the potential to evolve antibiotic resistance in coastal environments and could spread to humans swimming in these waters so posing serious risks to human health.

TABLE 1 Pearson's correlation analysis among the normalized abundances of ARGs and MGEs.

	MGEs	Integrons	Transposase
Aminoglycoside	0.78**	0.25	0.82**
Beta_Lactamase	0.15	0.54	0.027
Chloramphenicol	0.94**	0.32	0.98**
MLSB	0.99**	0.48	0.99**
Multidrug	0.73*	0.60	0.66*
Sulfonamide	0.67*	0.50	0.63
Tetracycline	0.98**	0.46	0.98**
Vancomycin	-0.04	0.33	-0.13

*$p < 0.05$, and **$p < 0.01$.

Relationships among bacteria communities, mobile genetic elements, environmental factors and antibiotic resistance genes

The relationship between microbial communities, MGEs, environmental factors, and ARGs were explored by RDA analysis (Figure 5A). Taken together, the selected environmental variables (NH4+-N, NO3–N, NO2–N, PO43-, salinity, pH), MGEs, and bacterial communities explained 99.8% of the variation in ARGs. MGEs, salinity, and NH4+-N were significantly positively correlated with the first axis and ARGs from the estuaries of the Tang, Xinkai and Shi Rivers. PO43-, pH, NO3–N, Litoreibacter, and Psychrobacter were significantly positively correlated with ARGs in the RCWs of the Xinkai, Nandai, and Yang Rivers. Partial RDA was performed to further distinguish the effects of environmental factors, MGEs and bacterial communities on antibiotic resistomes in water samples. Based on partial RDA, the bacterial communities accounted for 50.3% of the total ARG variations, much more than the sum of the contribution of MGEs (18.1%) and environmental factors (8.3%). The interaction between environmental factors and microbial community structure, as well as those between MGEs and the bacterial community accounted for 5.9% and 15.2% of total resistome variation, respectively. Mantel correlation based on Bray-Curtis distance showed significant correlations between bacterial communities and antibiotic resistomes in the coastal environments studied (r2 = 0.4591, p = 0.008). The contributions of microbial communities, MGEs and environmental factors to the relative abundance of ARGs in the samples were further explored separately using ABT analysis. Figure S6 shows the relative

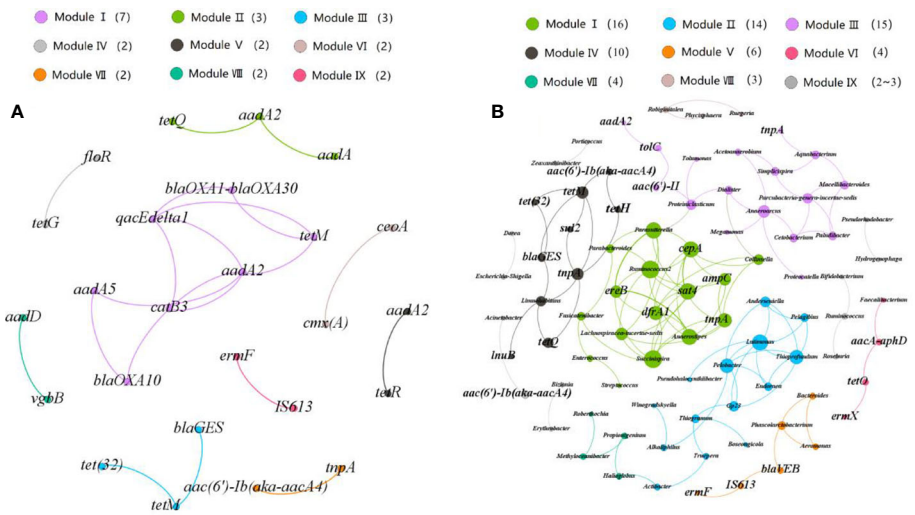

FIGURE 4
Network analysis revealing **(A)** co-occurrence patterns among ARGs and **(B)** co-occurrence patterns between ARGs and microbial taxa at genus level. Nodes are colored according to modularity classes. A connection between nodes indicated a strong ($r > 0.8$) and ($P < 0.01$) significant correlation. The size of each node is proportional to the number of connections.

importance of these indicators. The greater the value, the higher the importance of an indicator. MGEs strongly influenced the occurrence of ARGs in the waters. In addition, the concentration of NO2- (0.011-0.02 mg/L) also had a strong effect on the relative abundance of ARGs. In terms of microbial communities, Acidobacteria had the greatest influence on the resistomes in RCWs and their adjacent estuaries. Coexistence of multiples integrative and conjugative elements has been found in the chromosome of Acidobacteria (Gonçalves and Santana, 2021). Therefore, they could easily become resistant to antibiotics and contribute to the dissemination of ARGs, mediated by the MGEs in estuaries and RCWs.

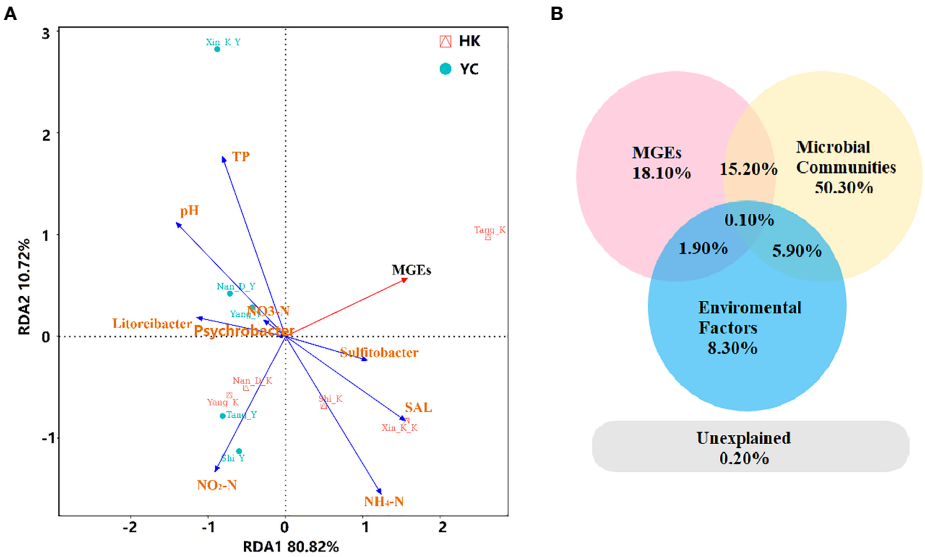

FIGURE 5
(A) Redundancy analysis (RDA) and **(B)** partial RDA assess the effects of environmental factors including pH, NH_4-N, NO_3-N and NO_2-N, MGEs and microbial communities (relative abundance of phylum) on the difference of overall ARGs. TP, total phosphorus; SAL, salinity; MGEs, mobile genetic elements.

Discussion

ARGs and MGEs were widely distributed in RCWs

An abundance of diverse ARGs are alarmingly widespread in estuarine environments. Our study detected a broad spectrum of ARGs in RCWs using HT-qPCR techniques, and their normalized copy numbers were close to, or even higher than, those in adjacent estuaries. In particular, 95 and 72 ARGs were detected in the RCWs adjacent to the estuaries of Tang and Xinkai rivers, respectively. The corresponding relative abundances were as high as 2.6 and 1.3/16S rRNA gene, respectively. Clearly, human exposure to these ARGs in RCWs (for example by aerosol inhalation, dermal, eye or ear contact, and oral intake) may represent potential health risks to those swimming in recreational bathing waters, despite there being no currently known infectious dose of antibiotic resistant bacteria or ARGs. In addition, waterborne pathogens also present major threats to public health. Arcobacter spp. were only identified in estuarine samples by the Illumina sequences of their 16S rRNA genes. Whether these species are pathogenic depends on their expression of a few virulence factors. There have been reports of the widespread occurrence of pathogenic marker genes in RCWs, such as the virulence factors of Acanthamoeba spp., Clostridium perfringens, enteropathogenic Escherichia coli, Klebsiella pneumoniae, Vibrio cholera/V. parahaemolyticus and Legionella spp (An et al., 2020). Co-contamination of waters with pathogens and ARGs could probably contribute to the evolution antibiotic resistant pathogenic bacteria. Therefore, the routine monitoring of waterborne ARGs and pathogens is imperative to improve or safeguard human, animal and environmental health, as emphasized in the various "One-Health" initiatives.

The normalized copy numbers of ARGs detected in the RCWs and estuaries of the Tang and Xinkai rivers were even higher than those in some other environmental samples, such as aquaculture waters (P. Gao et al., 2012), estuarine sediments (Y. G. Zhu et al., 2017), and soils (Y. G. Zhu et al., 2013). The high abundance of ARGs in these two estuaries could be explained by the particularly dense populations in these watersheds. Intensive human activities, such as increased sewage discharge and large aquacultural developments might contribute to the relatively high abundance of ARGs in the Tang and Xinkai Rivers and their accumulation in the estuarine environments. Intensive human activity has been reported to facilitate the spread of ARGs, and population density has been positively correlated with the abundance of ARGs (Uyaguari et al., 2013; Berglund, 2015).

ARGs and MGEs associated with clinical setting have been commonly detected in coastal environments, and can often be traced back to particular hospitals and sewage discharges. For example, vancomycin is only used as the "last line" in the treatment of human bacterial infections. Previous studies have detected the vancomycin resistant gene (vanA) in ancient permafrost sediments predating the use of antibiotics (D'Costa et al, 2011), indicating that it occurs naturally. In 2017, the normalized copy number of vancomycin in estuarine sediment around China was as high as 9.3 × 10-3/16S rRNA genes (Zhu et al., 2017). We found vancomycin resistant genes in all of the estuaries and RCWs, with the relative abundances ranging from 3.7 × 10-4 ~ 2.4×10-3 and 1.5 × 10-3 ~ 1.1×10-1/16S rRNA genes, respectively, which could be related to overuse of vancomycin or unregulated wastewater from hospitals or medical facilities. The growing occurrence and abundance of vancomycin resistance presents an urgent problem. The β-Lactamase blaTEM gene had the highest relative abundance in the samples, possibly due to overuse of the antibiotic cephalosporin in clinical settings. It is worth noticing that blaTEM gene has the potential to encode TEM-1 β-lactamase, which requires only a few specific single nucleotide hydrolytic polymorphisms to evolve into a gene encoding an extended-spectrum β-lactamase that degrades all cephalosporins including ceftriaxone (Muhammad et al., 2014). Diversity of clinically relevant antimicrobial resistance genes was found in urban beaches. The clinical intI1 gene commonly detected in RCWs occurs in a variety of clinical pathogenic bacteria and in the human intestinal flora and can be used as a biomarker for municipal sewage pollution and is closely related to human health risks (Zheng et al., 2020). The results were in consistence with previously published paper indicating that diverse clinically relevant ARGs have been found in urban beaches (Furlan et al., 2021). Together, our study indicated that estuaries and RCWs may be polluted by medical and municipal sewage.

ARGs patterns was strongly affected by bacterial phylogenetic compositions in coastal water environments

The RCW samples analyzed in this study were collected along the coastline of Qinhuangdao. However, the two estuaries with the highest normalized copy numbers (the Tang and Xinkai Rivers) were not adjacent to each other, and there was no overall spatial pattern in antibiotic resistomes in the estuarine areas. These results suggested that environmental factors such as tides or latitude did not the drive the occurrence of ARGs in these estuarine environments. Human activities is frequent in this area and people can either acquire ARGs through direct exposure when swimming there and also introduce new ARGs, so promoting their horizontal transfer of ARGs (Chaturvedi et al., 2021). In order to minimize the impact of human activities on the ARGs detected in RCWs, water samples were collected in winter to minimize the anthropogenic variation in the data. ARGs profiles (qPCR data) were significantly correlated

with bacterial community (16S rRNA genes, OTU data), as shown by the Mantel test. Environmental factors (NH4+-N, NO3–N, NO2–N, PO43-, salinity, pH), bacterial community compositions (relative abundance of major bacterial phyla), and MGEs accounted for 99.8% of total variation in ARGs profiles in the RCWs. Separation of the variations explained by subsets of these factors indicated that MGEs accounted for 18.1% of the subset variation, while bacterial compositions accounted for a much higher percentage of the variation in ARGs (50.3%, Figure 5B). These data indicated that the particular microbial community was a driving force in the variation of ARGs in these estuarine areas. Thus, any factors that disturb the microbial community, such as salinity, nutrient level, organic pollutants, and storm and runoff levels, may exert previously underestimated increases in abundances of ARGs,.

MGEs are vehicles for horizontal transfer of ARGs, and have been shown to promote transmission and enrichment of ARGs many other environments (Wright et al., 2008; Hoa et al., 2011; K. Zhang et al., 2021). In this study, MGEs accounted for 18.1% of the total variation in ARGs according to the pRDA analysis. Based on the network analysis of ARGs, MGEs, and microbial genera, the correlation between transposons (TnpA) and aminoglycoside resistant gene (aac(6')-Ib(aka aacA4)) indicated that conjugation may play a role in the dissemination of ARGs in RCWs. Transposons can transfer themselves and related resistant genes at random to a new location within the cell, including plasmids, while integrons can transfer resistant genes between defined sites by site-specific recombination (Cox and Wright, 2013). Although no correlations between ARGs and integrons were detected, the role of MGEs in the enrichment of ARGs in estuarine areas should not be overlooked. It is noteworthy that Acinetobacter, an opportunistic pathogen, was also significantly associated with the aac(6')-Ib(aka aacA4) gene and may express aminoglycoside resistance. Acinetobacter may cause lung infection through oral inhalation or direct exposure (Wong et al., 2017). In recent years, the occurrence of antibiotic resistant Acinetobacter has been increasing, and ampicillin resistance has remained at a relatively high level (Kutlu et al., 2008). Previous studies have also reported marker genes for Acinetobacter baumanii AB0057 and Acinetobacter oleivorans DR1 in marine recreational beaches around Xiamen City, China (An et al., 2020). Our study showed that coastal environments are ideal places for bacteria or even pathogens to acquire ARGs, and that recreational activities in coastal water may put human beings at risk of antibiotic resistant bacteria infections.

Impacts of estuaries on adjacent recreational coastal waters

PCoA and hierarchical cluster analysis based on Bray-Curtis distance revealed the consistency of ARG occurrences between estuaries and their corresponding RCWs, indicating that estuaries may, to some extent, impact the ARGs in adjacent bathing waters through currents or water exchange. The "Qinhuangdao Recreational Coastal Water Management Regulations", established to avoid contamination from estuaries, state that the RCWs should be located at least 500 m away from an estuary. However, this distance cannot totally avoid the potential threat of ARGs. ARGs from livestock farms, municipal sewage, medical wastewater, and agricultural sewage outlets may spread to bathing waters through estuaries and threaten human health. Previous studies have reported that if RCWs located downstream from poultry farms or municipal sewage discharge points, people swimming are likely to be exposed to Escherichia coli expressing broad-spectrum β-lactamase (Schijyen et al., 2015). Besides, the diverse and abundant ARGs in RCWs could be due to the fact that frequent human activities contribute to permanent changes in properties of RCWs. For example, changes in environmental factors such as differences in organic matter level (Lin et al., 2019), total nitrogen (J. Chen et al., 2019), and temperature (Liao et al., 2018) have been proven to drive the shift of bacterial communities and promote the propagation of ARGs in aquatic environments. Based on ABT analysis, the concentration of NO2- also had an important effect on the relative abundance of ARGs. We found that NO2—N in RCWs was generally higher than in estuaries. According to Cen et al. (2020), nitrite higher than 1 mg/ml could stimulate free radical-induced RpoS regulators and SOS responses, increase cell membrane permeability, and regulate binding transfer-related genes, thus promoting the horizontal transfer of ARGs. Together, these results indicated that multiple factors could result in the propagation of ARGs and further emphasize the importance of routine surveillance of ARGs in RCWs.

Conclusions

The results of this study showed that the abundance of ARGs in RCWs ranged from 9.9×10-2 to 2.1/16S rRNA gene, higher than in many other environments such as soil, estuarine sediments, and aquacultural developments. The consistency between RCW and their adjacent estuaries indicated that estuaries, to some extent, may have an impact on ARGs in RCWs. Thus, the current rules regulating RCWs cannot avoid the threat of ARGs to human health, and humans may be exposed to ARGs when swimming in RCWs. The Mantel test suggested that microbial community structure is the main force driving the occurrence of ARGs in coastal water environment. Besides the selective pressure of antibiotics, attention should be paid to the spread and enrichment of ARGs that may be overlooked when any perturbation disturbs the microbial composition of swimming waters, such as changes in

temperatures, N and P levels, or even algal abundances. Moreover, the consistency between antibiotic resistomes in RCWs and their adjacent estuaries suggested that ARGs from estuaries could contaminate adjacent RCWs. Therefore, proper regulations of bathing areas and reducing the discharge of ARG into terrigenous runoff may be useful in controlling ARG levels in RCWs, and so control the risks to public health. More work is needed to determine the infectious concentrations and risk levels of ARGs to better assess the potential public health risk of ARGs in RCWs. ARG levels and microbial community composition in bathing waters should be routinely detected in real-time.

Data availability statement

The original contributions presented in the study are included in the article/Supplementary Material. Further inquiries can be directed to the corresponding author.

Author contributions

YH: Conceptualization, Methodology, Formal analysis, Data curation, Writing – original draft, Writing – review & editing. YKH: Formal analysis, Conceptualization, Writing – review & editing. HXW: Conceptualization, Formal analysis, Writing – review & editing. YWL: Writing – review & editing. JYW: Data curation. YCZ: Methodology. HW: Writing – review & editing. All authors contributed to the article and approved the submitted version.

Funding

This work has been funded by Natural Science Foundation of Hebei Province, China (B2020203005), Cultivation Project for Basic Research and Innovation of Yanshan University (2021LGQN027) and Open Foundation of Key Laboratory of Industrial Ecology and Environmental Engineering, MOE (KLIEEE-20-05).

Conflict of interest

The authors declare that the research was conducted in the absence of any commercial or financial relationships that could be construed as a potential conflict of interest.

Publisher's note

All claims expressed in this article are solely those of the authors and do not necessarily represent those of their affiliated organizations, or those of the publisher, the editors and the reviewers. Any product that may be evaluated in this article, or claim that may be made by its manufacturer, is not guaranteed or endorsed by the publisher.

Supplementary Material

The Supplementary Material for this article can be found online at: https://www.frontiersin.org/articles/10.3389/fmars.2022.976438/full#supplementary-material

References

Ali, L., Wang, Y. Q., Zhang, J., Ajmal, M., Xiao, Z. R., Wu, J. R., et al. (2016). Nutrient-induced antibiotic resistance in enterococcus faecalis in the eutrophic environment. *J. Glob. Antimicrob. Resist.* 7, 78–83. doi: 10.1016/j.jgar.2016.07.014

An, X. L., Wang, J. Y., Pu, Q., Li, H., Pan, T., Li, H. Q., et al. (2020). High-throughput diagnosis of human pathogens and fecal contamination in marine recreational water. *Environ. Res.* 190, 109982. doi: 10.1016/j.envres.2020.109982

Berglund, B. (2015). Environmental dissemination of antibiotic resistance genes and correlation to anthropogenic contamination with antibiotics. *Infect. Ecol. Epidemiol.* 5, 28564–28564. doi: 10.3402/iee.v5.28564

Bigus, K., Astel, A., and Niedzielski, P. (2016). Seasonal distribution of metals in vertical and horizontal profiles of sheltered and exposed beaches on polish coast. *Mar. pollut. Bull.* 106 (1-2), 347–359. doi: 10.1016/j.marpolbul.2016.03.009

Bi Weihong, Li Yu, Jiancheng, S., Yajie, J., Pingjie, H., and Fei, Xu (2022). Research review and development trend of marine total organic carbon detection based on spectral technology. *J. YanShan Univ.* 46 (1), 1–8. doi: 10.3969/j.issn.1007-791X.2022.01.001

Blahova, J., Kralikova, K., and Krcmery, V. (1999). Reservoirs, interactions and stability of genetic resistance to antibiotics. the "easy to get–hard to lose" syndrome. [Rezervoary, interakcie a stabilita genov rezistencie na antibiotika. syndrom "easy to get–hard to lose".]. *Cas. lek. Cesk.* 138 (14), 424–428.

Cen, T., Zhang, X., Xie, S., and Li, D. (2020). Preservatives accelerate the horizontal transfer of plasmid-mediated antimicrobial resistance genes *via* differential mechanisms. *Environ. Int.* 138, 105544. doi: 10.1016/j.envint.2020.105544

Chaturvedi, P., Chowdhary, P., Singh, A., Chaurasia, D., Pandey, A., Chandra, R., et al. (2021). Dissemination of antibiotic resistance genes, mobile genetic elements, and efflux genes in anthropogenically impacted riverine environments. *Chemosphere* 273, 129693. doi: 10.1016/j.chemosphere.2021.129693

Chen, J., Deng, W. J., Liu, Y. S., Hu, L. X., He, L. Y., Zhao, J. L., et al. (2019). Fate and removal of antibiotics and antibiotic resistance genes in hybrid constructed wetlands. *Environ. pollut.* 249, 894–903. doi: 10.1016/j.envpol.2019.03.111

Chen, H., and Zhang, M. M. (2013). Effects of advanced treatment systems on the removal of antibiotic resistance genes in wastewater treatment plants from hangzhou, China. *Environ. Sci. Technol.* 47 (15), 8157–8163. doi: 10.1021/es401091y

Cox, G., and Wright, G. D. (2013). Intrinsic antibiotic resistance: Mechanisms, origins, challenges and solutions. *Int. J. méd. Microbiol. Int. J. Med. Microbiol.* 303 (6-7), 287–292. doi: 10.1016/j.ijmm.2013.02.009

Culliton, T. J. (1998) *Population: Distribution, density, and growth*. Available at: https://www.researchgate.net/publication/247207344_Population_Distribution_Density_and_Growth.

D'Costa, V. M., King, C. E., Kalan, L., Morar, M., Sung, W. W. L., Schwarz, C., et al. (2011). Antibiotic resistance is ancient. *Nature* 377 (7365), 457–461. doi: 10.1038/nature10388

Dalcin, E., and Jackson, P. W. (2018). A network-wide visualization of the implementation of the global strategy for plant conservation in Brazil. *Rodriguésia.* 69 (4), 1613–1639. doi: 10.1590/2175-7860201869411

Forsberg, K. J., Patel, S., Gibson, M. K., Lauber, C. L., Knight, R., Fierer, N., et al. (2014). Bacterial phylogeny structures soil resistomes across habitats. *Nature.* 509 (7502), 612–615. doi: 10.1038/nature13377

Freeman, C. N., Scriver, L., Neudorf, K. D., Hansen, L. T., and Jamieson, R. C. (2018). Antimicrobial resistance gene surveillance in the receiving waters of an upgraded wastewater treatment plant. *Facets* 3, 128–138. doi: 10.1139/facets-2017-0085

Furlan, J. P. R., Ramos, M. S., dos Santos, L. D. R., Gallo, I. F. L., Lopes, R., and Stehling, E. G. (2021). Appearance of *mcr-9*, *blaKPC*, *cfr* and other clinically relevant antimicrobial resistance genes in recreation waters and sands from urban beaches, Brazil. *Mar. pollut. Bull.* 167, 112334. doi: 10.1016/j.marpolbul.2021.112334

Gao, F. L., Li, J. X., Hu, J., Sui, B. L., Wang, C. A. X., Sun, C. J., et al. (2021). The seasonal distribution characteristics of microplastics on bathing beaches along the coast of qingdao, China. *Sci. Total Environ.* 783, 146969. doi: 10.1016/j.scitotenv.2021.146969

Gao, P., Mao, D., Luo, Y., Wang, L., Xu, B., and Xu, L. (2012). Occurrence of sulfonamide and tetracycline-resistant bacteria and resistance genes in aquaculture environment. *Water Res.* 46 (7), 2355–2364. doi: 10.1016/j.watres.2012.02.004

Gonçalves, O. S., and Santana, M. F. (2021). The coexistence of monopartite integrative and conjugative elements in the genomes of acidobacteria. *Gene* 777, 145476. doi: 10.1016/j.gene.2021.145476

Hoa, P. T. P., Managaki, S., Nakada, N., Takada, H., Shimizu, A., Anh, D. H., et al. (2011). Antibiotic contamination and occurrence of antibiotic-resistant bacteria in aquatic environments of northern Vietnam. *Sci. Total Environ.* 409 (15), 2894–2901. doi: 10.1016/j.scitotenv.2011.04.030

Huang, H. W., Zeng, S. Y., Dong, X., Li, D., Zhang, Y., He, M., et al. (2019). Diverse and abundant antibiotics and antibiotic resistance genes in an urban water system. *J. Environ. Manage.* 231, 494–503. doi: 10.1016/j.jenvman.2018.10.051

Huang, H. N., Zheng, X., Chen, Y. G., Liu, H., Wan, R., and Su, Y. L. (2017). Alkaline fermentation of waste sludge causes a significant reduction of antibiotic resistance genes in anaerobic reactors. *Sci. Total Environ.* 580, 380–387. doi: 10.1016/j.scitotenv.2016.11.186

Jacoby, G. A. (2006). β-lactamase nomenclature nomenclature. *Antimicrob. Agents Chemother.* 50 (4), 1123–1129. doi: 10.1128/AAC.50.4.1123-1129.2006

Jang, H. M., Kim, Y. B., Choi, S., Lee, Y., Shin, S. G., Unno, T., et al. (2018). Prevalence of antibiotic resistance genes from effluent of coastal aquaculture, south Korea. *Environ. pollut.* 233, 1049–1057. doi: 10.1016/j.envpol.2017.10.006

Kutlu, S. S., Sacar, S., Suzer, T., Cevahir, N., Okke, D., Caylak, S. D., et al. (2008). Successful treatment of a patient with multidrug resistant acinetobacter baumannii meningitis with high dose ampicillin-sulbactam. *Mikrobiyol Bul.* 42 (2), 353–358.

Liao, H., Lu, X., Rensing, C., Friman, V. P., Geisen, S., Chen, Z., et al. (2018). Hyperthermophilic composting accelerates the removal of antibiotic resistance genes and mobile genetic elements in sewage sludge. *Environ. Sci. Technol.* 52 (1), 266–276. doi: 10.1021/acs.est.7b04483

Lin, W. F., Wan, K., Zeng, J., Li, J. J., Li, X., and Yu, X. (2019). Low nutrient levels as drinking water conditions can reduce the fitness cost of efflux pump-mediated ciprofloxacin resistance in pseudomonas aeruginosa. *J. Environ. Sci(China)* . 83, 123–132. doi: 10.1016/j.jes.2019.03.022

Magoc, T., and Salzberg, S. L. (2011). FLASH: fast length adjustment of short reads to improve genome assemblies. *Bioinformatics.* 27 (21), 2957–2963. doi: 10.1093/bioinformatics/btr507

Marti, E., Variatza, E., and Balcazar, J. L. (2014). The role of aquatic ecosystems as reservoirs of antibiotic resistance. *Trends Microbiol.* 22 (1), 36–41. doi: 10.1016/j.tim.2013.11.001

Muhammad, I., Golparian, D., Dillon, J. A. R., Johansson, A., Ohnishi, M., Sethi, S., et al. (2014). Characterisation of bla(TEM) genes and types of beta-lactamase plasmids in neisseria gonorrhoeae - the prevalent and conserved bla(TEM-135) has not recently evolved and existed in the Toronto plasmid from the origin. *BMC Infect. Dis. BMC Infect. Dis.* 14, 454. doi: 10.1186/1471-2334-14-454

O' Neil, J. (2014)Review on antimicrobial resistance antimicrobial resistance: tackling a crisis for the health and wealth of nations. In: *Review on antimicrobial resistance.* Available at: https://amr-review.org/sites/default/files/AMR%20Review%20Paper%20-%20Tackling%20a%20crisis%20for%20the%20health%20and%20wealth%20of%20nations_1.pdf (Accessed 9 March 2022).

Ouyang, W. Y., Huang, F. Y., Zhao, Y., Li, H., and Su, J. Q. (2015). Increased levels of antibiotic resistance in urban stream of jiulongjiang river, China. *Appl. Microbiol. Biotechnol.* 99 (13), 5697–5707. doi: 10.1007/s00253-015-6416-5

Pruden, A., Pei, R. T., Storteboom, H., and Carlson, K. H. (2006). Antibiotic resistance genes as emerging contaminants: Studies in northern Colorado. *Environ. Sci. Technol.* 40 (23), 7445–7450. doi: 10.1021/es060413l

Qinhuangdao Municipal People's Government (2019) *Regulations of qinhuangdao municipality on the administration of bathing beaches.* Available at: http://www.qhd.gov.cn/front_pcthi.do?uuid=8F0D6662565323FFB03AC4C9AE146E42 (Accessed 9 March 2022).

Rider, B. F., and Mellon, M. G. (1946). Colorimetric determination of nitrites. *Ind. Eng. Chem. Analytical Ed.* 18 (2), 96–99. doi: 10.1021/i560150a003

Rodriguez-Mozaz, S., Chamorro, S., Marti, E., Huerta, B., Gros, M., Sanchez-Melsio, A., et al. (2015). Occurrence of antibiotics and antibiotic resistance genes in hospital and urban wastewaters and their impact on the receiving river. *Water Res.* 69, 234–242. doi: 10.1016/j.watres.2014.11.021

Rognes, T., Flouri, T., Nichols, B., Quince, C., and Mahe, F. (2016). VSEARCH: a versatile open source tool for metagenomics. *Peerj* 4, e2584. doi: 10.7717/peerj.2584

Sarkar, S. K., and Chang, C. K. (1997). The simes method for multiple hypothesis testing with positively dependent test statistics. *J. Am. Stat. Assoc.* 92 (440), 1601–1608. doi: 10.2307/2965431

Schijyen, J. F., Blaak, H., Schets, F. M., Husman, A. M., and d., R. (2015). Fate of extended-spectrum beta-Lactamase-Producing escherichia coli from faecal sources in surface water and probability of human exposure through swimming. *Environ. Sci. Technol.* 49 (19), 11825–11833. doi: 10.1021/acs.est.5b01888

Stepanauskas, R., Glenn, T. C., Jagoe, C. H., Tuckfield, R. C., Lindell, A. H., King, C. J., et al. (2006). Coselection for microbial resistance to metals and antibiotics in freshwater microcosms. *Environ. Microbiol.* 8 (9), 1510–1514. doi: 10.1111/j.1462-2920.2006.01091.x

Stewart, J. R., Gast, R. J., Fujioka, R. S., Solo-Gabriele, H. M., Meschke, J. S., Amaral-Zettler, L. A., et al. (2008). The coastal environment and human health: microbial indicators, pathogens, sentinels and reservoirs. *Environ. Health* 7, s3. doi: 10.1186/1476-069x-7-s2-s3

Su, J., Fan, J., Ming, H., Guo, G., Fu, Y., Zhao, X., et al. (2022). The municipal sewage discharge may impact the dissemination of antibiotic-resistant escherichia coli in an urban coastal beach. *Water* 14, 1639. doi: 10.3390/w14101639

Sun, J. T., Jin, L., He, T. T., Wei, Z., Liu, X. Y., Zhu, L. Z., et al. (2020). Antibiotic resistance genes (ARGs) in agricultural soils from the Yangtze river delta, China. *Sci. Total Environ.* 740, 140001. doi: 10.1016/j.scitotenv.2020.140001

Su, J. Q., Wei, B., OuYang, W. Y., Huang, F. Y., Zhao, Y., Xu, H. J., et al. (2015). Antibiotic resistome and its association with bacterial communities during sewage sludge composting. *Environ. Sci. Technol.* 49 (12), 7356–7363. doi: 10.1021/acs.est.5b01012

Tamminen, M., Karkman, A., Lohmus, A., Muziasari, W. I., Takasu, H., Wada, S., et al. (2011). Tetracycline resistance genes persist at aquaculture farms in the absence of selection pressure. *Environ. Sci. Technol.* 45 (2), 386–391. doi: 10.1021/es102725n

Tandukar, M., Oh, S., Tezel, U., Konstantinidis, K. T., and Pavlostathis, S. G. (2013). Long-term exposure to benzalkonium chloride disinfectants results in change of microbial community structure and increased antimicrobial resistance. *Environ. Sci. Technol.* 47 (17), 9730–9738. doi: 10.1021/es401507k

Tomova, A., Ivanova, L., Buschmann, A. H., Rioseco, M. L., Kalsi, R. K., Godfrey, H. P., et al. (2015). Antimicrobial resistance genes in marine bacteria and human uropathogenic escherichia coli from a region of intensive aquaculture. *Environ. Microbiol. Rep.* 7 (5), 803–809. doi: 10.1111/1758-2229.12327

Uyaguari, M. I., Scott, G. I., and Norman, R. S. (2013). Abundance of class 1-3 integrons in south Carolina estuarine ecosystems under high and low levels of anthropogenic influence. *Mar. pollut. Bull.* 76 (1-2), 77–84. doi: 10.1016/j.marpolbul.2013.09.027

von Wintersdorff, C. J. H., Penders, J., van Niekerk, J. M., Mills, N. D., Majumder, S., van Alphen, L. B., et al. (2016). Dissemination of antimicrobial resistance in microbial ecosystems through horizontal gene transfer. *Front. Microbiol.* 7. doi: 10.3389/fmicb.2016.00173

Wang, Q., Garrity, G. M., Tiedje, J. M., and Cole, J. R. (2007). Naive Bayesian classifier for rapid assignment of rRNA sequences into the new bacterial taxonomy. *Appl. Environ. Microbiol.* 73 (16), 5261–5267. doi: 10.1128/aem.00062-07

Wang, Y. Q., Lu, S. Y., Liu, X. H., Chen, J., Han, M. Z., Wang, Z., et al. (2021). Profiles of antibiotic resistance genes in an inland salt-lake ebinur lake, xinjiang, China: The relationship with antibiotics, environmental factors, and microbial communities. *Ecotoxicol. Environ. Saf.* 221, 112427. doi: 10.1016/j.ecoenv.2021.112427

Wei, Z. L., Miao, J., Yang, Z. W., Shi, D. Y., Wu, H. Y., Yang, D., et al. (2020). Contamination sources of the enteric virus in recreational marine water shift in a seasonal pattern. *Sci. Total Environ.* 743, 140641. doi: 10.1016/j.scitotenv.2020.140641

Wen, H.-q., Shi, J., Xun, H., and Deng, H. P. (2015). Distribution, dissemination and removal of antibiotic resistant genes (ARGs) in the aquatic environment. *J. Appl. Ecol.* 26 (2), 625–635.

Wong, D., Nielsen, T. B., Bonomo, R. A., Pantapalangkoor, P., Luna, B., and Spellberg, B. (2017). Clinical and pathophysiological overview of acinetobacter infections: a century of challenges. *Clin. Microbiol. Rev.* 30 (1), 409–447. doi: 10.1128/cmr.00058-16

Wright, M. S., Baker-Austin, C., Lindell, A. H., Stepanauskas, R., Stokes, H. W., and McArthur, J. V. (2008). Influence of industrial contamination on mobile genetic elements: class 1 integron abundance and gene cassette structure in aquatic bacterial communities. *ISME J.* 2 (4), 417–428. doi: 10.1038/ismej.2008.8

Wu, D., Ma, R. Q., Wei, H. W., Yang, K., and Xie, B. (2018). Simulated discharge of treated landfill leachates reveals a fueled development of antibiotic resistance in receiving tidal river. *Environ. Int.* 114, 143–151. doi: 10.1016/j.envint.2018.02.049

Wu, B., Song, J. M., and Li, X. G. (2014). Evaluation of potential relationships between benthic community structure and toxic metals in laizhou bay. *Mar. pollut. Bull.* 87 (1-2), 247–256. doi: 10.1016/j.marpolbul.2014.07.052

Yang, J., Wang, H., Roberts, D. J., Du, H. N., Yu, X. F., Zhu, N. Z., et al. (2020). Persistence of antibiotic resistance genes from river water to tap water in the Yangtze river delta. *Sci. Total Environ.* 742, 140592. doi: 10.1016/j.scitotenv.2020.140592

Yang, J., Wang, C., Shu, C., Liu, L., Geng, J., Hu, S., et al. (2013). Marine sediment bacteria harbor antibiotic resistance genes highly similar to those found in human pathogens. *Microb. Ecol.* 65 (4), 975–981. doi: 10.1007/s00248-013-0187-2

Zhang, Y. J., Hu, H. W., Yan, H., Wang, J. T., Lam, S. K., Chen, Q. L., et al. (2019). Salinity as a predominant factor modulating the distribution patterns of antibiotic resistance genes in ocean and river beach soils. *Sci. Total Environ.* 668, 193–203. doi: 10.1016/j.scitotenv.2019.02.454

Zhang, T., Li, J., Wang, N., Wang, H., and Yu, L. (2021). Metagenomic analysis reveals microbiome and resistome in the seawater and sediments of kongsfjorden (Svalbard, high Arctic). *Sci. Total Environ.* 809, 151937. doi: 10.1016/j.scitotenv.2021.151937

Zhang, K., Xin, R., Zhao, Z., Li, W. P., Wang, Y. N., Wang, Q., et al. (2021). Mobile genetic elements are the major driver of high antibiotic resistance genes abundance in the upper reaches of huaihe river basin. *J. Hazard. Mater* 401, 123271. doi: 10.1016/j.jhazmat.2020.123271

Zheng, W. L., Huyan, J. Q., Tian, Z., Zhang, Y., and Wen, X. H. (2020). Clinical class 1 integron-integrase gene - a promising indicator to monitor the abundance and elimination of antibiotic resistance genes in an urban wastewater treatment plant. *Environ. Int.* 135, 105372. doi: 10.1016/j.envint.2019.105372

Zhuang, M., Achmon, Y., Cao, Y. P., Liang, X. M., Chen, L., Wang, H., et al. (2021). Distribution of antibiotic resistance genes in the environment star. *Environ. pollut.* 285, 117402. doi: 10.1016/j.envpol.2021.117402

Zhu, Y. G., Johnson, T. A., Su, J. Q., Qiao, M., Guo, G. X., Stedtfeld, R. D., et al. (2013). Diverse and abundant antibiotic resistance genes in Chinese swine farms. *P. Natl. Acad. Sci. U.S.A.* 110 (9), 3435–3440. doi: 10.1073/pnas.1222743110

Zhu, L. H., Wu, J. Z., Xu, Z. Q., Xu, Y. C., Lin, J., and Hu, R. J. (2014). Coastline movement and change along the bohai Sea from 1987 to 2012. *J. Appl. Remote. Sens* 8, 083585. doi: 10.1117/1.jrs.8.083585

Zhu, Y. G., Zhao, Y., Li, B., Huang, C. L., Zhang, S. Y., Yu, S., et al. (2017). Continental-scale pollution of estuaries with antibiotic resistance genes. *Nat. Microbiol.* 2 (4), 7. doi: 10.1038/nmicrobiol.2016.270

frontiers | Frontiers in Marine Science

TYPE Original Research
PUBLISHED 17 October 2022
DOI 10.3389/fmars.2022.1035268

OPEN ACCESS

EDITED BY
Songzhe Fu,
Dalian Ocean University, China

REVIEWED BY
Duochun Wang,
National Institute for Communicable Disease Control and Prevention (China CDC), China
Ruijun Li,
Dalian Ocean University, China
Pimonsri Mittraparp-arthorn,
Prince of Songkla University, Thailand

*CORRESPONDENCE
Xiaojun Zhang
zxj9307@163.com

SPECIALTY SECTION
This article was submitted to Marine Fisheries, Aquaculture and Living Resources, a section of the journal Frontiers in Marine Science

RECEIVED 02 September 2022
ACCEPTED 29 September 2022
PUBLISHED 17 October 2022

CITATION
Jiang Z, Gu S, Qian Q, Li J, Ji P, Wu C, Zhang Y, Gao X, Jiang Q and Zhang X (2022) Survival virulent characteristics and transcriptomic analyses of *Vibrio mimicus* exposed to starvation. *Front. Mar. Sci.* 9:1035268. doi: 10.3389/fmars.2022.1035268

Survival virulent characteristics and transcriptomic analyses of *Vibrio mimicus* exposed to starvation

Ziyan Jiang, Shuwen Gu, Qieqi Qian, Jie Li, Peng Ji, Congcong Wu, Yingjie Zhang, Xiaojian Gao, Qun Jiang and Xiaojun Zhang*

College of Animal Science and Technology, Yangzhou University, Yangzhou, China

Vibrio mimicus is a global causative agent of vibriosis in a variety of aquatic animals and causes major economic losses to aquaculture. It could survive in water for extended periods of time under environmental stress, but its survival strategy remains unknow. This study described the survival, virulent and gene expression changes of *V. mimicus* cells undergoing starvation stress. After 4 weeks' cultivation in media without nutrients, *V. mimicus* Y4 showed reduced rates of activity with marked changes in morphology and physiological activities. The culturable cell counts declined gradually to 10^4 CFU/mL and the shape changed from rod-shaped to coccoid with short rods or spherical. The motility of starved cells decreased after starvation and the biofilm production was significantly lower than wild cells. The starved cells still produced β-hemolysis, lecithinase and caseinase, but its infectivity to *Macrobrachium nipponense* was weakened. To investigate the mechanism behind morphological and physiological changes, we further analyzed differently expressed genes (DEGs) between starved and wild cells at the whole transcriptional level. The RNA-seq analysis demonstrated that large-scale DEGs were involved in transferase, membrane, dehydrogenase, synthase, flagellar, hemolysin, pilus assembly, and starvation, etc. Among them, the well-known virulence-related genes were downregulated significantly, including *vmh*, *pilA*, *vipA*, *capB*, *tadC*, *huvX*, *ompA*, etc. These data provide a key resource to understand the regulatory mechanisms of *V. mimicus* to starvation stress.

KEYWORDS

***Vibrio mimicus*, starvation stress, survival, virulent changes, transcriptome analysis**

Introduction

Vibrio mimicus is a gram-negative bacterial pathogen distributing widely in both freshwater and estuarine environments. It is one of the most prevalent pathogens in aquaculture, which could induce high mortality among aquatic animals, impeding healthy and sustainable development of aquaculture (Vieira et al., 2001). For example, the outbreak of white spot disease (WSD) in *Penaeus monodon* was reported to be related with the infection of *V. mimicus* (Ramalingam et al., 2017), and it also could infect freshwater catfish and prawns and induce mortality with short disease duration (Geng et al., 2014; Yu et al., 2020; Jiang et al., 2021). Furthermore, consumption of freshwater fish and seafood contaminated with *V. mimicus* might cause symptoms of gastroenteritis, diarrhea and food poisoning in humans (Chitov et al., 2009; Kay et al., 2012; Tercero-Alburo et al., 2014; Muller et al., 2016). The severe impact of *V. mimicus* on aquaculture industry and human health attracts people's attention, and an increasing number of studies focused on its detection and pathogenesis have been conducted (Neogi et al., 2018; Yu et al., 2020).

Bacteria can be subject to multiple environmental stresses during their life, including nutrient limitation, extreme temperature, osmotic concentrations, oxygen, copper stress and organic pollutants (Oliver, 2010; Fu, et al., 2014). Among them, nutrient deficiency is the most common stress which microorganisms routinely encounter in natural ecosystems (Gao et al., 2018). It has been reported that *Vibrio* spp. can differentiate into the viable but nonculturable (VBNC) state to maintain viability and survive several years in food deprived condition (Abdallah et al., 2009; Kim et al., 2018), which could contribute to the spreading of *V. mimicus* in the environment and hazarding public health. A common feature of bacteria subjected to starvation is the 'rounding up' phenomenon, which cells become rounder and adopt a coccus shape (Carroll et al., 2001). In addition, the growth, survival rate, and pathogenicity were also reported to be reduced compared to the non-starved cells (Eguchi et al., 2000; Amel et al., 2008; Chen et al., 2009). These phenotypic signs induced by starvation were found in *Vibrio* spp. (Alonso et al., 2002; Citterio et al., 2004), but the response of *V. mimicus* in survival and pathogenicity under starvation stress are not clear.

This study assessed the potential of *V. mimicus* to survive under starvation stress and further investigated the changes in morphology, motility, and pathogenicity induced by starvation. Besides, to reveal the molecular mechanism behind phenotypic changes, transcriptomic analyses between starved and wild cells were examined at the whole transcriptional level. These results will shed new light on understanding of the stress response mechanisms of *V. mimicus* under starvation.

Materials and methods

Bacterial strains and starvation stress

V. mimicus Y4 was isolated from *Macrobrachium nipponense* with red body disease in Jiangsu province, China (Jiang et al., 2021). It was preserved in 30% glycerol at -80°C in our lab, and the individual colony of the isolate Y4 were incubated in 100 mL of LB liquid medium at 28°C while shaking (180 rpm) for 18 h. *V. mimicus* cells were harvested by centrifugation at 6,000 g for 10 min and washed twice with sterile saline solution (0.9% w/v NaCl). The cells were resuspended in sterile Erlenmeyer glass flasks containing 100 mL of sterile saline with a final concentration of 1×10^9 CFU/mL and incubated at 28°C in sterile saline solution without nutrients for 4 weeks. Experiments were performed in triplicates for statistical analysis. The culturable number of bacterial cells was obtained using LB plates. The freshly prepared log-phase *V. mimicus* cell culture without starvation treatment was used as the control.

Growth curve

The wild and 4-week starved strain was incubated at 28°C to the initial exponential (OD_{570} = 0.2). The values of OD_{570} were recorded at 0-24 h. From the OD_{570} data, growth curves were plotted comparing the wild and 4-week starved strain. Three independent biological replicates were performed for each data point.

Ultrastructural analysis

Morphological changes between 4-week starved and wild cells were monitored under scanning electronic microscope (SEM) as previously described with minor modification (Arias et al., 2012). Briefly, 10 µL of bacteria was fixed in 2.5% glutaraldehyde (v/v) on 8 × 8 mm glass slides at 4°C overnight. Then, samples were dehydrated in a graded ethanol series (50, 70, 90, and 100%), coated with gold palladium alloy in an EMS 550X (Electron Microscopy Science), and examined under Zeiss EVO 50 electronic microscope (Zeiss, Germany).

Bacterial motility test

After 4-week starvation, the motility of *V. mimicus* strain Y4 was measured as described previously (Xu et al., 2014). Briefly, a puncture inoculated a single colony in the middle of the plates containing 0.4% agar. The diameter of the halo surrounding the punctured portion of the agar media was measured 24 h post-inoculation.

Microtiter plate biofilm production assay

Biofilm formation in microplates was quantified by crystal violet staining according to a previously described method (Dueholm et al., 2013), with minor modifications. Overnight cultures of wild-type and 4-week starved strain were diluted at a 1:1000 ratio in fresh sterile LB, added to 96-well microtiter plates at a volume of 200 μL per well, and incubated at 28°C with shaking for 12-72 h. The wells were aspirated and washed with 0.1 M phosphate buffer (PBS). The biofilms were stained with 250 μL of 1% crystal violet for 15 min, then washed twice with PBS, solubilized the crystal violet with ethanol for 15 min, and measured the absorbance (OD_{570}) using a Synergy HT microplate reader.

Determination of extracellular enzymes and hemolysin

The presence of lecithinase, caseinase, and lipase of the 4-week starved cells were determined by directly culturing the starved cells on LB nutrient agar containing 10% egg yolk (lecithinase test), 10% skim milk (caseinase test), 1% Tween-80 (lipase test), and 7% rabbit erythrocytes (β-hemolytic activity test) as substrate. These plates were incubated at 28°C for 24-48 h, and the presence of the lytic halo around the colonies was observed.

Bacterial virulence assay

To examine the pathogenicity, healthy *M. nipponense* was infected by bath immersion with 4-week starved and wild *V. mimicus*. Experimental *M. nipponense* (average weight was 1.64 ± 0.6 g) were provided by an aquaculture farm located at Changzhou Country of Jiangsu Province, China. A total of 330 prawns were divided into 11 groups and continuously immersed with five different doses (3.6×10^8, 3.6×10^7, 3.6×10^6, 3.6×10^5 and 3.6×10^4 CFU/mL), respectively, and prawns in the rest tank were maintained in freshwater as control group. During the experiment, prawns were maintained in 30-L aquarium at 26 ± 0.5°C water temperature, and the water was aerated with 5.0 mg/L of dissolved oxygen. The mortality of prawns were checked during 7 d post infection. All experiments were repeated three times and the mean value was taken for the calculation of the median lethal dose (LD_{50}) values according to the description of Saganuwan (Saganuwan, 2011) (Supplementary Table 1).

Transcriptome analysis

Samples of 4-week starved and wild cells (n=3) were sent to Beijing Novogene Co., Ltd, and subjected to total RNA isolation and cDNA preparations. The library was sequenced on the Illumina Hiseq 2500 platform. The clean reads of starved and wild cells were filtered from the raw data, and aligned to the reference genome and sequence using Bowtie 2. The DESeq R package was used to determine the differentially expressed genes (DEGs) between the starved and wild cells samples, and the q-value <0.05 and |log2(FoldChange)|>1 was adjusted as the threshold for significantly different expression. These DEGs was identified by GO and KEGG database annotations (Conesa et al., 2005; Minoru et al., 2013). The sequencing data has been successfully deposited in SRA database (PRJNA770024).

Validation of DEGs using qRT-PCR

Fourteen genes were selected to confirm the RNA-seq results by qRT-PCR. Primers were used for qRT-PCR and 16S rRNA gene was used to normalize the expression level (Table 1). The relative gene expressions were determined using $2^{-\Delta\Delta Ct}$ method. Expression of the detected genes was analyzed by one-Way ANOVA using SPSS 16.0. All quantitative data were expressed as means ± SD.

Results

Survival under starvation stress

The survival rate of *V. mimicus* Y4 under starvation at 28°C was determined over a 4-week period (Figure 1A). Overall, *V. mimicus* Y4 was still culturable after 4-week starvation. The percentage of the strain Y4 culturable bacterial cells was reduced to 68.13% of their initial level during starvation period with Log_{10} CFU/mL changing from 10.4028 ± 0.1991 to 7.0878 ± 0.1102. In addition, the viability of starved cells is maintained and no significant change in growth capacity was observed at 4-week-starved cells compared with the wild strain, and the growth curve was shown in Figure 1B.

Phenotype changes of *V. mimicus* after starvation stress

The wild *V. mimicus* cells were changed from rods shape to short rods, and the average cell length of the initial *V. mimicus* had significantly decreased from 1.6 ± 0.2 μm to 1.0 ± 0.2 μm by using scanning electron micrograph (Figures 1C, D). Furthermore, *V. mimicus* had significantly decreased in motility (from 2.2 ± 0.2 μm to 1.2 ± 0.2 μm) after starvation (Figures 1E, F). In addition, biofilm production of the starved cells was decreased with 0.24, 0.67, 0.40 and 0.54 fold than wild cells over a period of 12-72 h, respectively (Figure 2). The

TABLE 1 Primers used for the detection of DEGs by qRT-PCR.

Target gene	PCR primers sequence (5′-3′)	Gene ID
flgD-F	GCCTCATCACTGGTAGGTCG	Y4_GM001751
flgD-R	CTTTGGCGCCCACATCAAAA	
ompA-F	GCGCGATTGAACCAGCATTT	Y4_GM002845
ompA-R	GACGCGATTCGGCGTTATAC	
tonB-F	CGATAACCAGTACCGTCGCA	Y4_GM000418
tonB-R	GAGATATGCGTGCGAGACGA	
luxS-F	CTGCGATGCAGGATGTGTTG	Y4_GM003602
luxS-R	CGCAATCACTTTCTGTGCGA	
cpaB-F	TAGCTCAGCGTTTAGGGGTG	Y4_GM004038
cpaB-R	TGACACTTGCTCATCCCACA	
pilA-F	AGGGTGCAACAGCGATTGAG	Y4_GM004040
pilA-R	ATTCGCCACTGCTACTCATGTT	
vipA-F	ATGCTGAGCTTCCGGTTGAG	Y4_GM000515
vipA-R	CAGAGACTGCAAACGCTCAC	
tadC-F	GAAGCTGGTCTGTCGTTGGA	Y4_GM004032
tadC-R	CGCCAAGCCAGCTTTTTCAT	
huvX-F	CGATGGCAAACATGCGCAAA	Y4_GM000421
huvX-R	CCGTCTCTCCCCATCAGGTT	
vmh-F	GCGAAGCTAGAGGCAAAAGC	Y4_GM000397
vmh-R	GTCGAGCGGTTAAGCAAGGA	
matE-F	GGGCAGCTGTATCCATTCGT	Y4_GM002755
matE-R	AGCCTGTCATCAAGCCAACA	
lysE-F	ATTGCTCTGAGCCGACCATC	Y4_GM002415
lysE-R	CGCAAACACTAGCGCAATCA	
lysM-F	GCGATCAAGGCAACAAAGGG	Y4_GM003624
lysM-R	TCCCATGGTGGCGATTTTCT	
dnaJ-F	TATCGCCGCTCTGTTGGTAG	Y4_GM000347
dnaJ-R	CGCCATGTTTTGCGGATCTC	

significant difference was found between biofilm formation at all time points.

Virulence factors and pathogenicity of the starved strain

Consistent with the wild strain, 4-week-starved *V. mimicus* still could produce β-hemolysis, lecithinase and caseinase, and did not produce lipase (Figure 3). However, the lytic halo around the colonies reduced in the starved strain. To further examine the pathogenicity changes, the wild and 4-week-starved *V. mimicus* were used to infect healthy *M. nipponense*.

Table 2 showed that the virulence of starved cells decreased with an LD_{50} value (2.45×10^6 CFU/mL), compared with wild cells (3.09×10^5 CFU/mL). These indicated that the LD_{50} of *V. mimicus* Y4 decreased by an order of magnitude after starvation stress, suggesting that starvation might affect the virulence of bacteria.

Transcriptional changes during starvation

DEGs analysis

A total of 435 DEGs (119 up-regulated genes and 316 downregulated genes) were identified in the 4-week starved cells by comparison with the wild cells (Supplementary Figure 1). Figure 4 showed DEGs analysis in the wild and starved *V. mimicus*. Most of the anabolism related genes (44 out of 49, 89.8%) showed decreased expression level under starvation stress, and similar expression changes were found in catabolism related genes with 102 downregulated and 39 up-regulated (Supplementary Table 2). The expression changes of metabolically related gene implied that the *V. mimicus* stringent response increases the capacity of the cell to respond to a wider range of nutrient sources. Further, most of virulent-related genes involved in hemolysin, hume utilization, pilus assembly, toxin, secretion, etc. were also downregulated, which is consistent with the weakened virulence described above. Remarkably, a large number of flagellar assembly protein-related genes showed significantly downregulated

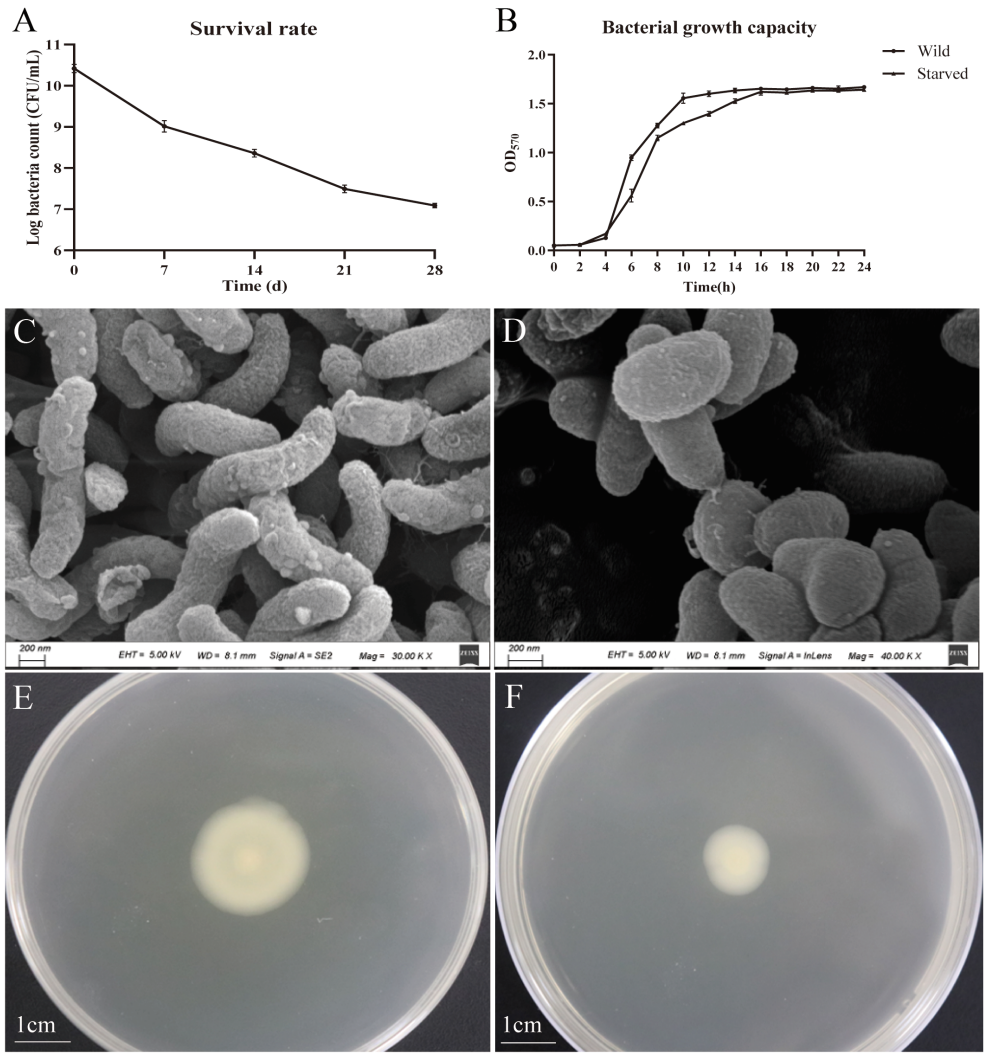

FIGURE 1
Survival, growth curves, morphological and motility changes of *V. mimicus* Y4 under starvation stress. Error bars: ± SD. **(A)** Survival rates; **(B)** Bacterial growth capacity. **P*<0.05, ***P*<0.01. *n*=3; **(C)** morphological character of wild cells; **(D)** morphological character of 4-week starved cells; **(E)** motility of wild cells; **(F)** motility of 4-week starved cells.

expression after starvation, including *flgD* gene, *flgF* gene and *fliF* gene, etc., which might reduce the flagella synthesis, affect the motility of *V. mimicus*, and further decrease the bacterial adhesion and invasion ability to the host. Meanwhile, biofilm formation related genes, including *rbmA*, *rbmB*, *ompU*, *toxT* and *luxS*, etc., and capsular polysaccharide synthesis enzyme *cpsA*, *cpsC* were also downregulated after starvation, which influence to form the biofilm in *V. mimicus*. In addition, many genes with unknown function were regulated by starvation, which will be further studied.

GO and KEGG enrichment analysis of DEGs

The DEGs of *V. mimicus* after starvation stress were enriched and classified into three major categories: biological process, cellular component, and molecular function *via* GO enrichment analysis (Figure 5A; Supplementary Table 3). In the biological process category, small molecule metabolic process was the most highly represented. In the cellular component category, the most abundant category of the DEGs was membrane, which can improve tolerance in stress. Moreover, oxidoreductase activity was the most dominant category in molecular function category, indicative of starvation stress response.

A total of 60 biochemical metabolism and signal pathways were enriched by KEGG enrichment analysis of DEGs. A majority of the DEGs in the enriched KEGG pathways were downregulated with a percentage of 89.6%. The top three enriched KEGG pathways were biosynthesis of secondary metabolites, microbial metabolism in diverse environments and carbon metabolism, which might

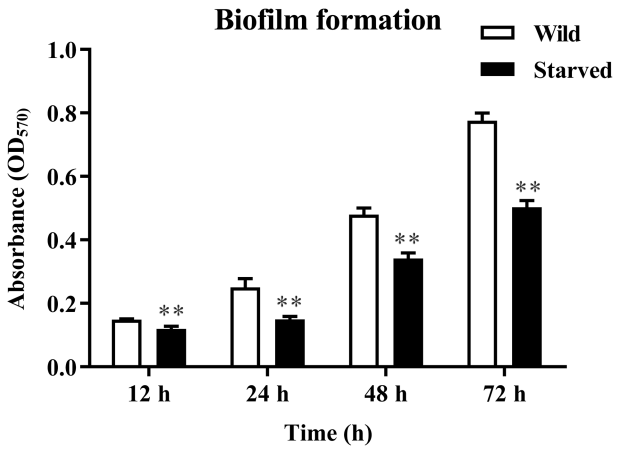

FIGURE 2
Biofilm production of wild and starved strains incubated at 28°C for 24 h and 48 h. **P<0.01. n=3.

improve *V. mimicus* survival by regulating the requirements of energy (Figure 5B).

Verification of the DEGs by qRT-PCR

To further verify the accuracy of sequencing, fourteen DEGs in the transcriptome data were purposefully chosen for relative qRT-PCR. Among them, the expression of *flgD*, *ompA*, *tonB*, *luxS*, *capB*, *pilA*, *tadC*, *huvX*, and *vmh* were down-regulated and the expression of *matE*, *lysE*, *lysM* and *dnaJ* were up-regulated. The qRT-PCR results showed similar expression trends with transcriptome profiling, confirming the reliability of transcriptome sequencing results (Figure 6).

Discussion

Bacteria are usually challenged by various degrees of nutrient deprivation and starvation at some point in their life cycle, and they

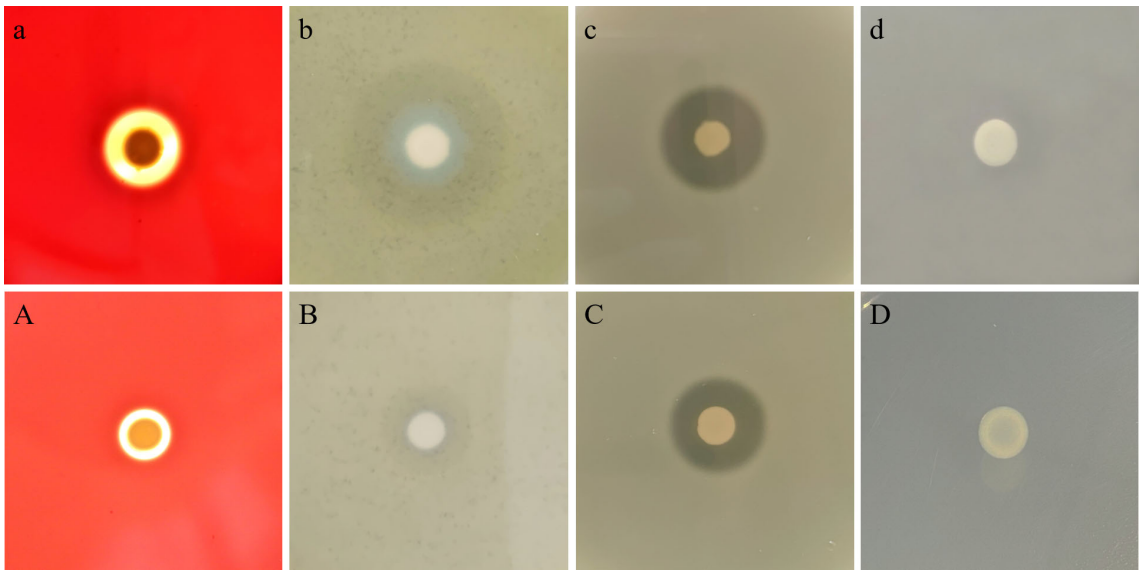

FIGURE 3
Virulence factors determination of *V. mimicus* Y4 after starvation stress. **(A–D)**: hemolysin, lecithinase, caseinase, and lipase activities of 4-week starved cells; **(a–d):** hemolysin, lecithinase, caseinase, and lipase activities of wild cells.

TABLE 2 Pathogenicity of wild and starved *V. mimicus* in *M. nipponense*.

Group	Infected amount	Bacterial concentration	Time (d) and amount of mortality														Mortality (%)
		(CFU/mL)	1	2	3	4	5	6	7	8	9	10	11	12	13	14	total	
Non-starved cells	30	3.6×10^{8}	25	5	0	0	0	0	0	0	0	0	0	0	0	0	30	100%
	30	3.6×10^{7}	16	10	4	0	0	0	0	0	0	0	0	0	0	0	30	100%
	30	3.6×10^{6}	12	7	7	0	1	1	0	0	0	0	0	0	0	0	28	86.7%
	30	3.6×10^{5}	1	4	6	3	2	0	0	0	0	0	0	0	0	0	16	53.3%
	30	3.6×10^{4}	0	1	1	2	1	0	0	0	0	0	0	0	0	0	5	16.7%
Starved cells	30	3.6×10^{8}	22	6	2	0	0	0	0	0	0	0	0	0	0	0	30	100%
	30	3.6×10^{7}	8	8	5	3	0	0	0	0	0	0	0	0	0	0	24	80%
	30	3.6×10^{6}	6	4	2	1	1	0	0	0	0	0	0	0	0	0	14	46.7%
	30	3.6×10^{5}	0	4	1	1	1	1	0	0	0	0	0	0	0	0	8	26.7%
	30	3.6×10^{4}	1	2	0	1	0	0	0	0	0	0	0	0	0	0	4	13.3%
Control	30	0	0	0	0	0	0	0	0	0	0	0	0	0	0	0	0	0

can sense and respond to this stress through changing their phenotypic and genetic repertoire (Rosen et al., 2006; Gao et al., 2018). In general, starvation-induced activities often differentiate into resistant forms to remain viable in starvation condition (Arias et al., 2012). This study described the ability of *V. mimicus* to survive under starvation stress for a period of 4 weeks, and further investigate the changes of morphological, viability, culturability, virulence and gene expression changes. Results in this study indicated that *V. mimicus* undergoes survival and virulent changes in the starvation stress, representing adaptative evolution to new environmental conditions.

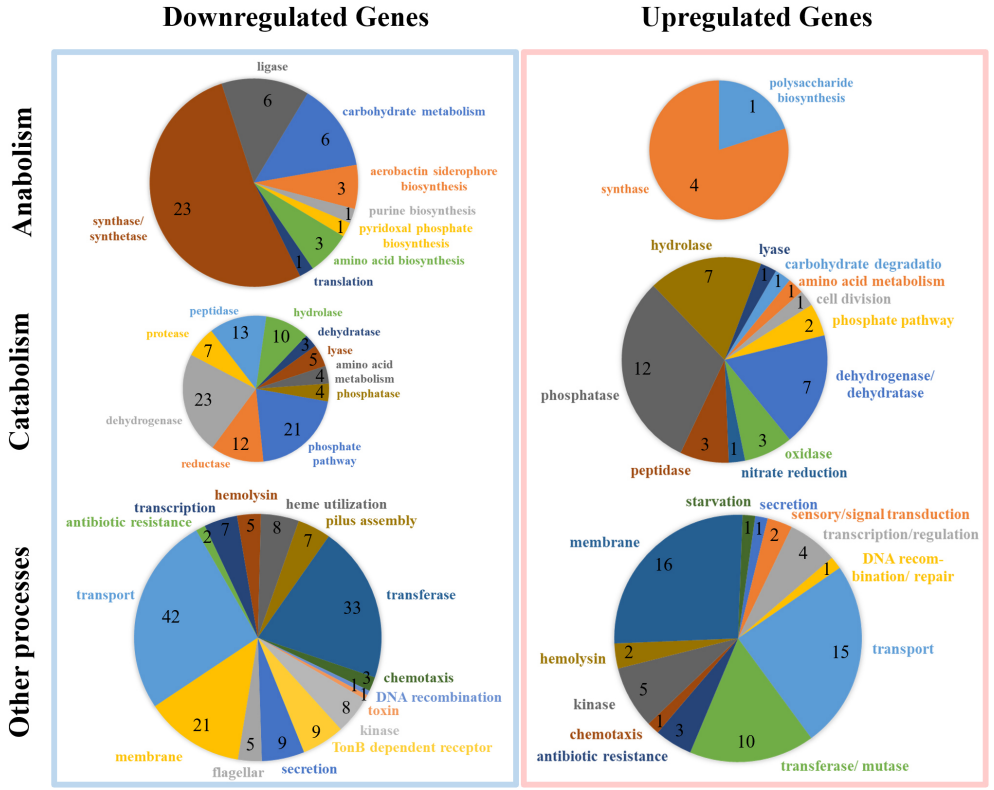

FIGURE 4
DEGs analysis in the wild and starved *V. mimicus*.

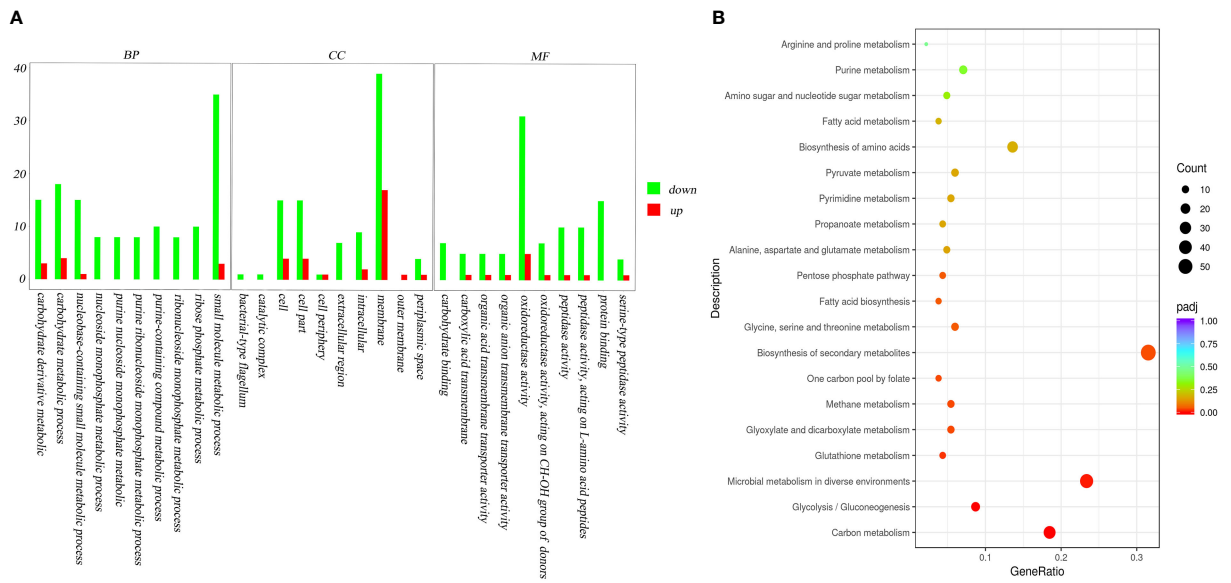

FIGURE 5
GO analysis and KEGG pathways of DEGs to the initial and the 4-week starved *V. mimicus*. **(A)**: GO analysis; **(B)**: KEGG pathways The x-axis indicates percentages of DEGs belonging to the corresponding pathway. The left y-axis represents the top 20 pathways. The sizes of the bubbles represent the number of DEGs in the corresponding pathway, and the colors of the bubbles represent the enrichment p-value of the corresponding pathway. KEGG terms with P-value <0.05 were considered significantly enriched by DEGs.

The reduction in cell size has been observed in many bacteria after long-term nutrient limitation (Gray et al., 2019), including *Vibrio* spp. such as *V. parahaemolyticus* (Chen et al., 2009; Su et al., 2013) and *V. fluvialis* (Amel et al., 2008). In addition, *Vibrio* can obtain a better survival ability in their environment by forming biofilm, growing rapidly to a certain population density, or the expression of genes in bacteria responding to environmental stress (Huang et al., 2020); for instance, sigma factors, two-component system, quorum sensing, flagellar assembly, etc. regulate natural competence in *V. cholereae*

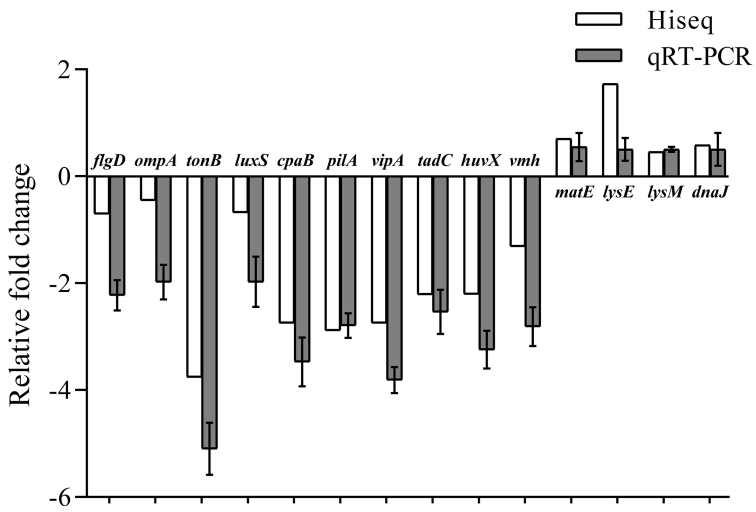

FIGURE 6
Comparative analysis of qRT-PCR and transcriptome sequencing results of DEGs of *V. mimicus* before and after starvation stress.

(Gao, et al., 2022). In our study, the size reduction in *V. mimicus* was also found after starvation, which might contribute to reduce the requirements for cell maintenance and to protect bacteria from environmental stress. Meanwhile, morphological changes, swimming motility of *V. mimicus* also decreased significantly after starvation. The bacterial motility mode is driven by rotating flagella (Berg, 2003; Gao et al., 2018). The RNA-seq results showed that dozens of flagellar assembly related genes, including *flgG*, *fliK*, *flrC*, etc., were downregulated after starvation which well explained the decreased motility. Reportedly, flagellar assembly KEGG pathway was also downregulated in starved cells of *V. cholerae* (Gao, et al., 2022). Apart from motility, flagella can also influence biofilm formation by affecting bacterial adhesion (Choy et al., 2004). In this study, biofilm formation was reduced in *V. mimicus* Y4 after starvation which is in consistence with that in *Campylobacter jejuni* (Svensson et al., 2014). Changes of morphology, swimming motility and biofilm formation are important feature for *V. mimicus* to increase adaptability.

Like many other food-borne pathogens, *V. mimicus* can survive long periods in low nutrient conditions on account of the genes used to adapt to environmental stress (Klancnik et al., 2009). A global view of up-regulated and down-regulated genes indicated that a large proportion of DEGs were involved in metabolism, transport and membrane. Metabolism plays an important role in reactivating starved cells in VBNC state (Villarino et al., 2000). A major of DEGs involved in metabolism were downregulated, especially in the anabolism, which indicated *V. mimicus* Y4 minimized the requirements for cell maintenance to survive starvation. The transport adaptation is the clearest example of starvation response, and some transport-related proteins, including some ABC transporter components and fructose specific PTS enzyme, may contribute to the uptake of alternative sources (Voigt et al., 2007). Membrane systems can change their composition and the concentrations of unsaturated fatty acids, phospholipids, and peptidoglycans to improve tolerance (Margrete et al., 2014). The expression changes of genes involved in metabolism, transport and membrane indicated their role in protecting the cells from stresses, but the function and regulatory mechanism need to be further studied. In addition, previous research found that limitation of nutrients leads to the significant downregulation of genes controlling central carbon metabolism, biosynthesis of lipids, amino acids, and nucleotides (Montánchez et al., 2014). The abundant KEGG pathways of downregulated genes included carbon metabolism, biosynthesis of amino acids, fatty acid biosynthsis, which are similar with the previous research.

Pathogenic bacteria subvert host life through adhering and colonizing the host surface, penetrating and proliferating in the host tissue, producing toxins to destroy cell function, and eventually causing organ infection (Hao et al., 2013). The drastic changes in morphology, swimming motility and biofilm formation induced by starvation might affect the attachment and colonization ability of the pathogen Y4, and results in bacterial virulence assay verified this hypothesis. Although the starved cells could still produce β-hemolysis, lecithinase and caseinase, the lytic halo around the colonies reduced compared with the wild strain. Besides, virulence-related genes showed downregulated expression level and the infectivity of Y4 to *M. nipponense* also decreased after starvation. Therefore, some virulent genes were downregulated, such as *flgD*, *ompA*, *luxS*, *vmh*, and *pilA*, which also contribute to the decrease of pathogenicity. Weakened virulence under starvation stress was also reported in other bacteria. Similarly, *V. anguillarum* starved cells presented a decline of the ability to cause infection and the expression of virulence genes compared to the non-starved cells (Gao et al., 2018). The downregulated expression levels of virulence regulator gene were found in *V. harveyi* under starvation stress (Liu et al., 2020). These results indicate that starvation can weaken the virulence of bacteria.

This study demonstrated that *V. mimicus* cells were still culturable after 4-week starvation, but showed reduction in size, changed morphology from rods to short rods, and weakened pathogenicity. Genes involved in metabolism, virulence and adaptive evolution were differently expressed which might contribute to the survival and virulent changes under starvation. These data provide a key resource to determine the specific response of *V. mimicus* to starvation stress.

Data availability statement

The datasets presented in this study can be found in online repositories. The names of the repository/repositories and accession number(s) can be found in the article/Supplementary Material.

Ethics statement

All treatments involving animals were carried out under the strict guidelines of Animal Experiment Ethics Committee of Yangzhou University.

Author contributions

ZJ, XG, QJ, and XZ conceived the project and designed the experiments. ZJ, QQ, CW, and YZ performed the experiments. SG, JL, and PJ analyzed the data. ZJ wrote the manuscript. All authors contributed to the article and approved the submitted version.

Funding

This work was supported by the National Natural Science Fund (31972830, 32202982), the earmarked fund for Jiangsu Agricultural Industry Technology System (JATS [2022] 501, JATS [2022] 504), the National Key Research and Development Project (2019YFD0900305), Revitalizing of Seed Industry - the Open Competition Mechanism to Select the Best Candidates Projects (JBGS [2021] 120), Natural Science Foundation of Jiangsu Province (BK20220584).

Conflict of interest

The authors declare that the research was conducted in the absence of any commercial or financial relationships that could be construed as a potential conflict of interest.

Publisher's note

Supplementary material

The Supplementary Material for this article can be found online at: https://www.frontiersin.org/articles/10.3389/fmars.2022.1035268/full#supplementary-material

SUPPLEMENTARY FIGURE 1
Different expressed genes in the wild and 4-weeks starved *V. mimicus*.

References

Abdallah, F. B., Kallel, H., and Bakhrouf, A. (2009). Enzymatic, outer membrane proteins and plasmid alterations of starved *Vibrio parahaemolyticus* and *Vibrio alginolyticus* cells in seawater. *Arch. Microbiol.* 191 (6), 493–500. doi: 10.1007/s00203-009-0477-8

Alonso, J. L., Mascellaro, S., Moreno, Y., Ferrus, M. A., and Hernandez, J. (2002). Double-staining method for differentiation of morphological changes and membrane integrity of *Campylobacter coli* cells. *Appl. Environ. Microbiol.* 68 (10), 5151–5154. doi: 10.1128/AEM.68.10.5151-5154.2002

Amel, K. N., Amine, B., and Amina, B. (2008). Survival of *Vibrio fluvialis* in seawater under starvation conditions. *Microbiol. Res.* 163 (3), 323–328. doi: 10.1016/j.micres.2006.06.006

Arias, C. R., LaFrentz, S., Cai, W., and Olivares-Fuster, O. (2012). Adaptive response to starvation in the fish pathogenFlavobacterium columnare: cell viability and ultrastructural changes. *Bmc. Microbiol.* 12 (1), 266. Available at: http://www.biomedcentral.com/1471-2180/12/266

Berg, H. C. (2003). The rotary motor of bacterial flagella. *Annu. Rev. Biochem.* 72 (1), 19. doi: 10.1146/annurev.biochem.72.121801.161737

Carroll, J. W., Mateescu, M. C., Chava, K., Colwell, R. R., and Bej, A. K. (2001). Response and tolerance of toxigenic *Vibro cholerae* O1 to cold temperatures. *Anto. Van. Leeuw.* 79 (3-4), 377. doi: 10.1023/A:1012004725373

Chen, S. Y., Jane, W. N., Chen, Y. S., and Wong, H. C. (2009). Morphological changes of *Vibrio parahaemolyticus* under cold and starvation stresses. *Int. J. Food. Microbiol.* 129 (2), 157–165. doi: 10.1016/j.ijfoodmicro.2008.11.009

Chitov, T., Kirikaew, P., Yungyune, P., Ruengprapan, N., and Sontikun, K. (2009). An incidence of large foodborne outbreak associated with *Vibrio mimicus*. *Eur. J. Clin. Microbiol.* 28 (4), 421–424. doi: 10.1007/s10096-008-0639-7

Choy, W. K., Zhou, L., Syn, K. C., Zhang, L. H., and Swarup, S. (2004). MorA defines a new class of regulators affecting flagellar development and biofilm formation in diverse *Pseudomonas* species. *J. Bacteriol.* 186 (21), 7221. doi: 10.1128/JB.186.21.7221-7228.2004

Citterio, B., Casaroli, A. L., Pierfelici, L., Battistelli, M., and Baffone, W. (2004). Morphological changes and outer membrane protein patterns in *Helicobacter pylori* during conversion from bacillary to coccoid form. *New Microbiologica* 27 (4), 353–360. Available at: http://europepmc.org/article/MED/15646049

Conesa, A., Gotz, S., Garcia-Gomez, J. M., Terol, J., Talon, M., and Robles, M. (2005). Blast2GO: A universal tool for annotation, visualization and analysis in functional genomics research. *Bioinformatics.* 21 (18), 3674–3676. doi: 10.1093/bioinformatics/bti610

Dueholm, M. S., Sndergaard, M. T., Nilsson, M., Christiansen, G., and Nielsen, P. H. (2013). Expression of fap amyloids in *Pseudomonas aeruginosa*, *P. fluorescens*, and *P. putida* results in aggregation and increased biofilm formation. *MicrobiologyOpen.* 2 (3), 365–382. doi: 10.1002/mbo3.81

Eguchi, M., Fujiwara, E., and Miyamoto, N. (2000). Survival of *Vibrio anguillarum* in freshwater environments: Adaptation or debilitation. *J. Infect. Chemother.* 6 (2), 126–129. doi: 10.1007/PL00012152

Fu, X., Liang, W., Du, P., Yan, M., and Kan, B. (2014). Transcript changes in *Vibrio cholerae* in response to salt stress. *Gut. Pathog.* 6, 47. doi: 10.1186/s13099-014-0047-8

Gao, X., Pi, D., Chen, N., Li, X., Liu, X., Yang, H., et al. (2018). Survival, virulent characteristics, and transcriptomic analyses of the pathogenic *Vibrio anguillarum* under starvation stress. *Front. Cell. Infect. Mi.* 8, 389. doi: 10.3389/fcimb.2018.00389

Gao, X., Zhang, Z., Qian, Q., Chen, Q., Gu, S., Li, J., et al. (2022). Survival characteristics and transcriptomic analyses analyses reveal the adaptive response of the aquatic pathogen Non-O1/O139*Vibrio cholerate* to starvation stress. *Microbiol Spectr.* 10(3), 01939–21. doi: 10.1128/spectrum.01939-21

Geng, Y., Liu, D., Han, S., Zhou, Y., Wang, K. Y., Huang, X. L., et al. (2014). Outbreaks of vibriosis associated with vibrio mimicus in freshwater catfish in China. *Aquaculture.* 433, 82–84. doi: 10.1016/j.aquaculture.2014.05.053

Gray, D. A., Dugar, G., Gamba, P., Strahl, H., Jonker, M. J., and Hamoen, L. W. (2019). Extreme slow growth as alternative strategy to survive deep starvation in bacteria. *Nat. Commun.* 10 (1), 890. doi: 10.1038/s41467-019-08719-8

Hao, B., Mo, Z. L., Xiao, P., and Pan, H. J. (2013). Role of alternative sigma factor 54 (*RpoN*) from *Vibrio anguillarum* M3 in protease secretion, exopolysaccharide production, biofilm formation, and virulence. *Appl. Microbiol. Biot.* 97 (6), 2575–2585. doi: 10.1007/s00253-012-4372-x

Huang, Z., Yu, K., Fang, Y., Dai, H., Cai, H., Li, Z., et al. (2020). Comparative genomics and transcriptomics analyses reveal a unique environmental adaptability of *Vibrio fujianensis*. *Microorganisms.* 8, 555. doi: 10.3390/microorganisms8040555

Jiang, Z., Gao, X., Jiang, Q., Zhu, X., Zhou, Y., Zhang, Z., et al. (2021). Genomic characterization and pathogenicity analysis of the *Vibrio mimicus* Y4 causing red body disease in *Macrobrachium nipponense*. *Aquaculture.* 548 (2), 737701. doi: 10.1016/j.aquaculture.2021.737701

Kay, M. K., Cartwright, E. J., Maceachern, D., Mccullough, J., Barzilay, E., Mintz, E., et al. (2012). *Vibrio mimicus* infection associated with crayfish consumption, Spokane, washingto. *J. Food. Protect.* 75 (4), 762–764. doi: 10.4315/0362-028X.JFP-11-410

Kim, J. S., Chowdhury, N., Yamasaki, R., and Wood, T. K. (2018). Viable but non-culturable and persistence describe the same bacterial stress state. *Environ. Microbiol.* 20 (6). doi: 10.1111/1462-2920.14075

Klancnik, A., Guzej, B., Jamnik, P., Vukovi, D., Abram, M., and Možina, S. S. (2009). Stress response and pathogenic potential of *Campylobacter jejuni* cells exposed to starvation. *Res. Microbiol.* 160 (5), 345–352. doi: 10.1016/j.resmic.2009.05.002

Liu, X., Gao, X., Chen, N., Zhang, Y., Li, X., Zhang, Y., et al. (2020). Transcriptional responses to starvation of pathogenic *Vibrio harveyi* strain DY1. *J. Oceanol. Limnol.* 38 (2), 579–587. doi: 10.1007/s00343-019-8350-3

Margrete, S., Leanti, L., Thomas, M., Snipen, L. G., Nes, I. F., Anders, B. D., et al. (2014). Transcriptomic and functional analysis of NaCl-induced stress in *Enterococcus faecalis*. *PloS One* 9 (4), e94571. doi: 10.1371/journal.pone.0094571

Minoru, K., Susumu, G., Yoko, S., Masayuki, K., Miho, F., and Mao, T. (2013). Data, information, knowledge and principle: Back to metabolism in KEGG. *Nucleic. Acids Res.* 42 (D1), 199–205. doi: 10.1093/nar/gkt1076

Montánchez, I., Arana, I., Parada, C., Garaizabal, I., Orruño, M., Barcina, I., et al. (2014). Reprogramming of *Vibrio harveyi* gene expression during adaptation in cold seawater. *FEMS. Microbiol. Ecol.* 87 (1), 193–203. doi: 10.1111/1574-6941.12216

Muller, S., Chau, H., and Boudreaux, K. (2016). *Vibrio mimicus* as the rare cause of acute diarrheal illness. *J. Louisiana State Med. Soc.* 168 (6), 192–193. Available at: http://europepmc.org/article/med/28045686

Neogi, S. B., Chowdhury, N., Awasthi, S. P., Asakura, M., and Yamasaki, S. (2018). Novel cholera toxin variant and ToxT regulon in environmental *Vibrio mimicus* isolates: Potential resources for the evolution of *Vibrio cholerae* hybrid strains. *Appl. Environ. Microb.* 85 (3), e01977–e01918. doi: 10.1128/AEM.01977-18

Oliver, J. D. (2010). Recent findings on the viable but nonculturable state in pathogenic bacteria. *FEMS. Microbiol. Rev.* 34 (4), 415–425. doi: 10.1111/j.1574-6976.2009.00200.x

Ramalingam, A. R., Akshaya, P., Debasis, D., and Sujeet, K. (2017). Investigations on white spot disease outbreak in *Penaeus monodon* (Fabricius 1798) in association with *Vibrio mimicus* infection in the sunderbans, West Bengal, India. *Indian. J. Fish.* 64 (1), 56–60. doi: 10.21077/ijf.2017.64.1.54833-09

Rosen, R., Matthysse, A. G., Becher, D., Biran, D., Yura, T., Hecker, M., et al. (2006). Stress-induced proteins of *Agrobacterium tumefaciens*. *Fems. Microbiol. Ecol.* 35 (3), 277–285. doi: 10.1111/j.1574-6941.2001.tb00813.x

Saganuwan, S. A. (2011). A modified arithmetical method of reed and muench for determination of a relatively ideal median lethal dose (LD_{50}). *Afr J. Pharm. Pharmaco.* 5 (12), 1543–1546. doi: 10.5897/AJPP11.393

Su, C. P., Jane, W. N., and Wong, H. C. (2013). Changes of ultrastructure and stress tolerance of *Vibrio parahaemolyticus* upon entering viable but nonculturable state. *Int. J. Food. Microbiol.* 160 (3), 360–366. doi: 10.1016/j.ijfoodmicro.2012.11.012

Svensson, S. L., Mark, P., Gaynor, E. C., and Roop, R. M. (2014). Flagella-mediated adhesion and extracellular DNA release contribute to biofilm formation and stress tolerance of *Campylobacter jejuni*. *PloS One* 9 (8), e106063. doi: 10.1371/journal.pone.0106063

Tercero-Alburo, J. J., González-Márquez, H., Bonilla-González, E., Quiñones-Ramírez, E., and Vázquez-Salinas, C. (2014). Identification of capsule, biofilm, lateral flagellum, and type IV pili in *Vibrio mimicus* strains. *Microb. Pathogenesis.* 76, 77–83. doi: 10.1016/j.micpath.2014.09.012

Vieira, V. V., Teixeira, L. F. M., Vicente, A. C. P., Momen, H., and Salles, C. A. (2001). Differentiation of environmental and clinical isolates of *Vibrio mimicus* from *Vibrio cholerae* by multilocus enzyme electrophoresis. *Appl. Environ. Microb.* 67 (5), 2360–2364. doi: 10.1128/AEM.67.5.2360-2364.2001

Villarino, A., Bouvet, O. M., Regnault, B., Martin-Delautre, S., and Pad, G. (2000). Exploring the frontier between life and death in *Escherichia coli*: evaluation of different viability markers in live and heat- or UV-killed cells. *Res. Microbiol.* 151 (9), 755–768. doi: 10.1016/S0923-2508(00)01141-4

Voigt, B., Hoi, L. T., Jürgen, B., Albrecht, D., Ehrenreich, A., Vieth, B., et al. (2007). The glucose and nitrogen starvation response of *Bacillus licheniformis*. *PROTEOMICS.* 7 (3), 413–423. doi: 10.1002/pmic.200600556

Xu, X., Wu, Q., Zhang, J., Cheng, J., Zhang, S., and Wu, K. (2014). Prevalence, pathogenicity, and serotypes of *Vibrio parahaemolyticus* in shrimp from Chinese retail markets. *Food. Control.* 46, 81–85. doi: 10.1016/j.foodcont.2014.04.042

Yu, Z. H., Wang, E. L., Geng, Y., Wang, K. Y., Chen, D. F., Huang, X. L., et al. (2020). Complete genome analysis of *Vibrio mimicus* strain SCCF01, a highly virulent isolate from the freshwater catfish. *Virulence.* 11 (1), 23–31. doi: 10.1080/21505594.2019.1702797

frontiers | Frontiers in Marine Science

TYPE Original Research
PUBLISHED 09 December 2022
DOI 10.3389/fmars.2022.1044260

OPEN ACCESS

EDITED BY
Juan Feng,
Chinese Academy of Fishery Sciences (CAFS), China

REVIEWED BY
Ying Han,
Yanshan University, China
Xiaolei Wang,
Ocean University of China, China

*CORRESPONDENCE
Jingfeng Fan
jffan@nmemc.org.cn

†These authors have contributed equally to this work and share first authorship

SPECIALTY SECTION
This article was submitted to Marine Fisheries, Aquaculture and Living Resources, a section of the journal Frontiers in Marine Science

RECEIVED 14 September 2022
ACCEPTED 22 November 2022
PUBLISHED 09 December 2022

CITATION
Huang H, Zan S, Ming H, Li M, Xu J, Xie Y, Wang W and Fan J (2022) 16S Next-generation sequencing and quantitative PCR reveal the distribution of potential pathogens in the Liaohe Estuary. *Front. Mar. Sci.* 9:1044260. doi: 10.3389/fmars.2022.1044260

16S Next-generation sequencing and quantitative PCR reveal the distribution of potential pathogens in the Liaohe Estuary

Huiling Huang[1,2†], Shuaijun Zan[3†], Hongxia Ming[1], Mengfei Li[1], Jianrong Xu[1,2], Yuyang Xie[1,2], Wenjing Wang[1,4] and Jingfeng Fan[1,2,4*]

[1]State Environmental Protection Key Laboratory of Coastal Ecosystem, National Marine Environmental Monitoring Center, Dalian, China, [2]College of Marine Ecology and Environment, Shanghai Ocean University, Shanghai, China, [3]Groundwater Provincial Engineering Research Center for Urban Water Recycling and Environmental Safety, Shenzhen International Graduate School, Tsinghua University, Shenzhen, China, [4]College of Marine Technology and Environment, Dalian Ocean University, Dalian, China

The existence of potentially pathogenic bacteria seriously threatens aquatic animals and human health. Estuaries are closely related to human activities, and the detection of pathogens is important for aquaculture and public health. However, monitoring only indicator microorganisms and pathogens is not enough to accurately and comprehensively estimate water pollution. Here, the diversity of potentially pathogenic bacteria in water samples from the Liaohe estuary was profiled using 16S next-generation sequencing (16S NGS) and quantitative polymerase chain reaction (qPCR) analysis. The results showed that the dominant genera of environmental pathogens were *Pseudomonas*, *Vibrio*, *Mycobacterium*, *Acinetobacter*, *Exiguobacterium*, *Sphingomonas*, and *Legionella*, and the abundance of enteric pathogens was significantly less than the environmental pathogens, mainly, *Citrobacter*, *Enterococcus*, *Escherichia-Shigella*, *Enterobacter*, *Bacteroides*. The qPCR results showed that the 16S rRNA genes of *Vibrio* were the most abundant, with concentrations between 7.06 and 9.48 lg copies/L, followed by *oaa* gene, *fliC* gene, *trh* gene, and *uidA* gene, and the temperature and salinity were the main factors affecting its abundance. Variance partitioning analysis (VPA) analysis of spatial factors on the potential pathogen's distribution (19.6% vs 5.3%) was greater than environmental factors. In addition, the co-occurrence analysis of potential pathogens in the estuary revealed significant co-occurrence among the opportunistic pathogens *Testosteronemonas*, *Brevimonas vesicularis*, and *Pseudomonas putida*. Our findings provide an essential reference for monitoring and occurrence of potentially pathogenic bacteria in estuaries.

KEYWORDS

potential pathogens, spatial distribution, co-occurrence, estuary, quantitative polymerase chain reaction (qPCR), 16S next-generation sequencing (16S NGS)

Introduction

The estuarine ecosystem is a highly productive and dynamic buffer zone between freshwater and oceans (McLusky and Elliott, 2004). Population growth, urbanization, and industrialization have increased the input of organic and inorganic matter (such as sewage from human activities, agricultural wastewater, and industrial waste) into coastal water (Yeleliere et al., 2018), resulting in eutrophication with a large influx of pathogenic microorganisms into the estuaries and finally into the sea (Mei Liu et al., 2011; Wang et al., 2015). According to reports, at least 80% of the wastewater generated by human activities is discharged into rivers and oceans without any treatment (Unesco, 2017), and the burden of human diseases caused by marine pathogens has been estimated to be 4 million people lost annually (Leal Diego et al., 2013). Therefore, it is vital to study the pathogenic bacteria in estuaries.

Pathogens are divided into two categories: enteric and environmental (Leclerc et al., 2008; Percival, 2014). Enteric pathogens are mainly derived from fecal contamination and do not easily proliferate *in-vitro* but survive for a long time under favorable conditions (Brookes et al., 2004). In contrast, the distribution of environmental pathogens is related to various environmental factors (Jacobs et al., 2009). Recent studies have shown that few environmental pathogens, such as *Legionella pneumophila* and *Pseudomonas aeruginosa*, were responsible for increasing outbreaks (Percival, 2014; Liang et al., 2020). Some enteric pathogens, such as *Vibrio*, *Escherichia coli*, and *Salmonella* spp., are attributed to an increase in seafood disease outbreaks (Ramaiah, 2002; Rodrigues et al., 2011; Khandeparker et al., 2015), particularly *Vibrio parahaemolyticus* and *Vibrio vulnificus* (Ruiz-Cayuso et al., 2021). Vibrio-infected oysters caused the first major outbreak in Europe in 1999 (Lozano-León et al., 2003). Although in recent years, studies on estuaries focused mainly on fecal indicator bacteria, such as pathogenic *E. coli* and *Enterococci* (Griffith et al., 2009), there is a lack of understanding of potentially pathogenic bacteria. Poor correlations between fecal indicator bacteria (FIB) and pathogens (Boehm et al., 2003; Harwood et al., 2005) suggest that relying solely on FIB levels to indicate fecal contamination is problematic. Extra-intestinal sources of FIB, such as sediments, soil, and aquatic vegetation, can confuse the relationship between pathogens and FIB (Lamb et al., 2017). Furthermore, many environmental factors may affect the abundance of pathogenic bacteria, with eutrophic conditions, salinity, and temperature considered the most important (Campbell and Kirchman, 2013; Wu et al., 2019a). However, there is limited research on the distribution and factors that influence the spatial morphology of estuaries. Therefore, contemporary research is critical to understanding the diversity of the pathogen community and its coexistence patterns in estuaries.

Good management of the quality of potential pathogens in estuarine water and efficient and exhaustive pathogen monitoring is critical to detect the dominant pathogens. In previous studies, the distribution of pathogens (e.g., *Vibrio*, FIB, or several enteric pathogens) in estuarine waters was studied primarily by culture or quantitative polymerase chain reaction (qPCR) (Baliarsingh et al., 2021; Soueidan et al., 2021). Compared to culture-dependent methods, qPCR has the advantages of specificity and sensitivity and is widely used to detect pathogenic bacteria. Typically, the researcher chooses the target, thus overlooking some key pathogens in complex environments. Recently, next-generation sequencing (NGS) methods of the 16S rRNA gene have been used to study bacterial pathogens in water (Cui et al., 2019). Studies have shown that while this method can detect hundreds of pathogens, the results are incompletely quantified for potential pathogens. In conclusion, there are limitations in monitoring potentially pathogenic bacteria by traditional culturable and single qPCR or 16S NGS methods.

In this study, surface seawater from eutrophication was collected from the Liaohe estuary, and 16S rRNA gene-targeted NGS technology was used to analyze diversity. Our study aimed to 1) characterize the diversity and abundance of potentially pathogenic bacteria in the Liaohe estuary, 2) uncover distribution factors affecting potential pathogenic bacteria, and 3) identify co-occurrence patterns among potentially pathogenic bacteria.

Materials and methods

Sampling and collection

The samples were collected in the Liaohe estuary during the wet season (September 2017). Ten sampling points were established according to salinity and distance from the estuary, which was divided into three areas: near-shore area (N), central area (C) and offshore area (O) (Figure 1). A ZH6547 sampler was used to collect about 4L of seawater from the surface (15-30 cm) and stored in sterile plastic bottles in triplicate. The seawater samples were transported in ice bags (4°C) and delivered to the laboratory within 24 h. Each seawater sample was used for DNA extraction.

Water physicochemical properties

Physicochemical properties for each seawater sample, i.e., seawater depth (Depth), pH, T (Temperature), salinity (Sal), chemical oxygen demand (COD), and dissolved oxygen (DO) were tested using a YSI (Yellow Springs Instrument Company) multi-meter. Phosphate (PO_4^{3-}) was measured spectrophotometrically (State Oceanic Administration, 2007a),

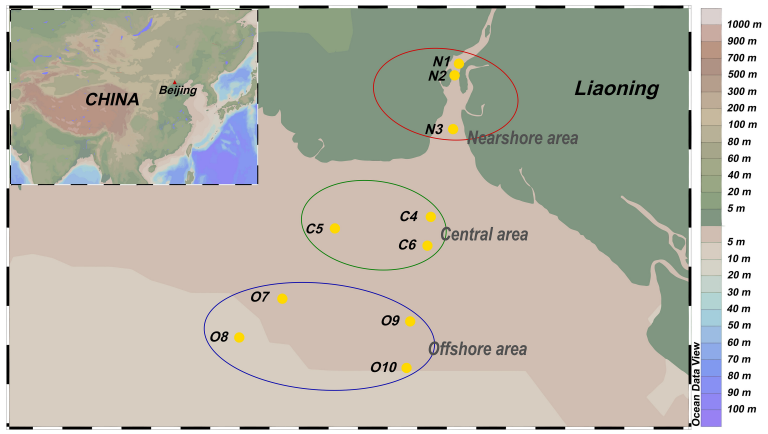

FIGURE 1
Sampling sites of seawater samples in Liaohe estuary.

while nitrate (NO_3^-), nitrite (NO_2^-), and ammonia (NH_4^+) concentrations were determined following the marine monitoring specification (State Oceanic Administration, 2007b). Cu, Zn, Pb, Cd, and Cr were measured using flame or flameless atomic absorption spectrophotometry (Cd and Cr) (State Oceanic Administration, 2007c). Suspended solids(SS) were measured by the gravimetric method (National Environmental Protection Agency, 1989).

DNA extraction, sequencing, and data processing

The seawater sample (1L) was filtered through a 0.22 μm filter (Sterivex-GS, Millipore, Billerica, MA, USA), and the DNA was extracted using the Power Seawater® DNA Isolation Kit (MO BIO Inc., Carlsbad, CA, USA). The extracted DNA samples were sent to BOZERON Bioinformatics Institute (Shanghai, China) in triplicate and sequenced using 2 × 300 bp paired-end sequencing through an Illumina MiSeq platform. The extracted DNA was amplified by the V4 and V5 regions of the 16S rRNA gene using the primers 515F: 5′-GTGCCAGCMGCCGCGGTAA-3′ and 907R: 5′-GGACTACHVGGGTWTCTAAT -3′ by PCR (Ge and Yu, 2017). The raw Illumina sequences were splitting the sequencing data and the construction of barcodes by using the QIIME2 (Bolyen et al., 2019), the sequences were processed by USEARCH(version 7.1) (Edgar, 2010), combined paired-end sequences with the -fasteq_mergepairs command, then the primers were excised (-fastx_truncate), subsequently, the low-quality sequences (-fastq_filter) and redundancy (-fastx_uniques) were filtered and removed, respectively. Then, the operational taxonomic units (OTUs) with 97% similarity were clustered by the -cluster_otus command based on the UPARSE algorithm. Finally, the characteristic sequences were obtained after removing the chimera and the host based on the SILVA v119 database (Yilmaz et al., 2014), and to the OTU table were compared and generated using the -otutab command of USEARCH (-id 0.97).

Accession number

The datasets presented in this study can be found in online repositories. The names of the repository/repositories and accession number(s) can be found below: NCBI, PRJNA855276.

Potential pathogen identification based on 16S NGS

Potential pathogens in the sequencing data were identified from the pathogen databases. A reference database of pathogenic bacteria was created from the literature and the National Marine Environment Monitoring Center pathogen database (https://microbiol.nmemc.org.cn/) and reference lists from other studies, including (59 genera and 177 species) (Wu et al., 2019b) (Table S1). The data included bacterial pathogens from breeding areas, bathing pathogenic microorganisms, and estuarine areas. The representative 16S rRNA gene sequences of the bacterial pathogen species were extracted from NCBI's Reference Sequence (RefSeq) database. Sequences were annotated to the genus level by SILVA. For further analysis at the species level, unique reads classified for the genera in the reference database of human pathogenic bacteria were screened and aligned with representative sequences of pathogenic species within the same genera using BLAST.

qPCR

A total of five representative potential pathogenic bacterial genes were selected for qPCR amplification, including the *uidA* gene of *E. coli*, *oaa* gene of *P. aeruginosa*, *fliC* gene of *Vibrio alginolyticus*, 16S rRNA gene of *Vibrio*, *trh* gene of *Vibrio parahaemolyticus* because of their prevalence at both the genus and species levels in the screening results by 16S NGS and representative in an estuary. *E. coli* was considered a fecal contamination indicator and a common enteric waterborne potential pathogen.

Primer information and qPCR conditions are listed in Table S2. The qPCR analysis was performed using an ABI Prism 7500 Sequence Detection System (Applied Biosystems, US) with a 20 μL reaction volume containing 10 μL of TB Green Premix Ex Taq II (Takara, Dalian, China), 0.4 μL of each primer (10 mM), 0.4 μL of ROX II (50X) (Takara, Dalian, China), 2 μL of template DNA and double-distilled water (ddH2O). For the TaqMan qPCR reactions,10 μL consisted of Premix Ex Taq (2X), 0.4 μL of each primer (10 mM), 0.8 μL probe, 0.2 μL ROX Reference Dye (50X), 2 μL of template DNA, and double-distilled water (ddH_2O).

The calibration curves based on the appropriate ten-fold dilution series of the corresponding gene standards were run with the test samples and the amplification efficiency was determined to be 80- 105% by the qPCR test, with $R^2 > 0.99$.

Statistical analysis

All statistical analyses were performed using the R program (http://cran.r-project.org/) implemented with various packages. A set of spatial variables was first generated based on the latitude and longitude coordinates of the sampling points, employing a neighborhood matrix principal coordinates (PCNM) analysis method (Borcard and Legendre, 2002). Redundancy Analysis (RDA) was used to analyze the potential pathogen community composition and environmental/spatial variables in the studied estuary. The environmental and spatial variables were screened by the R package 'vegan' prior to RDA analysis (Blanchet et al., 2008), using the '*varpart*' function of the "vegan" package. Only significant ($p < 0.05$) environmental and spatial variables were selected to perform a Variance partitioning analysis (VPA) to assess the relative impact of environmental and spatial variables on the distribution of potential pathogens. Environmental (E) and spatial (S) variables were explained using pure environmental variables (E|S), pure spatial variables (S|E), and the combined effect of both components (E∩S). The remaining proportion of the differences cannot be explained. Boxplots were drawn using the R package "ggpubr." A symbiotic network of potentially pathogenic bacteria was inferred from Spearman's correlation matrix based on estimating abundances of 16S rRNA gene of the potentially pathogenic bacterial species and environmental factors. The "iGraph" package was used for network analysis and drawn using Cytoscape software (version 3.9.0). All statistical tests at $p < 0.05$ were considered significant.

Results

Physicochemical attributes of the estuary water

The physicochemical parameters of the samples from ten stations in the Liaohe estuary are shown in Table 1. The surface seawater temperature was between 19.80 and 23.10°C, with the highest recorded in the N area and the lowest in the O area. The salinity gradually increased from the N to the O area, ranging from 24.23-29.12 ‰. Nitrate content was between 16.10-328.00 μg/L, and the ammonia was 42.30-102.00 μg/L. The highest nitrate and ammonia content was found in the N area, the lowest nitrate content was found in the O area, and the lowest ammonia

TABLE 1 Physicochemical attributes of the estuary.

Sites	Salinity (‰)	pH	Temperature (°)	Depth (m)	COD (mg/L)	DO (mg/L)	SS (mg/L)	PO_4^{3-} (ug/L)	NO_2^- (ug/L)	NO_3^- (ug/L)	NH_4^+(ug/L)	Cu (ug/L)	Pb (ug/L)	Zn (ug/L)	Cd (ug/L)	Cr (ug/L)
N1	24.23	8.11	23.10	2.50	2.64	6.65	60.05	23.90	32.10	328.00	102.00	3.50	0.39	7.30	0.13	1.10
N2	24.87	8.11	23.10	3.60	2.35	5.98	45.22	20.00	24.00	273.00	89.00	3.60	0.40	6.50	0.24	1.30
N3	25.96	8.07	22.90	5.00	2.39	6.03	32.64	16.00	15.20	217.00	78.40	3.10	0.48	5.40	0.10	1.10
C4	27.76	8.03	21.90	7.00	2.40	7.72	23.49	10.90	7.05	131.00	73.30	3.70	0.28	7.60	0.11	1.40
C5	28.18	8.13	21.40	5.00	2.25	7.56	52.70	7.15	9.77	146.00	68.30	3.00	0.29	5.60	0.17	1.00
C6	28.11	8.00	21.50	6.00	2.24	7.47	28.63	6.76	6.95	102.00	60.90	3.90	0.46	6.70	0.17	1.00
O7	29.01	8.11	20.70	7.00	1.88	7.32	44.55	3.42	5.73	76.70	42.30	3.60	0.26	7.20	0.13	0.90
O8	29.12	8.03	19.90	11.00	2.15	9.96	39.34	2.82	1.88	16.10	49.10	3.40	0.29	6.80	0.11	1.20
O9	28.35	8.05	20.80	8.80	2.16	7.85	22.44	3.72	4.21	49.30	42.90	3.60	0.57	5.60	0.09	1.20
O10	28.68	8.10	19.80	9.50	2.40	7.71	37.05	9.17	8.49	97.80	70.40	3.60	0.26	5.60	0.24	1.60

was found in the C area. Phosphate content ranged from 2.82 to 23.90 μg/L, with a similar trend as nitrate. The heavy metal content showed little change between the stations. The concentration ranges were Cu 3.00-3.90 μg/L, Pb 0.26-0.57 μg/L, Zn 5.40-7.60 μg/L, Cd 0.09-0.24 μg/L, Cr 0.90-1.60 μg/L.

Diversity of potential pathogenic bacteria community by 16S NGS

In total, 496,527 qualified sequence reads were obtained from the water samples, averaging 49,653 reads per sample. According to the bacterial database, 15 genera and 31 species were identified as potentially pathogenic bacteria. Five genera of potential enteric pathogens dominated, including *Citrobacter*, *Enterococcus*, *Escherichia-Shigella*, *Enterobacter*, and *Bacteroides*, while the potential environmental pathogen genera were more diverse, including *Pseudomonas*, *Vibrio*, *Mycobacterium*, *Acinetobacter*, *Exiguobacterium*, *Sphingomonas* and *Legionella*, predominated (Figure 2A). The relative abundance and Shannon-Wiener diversity index of dominant potential pathogen species in the estuary are shown in Figure 2B. At the genus level, the relative abundance of *Pseudomonas* (44.42% and 51.80%) was comparatively high in the N and C areas, while the O area had the highest relative abundance of *Vibrio* (72.10%). Similarly, *Mycobacterium* and *Acinetobacter* were detected in several samples (6 out of 10 samples), and their highest relative abundance was detected in the N area (3.13% and 2.23%) samples. The highest relative abundances of *Enterobacter* (0.36%) and *Bacteroides* (0.03%) were mainly concentrated in the C4 site of the C area. *Brevundimonas* was the most commonly detected potential pathogen in the estuary, with higher relative abundance in the N (0.57%) and O areas (0.24%). Related sequences of *Brevundimonas* were identified as potential opportunistic pathogens associated with bacteremia.

Pseudomonas stutzeri, Mycobacterium fortuitum, and *Acinetobacter johnsonii* were the main environmental pathogen at the species level. *P. stutzeri* (51.44%) showed the highest abundance in the C area. *V. alginolyticus* and *V. parahaemolyticus* were the main potential pathogenic bacteria in the estuary, and the abundance trend was from the N (13,47% and 7.45%) to the O (38.38% and 65.63%) area, which initially decreased and then increased. *Comamonas testosteroni* and *Brevundimonas vesicularis* were potential opportunistic pathogens in the estuary and found most abundant in the N (1.32% and 0.57%) area. *Legionella feeleii* (0.09%) from the animal and human intestinal tract had the highest abundance in the N area. According to the relative abundance of potential pathogen species and the Shannon-Wiener diversity index, the N2 site in the N area and the O9 site in the O area had the highest proportion of potential pathogen species.

Quantification of typical pathogenic bacteria by qPCR

The abundance of five genes, *uidA* gene, *oaa* gene, *fliC* gene,16S rRNA gene of *Vibrio*, and *trh* gene, in the ten water samples were obtained using qPCR (Figure 3). The abundance of the *uidA* gene was between 0 and 3.80 lg copies/L; however, they were not detected in some sites in N and C areas. The abundance of the 16S rRNA *Vibrio* gene was 7.06 to 9.48 lg copies/L. The abundance of *trh* and *fliC* genes showed the same characteristics. *trh* gene showed the highest abundance in water from the N area (3.93 and 5.51 lg copies/L), while the abundance of *fliC* gene was about 10^2 of the *trh* gene. The abundance of the *oaa* gene

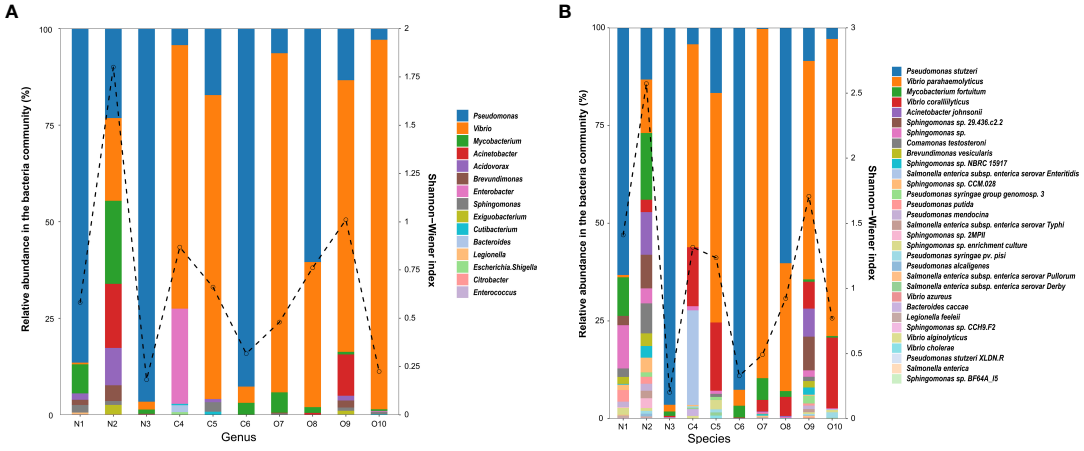

FIGURE 2
Relative abundance of the potentially pathogenic bacterial genus **(A)** and species **(B)** in the estuary. The dashed line indicates the Shannon-Wiener index.

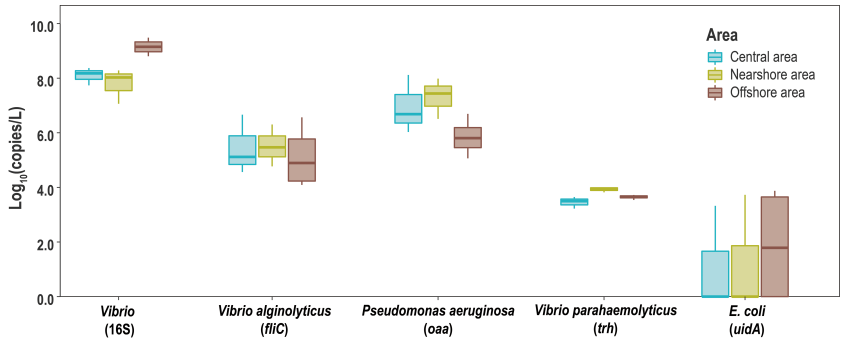

FIGURE 3
Boxplot of 16S rRNA gene of *Vibrio* and maker genes of V. alginolyticus, *V. parahaemolyticus*, *P. aeruginosa*, and *E. coli*.

decreased sequentially from nearshore to distant sea, with the highest value in the N area (7.31 lg copies/L) and the lowest in the O area (5.84 lg copies/L).

Impact factors in the distribution of potential pathogens

Correlation analysis of quantitative potential pathogenic bacteria with environmental factors was performed to investigate the relationship between environmental factors and potentially pathogenic bacteria. The 16S rRNA gene of *Vibrio* abundance showed a positive correlation with salinity (Spearman's correlation, r = 0.806, p<0.01) (Figure 4) and a negative correlation with N, P Nutrients (PO_4^{3-}, NO_3^-, NO_2^-, NH_4^+) and temperature (r =-0.772, p<0.01). 16S NGS potential pathogenic results were correlated with environmental factors, and it was concluded that *P. stutzeri* showed a positive correlation with Pb (Spearman's correlation, r = 0.798, p<0.01) (Figure 5) and *Salmonella enterica* subsp. *enterica serovar enteritidis* showed a positive correlation with Cu (Spearman's correlation, r = 0.697, p<0.01). *V. alginolyticus* showed a negative correlation with temperature (Spearman's correlation, r =-0.675, p<0.01) and a positive correlation with salinity (Spearman's correlation, r = 0.624, p<0.01).

The effects of spatial and environmental variables on potential pathogenic bacteria in the estuary were explored by statistical analysis, which indicated that four environmental (i.e., pH, COD, Pb, Cu) and two spatial variables (i.e., PCNM1, PCNM2) had a significant (p < 0.05) influence on the distribution of potentially pathogenic bacteria in the water samples (Figure 6). RDA1 and RDA2 contributed 46.42% and 22.55% of the total variation, respectively. The RDA biplot indicated that four environmental (i.e., pH, COD, Pb, Cu) and two spatial variables (i.e., PCNM1, PCNM2) had a major influence on the composition of the bacterial community. VPA showed that environmental and spatial factors explained 5.3% and 19.6% (Figure 7) of the potentially pathogenic bacteria distribution variation in the studied estuary, respectively. However, a large amount of variation (85.3%) remained unexplained.

Co-occurrence patterns of potentially pathogenic bacteria in estuary

The co-occurrence characteristics of potentially pathogenic bacteria distribution had 22 network nodes representing potential pathogenic bacteria species and 43 edges representing the correlations between co-occurrence (Figure 8). Our results showed that *Pseudomonas putida* co-occurred with *Sphingomonas* spp. and had a significant positive correlation with *Sphingomonas* sp. CCM-028, *Sphingomonas* sp. 29-436-c2-2, and *Sphingomonas* sp. NBRC15917 (p<0.05). Furthermore, three potential opportunistic pathogens, such as *C. testosterone*, *B. vesicularis* and *P. putida*, co-occurred.

Discussion

Co-detection of pathogens by 16S NGS and qPCR

16S rRNA gene sequencing can be used for microbial identification in diagnostic laboratories (Janda and Abbott, 2007). Thus, this method can improve the reference potential pathogen species library by increasing the number of genera and species and avoiding false positives. Potential pathogens that were relatively high in 16S NGS results, such as *V. parahaemolyticus* and *V. alginolyticus*, were also detected in our study by qPCR assays (Figure 3). Meanwhile, the potential pathogen targets with low abundances or undetected by 16S NGS, such as *Pseudomonas aeruginosa*, were more abundant when determined by qPCR than by 16S NGS. This may be due to the lower resolution of 16S NGS, consistent with the results of

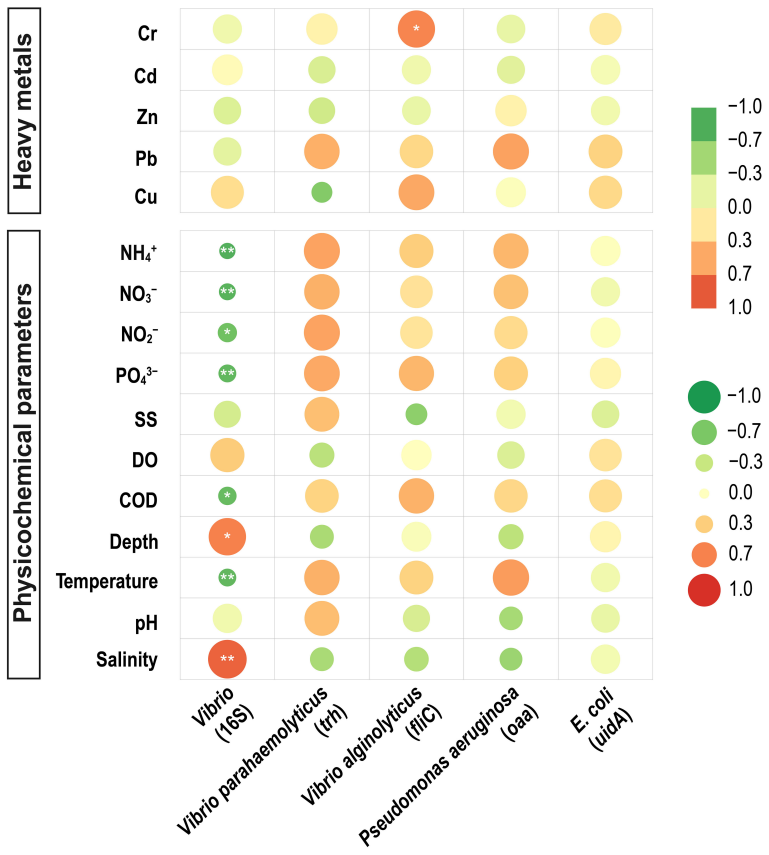

FIGURE 4
Correlation between abundance, maker genes, and environmental factors. Horizontal axes represent the gene abundance (*Vibrio*16S rRNA, *V. parahaemolyticus trh*, *V. alginolyticus fliC*, *P. aeruginosa oaa*, *E. coli uidA*). The vertical axis represents the environmental factors. The circle's color inside the grid indicates a positive or negative Pearson's correlation; the circle's color depth and size denote the correlation's strength. The deeper the red, the higher the positive correlation between the two factors; the deeper the green, the higher the negative correlation. *significant correlation at 0.05 level, **significant correlation at 0.01 level.

Cui et al. (Cui et al., 2017). Related studies have shown that increasing reads by at least 500 bp can improve 16S NGS resolution (Janda and Abbott, 2007). We speculate that the cause could be that *P. aeruginosa* was in low abundance, necessitating more sequencing reads per sample. Therefore, combining 16S NGS with qPCR can be advantageous, and the potential pathogen diversity that 16S NGS can reveal could provide preliminary potential pathogen screening information and relative abundance for comprehensive and further qPCR analysis.

Distribution of potential pathogens in the estuary

The 16S NGS results showed that the distribution of potentially pathogenic bacteria in the Liaohe estuary was mainly abundant in the nearshore N area. According to previous studies (Ming et al., 2020), the estuary had the characteristics of high sewage discharge, high population density, and eutrophication which could be the main reason for the high abundance of potentially pathogenic bacteria in the nearshore N area. Our study detected *Vibrio* with high abundance using both 16S NGS and qPCR techniques. *Vibrio* is a symbiotic bacterium that lives in various environments and is an important potential pathogen in estuaries. In this experiment, the abundance of *Vibrio* in the Liaohe estuary was relatively high compared to the eutrophic estuarine environments such as the Yangtze river estuary (Wang et al., 2020), Sydney harbor (Siboni et al., 2016) and Shandong bay (Xu et al., 2020). This is due to seasonal rainfall or hydrodynamic processes (such as tides and storms) in the Liaohe estuary may have resuspended sediment particles and their attached pathogens into the water column, leading to irregular elevated levels of pollution. Consistent with our hypothesis and influencing factors is the study by Perkins et al. (Perkins et al., 2014), who conducted experiments on the effect of estuarine hydrodynamics on the abundance of pathogenic microorganisms and found that

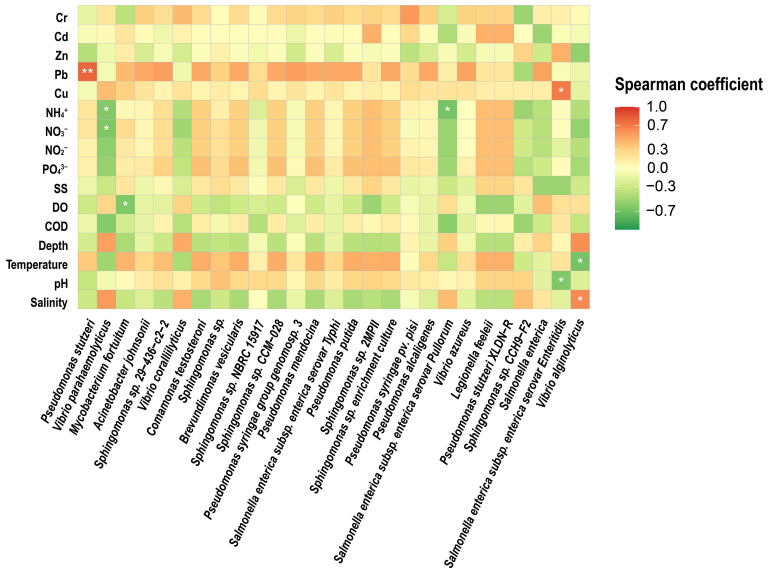

FIGURE 5
Heatmap showing the Spearman correlations between the 16S rRNA gene abundances of potentially pathogenic bacterial species and environmental variables in the studied estuary samples. *significant correlation at 0.05 level, **significant correlation at 0.01 level.

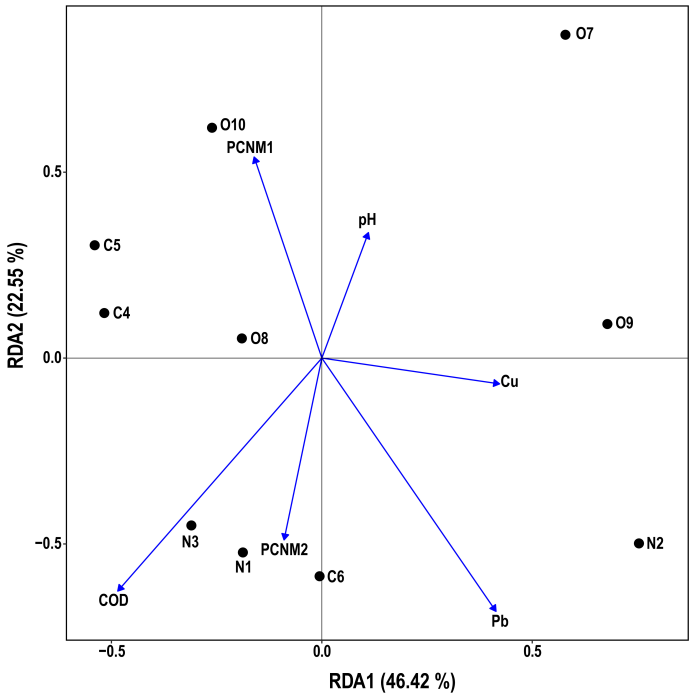

FIGURE 6
A Redundancy analysis (RDA) of environmental/spatial variables and potentially pathogenic bacterial community structure.

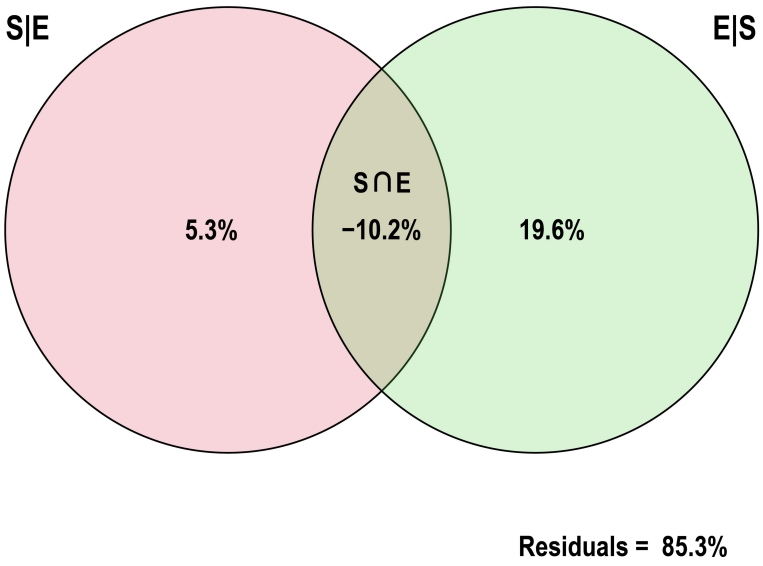

FIGURE 7
Variation partitioning analysis (VPA) showing the relative influence of spatial and environmental properties on the potentially pathogenic bacterial distribution in the studied estuary samples.

sediment resuspension is an important factor increasing public health risks in seawater.

Interestingly, an unusually high abundance of *Vibrio coralliilyticus* was observed, suggesting that the symbiotic features benefit both parties in distinct *Vibrio* spp. *Vibrio* was found to control virulence factors by density-related synthesis and co-infection with other potential pathogens that produce population sensing molecules (Wendling et al., 2014; Lemire et al., 2015; Tout et al., 2015), indicating that interactions between different bacterial species or the community affect the abundance of *V. coralliilyticus*. Secondly, the temperature may be one of the important factors. A study revealed that late summer is beneficial for the growth of *V. coralliilyticus* (Gradoville et al., 2018), which is comparable with the sampling season of our study, suggesting that temperature had a significant impact on the growth of *V. coralliilyticus*. Third, *V. coralliilyticus* grew more quickly because of favorable estuarine circumstances. According to studies (Macián Rovira et al., 2000;

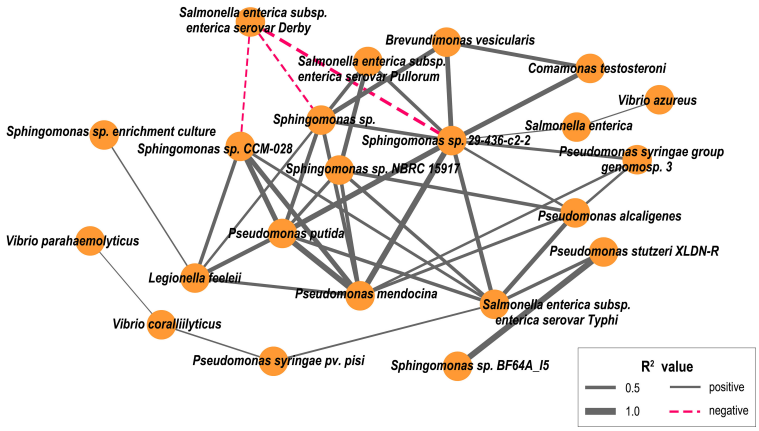

FIGURE 8
Connections between pathogenic bacteria indicate ($p < 0.05$) Spearman rank correlations between them. Line thickness reflects the strength of the correlation relationship between pathogenic species (R^2 value), and the line color reflects the relationship between pathogenic species, with positive correlations (solid line, gray) and negative correlations (dashed line, red).

Froelich et al., 2012), high estuarine salinity promoted the growth of *V. coralliilyticus* while decreasing the abundance of *Vibrio vulnificus* to almost zero. A similar phenomenon occurred in our experiment, which confirmed the importance of estuarine hydrological conditions for *V. coralliilyticus*. Fourth, the higher abundance of or growth of *V. corallilyticus* may be related to ocean conditions. Some researchers have hypothesized that upwelling may transport high concentrations of *V. corallilyticus* to the coast (Elston et al., 2008), and that rising water temperatures may also drive the explosive growth of *V. corallilyticus* (Tout et al., 2015; Amin et al., 2016).

Typical enteric potential pathogenic *E. coli* mostly enter the estuary from domestic and industrial wastewater (Jeamsripong et al., 2018). Compared to the results of other estuaries (He et al., 2017), our findings suggested that fecal pollution in the Xinhai estuary was more severe, as the abundance of *E. coli* in the Liaohe estuary was lower than that in the Xinhai estuary. Some studies showed that the lower the salinity, the higher the FIB level, and thus, FIB is more sensitive to high salinity (He et al., 2007; Soueidan et al., 2021). However, in this study, the highest abundance was found in the lower part of the estuary, suggesting that it may be due to rainfall and runoff, where *E. coli* was washed into distant waters.

Influencing factors on the distribution of potential pathogens in estuary

Our experimental results showed little correlation between most potential pathogens and environmental factors, which demonstrated no association between the majority of possible pathogens and environmental parameters. This conclusion is supported by the findings of López-Hernández et al. (López-Hernández et al., 2015), who evaluated the effect of environmental parameters on the seasonal density of potentially pathogenic *V. parahaemolyticus* in American oysters by regression analysis, they found that there was no correlation between environmental conditions and *V. parahaemolyticus* densities, which was thought to be related to changes in water temperature in the study waters. However, our study found a strong association between environmental factors and a common potential pathogen, *Vibrio*. According to the quantitative qPCR data, temperature and salinity were correlated with *Vibrio*, and our conclusions are supported by the experimental results of Oberbeckmann et al. and Vezzulli et al. Oberbeckmann et al. (Oberbeckmann et al., 2012) used Spearman's analysis techniques to model the seasonal dynamics of *Vibrio* populations offshore the North Sea, where temperature and salinity were identified as the main determinants of *Vibrio* abundance. A generalized additive model used by Vezzulli et al. (Vezzulli et al., 2016) demonstrated that an increase in sea surface temperature led to a long-term increase in *Vibrio* abundance, showing the importance of temperature for *Vibrio*. However, the correlation between temperature and *Vibrio* abundance is currently controversial. In our study, we found that not all *Vibrio* spp. were correlated with temperature, but with the span of water temperature in the season in the Liaoning River estuary. For example, Liang et al. (Liang et al., 2019) showed a significant association between temperature and *Vibrio* abundance in seasons with a broad temperature range, but the correlation was insignificant in the summer, indicating the significance of the temperature range setting. In addition, we found very low abundance of *V. vulnificus* in 16S NGS results, which may be related to seawater salinity. According to Tamplin et al. (Tamplin, 2001), the abundance of *V. vulnificus* decreases to a level not related to human health in environments with salinity above 20 ppt, from which it can be inferred that the Liaoning estuary is not suitable for *V. vulnificus*.

The relationship between temperature and *Vibrio* virulence genes is a hot research topic. Recent investigations have revealed a strong correlation between temperature and the expression of *Vibrio* virulence genes, raising the possibility that warm waters could increase its pathogenic potential and endanger public health (Green et al., 2019; Canellas et al., 2021). Previous studies have shown that *trh* gene is the main virulence gene commonly found in *V. parahaemolyticus* (López-Hernández et al., 2015; Canellas et al., 2021). In our experiments, *trh* gene and *fliC* gene were selected as virulence genes for *Vibrio*. The *fliC* gene was chosen as a target gene for the detection of *V. alginolyticus* because it is an important, highly conserved gene in bacteria and that allows it to swim in highly viscous liquid or semi-solid environments (Tang and Grossart, 2007; Lippolis et al., 2016) as well as aids in seeking nutrients and settling on particles to escape bacterial predation (Matz et al., 2005; Asplund et al., 2011). A similar distribution pattern of *trh* gene in *V. parahaemolyticus* and *fliC* gene in *V. alginolyticus* confirmed Mookerjee's findings (Mookerjee et al., 2015), indicating that horizontal gene transfer of these virulence genes occurs in this context. Additionally, because *V. alginolyticus* is a potential opportunistic pathogen whose virulence is influenced by environmental factors (McDevitt-Irwin et al., 2017), it is possible to infer that the existing environmental factors in the Liaohe estuary were favorable to its proliferation.

Compared to the environmental temperature, salinity is a more compelling critical factor (Takemura et al., 2014). Most experiments showed a significant positive correlation between *Vibrio* and salinity (Perkins et al., 2014; Krishna et al., 2021), consistent with our results. According to a study, the potential opportunistic pathogenic *V. alginolyticus* and *V. parahaemolyticus* are halotolerant (Mookerjee et al., 2015), and thus the 16S NGS results of this experiment showed that their distribution patterns showed dominance at high salinity. In addition, there is a complex relationship between nutrients and *Vibrio*, such as the abundance of *V. parahaemolyticus* associated with allochthonous inputs (He et al., 2017; Krishna et al., 2021). In the moderately high saline

downstream areas of estuaries, mixing estuarine water with flows such as sewers during the rainy season may be a second peak of *Vibrio* outbreaks.

The examination of spatial components and analysis of environmental factors also revealed a significant effect on potentially pathogenic bacteria in water ($p<0.05$). It was shown that one of the key mechanisms of potentially pathogenic bacteria transmission in the ocean is the movement of water masses (Krishna et al., 2021), suggesting that estuarine hydrodynamics may be an important determinant. Additionally, spatial variables can strongly explain potential pathogenic bacteria aggregation patterns and provide a favorable reference for coexistence among potential pathogenic bacteria, such as cooperation or competition in terms of nutrition, space, and material use (Deng et al., 2012). A large proportion (85.3%) of the potentially pathogenic bacteria distribution in this study is unexplained, and many key factors were not identified, which may be explained on the one hand by the fact that most potential bacterial communities have processes of growth, mortality, migration, deposition, and extinction that are jointly determined by spatial scales and environmental gradients. For example, Hanson et al. (Hanson et al., 2012) suggested that microorganisms are mainly influenced by evolutionary and ecological effects, where selection, dispersal, drift, and mutation are the main processes of interaction between microorganisms and the environment, and Berga et al. (Berga et al., 2015) suggested that processes such as viral lysis or predation can be influenced by environmental factors and thus may lead to changes in the microbial community. On the other hand, the unexplained part and the high autocorrelation between spatial and environmental factors may be the difference between VPA and other methods.

Co-occurrence patterns of potentially pathogenic bacteria in the estuary

Microbial network analysis is an important method for studying potential interactions between bacteria. This study found that some potentially pathogenic bacteria were present in the estuaries studied simultaneously, possibly due to potential pathogenic bacteria from a common source of pollution (such as feces and sewage). *Salmonella* and *Legionella* originate from the same source of contamination and have co-existed (Pandey et al., 2014), suggesting that the source of contamination is one of the factors affecting the potential pathogen's coexistence. Furthermore, *Brevundimonas vesicularis* (Denet et al., 2017), *Comamonas testosterone* (Orsini et al., 2014), and *Pseudomonas putida* were found to be potential human pathogens (Fernández et al., 2015), which may be co-existing.

The potential pathogens are affected by heavy metals and water temperature. Many potential pathogens are subjected to environmental stress to carry the commonality of heavy metal resistance genes. Therefore, co-existing potential pathogens may have similar ecological niches, and the co-occurrence of potential opportunistic pathogens in estuarine areas should be treated with caution. We also found that bacterial populations (*Pseudomonas* and *Sphingomonas*) correlated highly with pollutant degradation. Several studies reported the degradation of pollutants by bacteria, *Pseudomonas* and *Sphingomonas* being the main strain for the degradation of aromatic pollutants (Li et al., 2020), and *Pseudomonas stutzeri* can contribute to organic pollutants (Gao et al., 2020). Biodegradation processes can also remove heavy metals. *Pseudomonas Putida* can remediate oil-contaminated soils (Titah et al., 2021), *Brevundimonas vesicularis* can remove lead from wastewater (Resmi et al., 2010), and *Acinetobacter johnsonii* can degrade organophosphorus pesticides and are resistant to heavy metals (Xie et al., 2009). Thus, these suggested that the coexistence of potentially pathogenic bacteria is due to functional redundancy, and the functional coherence of potential bacteria can maintain ecological functions in response to rapid environmental perturbations.

Conclusion

This study revealed the distribution and factors that influence the distribution and coexistence of potentially pathogenic bacteria in the Liaohe estuary using 16S NGS and qPCR methods. It was found that most potentially pathogenic bacteria in the estuary area were mainly environmental pathogens, while the proportion of enteric pathogens was small, indicating that sewage discharge was the primary source of estuarine pollution. Secondly, the influence of spatial factors on potential pathogenic bacteria was found to be much greater than that of environmental factors, but temperature and salinity were still critical factors that influenced the typical potential pathogenic bacteria *Vibrio*. In addition, co-occurrence analysis of potential pathogens showed that some potential opportunistic pathogens might increase the risk of multiple infections. These findings guide the safe monitoring of estuarine waters. More research is needed to identify possible pathogenic bacteria in future estuarine water quality safety monitoring to assess the potential risk of potentially pathogenic bacteria.

Data availability statement

The datasets presented in this study can be found in online repositories. The names of the repository/repositories and accession number(s) can be found in the article/Supplementary Material.

Author contributions

HH analyzed all samples and data, contributed to the experimental design and wrote the manuscript. SZ wrote

reviews and edited, and contributed to manuscript writing. HM collected all samples and contributed to the experimental design. ML participated in the experiments. JX analyzed the experimental results. YX revised the manuscript. WW participated in the experiment. JF designed the experiments and supported the study. All authors contributed to the article and approved the submitted version.

Funding

This work was funded by People's Livelihood Science and Technology Project of Liaoning Province, China (2021JH2/10300001), Millions of Talent Projects of Liaoning Province, China, Dalian high level talent innovation support plan (2021RD04), the National Key R & D Program of China (2017YFC1404500).

Acknowledgments

The National Marine Environmental Monitoring Center (China), State Environmental Protection Key Laboratory of Coastal Ecosystem, is acknowledged by the authors for providing the experimental settings.

Conflict of interest

The authors declare that the research was conducted in the absence of any commercial or financial relationships that could be construed as a potential conflict of interest.

Publisher's note

All claims expressed in this article are solely those of the authors and do not necessarily represent those of their affiliated organizations, or those of the publisher, the editors and the reviewers. Any product that may be evaluated in this article, or claim that may be made by its manufacturer, is not guaranteed or endorsed by the publisher.

Supplementary material

The Supplementary Material for this article can be found online at: https://www.frontiersin.org/articles/10.3389/fmars.2022.1044260/full#supplementary-material

References

Amin, A. K. M. R., Feng, G., Al-saari, N., Meirelles, P. M., Yamazaki, Y., Mino, S., et al. (2016). The first temporal and spatial assessment of vibrio diversity of the surrounding seawater of coral reefs in ishigaki, Japan. *Front. Microbiol.* 7. doi: 10.3389/fmicb.2016.01185

Asplund, M. E., Rehnstam-Holm, A.-S., Atnur, V., Raghunath, P., Saravanan, V., Härnström, K., et al. (2011). Water column dynamics of vibrio in relation to phytoplankton community composition and environmental conditions in a tropical coastal area. *Environ. Microbiol.* 13, 2738–2751. doi: 10.1111/j.1462-2920.2011.02545.x

Baliarsingh, S. K., Lotliker, A. A., Srichandan, S., Basu, A., Nair, T. M. B., and Tripathy, S. K. (2021). Effect of tidal cycle on escherichia coli variability in a tropical estuary. *Bull. Environ. Contam Toxicol.* 106, 622–628. doi: 10.1007/s00128-021-03106-w

Berga, M., Östman, Ö., Lindström, E. S., and Langenheder, S. (2015). Combined effects of zooplankton grazing and dispersal on the diversity and assembly mechanisms of bacterial metacommunities. *Environ. Microbiol.* 17, 2275–2287. doi: 10.1111/1462-2920.12688

Blanchet, F. G., Legendre, P., and Borcard, D. (2008). Forward Selection of Explanatory Variables. *Ecology* 89, 2623–2632. doi: 10.1890/07-0986.1

Boehm, A. B., Fuhrman, J. A., Mrše, R. D., and Grant, S. B. (2003). Tiered approach for identification of a human fecal pollution source at a recreational beach: case study at Avalon bay, Catalina island, California. *Environ. Sci. Technol.* 37, 673–680. doi: 10.1021/es025934x

Bolyen, E., Rideout, J. R., Dillon, M. R., Bokulich, N. A., Abnet, C. C., Al-Ghalith, G. A., et al. (2019). Reproducible, interactive, scalable and extensible microbiome data science using QIIME 2. *Nat. Biotechnol.* 37, 852–857. doi: 10.1038/s41587-019-0209-9

Borcard, D., and Legendre, P. (2002). All-scale spatial analysis of ecological data by means of principal coordinates of neighbour matrices. *Ecological Modelling* 153, 51–68. doi: 10.1016/S0304-3800(01)00501-4

Brookes, J. D., Antenucci, J., Hipsey, M., Burch, M. D., Ashbolt, N. J., and Ferguson, C. (2004). Fate and transport of pathogens in lakes and reservoirs. *Environ. Int.* 30, 741–759. doi: 10.1016/j.envint.2003.11.006

Campbell, B. J., and Kirchman, D. L. (2013). Bacterial diversity, community structure and potential growth rates along an estuarine salinity gradient. *ISME J.* 7, 210–220. doi: 10.1038/ismej.2012.93

Canellas, A. L. B., Lopes, I. R., Mello, M. P., Paranhos, R., de Oliveira, B. F. R., and Laport, M. S. (2021). Vibrio species in an urban tropical estuary: Antimicrobial susceptibility, interaction with environmental parameters, and possible public health outcomes. *Microorganisms* 9, 1007. doi: 10.3390/microorganisms9051007

Cui, Q., Fang, T., Huang, Y., Dong, P., and Wang, H. (2017). Evaluation of bacterial pathogen diversity, abundance and health risks in urban recreational water by amplicon next-generation sequencing and quantitative PCR. *J. Environ. Sci.* 57, 137–149. doi: 10.1016/j.jes.2016.11.008

Cui, Q., Huang, Y., Wang, H., and Fang, T. (2019). Diversity and abundance of bacterial pathogens in urban rivers impacted by domestic sewage. *Environ. pollut.* 249, 24–35. doi: 10.1016/j.envpol.2019.02.094

Denet, E., Coupat-Goutaland, B., Nazaret, S., Pélandakis, M., and Favre-Bonté, S. (2017). Diversity of free-living amoebae in soils and their associated human opportunistic bacteria. *Parasitol. Res.* 116, 3151–3162. doi: 10.1007/s00436-017-5632-6

Deng, Y., Jiang, Y.-H., Yang, Y., He, Z., Luo, F., and Zhou, J. (2012). Molecular ecological network analyses. *BMC Bioinf.* 13, 113. doi: 10.1186/1471-2105-13-113

Edgar, R. C. (2010). Search and clustering orders of magnitude faster than BLAST. *Bioinformatics* 26, 2460–2461. doi: 10.1093/bioinformatics/btq461

Elston, R. A., Hasegawa, H., Humphrey, K. L., Polyak, I. K., and Häse, C. C. (2008). Re-emergence of vibrio tubiashii in bivalve shellfish aquaculture: severity, environmental drivers, geographic extent and management. *Dis. Aquat. Organisms* 82, 119–134. doi: 10.3354/dao01982

Fernández, M., Porcel, M., de la Torre, J., Molina-Henares, M. A., Daddaoua, A., Llamas, M. A., et al. (2015). Analysis of the pathogenic potential of nosocomial pseudomonas putida strains. *Front. Microbiol.* 6. doi: 10.3389/fmicb.2015.00871

Froelich, B. A., Williams, T. C., Noble, R. T., and Oliver, J. D. (2012). Apparent loss of vibrio vulnificus from north Carolina oysters coincides with a drought-induced increase in salinity. *Appl. Environ. Microbiol.* 78, 3885–3889. doi: 10.1128/AEM.07855-11

Gao, J., Zhu, T., Liu, C., Zhang, J., Gao, J., Zhang, J., et al. (2020). Ammonium removal characteristics of heterotrophic nitrifying bacterium pseudomonas stutzeri GEP-01 with potential for treatment of ammonium-rich wastewater. *Bioprocess Biosyst. Eng.* 43, 959–969. doi: 10.1007/s00449-020-02292-x

GB11901-89(1989) .*Water Quality-Determination of Suspended Substance-Gravimetric Method*. (Beijing, China: Ministry of Ecology and Environment).

Ge, Y., and Yu, S. (2017). Next-generation sequencing for investigating the diversity of microorganisms and pathogenic bacteria in a water source. *Trop. J. Pharm. Res.* 16, 1503. doi: 10.4314/tjpr.v16i7.7

Gradoville, M. R., Crump, B. C., Häse, C. C., and White, A. E. (2018). Environmental controls of oyster-pathogenic vibrio spp. in Oregon estuaries and a shellfish hatchery. *Appl. Environ. Microbiol.* 84, e02156–e02117. doi: 10.1128/AEM.02156-17

Green, T. J., Siboni, N., King, W. L., Labbate, M., Seymour, J. R., and Raftos, D. (2019). Simulated marine heat wave alters abundance and structure of vibrio populations associated with the pacific oyster resulting in a mass mortality event. *Microb. Ecol.* 77, 736–747. doi: 10.1007/s00248-018-1242-9

Griffith, J. F., Cao, Y., McGee, C. D., and Weisberg, S. B. (2009). Evaluation of rapid methods and novel indicators for assessing microbiological beach water quality. *Water Res.* 43, 4900–4907. doi: 10.1016/j.watres.2009.09.017

Hanson, C. A., Fuhrman, J. A., Horner-Devine, M. C., and Martiny, J. B. H. (2012). Beyond biogeographic patterns: processes shaping the microbial landscape. *Nat. Rev. Microbiol.* 10, 497–506. doi: 10.1038/nrmicro2795

Harwood, V. J., Levine, A. D., Scott, T. M., Chivukula, V., Lukasik, J., Farrah, S. R., et al. (2005). Validity of the indicator organism paradigm for pathogen reduction in reclaimed water and public health protection. *Appl. Environ. Microbiol.* 71, 3163–3170. doi: 10.1128/AEM.71.6.3163-3170.2005

He, L.-M., Lu, J., and Shi, W. (2007). Variability of fecal indicator bacteria in flowing and ponded waters in southern California: Implications for bacterial TMDL development and implementation. *Water Res.* 41, 3132–3140. doi: 10.1016/j.watres.2007.04.014

He, Y., Sen, B., Shang, J., He, Y., Xie, N., Zhang, Y., et al. (2017). Seasonal influence of scallop culture on nutrient flux, bacterial pathogens and bacterioplankton diversity across estuaries off the bohai Sea coast of northern China. *Mar. pollut. Bull.* 124, 411–420. doi: 10.1016/j.marpolbul.2017.07.062

Jacobs, J., Rhodes, M., Sturgis, B., and Wood, B. (2009). Influence of environmental gradients on the abundance and distribution of mycobacterium spp. in a coastal lagoon estuary. *Appl. Environ. Microbiol.* 75, 7378–7384. doi: 10.1128/AEM.01900-09

Janda, J. M., and Abbott, S. L. (2007). 16S rRNA gene sequencing for bacterial identification in the diagnostic laboratory: Pluses, perils, and pitfalls. *J. Clin. Microbiol.* 45, 2761–2764. doi: 10.1128/JCM.01228-07

Jeamsripong, S., Chuanchuen, R., and Atwill, E. R. (2018). Assessment of bacterial accumulation and environmental factors in sentinel oysters and estuarine water quality from the phang nga estuary area in Thailand. *Int J Environ Res Publ Health* 15, 1–17. doi: 10.3390/ijerph15091970

Khandeparker, L., Anil, A. C., Naik, S. D., and Gaonkar, C. C. (2015). Daily variations in pathogenic bacterial populations in a monsoon influenced tropical environment. *Mar. pollut. Bull.* 96, 337–343. doi: 10.1016/j.marpolbul.2015.04.051

Krishna, K., Veettil, V. P., Anas, A., and Nair, S. (2021). Hydrological regulation of vibrio dynamics in a tropical monsoonal estuary: a classification and regression tree approach. *Environ. Sci. pollut. Res.* 28, 724–737. doi: 10.1007/s11356-020-10486-9

Lamb, J. B., van de Water, J. A. J. M., Bourne, D. G., Altier, C., Hein, M. Y., Fiorenza, E. A., et al. (2017). Seagrass ecosystems reduce exposure to bacterial pathogens of humans, fishes, and invertebrates. *Science* 355, 731–733. doi: 10.1126/science.aal1956

Leal Diego, A. G., Dores Ramos, A. P., Marques Souza, D. S., Durigan, M., Greinert-Goulart, J. A., Moresco, V., et al. (2013). Sanitary quality of edible bivalve mollusks in southeastern Brazil using an UV based depuration system. *Ocean Coast. Manage.* 72, 93–100. doi: 10.1016/j.ocecoaman.2011.07.010

Leclerc, H., Schwartzbrod, L., and Dei-Cas, E. (2008). Microbial agents associated with waterborne diseases. *Crit. Rev. Microbiol* 28, 371–409. doi: 10.1080/1040-840291046768

Lemire, A., Goudenège, D., Versigny, T., Petton, B., Calteau, A., Labreuche, Y., et al. (2015). Populations, not clones, are the unit of vibrio pathogenesis in naturally infected oysters. *ISME J.* 9, 1523–1531. doi: 10.1038/ismej.2014.233

Liang, J., Liu, J., Wang, X., Lin, H., Liu, J., Zhou, S., et al. (2019). Spatiotemporal dynamics of free-living and particle-associated vibrio communities in the northern Chinese marginal seas. *Appl. Environ. Microbiol.* 85, e00217–e00219. doi: 10.1128/AEM.00217-19

Liang, Z., Yu, Y., Ye, Z., Li, G., Wang, W., and An, T. (2020). Pollution profiles of antibiotic resistance genes associated with airborne opportunistic pathogens from typical area, pearl river estuary and their exposure risk to human. *Environ. Int.* 143, 105934. doi: 10.1016/j.envint.2020.105934

Li, Q., Huang, Y., Wen, D., Fu, R., and Feng, L. (2020). Application of alkyl polyglycosides for enhanced bioremediation of petroleum hydrocarbon-contaminated soil using sphingomonas changbaiensis and pseudomonas stutzeri. *Sci. Total Environ.* 719, 137456. doi: 10.1016/j.scitotenv.2020.137456

Lippolis, J. D., Brunelle, B. W., Reinhardt, T. A., Sacco, R. E., Thacker, T. C., Looft, T. P., et al. (2016). Differential gene expression of three mastitis-causing escherichia coli strains grown under planktonic, swimming, and swarming culture conditions. *mSystems* 1, e00064–e00016. doi: 10.1128/mSystems.00064-16

López-Hernández, K. M., Pardío-Sedas, V. T., Lizárraga-Partida, L., Williams, J., de, J., Martínez-Herrera, D., et al. (2015). Environmental parameters influence on the dynamics of total and pathogenic vibrio parahaemolyticus densities in crassostrea virginica harvested from mexico's gulf coast. *Mar. pollut. Bull.* 91, 317–329. doi: 10.1016/j.marpolbul.2014.11.015

Lozano-León, A., Torres, J., Osorio, C. R., and Martínez-Urtaza, J. (2003). Identification of tdh-positive vibrio parahaemolyticus from an outbreak associated with raw oyster consumption in Spain. *FEMS Microbiol. Lett.* 226, 281–284. doi: 10.1016/S0378-1097(03)00604-9

Macián Rovira, M. C., Rodríguez Arias, C., Aznar Novella, R., Garay Auban, E., and Pujalte Domarco, M. J. (2000). Identification of Vibrio spp. (other than V. vulnificus) recovered on CPC agar from marine natural samples. *Int. Microbiol.* 3, 51–53.

Matz, C., McDougald, D., Moreno, A. M., Yung, P. Y., Yildiz, F. H., and Kjelleberg, S. (2005). Biofilm formation and phenotypic variation enhance predation-driven persistence of vibrio cholerae. *Proc. Natl. Acad. Sci.* 102, 16819–16824. doi: 10.1073/pnas.0505350102

McDevitt-Irwin, J. M., Baum, J. K., Garren, M., and Vega Thurber, R. L. (2017). Responses of coral-associated bacterial communities to local and global stressors. *Front. Mar. Sci.* 4. doi: 10.3389/fmars.2017.00262

McLusky, D. S., and Elliott, M. (2004). *The Estuarine Ecosystem: Ecology, Threats and Management third ed.* (Oxford: Oxford University Press), 216 pp.

Mei Liu, S., Wei Li, L., and Zhang, Z. (2011). Inventory of nutrients in the bohai. *Continental Shelf Res.* 31, 1790–1797. doi: 10.1016/j.csr.2011.08.004

Ming, H., Fan, J., Chen, Q., Su, J., Song, J., Yuan, J., et al. (2020). Diversity and abundance of denitrifying bacteria in the sediment of a eutrophic estuary. *Geomicrobiol J.* 38, 199–209. doi: 10.1080/01490451.2020.1822959

Mookerjee, S., Batabyal, P., Sarkar, M. H., and Palit, A. (2015). Seasonal prevalence of enteropathogenic vibrio and their phages in the riverine estuarine ecosystem of south Bengal. *PloS One* 10, e0137338. doi: 10.1371/journal.pone.0137338

Oberbeckmann, S., Fuchs, B. M., Meiners, M., Wichels, A., Wiltshire, K. H., and Gerdts, G. (2012). Seasonal dynamics and modeling of a vibrio community in coastal waters of the north Sea. *Microb. Ecol.* 63, 543–551. doi: 10.1007/s00248-011-9990-9

Orsini, J., Tam, E., Hauser, N., and Rajayer, S. (2014). Polymicrobial bacteremia involving comamonas testosteroni. *Case Rep. Med.* 2014, e578127. doi: 10.1155/2014/578127

Pandey, P. K., Kass, P. H., Soupir, M. L., Biswas, S., and Singh, V. P. (2014). Contamination of water resources by pathogenic bacteria. *AMB Express* 4, 51. doi: 10.1186/s13568-014-0051-x

Percival, S. L. (2014). *Microbiology of waterborne diseases: microbiological aspects and risks. 2nd ed.* (Amsterdam: Elsevier, Academic Press).

Perkins, T. L., Clements, K., Baas, J. H., Jago, C. F., Jones, D. L., Malham, S. K., et al. (2014). Sediment composition influences spatial variation in the abundance of human pathogen indicator bacteria within an estuarine environment. *PloS One* 9, e112951. doi: 10.1371/journal.pone.0112951

Ramaiah, N. (2002) *Coliform and human pathogenic bacteria in tourism affected water bodies in north goa*. Available at: https://drs.nio.org/xmlui/handle/2264/1338.

Resmi, G., Thampi, S. G., and Chandrakaran, S. (2010). Brevundimonas vesicularis: A novel bio-sorbent for removal of lead from wastewater. *Int. J. Environ. Res.* 4, 281–288. doi: 10.22059/ IJER.2010.20

Rodrigues, V., Ramaiah, N., Kakti, S., and Samant, D. (2011). Long-term variations in abundance and distribution of sewage pollution indicator and human pathogenic bacteria along the central west coast of India. *Ecol. Indic.* 11, 318–327. doi: 10.1016/j.ecolind.2010.05.010

Ruiz-Cayuso, J., Trujillo-Soto, T., Rodriguez-Iglesias, M., and Almagro-Moreno, S. (2021). Effects of temperature and salinity interaction on vibrio spp and vibrio parahaemolyticus in the intercontinental Euro-African atlantic. doi: 10.21203/rs.3.rs-607386/v1

Siboni, N., Balaraju, V., Carney, R., Labbate, M., and Seymour, J. R. (2016). Spatiotemporal dynamics of vibrio spp. within the Sydney harbour estuary. *Front. Microbiol.* 7. doi: 10.3389/fmicb.2016.00460

Soueidan, J., Warren, A., Pearson, M., and Montie, E. W. (2021). A changing estuary: Understanding historical patterns in salinity and fecal coliform levels in the may river, SC. *Mar. pollut. Bull.* 168, 112384. doi: 10.1016/j.marpolbul.2021.112384

State Oceanic Administration (2007a). *The Specification for Marine Monitoring–Part 4: Seawater Analysis (GB17378.4-2007)*. (Beijing: Chinese. Standards Press of China) pp. 117–119.

State Oceanic Administration (2007b). *The specification for marine monitoring–part 4: Seawater analysis (GB17378.4-2007)*. (Beijing: Chinese. Standards Press of China) pp. 109–117.

State Oceanic Administration (2007c). *The specification for marine monitoring–part 4: Seawater analysis (GB17378.4-2007)*. (Beijing: Chinese. Standards Press of China) pp. 10–24.

Takemura, A., Chien, D., and Polz, M. (2014). Associations and dynamics of vibrionaceae in the environment, from the genus to the population level. *Front. Microbiol.* 5. doi: 10.3389/fmicb.2014.00038

Tamplin, M. L. (2001). Coastal vibrios: Identifying relationships between environmental condition and human disease. *Hum. Ecol. Risk Assessment: Int. J.* 7, 1437–1445. doi: 10.1080/20018091095113

Tang, K. W., and Grossart, H.-P. (2007). Iron effects on colonization behavior, motility, and enzymatic activity of marine bacteria. *Can. J. Microbiol.* 53, 968–974. doi: 10.1139/W07-059

Titah, H. S., Pratikno, H., Purwanti, I. F., and Wardhani, W. K. (2021). Biodegradation of crude oil spill using bacillus subtilis and pseudomonas putida in sequencing method. *J. Ecol. Eng.* 22, 157–167. doi: 10.12911/22998993/142913

Tout, J., Siboni, N., Messer, L. F., Garren, M., Stocker, R., Webster, N. S., et al. (2015). Increased seawater temperature increases the abundance and alters the structure of natural vibrio populations associated with the coral pocillopora damicornis. *Front. Microbiol.* 6. doi: 10.3389/fmicb.2015.00432

Unesco (2017). *Wastewater: the untapped resource* (Paris: UNESCO).

Vezzulli, L., Grande, C., Reid, P. C., Hélaouët, P., Edwards, M., Höfle, M. G., et al. (2016). Climate influence on vibrio and associated human diseases during the past half-century in the coastal north Atlantic. *Proc. Natl. Acad. Sci.* 113, E5062–E5071. doi: 10.1073/pnas.1609157113

Wang, X., Liu, J., Liang, J., Sun, H., and Zhang, X.-H. (2020). Spatiotemporal dynamics of the total and active vibrio spp. populations throughout the changjiang estuary in China. *Environ. Microbiol.* 22, 4438–4455. doi: 10.1111/1462-2920.15152

Wang, G., Peng, J., Yang, D., Zhang, D., and Li, X. (2015). Current levels, composition profiles, source identification and potentially ecological risks of polychlorinated biphenyls (PCBs) and polybrominated diphenyl ethers (PBDEs) in the surface sediments from bohai Sea. *Mar. pollut. Bull.* 101, 834–844. doi: 10.1016/j.marpolbul.2015.11.028

Wendling, C. C., Batista, F. M., and Wegner, K. M. (2014). Persistence, seasonal dynamics and pathogenic potential of vibrio communities from pacific oyster hemolymph. *PloS One* 9, e94256. doi: 10.1371/journal.pone.0094256

Wu, D.-M., Dai, Q.-P., Liu, X.-Z., Fan, Y.-P., and Wang, J.-X. (2019a). Comparison of bacterial community structure and potential functions in hypoxic and non-hypoxic zones of the changjiang estuary. *PloS One* 14, e0217431. doi: 10.1371/journal.pone.0217431

Wu, G., Yang, J., Jiang, H., Deng, Y., and Lear, G. (2019b). Distribution of potentially pathogenic bacteria in the groundwater of the jianghan plain, central China. *Int. Biodeterioration Biodegradation* 143, 104711. doi: 10.1016/j.ibiod.2019.05.028

Xie, S., Liu, J., Li, L., and Qiao, C. (2009). Biodegradation of malathion by acinetobacter johnsonii MA19 and optimization of cometabolism substrates. *J. Environ. Sci.* 21, 76–82. doi: 10.1016/S1001-0742(09)60014-0

Xu, W., Gong, L., Yang, S., Gao, Y., Ma, X., Xu, L., et al. (2020). Spatiotemporal dynamics of vibrio communities and abundance in dongshan bay, south of China. *Front. Microbiol.* 11. doi: 10.3389/fmicb.2020.575287

Yeleliere, E., Cobbina, S. J., and Duwiejuah, A. B. (2018). Review of ghana's water resources: the quality and management with particular focus on freshwater resources. *Appl. Water Sci.* 8, 93. doi: 10.1007/s13201-018-0736-4

Yilmaz, P., Parfrey, L. W., Yarza, P., Gerken, J., Pruesse, E., Quast, C., et al. (2014). The SILVA and "All-species living tree project (LTP)" taxonomic frameworks. *Nucleic Acids Res.* 42, D643–D648. doi: 10.1093/nar/gkt1209

frontiers | Frontiers in Marine Science

TYPE Original Research
PUBLISHED 19 December 2022
DOI 10.3389/fmars.2022.1042899

OPEN ACCESS

EDITED BY
Claudia R. Serra,
University of Porto, Portugal

REVIEWED BY
Min Yu,
Ocean University of China, China
Qingpi Yan,
Jimei University, China
Dan Gu,
Yangzhou University, China

*CORRESPONDENCE
Yiqin Deng
yiqindd@126.com
Juan Feng
juanfeng@scsfri.ac.cn

SPECIALTY SECTION
This article was submitted to Marine Fisheries, Aquaculture and Living Resources, a section of the journal Frontiers in Marine Science

RECEIVED 13 September 2022
ACCEPTED 06 December 2022
PUBLISHED 19 December 2022

CITATION
Su W, Deng Y, Zang S, Gao S and Feng J (2022) The global role of Lrp in *Vibrio alginolyticus* and its response to diverse physicochemical factors. *Front. Mar. Sci.* 9:1042899. doi: 10.3389/fmars.2022.1042899

The global role of Lrp in *Vibrio alginolyticus* and its response to diverse physicochemical factors

Wenxiao Su[1], Yiqin Deng[1]*, Shujun Zang[1,2], Si'ao Gao[1,3] and Juan Feng[1]*

[1]Key Laboratory of South China Sea Fishery Resources Exploitation & Utilization, Ministry of Agriculture, South China Sea Fisheries Research Institute, Chinese Academy of Fishery Sciences, Guangzhou, China, [2]National Demonstration Center for Experimental Fisheries Science Education, Shanghai Engineering Research Center of Aquaculture, Shanghai Ocean University, Shanghai, China, [3]Tianjin Key Laboratory of Aqua-ecology and Aquaculture, College of Fisheries, Tianjin Agricultural University, Tianjin, China

Leucine-responsive regulatory protein (Lrp) is an essential transcriptional regulator in prokaryotes. However, the regulatory role of *lrp* in *Vibrio alginolyticus* has still not been studied in detail. In this study, an *lrp* mutant strain was constructed to gain insight into the role of *lrp* in *Vibrio alginolyticus*. The absence of *lrp* significantly enhances swarming motility, biofilm formation, extracellular protease secretion activity, and tolerance to copper ions. The cumulative mortality of zebrafish (*Danio rerio*) challenged by intraperitoneal injection against the *lrp* mutant strain reached 68.89%, significantly higher than the 40.00% suffered by fish injected with the wild-type strain. The expression levels of *lrp* decreased gradually with increasing culture time under the influence of various physicochemical factors. The expression level of *lrp* was significantly increased after two hours of culture at pH 5, 22°C, 5% NaCl, the presence of 1 mM Cu^{2+}, 1/4/7 mM ferric citrate, 0.1 mg/L $NaNO_3$, and 0.1 mg/L KH_2PO_4. The mRNA level of *lrp* decreased significantly after six hours of culture at 37°C, 1% and 5% NaCl, and the presence of 1/7 mM ferric citrate, 0.1/5 mg/L $NaNO_3$, and 0.1/0.5/2.0 mg/L KH_2PO_4. The expression of *lrp* increased after ten hours of culture at pH 5/9, 22°C, 1% NaCl, and the presence of 1 mM Cu^{2+}, 7 mM ferric citrate, 5 mg/L $NaNO_3$, and 0.1 mg/L KH_2PO_4. Overall, this study indicates that *lrp* negatively controls the virulence of *V. alginolyticus*, probably by reducing its swarming motility, biofilm formation, extracellular protease secretion activity, and tolerance to copper ions, and that the expression of *lrp* is affected by numerous physicochemical factors, and is especially up-regulated after 2 hours of culture in bacterial growth.

KEYWORDS

***Vibrio alginolyticus*, *lrp*, biological characteristics, virulence regulation, physicochemical factors**

1 Introduction

Vibrio alginolyticus, a Gram-negative bacterium found throughout the ocean (Ren et al., 2013), has emerged as the primary aquatic pathogenic bacterium in recent years (Li et al., 2021). Diseases caused by *V. alginolyticus* can lead to epidermal bleeding, whitening of the kidneys, and congestion of the internal organs of animals. Its pathogenicity increases significantly in warmer temperatures in summer (Zuo et al., 2019) when it causes severe economic damage to the aquaculture industry (Mohamad et al., 2019; Fahmy and Hamed, 2021; Yang et al., 2021). In humans, *V. alginolyticus* infections can cause septicemia, eardrum infections, and intraocular inflammation (Li et al., 2009; Gaüzère et al., 2016; Baker-Austin et al., 2018). In total, *V. alginolyticus* can not only lead to large-scale mortality in aquatic animals with considerable negative economic impacts, but is also a potential source of human-aquatic animal co-morbidity, with a risk to human health. Current studies have shown that the pathogenic effects of *V. alginolyticus* are due to virulence factors such as extracellular products (Wang et al., 2007; Wang et al., 2008; Rui et al., 2009), bacterial adhesion (Wang and Leung, 2000), cell motility (Liu et al., 2020), and biofilm formation (Liu et al., 2011; Liu et al., 2011; Gu et al., 2019b).

Physicochemical factors have an impact on bacterial growth and reproduction. They can also directly influence the expression of bacterial virulence or virulence-regulating genes (DeAngelis et al., 2018), thereby affecting the risks to host organisms (Huang et al., 2015). For example, the abundance of *V. alginolyticus* is affected by factors such as nutrients, temperature, salinity, and phytoplankton (Oberbeckmann et al., 2011). Furthermore, the metabolism of *Vibrio* is significantly influenced by the environmental levels of nitrate, ammonia nitrogen, and phosphate (Unemoto et al., 1977; Oliver et al., 1983; Davis et al., 2017). The formation of *V. alginolyticus* blooms can be promoted by Saharan dust nutrients, which drive changes in its population dynamics (Westrich et al., 2016). Likewise, environmental conditions can substantially impact biofilm formation and adhesion of bacteria (Luo et al., 2016; Toyofuku et al., 2016). For example, the expression of the cytochrome C oxidase gene is effected by temperature, pH, and salinity, which alter the capacity of *V. alginolyticus* to adhere to the host (Huang et al., 2019). *Vibrio alginolyticus* is a conditionally pathogenic bacterium, and external environmental changes can also modulate the expression of pathogenesis-related proteins (Hoe and Goguen, 1993). Outer membrane proteins adapt and respond to environmental stress by altering the expression levels of specific proteins (Abdallah et al., 2012). Environmental factors change periodically both seasonally and geographically. Aquaculture systems are vulnerable to human activities, including overfeeding, drug usage, industrial pollution, and domestic sewage. The degree of these impacts have changed over time, posing additional challenges and threats, including those which affect the occurrence and development of pathogen virulence (Halpern et al., 2019). Therefore, understanding the influence of environmental factors on bacterial virulence factors or virulence regulators is of great significance in monitoring bacterial virulence and predicting disease occurrence, and can provide a theoretical basis for establishing virulence prevention and control measures based on environmental regulation.

Leucine-responsive regulatory protein (Lrp) belongs to the Leucine-responsive regulatory protein/asparagine synthase C gene product family (Lrp/AsnC family) of globally specific transcriptional regulators, also known as feast/famine regulatory proteins (Brinkman et al., 2003; Yokoyama et al., 2006). Lrp binds regulatory DNA *via* a helix-turn-helix motif, which strongly influences Lrp-DNA binding (Hart et al., 2011). Lrp primarily responds to exogenous amino acid effectors and globally impacts cellular metabolism (Thaw et al., 2006). Early studies found that Lrp can respond to leucine in *Escherichia. coli* (Chen et al., 2001). Further research found that Lrp is involved in the regulation of various metabolic functions, such as amino acid synthesis and catabolism (Brinkman et al., 2003), fimbriae biosynthesis, and pili phase-variation (Nou et al., 1993; Huisman et al., 1994; van der Woude and Low, 1994). As a global regulator, Lrp is associated with cytotoxicity, chemotaxis, and iron uptake in *Vibrio vulnificus* (Ho et al., 2017) and chromosome replication in *Vibrio cholerae* (Ciaccia et al., 2018). Furthermore, numerous studies have shown that Lrp plays a vital role in regulating the virulence of bacteria (Lin et al., 2007; Alice and Crosa, 2012; Hussa et al., 2015; Chen et al., 2019). Lin et al. (2007) found that Lrp could regulate the quorum-sensing regulator AphA, and then activate the expression of the virulence gene. However, in *Vibrio alginolyticus* the *lrp* gene has not yet been the subject of any detailed research, and its function is still unknown.

To understand the function of *lrp* in *V. alginolyticus*, we constructed a null mutant of the *lrp* gene, studied the biological properties and pathogenicity of the Δ*lrp* strain, and then used qRT-PCR to analyze the transcription levels of the *lrp* gene when stressed with different physicochemical factors. These results make a significant contribution to the functional study of *lrp* in *V. alginolyticus*, especially regarding the role of *lrp* in regulating the virulence of *V. alginolyticus* and the effects of physicochemical factors on *lrp* expression. The study will aid the monitoring of *V. alginolyticus* virulence to predict outbreaks of diseases caused by *V. alginolyticus*, as well as provide a theoretical basis for the establishment of the environmental regulation system of *V. alginolyticus* related diseases.

2 Materials and methods

2.1 Bacterial strains, plasmids, and construction of the *lrp* mutant strain

ZJ-T is a translucent variant of *V. alginolyticus* ZJ-51 (Deng et al., 2016a), and was used as the wild-type strain in this study. ZJ-T cells were cultured in LBS (Luria-Bertani medium with 3% sodium chloride) at 30°C. *E. coli* cells were cultured in LB medium at 37°C. Table 1 lists the bacterial strains and plasmids used in this study.

The *lrp* mutant strain was constructed by homologous recombination (Deng et al., 2016b). The plasmid pSW7848 was linearized with the pair primer pSW7848-F/R, and the two flanking regions of the desired deletion fragments of *lrp* were amplified using the primer pairs dlrp-U-F/R and dlrp-D-F/R, respectively (Table 2). The linearized plasmid and flanking fragments were assembled using a ClonExpress MultiS one-step cloning kit (Vazyme Biotech Co., Ltd., Nanjing, China) with an isothermal assembly. The recombinant plasmid was then introduced into *E.coli* II3813, followed by *E.coli* GEB883. After transformation, the integrity of the flanking fragments was examined using a pair primer Del-check-pSW7848-F/R. After that, the recombinant plasmid was transferred into *V. alginolyticus* ZJ-T by conjugation (Figure 1). The pSW7848 plasmid carries chloramphenicol resistance. D-glucose reduces while L-arabinose induces the expression of the virulence gene *ccdB* in the plasmid (Val et al., 2012). Two conjugation experiments were performed by screening colonies on TCBS plates with either D-glucose or L-arabinose. After conjugation, the mutant strains were obtained by PCR amplification and sequencing verification using the primer pairs Del-*lrp*-check-F/R.

2.2 Bacterial growth measurement

The monoclonal clones of *V. alginolyticus* ZJ-T (WT) and the *lrp* mutant strain (Δ*lrp*) were inoculated into LBS liquid medium and cultured overnight at 30°C with 200 rpm shaking. The overnight cultures were diluted to 0.01 at an optical density of OD600 nm (OD600 nm) in conical flasks and re-cultured at 30°C with 200 rpm continuous shaking. The change of absorbance during 36 h of bacterial growth was measured using a spectrophotometer (INESA Co., Ltd., Shanghai, China). The growth of bacteria in the LBS medium was observed. The experiments were conducted in triplicate, and the results were presented graphically. One-way ANOVA analysis of covariance was performed to analyze the effect of *lrp* deletion with time as a covariate against the OD600 nm values.

2.3 Iron absorption, copper ion and H_2O_2 resistance

The overnight cultures (described in 2.2) were diluted to OD600 nm = 5.0 and then gradient diluted in 10-fold steps (10^0 to 10^9) with fresh LBS medium. After that, 5 μL of each dilution were simultaneously spotted onto LBS plates alone or with either 0.003% H_2O_2, 4.5 mM $CuSO_4$, or 150 μM 2,2'-dipyridyl (DIP). Colony growth was observed after incubation at 30°C for 24 h.

2.4 Hemolytic activity

The effect of *lrp* on the hemolytic activity of *V. alginolyticus* was determined using the Mueller-Hinton blood agar plate method

TABLE 1 Strains and plasmids used in this study.

Strains or plasmids	Relevant characteristics	Source
V. alginolyticus		
ZJ-T (WT)	Ap^r (ampicillin resistant), *V. alginolyticus* ZJ-T, translucent/smooth variant of wild strain ZJ51, isolated from diseased *Epinephelus coioides* of the Southern China coast	(Huang et al., 2018b)
Δ*lrp*	Ap^r, *V. alginolyticus* ZJ-T carrying a deletion of *lrp*	This study
E. coli		
II3813	B462 Δ*thyA*:: (*erm-pir-116*), the intermediate host of suicide vector pSW7848	(Le Roux et al., 2007)
GEB883	*E.coli* K12 Δ*dapA*::*erm pirRP4-2* Δ*recAgyrA462*, *zei*298::*Tn10*; donor strain of conjuation	(Nguyen et al., 2018)
Plasmids		
pSW7848	Cm^r (chloramphenicol resistant), Pir protein and *ccdB* toxin gene are required for replication, suicide vectors with an R6K origin	(Val et al., 2012)
pSW7848-*lrp*up-*lrp*down	Cm^r, pSW848 containing the flanking region fragments in mutant allele of *lrp*	This study

TABLE 2 PCR primers used in this study.

Primers	Sequences(5′-3′)	Application
pSW7848_fwd	GTCTGATTCGTTACCAATTATGACAAC	Amplication of pSW7848
pSW7848_rev	GAATTCGATATCAAGCTTATCGATAC	
dlrp-U-F	ataagcttgatatcgaattcGTCTGTGACAACAAGCGTT	Amplification of upstream fragment for *lrp* allele exchange
dlrp-U-R	aactgtcactctcgtttggGTAAGGTGGCAGATGGAGATAA	
dlrp-D-F	ccatctgccaccttacCCAAACGAGAGTGACAGTT	Amplification of downstream fragment for *lrp* allele exchange
dlrp-D-R	taattggtaacgaatcagacTGGATCAACAGGGTCAGT	
Del-*lrp*-check-F	AAAGCGAACAACGCCAAAGC	Detection of *lrp* gene knockout
Del-*lrp*-check-R	TTGTAAGAGTGCCATCTGCTTTCC	
Del-check-pSW7848-F	TCACTGTCCCTTATTCGCACC	Detection of recombination
Del-check-pSW7848-R	CTGCTTTTGAGCACTACCCG	
q*lrp*-F	CAAAGGCTACCGAGCAGTAC	RT-PCR of *lrp*
q*lrp*-R	ACATTCCACCACCTCGTTTAC	
RT-16S-F	CCTACGGGAGGCAGCAG	RT-PCR reference gene
RT-16S-R	ATTACCGCGGCTGCTGG	

(HuanKai Microbial Sci&Tech. Co., Ltd., Guangdong, China). If the bacteria had caused hemolytic activity, hemolytic circles would appear on the plate. The overnight strain cultures (described in 2.2) were streaked onto Mueller-Hinton blood agar plates and hemolysis was observed after incubation at 30°C for 24 h.

2.5 Analysis of swimming and swarming motility

Overnight cultures of the WT and Δ*lrp* strains were prepared as described in 2.2. The cultures were diluted with fresh LBS medium to OD600 nm = 1.0. Three parallel 5 μL samples of the diluted WT and Δ*lrp* strains were spotted onto 0.3% agar and 1.5% agar LBS plates and the plates were incubated at 30°C for 16 h and 24 h, respectively. The culture diameters were measured to compare the differences in motility between the WT and Δ*lrp* strains.

2.6 Analysis of biofilm formation activity

Overnight cultures of the WT and Δ*lrp* strains were prepared as described in 2.2, and the bacteria were diluted to OD600 nm = 1.0. Samples were pipetted into sterilized 24-well plates with 1 mL per well. The plates were then incubated at 30°C for 48 h and used for biofilm quantification (O'Toole, 2011). After incubation, the wells were aspirated and fixed by adding 10% methanol. Then the biofilms were stained with 1% crystal violet and dissolved in 95% ethanol, followed by measurement of absorbance values of the biofilms at 550 nm using a microplate reader. The experiment was performed in triplicate and repeated three times.

2.7 Extracellular protease secretion assay

In this experiment, the extracellular protease secretion activity of the WT and Δ*lrp* strains were determined following Swift et al. (1999) with some modifications. Overnight cultures of the WT and Δ*lrp* strains were prepared as described in 2.2. The cultures were diluted to OD600 nm = 5.0, and 5 μL of the diluted cultures were spotted three times in parallel onto LBS plates containing 1% skimmed milk and then incubated at 30°C. The relative enzyme activity was calculated following Usman et al. (2021). The relative secretion abilities were measured as the diameter of the protein decomposition zone/the diameter of the colony after 24 h.

2.8 Antibiotic susceptibility assays

The effect of *lrp* deficiency on the susceptibility of *V.alginolyticus* to 23 antibiotics was determined using the Kirby-Bauer disk diffusion method (Yao et al., 2021). Overnight cultures of the WT and Δ*lrp* strains were prepared as described in 2.2. 200 μL overnight cultures were mixed with 10 mL fresh LBS liquid medium and poured onto LBS plates. After 10 min wetting, the remaining bacterial solution was poured off. The plates were air-dried, and antibiotic loaded

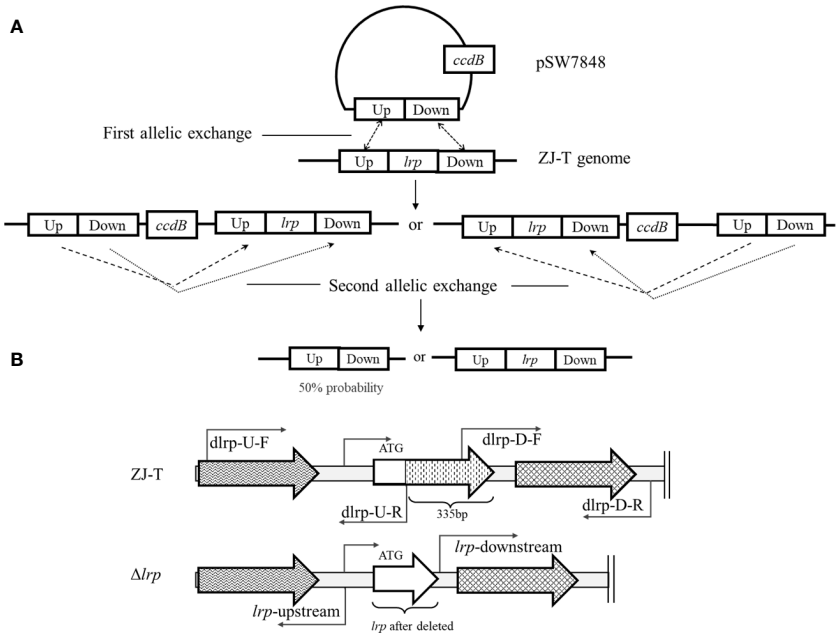

FIGURE 1
The conjugation between recombinant plasmid and *V. alginolyticus* genome **(A)**, and the structure of the *lrp* locus **(B)**. A: TCBS with 0.2% D-glucose and 20 μg/mL of Cm was used to select transconjugants in the first allelic exchange. TCBS with 0.2% L-arabinose was used to select the transconjugants that underwent plasmid excision in the second allelic exchange. The carried *ccdB* gene expressed was induced by L- arabinose, then pSW7848 was excised. B: 335 bp of the *lrp* ORF were deleted from the 33rd codon to the stop codon, giving rise to the *Δlrp* strain.

paper pills were placed onto them and then incubated at 30°C. After 24 h, the diameter of the inhibition circle on the plate was recorded, and the sensitivity results were determined by referring to the drug sensitivity instructions.

2.9 Zebrafish challenge assay

Zebrafish (average body weight, 0.35 ± 0.05 g) were purchased from an aquarium store in Guangzhou, Guangdong Province and acclimated for two weeks in an indoor laboratory at 30°C with continuous aeration.

Zebrafish challenge experiments were performed to determine the effect of *lrp* on the virulence of *V. alginolyticus*. The WT and *Δlrp* monoclonal strains were inoculated into LBS agar slant culture medium, then incubated overnight at 30°C. The colonies were then eluted with 3 mL of 0.85% sterile saline, and the bacterial concentration was determined and diluted to OD600 nm = 0.3. The zebrafish were challenged by intraperitoneal injection with 40 μL/fish ($2.55\sim2.71\times10^8$ CFU/fish). Each strain was injected into 60 fish equally divided into three tanks. The negative control was injected with 40 μL/fish of 0.85% sterile saline. Mortality was monitored every 24 h following the challenge, and the cumulative mortalities of four days (96 h) were calculated.

2.10 Effect of physicochemical factors on the expression of *lrp* during growth

The overnight cultures of the WT strain was diluted to OD600 nm = 0.01 in LBS medium with different pH (pH 5, 7, and 9), temperature (22°C, 30°C, and 37°C), salinity (1%, 3%, and 5% sodium chloride), copper ions (0.1 mg/L, 1.0 mg/L, and 5.0 mg/L copper sulfate), iron ions (1 mM, 4 mM, and 7 mM ferric citrate), nitrate (0.1 mg/L, 0.5 mg/L, and 2.0 mg/L sodium nitrate), and phosphate (1 mM, 4 mM, and 7 mM potassium dihydrogen phosphate) levels. The pH group, salinity group, and the groups with different concentration of added copper sulfate, ferric citrate, sodium nitrate, and potassium dihydrogen phosphate were cultured at 30°C with 200 rpm shaking. The temperature group were cultured at the different test temperature conditions with 200 rpm shaking. Bacteria cultured in LBS medium at pH 7, 30°C, and 3% NaCl were considered as the controls for the copper ions group, iron ions group, nitrate group, and phosphate group (the pH group use pH 7 as control, temperature group use 30°C as control, and salinity group use 3% NaCl as control). The *lrp* transcription levels of the bacteria cultured in the various conditions were analyzed after 2, 6, and 10 h of growth. RNAiso Plus reagent (Takara Bio Inc., Beijing, China) was used to extract total RNA from the cultures. Reverse transcription was performed using an

Evo M-MLV Mix Kit with gDNA Clean (Accurate Biology Co., Ltd., Hunan, China). RT-PCR amplification was performed to assess the expression of *lrp*, using a SYBR® Green Premix Pro Taq HS qPCR kit (Accurate Biology Co., Ltd., Hunan, China). The 16S rRNA gene was used as a control in the qRT-PCR. The primers used for RT-PCR are listed in Table 2. Gene expression analysis was performed using the $2^{-\Delta\Delta CT}$ method (Livak and Schmittgen, 2001).

2.11 Statistical analysis

The effects of *lrp* deletion on the phenotypes and virulence of *V. alginolyticus* and the effects of the various physicochemical factors on the expression of *lrp* were analyzed using Graphpad Prism 9 (Graphpad Software, San Diego, CA, USA). Mean ± SD values was calculated for the growth, motility, biofilm formation, extracellular protease, zebrafish challenge assay, and *lrp* expression experiments. Independent two-sample *t*-tests were used to analyze changes in motility, biofilm formation, and extracellular protease secretion activity following *lrp* deletion. A one-way ANOVA was conducted to assess the growth curves and *lrp* expression level assays in the same conditions at the three different time periods. Differences in cumulative mortalities caused by the WT and Δ*lrp* strains were analyzed using the Log-rank (Mantel-Cox) test. *P*-values < 0.05 were considered statistically significant.

3 Results

3.1 Construction of the *V. alginolyticus* ZJ-T *lrp* mutant strain

The *lrp* deletion strain was constructed using homologous recombination following Deng et al. (2016b) with some modifications. The linearized fragment of plasmid pSW7848 (3309 bp), and the upstream and downstream fragments of *lrp* (1025 bp and 904 bp) were successfully amplified using PCR (Figure 2, lane 1-3). The upstream and downstream fragments were then assembled with the linearized suicide vector pSW7848, and the fusion action was transformed into *E. coli* II3813. The fusion was identified using the primer pairs Del-check-pSW7848-F/R, resulting in a fragment of 2214 bp (Figure 2, lane 4). The resulting recombination plasmid pSW7848-*lrp*up-*lrp*down was subsequently transformed into *E. coli* GEB883. The allelic exchange was performed after the recombinant plasmid was transferred from *E. coli* GEB883 to *V. alginolyticus* ZJ-T by conjugation. The *lrp* disruptant was finally confirmed by sequencing, and the strain was named Δ*lrp* (Figure 2, lane 5-6).

3.2 Effect of *lrp* on the growth of *V. alginolyticus* under different conditions

The WT and Δ*lrp* strains were cultured in LBS medium. The growth of Δ*lrp* did not differ significantly from WT during any

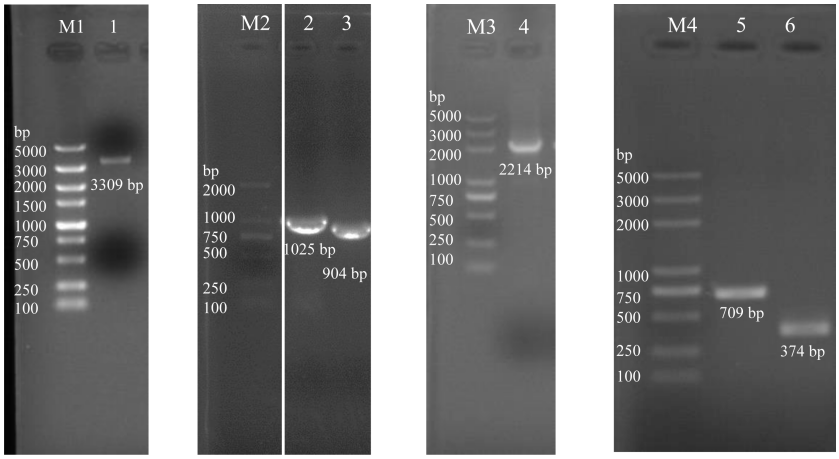

FIGURE 2
PCR identification of Δ*lrp* construction in *V. alginolyticus*. M1: 5,000 DNA marker (Guangzhou Dongsheng Biotech Co., Ltd.); M2: 2,000 DNA marker (Guangzhou Dongsheng Biotech Co., Ltd.); M3 and M4: 5,000 DNA marker (Tsingke Biotechnology Co., Ltd.); lane 1: pSW7848 linearized plasmid; lane 2: upstream fragment of *lrp*; lane 3: downstream fragment of *lrp*; lane 4: detecting of the recombination plasmid of pSW7848-*lrp*up-*lrp*down; lane 5: amplification fragment of wild strain with primers of Del-*lrp*-check-F/R; lane 6: amplification fragment of Δ*lrp* with primers of Del-*lrp*-check-F/R. This figure is the combination result of four gel pictures, and they are M1/1, M2/2/3, M3/4, and M4/5/6, respectively. In the gel M1/1, we cut all the lanes on the right of lane 1; in the gel M2/2/3, we cut a lane between lane M2 and lane 2, and cut all the lanes on the right of lane 3, then we spliced the lane M2 and lane 2/3, and there is a space between M2 and lane 2 showing the splicing; in the gel M3/4, we cut all the lanes on the right of lane 4; in the gel M4/5/6, we cut all the lanes on the right of lane 6.

growth period. During the 36 h of incubation, the first hour presented the latent period. The log phase began at 2 h and the stable phase was reached after 12 hours incubation (Figure 3A).

Neither the WT nor Δ*lrp* strains produced hemolytic circles on the Mueller-Hinton blood agar plate (Figure 3B). In the absence of *lrp*, there was no significant difference in the growth of *V. alginolyticus* on either the LBS plate or on the LBS plate with 150 μM DIP or with 0.003% H_2O_2 (Figure 3C). As shown in Figure 3C, there was a 10^5-fold difference in survival rate between the WT and the *lrp* mutant strains on the LBS agar plate containing 4.5 mM $CuSO_4$. Resistance of *V. alginolyticus* to copper ions was strengthened when *lrp* was absent (Figure 3C).

3.3 Absence of *lrp* increased the motility, biofilm formation, and extracellular secretion activity of *V. alginolyticus*

Both the WT and Δ*lrp* strains showed swimming motility on the 0.3% agar LBS plates, but no differences in extension diameter were observed. However, the swarming motility of the Δ*lrp* strain on the 1.5% agar LBS plates was significantly greater than the WT (Figure 4A and Figure 4B).

The biofilm circles were stained with crystal violet and eluted with acetic acid (Figure 4C). The purple biofilm precipitation could be seen at the bottom of the culture wells. The mean amount of Δ*lrp* strain biofilm formed was significantly greater than the WT strain (Figure 4D).

The ratio of the transparent proteolytic circle diameter to the colony diameter indicates the capacity for extracellular protease secretion (Figure 4E). The secretion activity of Δ*lrp* was significantly greater than that of WT (Figure 4F).

3.4 No significant effect of *lrp* on antibiotic resistance of *V. alginolyticus*

The bacterial inhibition circles produced around the 23 antibiotic paper tablets revealed that the absence of *lrp* did not significantly change the antibiotic resistance of *V. alginolyticus*. The results showed that the WT and Δ*lrp* strains were resistant to 13 antibiotics, including rifampicin, amoxicillin, sulfafurazole, medimycin, cephalexin, enrofloxacin, furazolidone, compound sulfamethoxazol, streptomycin, cefazolin, tetracycline, ampicillin, and vancomycin. In addition, the absence of *lrp* did not alter the susceptibility of *V. alginolyticus* to 10 antibiotics, including claricid, doxycycline, florfenicol, tobramycin, ciprofloxacin, gentamicin, erythromycin, chloramphenicol, ofloxacin, and norfloxacin (Table S1).

3.5 Enhanced virulence of the *lrp* mutant strain to zebrafish

The WT and Δ*lrp* strains were used to challenge experimental zebrafish. The cumulative zebrafish mortality rates in the WT group were 31.11%, 37.78%, 40.00%, and 40.00% for 24 h, 48 h, 72 h, and 96 h after intraperitoneal injection, respectively. The mortality of zebrafish after injection with Δ*lrp* appeared to be greater than for the WT, with cumulative mortality rates of 64.44%, 66.67%, 68.89%, and 68.89% for 24 h, 48 h, 72 h, and 96 h after intraperitoneal injection, respectively (Figure 5). The mortality difference between the WT and Δ*lrp* groups was statistically significant according to a Log Rank (Mantel-Cox) analysis. The results of

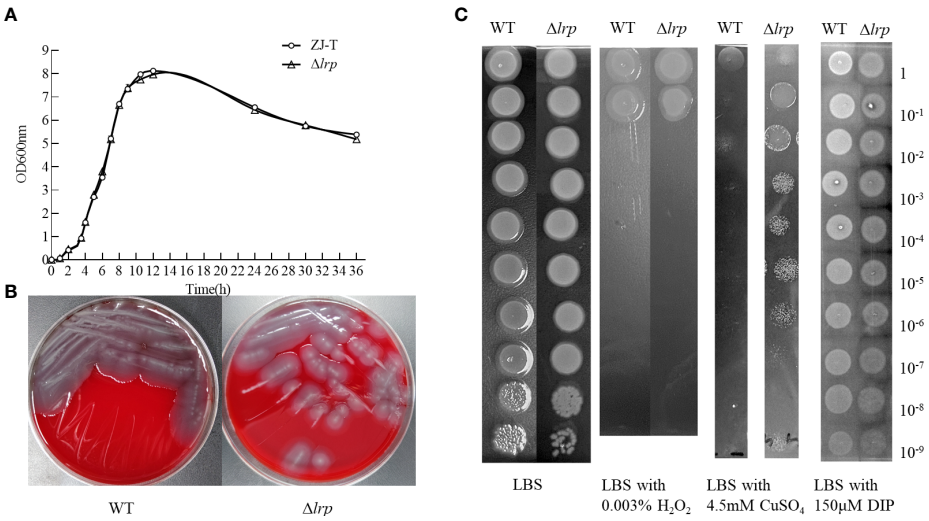

FIGURE 3
Growth, hemolysis, iron uptake capacity, copper ion and H_2O_2 tolerance of the WT and Δ*lrp* strains. The growth curve of WT and **(A)**, and the hemolytic activity on sheep blood agar plate **(B)**, as well as their sensitivity of them to H_2O_2, $CuSO_4$, and DIP on the LBS agar plate **(C)**.

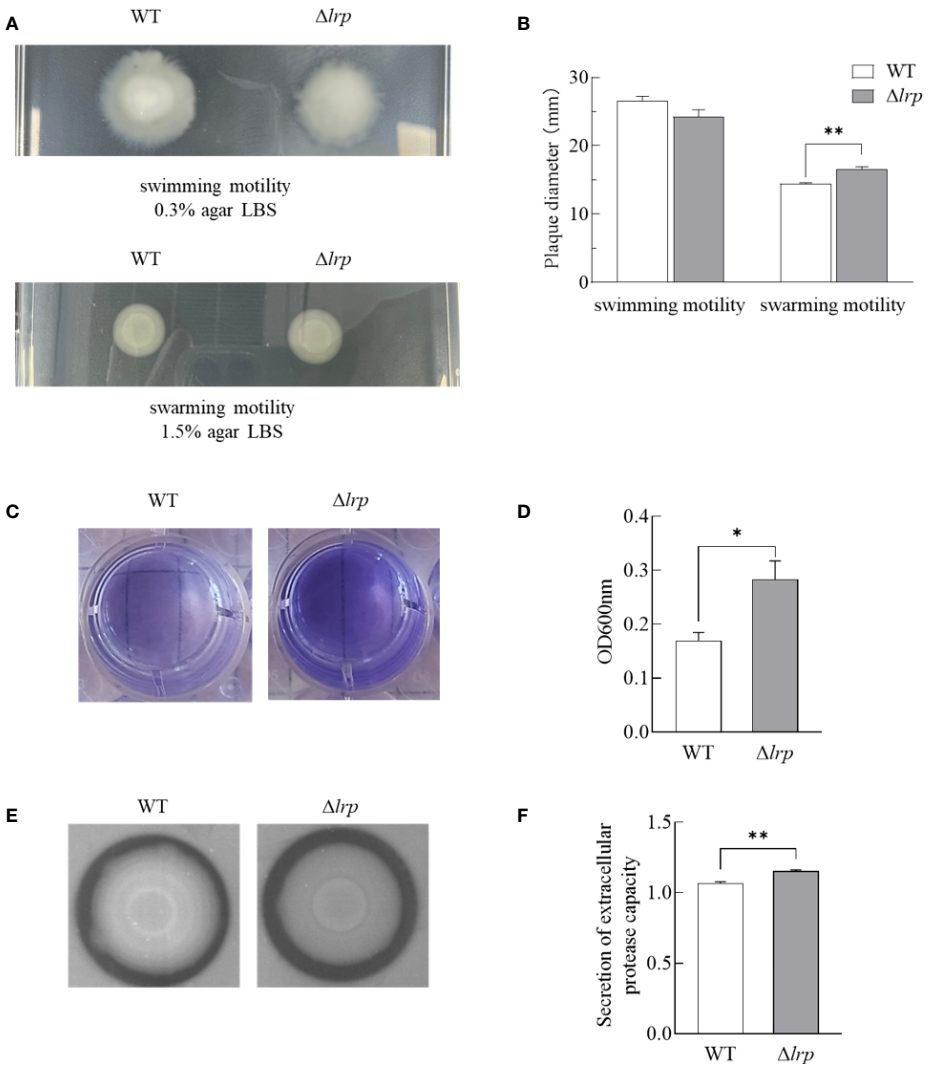

FIGURE 4
Motility, biofilm formation and extracellular protease secretion activity of WT and Δ*lrp* strains. **(A)**: the growth of the strains on the 0.3% and 1.5% agar LBS plate; **(B)**: the colony diameter statistical analysis; **(C)**: dissolved crystal violet-stained biofilm; **(D)**: the absorbance value of biofilm staining; **(E)**: strains growth on the skim milk plate; **(F)**: graph of extracellular protease secretion capacity, vertical coordinate is the ratio of outer circle diameter to inner circle diameter. (**, P<0.01; *, P<0.05).

the challenge experiment showed that the deletion of *lrp* enhanced the virulence of *V. alginolyticus* in zebrafish, and that *lrp* may negatively regulate *V. alginolyticus* virulence.

3.6 The expression of *lrp* was impacted by various physicochemical factors and was gradually downregulated

In general, the expression of *lrp* showed a gradual decrease with increasing growth under the same cultural conditions. Compared with the control group (pH 7), the expression of *lrp* increased at pH 5 after 2 h (3.43-fold, $P < 0.001$) and 10 h (1.59-fold, $P < 0.001$) (Figure 6A). At the same incubation time, *lrp* was expressed most at pH 5, followed by pH 7 and pH 9. Meanwhile, the pH 9 group showed a higher *lrp* expression level ($P < 0.01$) at 10 h (Figure 6A). The mRNA of *lrp* increased at a temperature of 22°C at 2 h (3.47-fold, $P < 0.01$) and 10 h (1.52-fold, $P < 0.05$) but decreased at a temperature of 37°C at 2 h (1.75-fold, $P < 0.05$); at 6 h (3.84-fold, $P < 0.001$); and at 10 h (2.13-fold, $P < 0.001$). Culture conditions at a temperature of 37°C could inhibit the expression of *lrp* (Figure 6B). The expression of *lrp* was significantly increased in the 5% NaCl group at 2 h (1.78-fold, $P < 0.01$), but significantly decreased at 6 h ($P < 0.05$) and 10 h

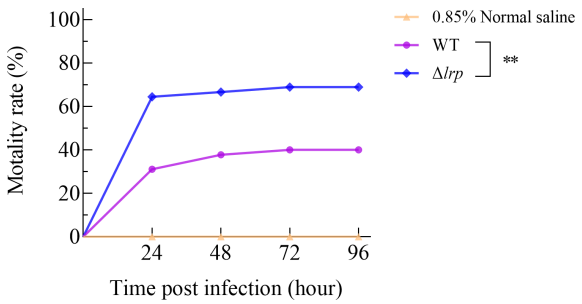

FIGURE 5
Cumulative mortality of zebrafish after injection of WT and Δ*lrp* strains. Cumulative mortality was recorded every 24 h. Differences in cumulative mortalities were analyzed by Log-rank (Mantel-Cox) test (**, P<0.01).

(P< 0.01). In the 1% NaCl group, its expression was significantly decreased at 6 h (2.63-fold, P < 0.001) but increased at 10 h (P < 0.05) (Figure 6C).

lrp mRNA was generally induced by $CuSO_4$. The 1 mM $CuSO_4$ group had a significantly higher *lrp* mRNA expression than the control when cultured for 2 h and 10 h (1.86-fold and 1.36-fold, P < 0.01, respectively). The expression of *lrp* increased at 6 h when the strain was grown in 3 mM $CuSO_4$ (1.49-fold, P < 0.01) (Figure 6D). The bacterial cultures with added Fe^{3+} (1 mM, 4 mM, and 7mM) showed relatively higher expression at 2 h compared with the control group, with 4.46-fold (P < 0.01), 1.69-fold (P < 0.01), and 1.87-fold (P < 0.05) increases, respectively. Meanwhile, under the same conditions, *lrp* was usually most expressed at 2 h (Figure 6E). The expression of *lrp* with the addition of 1 mM Fe^{3+} and 7 mM Fe^{3+} were significantly lower than the expression of *lrp* at 6 h (P < 0.01). The 7 mM Fe^{3+} group increased *lrp* transcription at 10 h (2.03-fold, P < 0.01) (Figure 6E). With the same concentration of $NaNO_3$, the expression of *lrp* was greatest at 2 h, and was significantly increased by the addition of 0.1 mg/L $NaNO_3$ (2.07-fold, P < 0.001). Appropriate concentrations of $NaNO_3$ decreased *lrp* expression at 6 h (0.1/5.0 mg/L $NaNO_3$, P < 0.05), while the expression of *lrp* was increased at 10 h in 5.0 mg/L $NaNO_3$ (1.59-fold, P < 0.001) (Figure 6F). The *lrp* expression of WT in LBS generally decreased with increasing concentrations of KH_2PO_4, except that the 0.1 mg/L KH_2PO_4 group significantly increased *lrp* expression at 2 h (1.55-fold, P < 0.05) and 10 h (2.10-fold, P < 0.001). The *lrp* expression of the 0.5 mg/L PO_4^{3-} and 2.0 mg/L PO_4^{3-} groups decreased at 2 h and 6 h, respectively (Figure 6G).

4 Discussion

In this study, a *lrp* mutant strain of *V. alginolyticus* was constructed to explore the role of Lrp and its biological properties and virulence. Biophenotype characterization revealed that the deletion of *lrp* did not significantly affect growth, iron absorption, radical oxygen resistance, hemolytic activity, antibiotic resistance, or swimming motility but increased swarming motility, biofilm formation, secretion of extracellular protease, and copper ion resistance. The virulence of *V. alginolyticus* to zebrafish was significantly enhanced after *lrp* deletion. *lrp* expression was affected by many physicochemical factors, including pH, temperature, salinity, and the presence of copper sulfate, ferric citrate, sodium nitrate, and potassium dihydrogen phosphate.

Bacteria move in highly viscous environments using their flagella, which help them to invade and colonize their hosts (McCarter and Silverman, 1990; Josenhans and Suerbaum, 2002). Many genes have been associated with bacterial motility (Yuan et al., 2022). Liu et al. (2021) showed that the RNA binding protein, CsrA, activates swarming motility by enhancing the expression of lateral flagellum-related genes. Deleting the quorum sensing-regulated extracellular protein gene *pep* leads to reduced motility and failure to generate lateral flagella (Cao et al., 2011). Biofilm formation is encouraged by bacterial spores and flagella (Yildiz and Visick, 2009) and helps bacteria to colonize of the host's interior or the surface of aquatic plankton (Tamplin et al., 1990). Motility therefore plays a crucial role in biofilm formation, pathogenicity, and environmental adaptation in many bacteria (Gu et al., 2019a). The lateral flagella support bacterial swarming motility over surfaces or through viscous environments (McCarter, 2004). Gu et al. (2019a) reported that a GntR family transcription factor may increase swarming motility by enhancing the transcription of lateral flagella genes in *Vibrio parahaemolyticus*. The flagellin-homologous proteins (FHPs) in *V. vulnificus* could enhance the exopolysaccharide-enriched biofilm matrix through excretion to the extracellular milieu. Therefore, the presence of FHPs involved in biofilm enhancement could promote the pathogenicity of bacteria (Jung et al., 2019). In this study, bacterial swimming motility was not affected by *lrp* deletion, while swarming motility was significantly increased. The absence of *lrp* may induce the flagella to move when crossing surfaces or in sticky environments. Lrp may affect biofilm formation and swarming motility by regulating FHPs secreted into the extracellular environment. Changes in biofilm formation and cell motility may lead to enhanced virulence of *V. alginolyticus* in zebrafish. Therefore, because of the changes in motility and biofilm formation after *lrp* deletion found in this study, we hypothesize that *lrp* may affect the expression of the flagella gene in *V. alginolyticus* to regulate its swarming motility, and so influence biofilm formation and lead to changes in virulence.

Extracellular protease secretion activity also increased after deletion of the *lrp* gene. Extracellular proteases are pathogenic factors and play an essential role in the infection process of *V. alginolyticus* (Watnick et al., 2001). Extracellular production of the alkaline serine protease has been reported to be lethal to fish (Lee et al., 1997), and the alkaline serine protease gene *asp* is regulated by the quorum sensing system, resulting in changes in

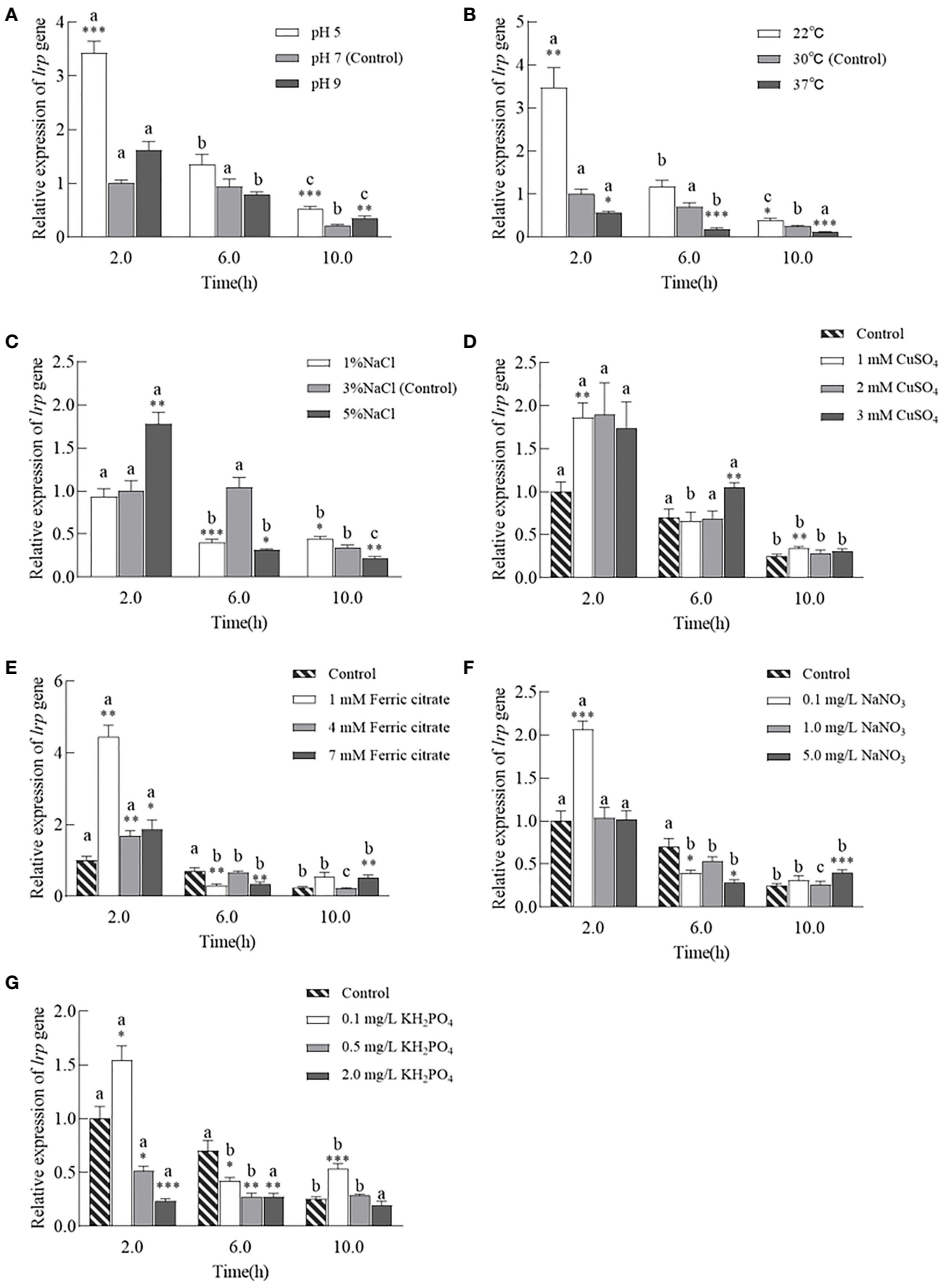

FIGURE 6
Expression profiles of WT strains under 7 incubate conditions. Expression levels of strains cultured in LBS with different pH **(A)**, temperature **(B)**, salinity **(C)**, and addition of different concentrations of copper ion **(D)**, iron ion **(E)**, nitrate **(F)**, phosphate **(G)**. Data are expressed as means ± SE relative to control group. Significant differences between control group and treatment groups at the same growth period are indicated with asterisks (*, $P<0.05$; **, $P<0.01$; ***, $P<0.001$). Take strains with the same culture conditions as a group and use different letters to indicate significant differences in the growth period of the same group ($P<0.05$).

virulence (Rui et al., 2009). The response regulator protein LuxO has multiple roles in regulating extracellular products, and the extracellular protease activity was significantly enhanced after *luxO* deletion (Wang et al., 2007). The results of this study are similar to those described above. After *lrp* mutation, extracellular protease secretory activity was significantly increased, as were swarming motility and biofilm formation. Further research is needed to determine whether Lrp can regulate virulence by inducing changes in extracellular protease activity, and interact with biofilm formation or flagellar gene expression.

Copper, in its two oxidation states, is involved in essential redox reactions and promotes the formation of reactive oxygen species, leading to cellular damage (Karlin, 1993). Copper efflux is essential to bacterial pathogens for host colonization and virulence and is primary prerequisite for *Vibrio* intracellular phases and cytotoxicity to hemocytes (Kong et al., 2015; Vanhove et al., 2016). Kong et al. (2015) found that the adhesion capacity of *V. alginolyticus* was significantly reduced after treatment with copper ions (50 mg/L). In *V. cholerae*, copper resistance proteins were reduced in *nqr* (electrogenic, sodium ion-translocating NADH: quinone oxidoreductase gene) deletion strains, resulting in diminished copper resistance (Toulouse et al., 2018). Vanhove et al. (2016) found that the primary mechanism of copper ion resistance was to prevent the host phagocytes killing pathogens, and to induce the cytolysis of host immune cells and host colonization. In this study, the mutant strain Δ*lrp* was less damaged by copper ion stress than the WT, indicating that its sensitivity to copper ions was reduced after the mutation ameliorated the toxicity of copper ions. It appears that Lrp may regulate the expression of copper resistance proteins in *V. alginolyticus*, decreasing its sensitivity to copper ions and enhancing its adhesion capacity.

Physicochemical factors can influence bacterial gene expression, thus regulating the biological properties relating to virulence. The attachment of *V. alginolyticus* was affected by temperature, which changed the expression of *rstA* and *rstB*. These two genes have a regulatory role in bacterial adhesion, biofilm production, motility, and hemolysis (Huang et al., 2018a). Appropriate salinity levels facilitated the adherence of *V. alginolyticus* to the skin mucus of *Sparus aurata*, and *V. alginolyticus* showed a higher adhesion rate in seawater (3.5% salinity) than in PBS and saline solution (Balebona et al., 1995). Studies have shown that the adhesion ability of *V. alginolyticus* was impaired under heavy metal (50 mg/L Cu^{2+}, 100 mg/L Pb^{2+}, 50 mg/L Hg^{2+}) and acidic stresses (Kong et al., 2015). VspR is the primary regulator in *V. alginolyticus*, and enables the formation/maintenance of biofilms by directly sensing phosphate levels (Hsieh et al., 2022). In this study, the expression of *lrp* was generally up-regulated by different physicochemical factors, and *lrp* usually showed its highest expression after 2 h of culture time. Many combinations of adverse environmental stresses could increase the expression of *lrp* (pH 5, 22°C, 5% NaCl, 1/4/7 mM Fe^{3+}, 0.1/5 mg/L NO^{3-}, and 0.1 mg/L PO_4^{3-} at 2 h; and pH 5, pH 9, 22°C, 1% NaCl, 1 mM Cu^{2+}, 7 mM Fe^{3+}, 5 mg/L NO_3^-, and 0.1 mg/L PO_4^{3+} at 10 h). The virulence of *V. alginolyticus* was reduced in the presence of *lrp*, indicating that increased *lrp* expression of ZJ-T in different conditions might also decrease its virulence. Some conditions could decrease the transcription level of *lrp* at 6 h, including 37°C, 1% NaCl, 5% NaCl, 1/7 mM iron ions, 0.1/5 mg/L nitrate, 0.1/0.5/2 mg/L phosphate. The significant decrease in *lrp* expression indicated that the virulence of *V. alginolyticus* might increase over a similar time in these culture conditions. These culture conditions may lead to changes in biological characteristics similar to those found in Δ*lrp*, such as motility, biofilm formation, and enhanced extracellular protease secretion. Therefore, various physicochemical factors that change the expression of *lrp* probably contribute to variations in adhesion, colonization, and toxin release of *V. alginolyticus*, thereby leading to changes in virulence. Especially after 2 h and 10 h of cultivation, the physicochemical factors tested tend to promote *lrp* expression, thereby probably inhibiting the virulence of *V. alginolyticus*. However, whether the increased expression of *lrp* in adverse environments is related to the maintenance of ZJ-T homeostasis or is involved in regulating the secretion of factors related to flagella, clearly requires further study.

5 Conclusions

After *lrp* deletion, *V. alginolyticus* displayed dramatically increased virulence, swarming motility, biofilm formation, extracellular protease activity, and resistance to copper ions. The expression of *lrp* showed a gradual decrease with time in any one cultural environment. After 2 h incubation time, cultivation with pH 5, 22°C, 5% NaCl, 1 mM Cu^{2+}, 1/4/7 mM Fe^{3+}, 0.1 mg/L NO_3^-, 0.1 mg/L PO_4^{3-} increased *lrp* expression, and at 37°C, 0.5 mg/L PO_4^{3-} and 2 mg/L PO_4^{3-} *lrp* expression was inhibited. After 6 h of culture at 37°C, 1/5% NaCl, 1/7 mM Fe^{3+}, 0.1/5 mg/L NO_3^-, 0.1/0.5/2 mg/L PO_4^{3-} the expression of *lrp* was inhibited. *lrp* expression was promoted after 10 h of culture at pH 5/9, 22°C, 1% NaCl, 1 mM Cu^{2+}, 7 mM Fe^{3+}, 5 mg/L NO_3^-, and 0.1 mg/L PO_4^{3-}, but was inhibited at 37°C and 5% NaCl. Therefore, Lrp was strongly affected by various physicochemical factors and may reduce the virulence of *V. alginolyticus* by inhibiting biofilm formation, swarming motility, and extracellular protease secretion. These results further the study of virulence regulation in *V. alginolyticus*. Future research should focus on: (1) how *lrp* affects motility, biofilm formation, and extracellular protease secretion, and ultimately the virulence of *V. alginolyticus* at the gene regulation level; and (2) the effects of various levels of virulence of *V. alginolyticus* on aquatic animals under different environmental conditions, including temperature, pH, salinity, and the presence of copper sulfate, ferric citrate, sodium nitrate, and potassium dihydrogen phosphate. The results of such work will help to establish precise virulence control strategies based on environmental regulation.

Data availability statement

The datasets presented in this study can be found in online repositories. The names of the repository/repositories and accession number(s) can be found below: https://www.ncbi.nlm.nih.gov/, CP016224.1.

Ethics statement

The animal study was reviewed and approved by the study protocol was approved by the Animal Care and Use Committee of the South China Sea Fisheries Research Institute, Chinese Academy of Fishery Sciences and performed in accordance with institutional regulations and guidelines.

Author contributions

WS: Completed experiment, Data curation, investigation, software, and writing. YD: Funding acquisition, conceptualization, resources, writing-review, and editing. SZ: Aided experiment conduct and validation, data collation. SG: Visualization, data curation, and validation. JF: Funding acquisition, project administration, supervision, writing-review and editing, validation. All authors contributed to the article and approved the submitted version.

Funding

This work was supported by the Central Public-Interest Scientific Institution Basal Research Fund, CAFS (2022GH03), the Guangzhou Science and Technology Program (202201010162), the National Natural Science Foundation of China (NSFC) (31902415), Central Public-interest Scientific Institution Basal Research Fund, South China Sea Fisheries Research Institute, CAFS (2021SD15), the Natural Science Fund of Guangdong (2019A1515011833), and the China Agriculture Research System (CARS-48).

Conflict of interest

The authors declare that the research was conducted in the absence of any commercial or financial relationships that could be construed as a potential conflict of interest.

Publisher's note

All claims expressed in this article are solely those of the authors and do not necessarily represent those of their affiliated organizations, or those of the publisher, the editors and the reviewers. Any product that may be evaluated in this article, or claim that may be made by its manufacturer, is not guaranteed or endorsed by the publisher.

Supplementary material

The Supplementary Material for this article can be found online at: https://www.frontiersin.org/articles/10.3389/fmars.2022.1042899/full#supplementary-material

References

Abdallah, F. B., Lagha, R., Ellafi, A., Namane, A., Rousselle, J.-C., Lenormand, P., et al. (2012). Identification of outer membrane proteins altered in response to UVC-radiation in vibrio parahaemolyticus and vibrio alginolyticus. *Indian J. Microbiol.* 52, 660–665. doi: 10.1007/s12088-012-0299-2

Alice, A. F., and Crosa, J. H. (2012). The TonB3 system in the human pathogen vibrio vulnificus is under the control of the global regulators lrp and cyclic AMP receptor protein. *J. Bacteriol.* 194, 1897–1911. doi: 10.1128/JB.06614-11

Baker-Austin, C., Oliver, J. D., Alam, M., Ali, A., Waldor, M. K., Qadri, F., et al. (2018). Vibrio spp. infections. *Nat. Rev. Dis. Primer* 4, 8. doi: 10.1038/s41572-018-0005-8

Balebona, M. C., Moriñigo, M. A., Faris, A., Krovacek, K., Månsson, I., Bordas, M. A., et al. (1995). Influence of salinity and pH on the adhesion of pathogenic vibrio strains to sparus aurata skin mucus. *Aquaculture* 132, 113–120. doi: 10.1016/0044-8486(94)00376-Y

Brinkman, A. B., Ettema, T. J. G., de Vos, W. M., and van der Oost, J. (2003). The lrp family of transcriptional regulators. *Mol. Microbiol.* 48, 287–294. doi: 10.1046/j.1365-2958.2003.03442.x

Cao, X., Wang, Q., Liu, Q., Rui, H., Liu, H., and Zhang, Y. (2011). Identification of a luxo-regulated extracellular protein pep and its roles in motility in vibrio alginolyticus. *Microb. Pathog.* 50, 123–131. doi: 10.1016/j.micpath.2010.12.003

Chen, K.-Y., Rathod, J., Chiu, Y.-C., Chen, J.-W., Tsai, P.-J., and Huang, I.-H. (2019). The transcriptional regulator lrp contributes to toxin expression, sporulation, and swimming motility in clostridium difficile. *Front. Cell. Infect. Microbiol.* 9. doi: 10.3389/fcimb.2019.00356

Chen, S., Rosner, M. H., and Calvo, J. M. (2001). Leucine-regulated self-association of leucine-responsive regulatory protein (lrp) from escherichia coli. *J. Mol. Biol.* 312, 625–635. doi: 10.1006/jmbi.2001.4955

Ciaccia, P. N., Ramachandran, R., and Chattoraj, D. K. (2018). A requirement for global transcription factor lrp in licensing replication of vibrio cholerae chromosome 2. *Front. Microbiol.* 9. doi: 10.3389/fmicb.2018.02103

Davis, B. J. K., Jacobs, J. M., Davis, M. F., Schwab, K. J., DePaola, A., and Curriero, F. C. (2017). Environmental determinants of vibrio parahaemolyticus in the Chesapeake bay. *Appl. Environ. Microbiol.* 83, e01147–e01117. doi: 10.1128/AEM.01147-17

DeAngelis, C. M., Saul-McBeth, J., and Matson, J. S. (2018). Vibrio responses to extracytoplasmic stress. *Environ. Microbiol. Rep.* 10, 511–521. doi: 10.1111/1758-2229.12693

Deng, Y., Chen, C., Zhao, Z., Huang, X., Yang, Y., and Ding, X. (2016a). Complete genome sequence of vibrio alginolyticus ZJ-T. *Genome Announc.* 4, e00912–e00916. doi: 10.1128/genomeA.00912-16

Deng, Y., Chen, C., Zhao, Z., Zhao, J., Jacq, A., Huang, X., et al. (2016b). The RNA chaperone hfq is involved in colony morphology, nutrient utilization and oxidative and envelope stress response in vibrio alginolyticus. *PloS One* 11, e0163689. doi: 10.1371/journal.pone.0163689

Fahmy, N. M., and Hamed, E. S. A. E. (2021). Isolation and characterization of vibrio alginolyticus strain Hat3 causing skin ulceration disease in cultured Sea cucumber holothuria atra (jaeger 1833). *Egypt. J. Aquat. Res.* 48, 75–81. doi: 10.1016/j.ejar.2021.11.007

Gaüzère, B.-A., Chanareille, P., and Vandroux, D. (2016). Septicémie À vibrio alginolyticus au décours d'une presque noyade À la réunion (océan indien). *Bull. Société Pathol. Exot.* 109, 151–154. doi: 10.1007/s13149-016-0505-2

Gu, D., Meng, H., Li, Y., Ge, H., and Jiao, X. (2019a). A GntR family transcription factor (VPA1701) for swarming motility and colonization of vibrio parahaemolyticus. *Pathogens* 8, 235. doi: 10.3390/pathogens8040235

Gu, D., Zhang, J., Hao, Y., Xu, R., Zhang, Y., Ma, Y., et al. (2019b). Alternative sigma factor RpoX is a part of the RpoE regulon and plays distinct roles in stress responses, motility, biofilm formation, and hemolytic activities in the marine pathogen vibrio alginolyticus. *Appl. Environ. Microbiol.* 85, e00234–e00219. doi: 10.1128/AEM.00234-19

Halpern, B. S., Frazier, M., Afflerbach, J., Lowndes, J. S., Micheli, F., O'Hara, C., et al. (2019). Recent pace of change in human impact on the world's ocean. *Sci. Rep.* 9, 11609. doi: 10.1038/s41598-019-47201-9

Hart, B. R., Mishra, P. K., Lintner, R. E., Hinerman, J. M., Herr, A. B., and Blumenthal, R. M. (2011). Recognition of DNA by the helix-Turn-Helix global regulatory protein lrp is modulated by the amino terminus. *J. Bacteriol.* 193, 3794–3803. doi: 10.1128/JB.00191-11

Hoe, N. P., and Goguen, J. D. (1993). Temperature sensing in yersinia pestis: Translation of the lcrf activator protein is thermally regulated. *J. Bacteriol.* 175, 7901–7909. doi: 10.1128/jb.175.24.7901-7909.1993

Ho, Y.-C., Hung, F.-R., Weng, C.-H., Li, W.-T., Chuang, T.-H., Liu, T.-L., et al. (2017). Lrp, a global regulator, regulates the virulence of vibrio vulnificus. *J. Biomed. Sci.* 24, 54. doi: 10.1186/s12929-017-0361-9

Hsieh, M.-L., Kiel, N., Jenkins, L. M. M., Ng, W.-L., Knipling, L., Waters, C. M., et al. (2022). The vibrio cholerae master regulator for the activation of biofilm biogenesis genes, vpsr, senses both cyclic di-gmp and phosphate. *Nucleic Acids Res.* 50, 4484–4499. doi: 10.1093/nar/gkac253

Huang, X., Chen, C., Ren, C., Li, Y., Deng, Y., Yang, Y., et al. (2018b). Identification and characterization of a locus putatively involved in colanic acid biosynthesis in vibrio alginolyticus zj-51. *Biofouling* 34, 1–14. doi: 10.1080/08927014.2017.1400020

Huang, L., Huang, L., Zhao, L., Qin, Y., Su, Y., and Yan, Q. (2019). The regulation of oxidative phosphorylation pathway on vibrio alginolyticus adhesion under adversities. *MicrobiologyOpen* 8, e00805. doi: 10.1002/mbo3.805

Huang, L., Hu, J., Su, Y., Qin, Y., Kong, W., Ma, Y., et al. (2015). Identification and characterization of three vibrio alginolyticus non-coding rnas involved in adhesion, chemotaxis, and motility processes. *Front. Cell. Infect. Microbiol.* 5. doi: 10.3389/fcimb.2015.00056

Huang, L., Xu, W., Su, Y., Zhao, L., and Yan, Q. (2018a). Regulatory role of the rstb-rsta system in adhesion, biofilm production, motility, and hemolysis. *MicrobiologyOpen* 7, e00599. doi: 10.1002/mbo3.599

Huisman, T. T., Bakker, D., Klaasen, P., and de Graaf, F. K. (1994). Leucine-responsive regulatory protein, Is1 insertions, and the negative regulator faea control the expression of the fae (k88) operon in escherichia coli. *Mol. Microbiol.* 11, 525–536. doi: 10.1111/j.1365-2958.1994.tb00333.x

Hussa, E. A., Casanova-Torres, A. M., and Goodrich-Blair, H. (2015). The global transcription factor lrp controls virulence modulation in xenorhabdus nematophila. *J. Bacteriol.* 197, 3015–3025. doi: 10.1128/JB.00272-15

Josenhans, C., and Suerbaum, S. (2002). The role of motility as a virulence factor in bacteria. *Int. J. Med. Microbiol. IJMM* 291, 605–614. doi: 10.1078/1438-4221-00173

Jung, Y.-C., Lee, M.-A., and Lee, K.-H. (2019). Role of flagellin-homologous proteins in biofilm formation by pathogenic vibrio species. *mBio* 10, e01793–e01719. doi: 10.1128/mBio.01793-19

Karlin, K. D. (1993). Metalloenzymes, structural motifs, and inorganic models. *Science* 261, 701–708. doi: 10.1126/science.7688141

Kong, W., Huang, L., Su, Y., Qin, Y., Ma, Y., Xu, X., et al. (2015). Investigation of possible molecular mechanisms underlying the regulation of adhesion in vibrio alginolyticus with comparative transcriptome analysis. *Antonie Van Leeuwenhoek* 107, 1197–1206. doi: 10.1007/s10482-015-0411-9

Lee, K. K., Yu, S. R., and Liu, P. C. (1997). Alkaline serine protease is an exotoxin of vibrio alginolyticus in kuruma prawn, penaeus japonicus. *Curr. Microbiol.* 34, 110–117. doi: 10.1007/s002849900153

Le Roux, F., Binesse, J., Saulnier, D., and Mazel, D. (2007). Construction of a vibrio splendidus mutant lacking the metalloprotease gene vsm by use of a novel counterselectable suicide vector. *Appl. Environ. Microbiol.* 73, 777–784. doi: 10.1128/AEM.02147-06

Lin, W., Kovacikova, G., and Skorupski, K. (2007). The quorum sensing regulator hapr downregulates the expression of the virulence gene transcription factor apha in vibrio cholerae by antagonizing lrp- and vpsr-mediated activation. *Mol. Microbiol.* 64, 953–967. doi: 10.1111/j.1365-2958.2007.05693.x

Liu, B., Gao, Q., Zhang, X., Chen, H., Zhang, Y., Sun, Y., et al. (2021). Csra regulates swarming motility and carbohydrate and amino acid metabolism in vibrio alginolyticus. *Microorganisms* 9, 2383. doi: 10.3390/microorganisms9112383

Liu, H., Wang, Q., Liu, Q., Cao, X., Shi, C., and Zhang, Y. (2011). Roles of hfq in the stress adaptation and virulence in fish pathogen vibrio alginolyticus and its potential application as a target for live attenuated vaccine. *Appl. Microbiol. Biotechnol.* 91, 353–364. doi: 10.1007/s00253-011-3286-3

Liu, R., Zheng, R., Liu, G., and Sun, C. (2020). The cyclic lipopeptides suppress the motility of vibrio alginolyticus *Via* targeting the na+ -driven flagellar motor component motx. *Environ. Microbiol.* 22, 4424–4437. doi: 10.1111/1462-2920.15144

Livak, K. J., and Schmittgen, T. D. (2001). Analysis of relative gene expression data using real-time quantitative PCR and the 2–ΔΔCT method. *Methods* 25, 402–408. doi: 10.1006/meth.2001.1262

Li, X. C., Xiang, Z. Y., Xu, X. M., Yan, W. H., and Ma, J. M. (2009). Endophthalmitis caused by vibrio alginolyticus. *J. Clin. Microbiol.* 47, 3379–3381. doi: 10.1128/JCM.00722-09

Li, X., Zhang, C., Wei, F., Yu, F., and Zhao, Z. (2021). Bactericidal activity of a holin-endolysin system derived from vibrio alginolyticus phage Hh109. *Microb. Pathog.* 159, 105135. doi: 10.1016/j.micpath.2021.105135

Luo, G., Huang, L., Su, Y., Qin, Y., Xu, X., Zhao, L., et al. (2016). Flra, flrb and flrc regulate adhesion by controlling the expression of critical virulence genes in vibrio alginolyticus. *Emerg. Microbes Infect.* 5, 1–11. doi: 10.1038/emi.2016.82

McCarter, L. L. (2004). Dual flagellar systems enable motility under different circumstances. *Microb. Physiol.* 7, 18–29. doi: 10.1159/000077866

McCarter, L., and Silverman, M. (1990). Surface-induced swarmer cell differentiation of vibrio parahaemoiyticus. *Mol. Microbiol.* 4, 1057–1062. doi: 10.1111/j.1365-2958.1990.tb00678.x

Mohamad, N., Mohd Roseli, F. A., Azmai, M. N. A., Saad, M. Z., Md Yasin, I. S., Zulkiply, N. A., et al. (2019). Natural concurrent infection of vibrio harveyi and v. alginolyticus in cultured hybrid groupers in Malaysia. *J. Aquat. Anim. Health* 31, 88–96. doi: 10.1002/aah.10055

Nguyen, A. N., Disconzi, E., Charrière, G. M., Destoumieux-Garzón, D., Bouloc, P., Le Roux, F., et al. (2018). csrB gene duplication drives the evolution of redundant regulatory pathways controlling expression of the major toxic secreted metalloproteases in vibrio tasmaniensis LGP32. *mSphere* 3, e00582–e00518. doi: 10.1128/mSphere.00582-18

Nou, X., Skinner, B., Braaten, B., Blyn, L., Hirsch, D., and Low, D. (1993). Regulation of pyelonephritis-associated pili phase-variation in escherichia coli: Binding of the papi and the lrp regulatory proteins is controlled by dna methylation. *Mol. Microbiol.* 7, 545–553. doi: 10.1111/j.1365-2958.1993.tb01145.x

Oberbeckmann, S., Wichels, A., Wiltshire, K. H., and Gerdts, G. (2011). Occurrence of vibrio parahaemolyticus and vibrio alginolyticus in the German bight over a seasonal cycle. *Antonie Van Leeuwenhoek* 100, 291–307. doi: 10.1007/s10482-011-9586-x

Oliver, J. D., Warner, R. A., and Cleland, D. R. (1983). Distribution of vibrio vulnificus and other lactose-fermenting vibrios in the marine environment. *Appl. Environ. Microbiol.* 45, 985–998. doi: 10.1128/aem.45.3.985-998.1983

O'Toole, G. A. (2011). Microtiter dish biofilm formation assay. *J. Vis. Exp. JoVE* 47, 2437. doi: 10.3791/2437

Ren, C., Hu, C., Jiang, X., Sun, H., Zhao, Z., Chen, C., et al. (2013). Distribution and pathogenic relationship of virulence associated genes among vibrio alginolyticus from the mariculture systems. *Mol. Cell. Probes* 27, 164–168. doi: 10.1016/j.mcp.2013.01.004

Rui, H., Liu, Q., Wang, Q., Ma, Y., Liu, H., Shi, C., et al. (2009). Role of alkaline serine protease, asp, in vibrio alginolyticus virulence and regulation of its expression by luxo-luxr regulatory system. *J. Microbiol. Biotechnol.* 19, 431–438. doi: 10.4014/jmb.0807.404

Swift, S., Lynch, M. J., Fish, L., Kirke, D. F., Tomás, J. M., Stewart, G. S. A. B., et al. (1999). Quorum sensing-dependent regulation and blockade of exoprotease production in aeromonas hydrophila. *Infect. Immun.* 67, 5192–5199. doi: 10.1128/IAI.67.10.5192-5199.1999

Tamplin, M. L., Gauzens, A. L., Huq, A., Sack, D. A., and Colwell, R. R. (1990). Attachment of vibrio cholerae serogroup O1 to zooplankton and phytoplankton of Bangladesh waters. *Appl. Environ. Microbiol.* 56, 1977–1980. doi: 10.1128/aem.56.6.1977-1980.1990

Thaw, P., Sedelnikova, S. E., Muranova, T., Wiese, S., Ayora, S., Alonso, J. C., et al. (2006). Structural insight into gene transcriptional regulation and effector binding by the Lrp/Asnc family. *Nucleic Acids Res.* 34, 1439–1449. doi: 10.1093/nar/gkl009

Toulouse, C., Metesch, K., Pfannstiel, J., and Steuber, J. (2018). Metabolic reprogramming of vibrio cholerae impaired in respiratory NADH oxidation is accompanied by increased copper sensitivity. *J. Bacteriol.* 200, e00761–e00717. doi: 10.1128/JB.00761-17

Toyofuku, M., Inaba, T., Kiyokawa, T., Obana, N., Yawata, Y., and Nomura, N. (2016). Environmental factors that shape biofilm formation. *Biosci. Biotechnol. Biochem.* 80, 7–12. doi: 10.1080/09168451.2015.1058701

Unemoto, T., Hayashi, M., and Terao, K. (1977). Lysis of halophilic vibrio alginolyticus and vibrio costicolus induced by chaotropic anions. *Biochim. Biophys. Acta* 500, 425–431. doi: 10.1016/0304-4165(77)90033-2

Usman, A., Mohammed, S., and Mamo, J. (2021). Production, optimization, and characterization of an acid protease from a filamentous fungus by solid-state fermentation. *Int. J. Microbiol.* 2021, 6685963. doi: 10.1155/2021/6685963

Val, M.-E., Skovgaard, O., Ducos-Galand, M., Bland, M. J., and Mazel, D. (2012). Genome engineering in vibrio cholerae: A feasible approach to address biological issues. *PloS Genet.* 8, e1002472. doi: 10.1371/journal.pgen.1002472

van der Woude, M. W., and Low, D. A. (1994). Leucine-responsive regulatory protein and deoxyadenosine methylase control the phase variation and expression of the sfa and daa pili operons in escherichia coli. *Mol. Microbiol.* 11, 605–618. doi: 10.1111/j.1365-2958.1994.tb00340.x

Vanhove, A. S., Rubio, T. P., Nguyen, A. N., Lemire, A., Roche, D., Nicod, J., et al. (2016). Copper homeostasis at the host vibrio interface: Lessons from intracellular vibrio transcriptomics. *Environ. Microbiol.* 18, 875–888. doi: 10.1111/1462-2920.13083

Wang, X. H., and Leung, K. Y. (2000). Biochemical characterization of different types of adherence of vibrio species to fish epithelial cells. *Microbiol. Read. Engl.* 146 (Pt 4), 989–998. doi: 10.1099/00221287-146-4-989

Wang, Q., Liu, Q., Cao, X., Yang, M., and Zhang, Y. (2008). Characterization of two tonb systems in marine fish pathogen vibrio alginolyticus: Their roles in iron utilization and virulence. *Arch. Microbiol.* 190, 595–603. doi: 10.1007/s00203-008-0407-1

Wang, Q., Liu, Q., Ma, Y., Rui, H., and Zhang, Y. (2007). LuxO controls extracellular protease, haemolytic activities and siderophore production in fish pathogen vibrio alginolyticus. *J. Appl. Microbiol.* 103, 1525–1534. doi: 10.1111/j.1365-2672.2007.03380.x

Watnick, P. I., Lauriano, C. M., Klose, K. E., Croal, L., and Kolter, R. (2001). The absence of a flagellum leads to altered colony morphology, biofilm development and virulence in vibrio cholerae O139. *Mol. Microbiol.* 39, 223–235. doi: 10.1046/j.1365-2958.2001.02195.x

Westrich, J. R., Ebling, A. M., Landing, W. M., Joyner, J. L., Kemp, K. M., Griffin, D. W., et al. (2016). Saharan Dust nutrients promote vibrio bloom formation in marine surface waters. *Proc. Natl. Acad. Sci. U. S. A.* 113, 5964–5969. doi: 10.1073/pnas.1518080113

Yang, B., Zhai, S., Li, X., Tian, J., Li, Q., Shan, H., et al. (2021). Identification of vibrio alginolyticus as a causative pathogen associated with mass summer mortality of the pacific oyster (crassostrea gigas) in China. *Aquaculture* 535, 736363. doi: 10.1016/j.aquaculture.2021.736363

Yao, H., Liu, J., Jiang, X., Chen, F., Lu, X., and Zhang, J. (2021). Analysis of the clinical effect of combined drug susceptibility to guide medication for carbapenem-resistant klebsiella pneumoniae patients based on the Kirby-Bauer disk diffusion method. *Infect. Drug Resist.* 14, 79–87. doi: 10.2147/IDR.S282386

Yildiz, F. H., and Visick, K. L. (2009). Vibrio biofilms: So much the same yet so different. *Trends Microbiol.* 17, 109–118. doi: 10.1016/j.tim.2008.12.004

Yokoyama, K., Ishijima, S. A., Clowney, L., Koike, H., Aramaki, H., Tanaka, C., et al. (2006). Feast/Famine regulatory proteins (ffrps): Escherichia coli lrp, asnc and related archaeal transcription factors. *FEMS Microbiol. Rev.* 30, 89–108. doi: 10.1111/j.1574-6976.2005.00005.x

Yuan, B., Zhao, L.-M., Zhuang, Z.-X., Wang, X.-R., Fu, Q., Huang, H.-B., et al. (2022). Transcriptomic and metabolomic insights into the role of the flgK gene in the pathogenicity of pseudomonas plecoglossicida to orange-spotted grouper (Epinephelus coioides). *Zool. Res.* 43, 952–965. doi: 10.24272/j.issn.2095-8137.2022.216

Zuo, Y., Zhao, L., Xu, X., Zhang, J., Zhang, J., Yan, Q., et al. (2019). Mechanisms underlying the virulence regulation of new vibrio alginolyticus ncrna Vvrr1 with a comparative proteomic analysis. *Emerg. Microbes Infect.* 8, 1604–1618. doi: 10.1080/22221751.2019.1687261

frontiers | Frontiers in Marine Science

TYPE Original Research
PUBLISHED 20 December 2022
DOI 10.3389/fmars.2022.1071371

OPEN ACCESS

EDITED BY
Songzhe Fu,
Dalian Ocean University, China

REVIEWED BY
Xiaojun Zhang,
Yangzhou University, China
Duochun Wang,
National Institute for Communicable Disease Control and Prevention (China CDC), China

*CORRESPONDENCE
Jingfeng Fan
jffan@nmemc.org.cn

SPECIALTY SECTION
This article was submitted to Marine Fisheries, Aquaculture and Living Resources, a section of the journal Frontiers in Marine Science

RECEIVED 16 October 2022
ACCEPTED 06 December 2022
PUBLISHED 20 December 2022

CITATION
Su J, Zhang Y, Hu T, Ming H, Xie Y, Jin Y, Shi T and Fan J (2022) Prevalence, antibiotic and heavy metal resistance of *Vibrio* spp. isolated from the clam *Meretrix meretrix* at different ages in Geligang, Liaohe estuary in China.
Front. Mar. Sci. 9:1071371.
doi: 10.3389/fmars.2022.1071371

Prevalence, antibiotic and heavy metal resistance of *Vibrio* spp. isolated from the clam *Meretrix meretrix* at different ages in Geligang, Liaohe estuary in China

Jie Su[1], Yingxue Zhang[1], Tian Hu[2], Hongxia Ming[1], Yuyang Xie[1,3], Yuan Jin[1], Tingting Shi[1] and Jingfeng Fan[1]*

[1]State Environmental Protection Key Laboratory of Coastal Ecosystem, National Marine Environmental Monitoring Center, Dalian, China, [2]College of Marine Technology and Environment, Dalian Ocean University, Dalian, China, [3]College of Marine Ecology and Environment, Shanghai Ocean University, Shanghai, China

Vibrio as one of the main pathogens of shellfish diseases can cause serious human seafoodborne gastroenteritis and even death. In this study, we analyzed the bacterial communities from the clam, and compared the resistance phenotypes and genotypes of *Vibrio* spp. from *Meretrix meretrix* at different growth stages. High-throughput sequencing analysis revealed the predominance of *Proteobacteria* (50%) in the bacterial community and *Vibrio* was one of the dominant genera in the clam hepatopancreas in the summer. *Vibrio* abundance in *Meretrix meretrix* positively correlated with the water temperature ($p<0.05$). A total of 73 *Vibrio* isolates from *Meretrix meretrix* were classified into 19 species and the dominant strains included *V. mediterranei* (19%) and *V. harveyi* (11%), *V. algolyticus* (10%), and *V. parahaemolyticus* (8%). The species and abundance of *Vibrio* spp. were the highest in the 3-year-old of *Meretrix meretrix* compared with clams of other ages in the summer. Among the 73 isolates, 68 *Vibrio* strains were resistant to other 15 antibiotics except for sulfamethoxazole-trimethoprim with 57 resistant phenotypes. The most prevalent resistance was toward clindamycin (76%), followed by amikacin (63%), ampicillin (62%), rifampicin (62%), vancomycin (57%), and amoxicillin (50%). The ARI values of *Vibrio* spp. in different ages ranged from 0.13 to 0.18, and ARI values of 3-year-old (ARI=0.18) clams are higher than that of other ages clam. Approximately 72% of the resistant isolates showed multidrug-resistant phenotypes with maximum resistance to 15 antibiotics. Tolerance to heavy metals including Cd, Zn, and Cu was detected in the majority of antibiotic resistant isolates. In addition to the co-resistance to the same class of antibiotics, resistance to cephalosporin (CFP, CEP, CZ) were significantly correlated with penicillins (AMP, AMC) ($p< 0.01$), tetracycline ($p < 0.001$), sulfanilamide (SXT) ($p< 0.01$) and quinolone (CIP) ($p< 0.01$). The heavy metal

resistance genes *copB* and *nccA* were significantly correlated with the clindamycin resistance phenotype ($p<0.01$). This study revealed that the habitat of *Meretrix meretrix* is in low exposure to antibiotics, and a link between heavy metal resistance genes and antibiotic resistance.

KEYWORDS

prevalence, antibiotic resistance, heavy metal resistance, *Vibrio* spp., *Meretrix meretrix*

1 Introduction

Shellfish mainly inhabit coastal and estuarine environments. Due to the nature of their habitats, shellfish contain a variety of bacterial microbiota, including the *Vibrio* spp. (Romalde et al., 2014). *Vibrio* is a Gram-negative bacterium with genetic and metabolic diversity and is an integral part of the global marine ecosystem (Thompson et al., 2004). *Vibrio* seriously affects shellfish farming. Moreover, it poses a potential danger to humans due to its high detection rate in shellfish farming. Twenty different pathogenic *Vibrio* species can cause large-scale death of shellfish. *Vibrio* infection-related diseases usually include gastrointestinal disorders with symptoms like diarrhea, abdominal cramps, nausea, vomiting, and fever (CDC, 2019b). These symptoms may occur within 24 h of ingestion and last for three days. Patients with low immunity or underlying diseases are at a higher risk of death (CDC, 2019a).

Presently, more than 120 species of *V*ibrio have been found; at least 12 species are known to cause human diseases. The list includes *Vibrio alginolyticus*, *Vibrio cincinnatiensis*, *Vibrio damsela*, *Vibrio fluvialis*, *Vibrio furnisii*, *Vibrio metschnikovii*, *Vibrio mimicus*, *Vibrio cholerae*, *Vibrio parahaemolyticus*, etc. (Oliver, 2015; Economopoulou et al., 2017; Huang et al., 2017; Zago et al., 2017). Antibiotics are often used to prevent and cure aquaculture diseases in recent years. However, the aquaculture industry lacks relevant drug regulations leading to the overuse of antibiotics. Consequently, the *Vibrio* develop antibiotic resistance, increasing the difficulty of treating human infections (Alsalem et al., 2018; Miranda et al., 2018). *Vibrio* spp. also showed resistant to the most clinically used antibiotics (Mala et al., 2014; Letchumanan et al., 2015). The incidence of human *Vibrio* infection and the drug resistance rate of drug-resistant bacteria are also increasing (Kitaoka et al., 2011). Therefore, it is imperative to detect pathogenic *Vibrio* in aquatic products and prevent food poisoning. The sudden outbreak of *Vibrio* will seriously affect marine biomass and cause severe economic loss to aquaculture (Moffitt and Cajas-Cano, 2014).

China remains the first major producer of fisheries and aquaculture in the world, with a 35 percent share of the total (FAO (Food and Agriculture Organization, 2022). In 2020, China's mariculture area covered 1996 thousand hectares. The shellfish occupied 1197 thousand hectares, accounting for 59.99% of the mariculture area. *Meretrix meretrix* is a beach-buried shellfish widely distributed in both the north and south coastal regions of China, especially in the estuary and tidal flat, such as Liaoning, Shandong, Jiangsu, and Guangxi. *Meretrix meretrix* grows in a wide range of temperatures and salinity and mainly feeds on planktonic and benthic diatoms. In 2020, the output of clam mariculture from the Liaoning Province was 1.353 million tons, and the area encompassed was 1,53,000 hectares, ranking first in China and far exceeding that of the other provinces (Ministry of Agriculture and Rural Affairs Fisheries Bureau et al., 2021). *Meretrix meretrix* is currently an important economic shellfish in the coastal mudflat culture in China. However, due to intensified aquaculture and the increasing eutrophication of coastal mudflats, *Vibrio* spp. as one of the primary pathogen have caused serious harm to the clam aquaculture industry and food safety (Li et al., 2018).

Geligang, as one of the important producing areas of clams *Meretrix meretrix* in northern China, is located in the east of Liaohe estuary, with an area of about 10000 ha. The annual output of *Meretrix meretrix* in Geligang area is more than 1000 t. In this study, we investigate the differences in the diversity and abundance of *Vibrio* isolated from *Meretrix meretrix*, and analyze antibiotic resistance and heavy metal resistance of *Vibrio* spp. in *Meretrix meretrix* at different ages in Geligang, Liaohe estuary in China. This study will support the need for food safety risk assessment of aquatic products.

2 Materials and methods

2.1 Sample collection

Meretrix meretrix samples of different ages were collected from the Geligang aquaculture area in Liaohe estuary in the spring (April), summer (July, August), and autumn (November) of 2019. The 1-year-old and 2-year-old clams were collected in spring. The 1-year-old, 2-year-old, 3-year-old, and 5-year-old of

clams were collected in the summer. The 1-year-old, 2-year-old, 3-year-old, and 5-year-old clams were collected in autumn. The collected samples were stored in sterile plastic bags at 4°C and transported to the laboratory for analysis within 24 h. Water temperature and salinity were measured *in situ* by the YSI ProQuatro Handheld Multiparameter Instrument (YSI, Xylem Inc., NY, USA).

2.2 Isolation and identification of the *Vibrio* strains

The samples of *Meretrix meretrix* were divided according to different growth cycles. The hepatopancreas samples of the same age were mixed by three independent samples, and 2–5 groups of parallel samples were set aside for preservation. The clam samples were washed with sterile saline. The clam hepatopancreas (200 g) samples were homogenized in phosphate-buffered saline (PBS; 2.5 mM KH_2PO_4; pH-7.2) with a blender and subsequently serially diluted with PBS. The homogenate diluents were further plated on Thiosulfate-Citrate-Bile Salts-Sucrose Agar (TCBS Agar; Oxoid, Thermo Fischer Scientific, UK) and incubated at 37°C for 24 h. The presumptive colonies on the TCBS agar plates were re-streaked on Tryptone Soy Agar (Oxoid, Thermo Fischer Scientific, UK) supplemented with 3% Sodium Chloride (TSA + 3% NaCl) and incubated at 37°C for 24 h to achieve a pure isolate (Sujeewa et al., 2009). *Vibrio* isolates were identified by PCR and sequencing of16S rDNA. Chromosomal DNA from the *Vibrio* cells were extracted using a QIAGEN DNA extraction kit following the manufacturer's instructions. 16S rRNA gene amplification and DNA purification were determined as described previously (Park et al., 2018) and sequenced by Sangon Biotech (Shanghai) Co., Ltd. (China). The obtained consensus sequences were subjected to BLAST search at NCBI (http://www.ncbi.nlm.nih.gov/pubmed) for sequence alignment analysis.

2.3 High-throughput sequencing

The genomic DNA was extracted from the clam hepatopancreas using the DNeasy Power Water Total DNA Isolation Kit (QIAGEN, Germany). Bacterial communities were identified using the 16S rRNA gene sequencing technology from Shanghai Personalbio Technology Co., Ltd. (China). The V3-V4 regions of the 16S rRNA gene were amplified using barcodes. The 175 primer sets with the forward primer 341F (5'-CCTACGGGNGGCWGCAG-3') and the reverse primer 765R with 176 primer sets (5'-GACTACNVGGGTATCTAAT-3') were used for sequencing. The PCR amplification was performed using the Pfu high-fidelity DNA polymerase (TransGen Biotech), and purification and recovery were managed with magnetic beads. The fluorescence of the PCR amplification product was quantified on the Fluorescence Microplate reader (BioTek, FLx800). The fluorescent reagent was used from the Quant-iT PicoGreen dsDNA Assay Kit. The sequencing library was prepared using the TruSeq Nano DNA LT Library Prep Kit (Illumina, Inc. (USA)). The community DNA fragments were sequenced using the Paired-end Illumina MiSeq platform.

2.4 Antimicrobial susceptibility and heavy metal resistance tests of the *Vibrio* isolates

The antimicrobial susceptibility of the *Vibrio* isolates was determined from the disk diffusion method according to the Clinical and Laboratory Standards Institute guidelines (Clinical Laboratory Standard Institute, 2016). The isolates were tested for susceptibility toward 16 antimicrobials: Cefazolin (CZ, 30 μg), Cephalotin (CEP, 30 μg), Cefoperazone (CFP, 75 μg), Cefuroxime (CXM, 30 μ g), Ampicillin (AMP, 10 μg), Amoxicillin (AMC, 10 μg), Streptomycin (STR, 10 μg), Gentamicin (GM, 10 μg), Amikacin (AN, 30 μ g), Sulfamethoxazole-Trimethoprim (SXT, 23.75–1.25 μg), Ciprofloxacin (CIP, 5 μg), Clindamycin (DA, 2 μg), Vancomycin (VA, 30 μg), Tetracycline (TCY, 30 μg), Erythromycin (ERY, 15 μg), and Rifampicin (RFP, 5 μg). The results were interpreted as susceptible (S), intermediate (I), and resistant (R) after 12 h of incubation at 30°C using the CLSI standards. Multiple Antibiotic Resistant (MAR) strain is defined as a bacterium resistant to three or more antibiotics (Manjusha et al., 2005). Antibacterial Resistance Index (ARI) was used to analyze the prevalence of resistant isolates from clam and calculated for the same age (Mohanta and Goel, 2014).

The heavy metal resistance of the *Vibrio* isolates was determined according to a previous method (Kang et al., 2016). The minimal inhibitory concentration (MIC) of the tested heavy metals against the isolates was measured using broth dilution testing (Clinical Laboratory Standard Institute, 2016). The heavy metals used in this study were $CdCl_2$, $ZnCl_2$, and $CuCl_2$.

2.5 Detection of antibiotic resistance genes and heavy metal resistance genes

From the results of the antibiotic and heavy metal resistance phenotypes of *Vibrio*, 13 resistant genes were selected. The six antibiotic resistance genes included the penicillins resistance gene(*ampR*), aminoglycosides resistance gene (*aadA*, *strA*, and *strB*) and glycopeptides resistance gene(*vanM*). The heavy metal resistance genes included *copA*, *copB*, and *copC* genes for Cu^{2+}, *nccA* and *cadD* genes for Cd^{2+}, and *zntA* and *zntB* resistance genes for Zn^{2+}. The primers and PCR conditions are presented in Table S1 (Sambrook, 2001; Kamika and Momba, 2013; Jiang

et al., 2014; Liu et al., 2014; Liu, 2016; Wu et al., 2019; Yang et al., 2020).

2.6 Statistical analyses

The statistical analyses of alpha diversity, beta diversity and differentially abundant taxa were carried out using QIIME2 2019.4. Pearson's correlation analysis was used to evaluate the relationship between the antibiotic resistant phenotypes and antibiotic resistant genotypes with SPSS version 25 (IBM, Armonk, NY, USA). p value < 0.05 was considered statistically significant.

3 Results

3.1 Microbial community analysis

3.1.1 Microbial alpha diversity

The alpha diversity was determined for each treatment and different seasons. The Good's Coverage index of 24 clam samples of different ages was >0.99, which means more than 99% of the species diversity was detected with a high coverage (Table S2). The Chao1, Shannon, and Simpson indices showed a trend of first increasing and then decreasing. The highest value was reached in the 3-year-old clams collected in August, and those collected in autumn contributed the lowest. The Chao1 index between the samples in spring and autumn (p <0.05) differed significantly; the Shannon and Simpson indices did not show a seasonal difference. The changing trend of the Good's Coverage index was autumn>spring>summer, indicating the difference in the sequencing coverage of samples in the four months. The samples in spring and summer were significantly different from those in autumn (p<0.05). Therefore, significant differences existed in the community richness but not in community diversity among the clam samples collected during different seasons (see Table 1; Figure 1).

3.1.2 Beta diversity

Beta diversity was used to analyze the similarities and differences in the structure of two or more communities. Only the 1-year-old and 2-year-old of *Meretrix meretrix* were detected in three seasons. Hence, the beta diversity analysis was conducted

TABLE 1 *Vibrio* spp. of clams in different ages.

Vibrio spp.	% of Vibrio spp.(No. of Isolates)			
	1-year-old (n=10)	2-year-old (n=10)	3-year-old (n=46)	5-year-old (n=7)
V. pacinii	10(1)	–	–	–
V. harveyi	20(2)	10(1)	8(4)	14(1)
V. mediterranei	40(4)	10(1)	15(7)	29(2)
V. tubiashii	–	20(2)	4(2)	–
V. campbellii	–	10(1)	4(2)	29(2)
V. parahaemolyticus	10(1)	20(2)	6(3)	–
V. brasiliensis	–	–	6(3)	14(1)
V. rotiferianus	10(1)	–	4(2)	14(1)
V. shilonii	10(1)	–	–	–
V. jasicida	–	10(1)	–	–
V. pelagius	–	20(2)	2(1)	–
V. hangzhouensis	–	–	8(4)	–
V. nereis	–	–	2(1)	–
V. alginolyticus	–	–	15(7)	–
V. diabolicus	–	–	8(4)	–
V. neocaledonicus	–	–	6(3)	–
V. natriegens	–	–	2(1)	–
V. azureus	–	–	2(1)	–
V. coralliilyticus	–	–	2(1)	–

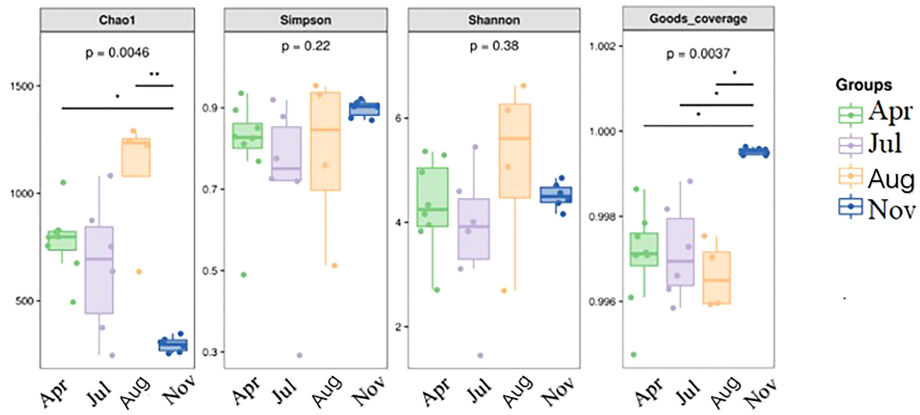

FIGURE 1
Differences in the Alpha Diversity Index of *Meretrix meretrix* Samples during different seasons.

only for the community structures of the 1-year-old and 2-year-old of *Meretrix meretrix*. Principal Coordinate Analysis (PCoA) revealed that the dissimilarities in community structure existed in different ages of *Meretrix meretrix*. Seasonal differences were prevalent in the bacterial community of the clam at the same age (see Figure 2).

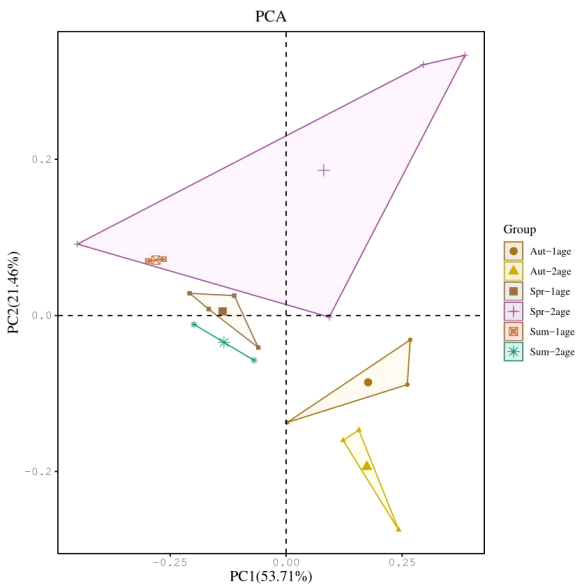

FIGURE 2
Comparison of the microbial community structures of *Meretrix meretrix* samples of the same age. Principal Coordinate Analysis (PCoA) of the 16S rRNA gene sequences using Bray-Curtis difference grouped by treatment.

3.1.3 Changes in the microbial community structure at different ages

Based on the high-throughput sequencing results, the dominant flora in the *Meretrix meretrix* included *Proteobacteria* (50%), *Firmicutes* (11%), *Bacteroides* (4%), *Spirochaetes* (1%), and *Cyanobacteria* (1%). *Proteobacteria* mainly included α- *Proteobacteria* (19%), γ- *proteobacteria* (19%), β- *Proteobacteria* (9%), and δ- *Proteobacteria* (0.5%).

The clam samples collected in the spring mainly comprised *Halomonas*, *Devosia*, *Cuprum*, *Lactobacillus*, *Paleobacterium* (1%), *Rhizobium* (1%), and *Sphingomonas* (1%). The dominant bacteria in the clam samples collected in the summer (July) included *Vibrio*, *Halomonas*, *Cuprum*, *Devosia*, *Palebacterium*, *Acinetobacter*, *Sphingomonas*, and *Seminibacterium*. The clam samples collected in mid-summer (August) mainly had *Vibrio* and *Palebacterium*. The dominant bacteria in the clam samples collected in autumn included *Ralstonia solanacearum*, *Devosia*, *Halomonas*, *Palebacterium*, *Pelomonas*, *Actinobacteria*, *Enterobacter*, *Staphylococcus*, sediment *Bacilli*, *Rhizobium*, and *Pseudomonas* (see Figure 3).

Vibrio accounted for 0.003%, 8%, 11%, and 0.1% of the bacterial community composition in the spring (April), summer (July), summer (August), and autumn (November), respectively. Thus, the *Vibrio* abundance in the clam samples increased first and then decreased with change in the season; it was the highest in summer. The relative abundance of *Vibrio* was the highest in the 3-year-old *Meretrix meretrix* in summer. *Ralstonia* caused the significant differences in the species abundance among the *Meretrix meretrix* during different seasons.

3.2 The abundance and species of *Vibrio*

The concentration of the culturable bacteria in the clam hepatopancreas ranged from 2.83×10^3 - 1.18×10^5 CFU/g in the

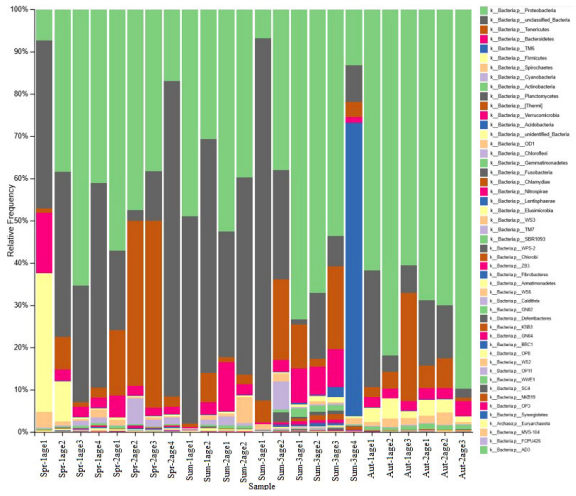

FIGURE 3
Bacterial community composition at the phylum level.

spring, summer, and autumn. The abundance of the culturable bacteria increased first and then decreased with the season. The bacterial abundance was the highest in summer, 1–2 orders of magnitude higher than in spring. In the same season, the abundance of the culturable bacteria in the hepatopancreas of the clams of different ages was different. The quantity of the culturable bacteria in the 1-year-old and 2-year-old of *Meretrix meretrix* collected during the spring, summer, and autumn differed by 2 and 1 orders of magnitude, respectively. Thus, the abundance of the culturable bacteria in the younger *Meretrix meretrix* was more susceptible to seasonal changes. There was a significant positive correlation between the abundance of the culturable bacteria and temperature ($p<0.05$).

Vibrio abundance in the clam hepatopancreas ranged from 33 to 1.10×10^5 CFU/g in the spring, summer, and autumn. The abundance of the *Vibrio* and culturable bacteria in the clam hepatopancreas showed the same seasonal variation trend, reaching the highest in summer. The ratio of the logarithmic abundance of *Vibrio* to culturable bacteria also increased first and then decreased with the season, ranging from 0.36 – 0.99. Moreover, the ratio reached the maximum in summer, ranging from 0.63 – 0.99, indicating that *Vibrio* was the dominant bacteria in the clam hepatopancreas in summer (see Figure 4).

The 16S rRNA gene sequencing technology identified 170 bacterial isolates, and a total of 73 *Vibrio* isolates of 19 species were obtained. *Vibrio mediterranei* (19%), *V. harveyi* (11%), *V. algolyticus* (10%), and *V. parahaemolyticus* (8%) were the dominant species. Among them, the 1-year-old, 2-year-old, 3-year-old, and 5-year-old of *Meretrix meretrix* contained 6, 7, 16, and 5 species of *Vibrio*, respectively. The species and number of *Vibrio* isolates in the 3-year-old of *Meretrix meretrix* were the highest (63%).

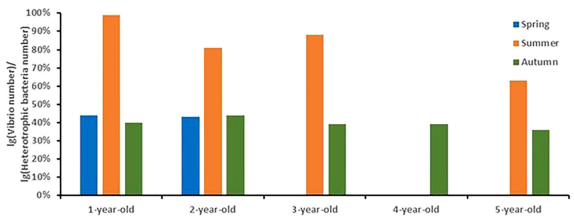

FIGURE 4
Seasonal variation of *Vibrio* spp. abundance in *Meretrix meretrix* at Different Ages.

3.3 Resistant phenotype analysis

All *Vibrio* isolates(n=73) were sensitive to sulfamethoxazole-trimethoprim. Among the 73 isolates, 68 *Vibrio* strains were resistant to other 15 antibiotics with 57 resistant phenotypes. *Vibrio* showed relatively high resistance to clindamycin (76%), amikacin (63%), ampicillin (62%), rifampicin (62%), vancomycin (57%) and amoxicillin (50%), respectively (Table 2). The ARI values of *Vibrio* spp. in different ages ranged from 0.13 to 0.18, and ARI values of 2-year-old (ARI=0.17) and 3-year-old (ARI=0.18) clams are higher than that of 1-year-old and 5-year-old clams. Forty-nine MAR *Vibrio* has been detected in the clams of different ages, and the proportion of MAR *Vibrio* in the clams at the 3-year-old is the highest (91%) compared with samples of other ages (Figure 5). Among the 49 multiple antibiotic-resistant isolates from the clam, 43 isolates were resistant to three to ten antibiotics and 1 isolate was resistant up to 15 antibiotics(Table S3). Sixteen isolates (24%) and fifteen isolates (22%) from clam samples showed resistance to four antibiotics and two antibiotics with high prevalence, respectively.

The MIC values of the 73 *Vibrio* strains for Cd^{2+}, Cu^{2+}, and Zn^{2+} metal ions were 25 – 125 mg/L, 25 - 300 mg/L, and 50 - 400 mg/L, respectively. The maximum MIC value of *Vibrio* showed the order of $Cd^{2+} < Cu^{2+} < Zn^{2+}$. The tolerance of *Vibrio* to Zn^{2+} increased with age (Table S4).

3.4 Resistant genotype analysis

Based on the results of the antibiotic-resistant phenotypes and heavy metal-resistant phenotypes of the 73 *Vibrio* strains, 13 associated resistance genes were selected for detection. The resistance genes with a higher detection rate were *nccA* (14%), *aadA* (14%), and *copB* (12%) (Table S5). The *copB* (20.00%) and *nccA* (20.00%) genes were the frequently detected resistant genes in the 1-year-old clam. The 2-year-old clam showed more resistance toward the *copA* (30.00%), *ampR* (20.00%), and *strA*

TABLE 2 Antibiotic resistance phenotypes of *Vibrio* isolates from *Meretrix meretrix* in different age.

Antibiotics		% of Resistance (No. of Isolates)			
		1-year-old (n=10)	2-year-old (n=10)	3-year-old (n=46)	5-year-old (n=7)
Cephalosporin	CZ	0	20(2)	35(16)	0
	CEP	0	10(1)	33(15)	0
	CFP	0	0	17(8)	0
	CXM	0	10(1)	20(9)	0
Penicillins	AMP	50(5)	50(6)	61(28)	43(3)
	AMC	30(3)	40(3)	54(25)	43(3)
Aminoglycosides	STR	0	10(1)	26(12)	14(1)
	GM	0	10(1)	30(14)	0
	AN	40(4)	70(7)	67(31)	14(1)
Sulfanilamide	SXT	0	0	0	0
	CIP	0	0	20(9)	0
Lincomycin	DA	30(3)	50(5)	93(43)	14(1)
Glycopeptides	VA	60(6)	60(6)	56(26)	14(1)
Tetracyclines	TCY	0	10(1)	6(3)	0
Macrolides	ERY	0	0	11(5)	0
Ansamycins	RFP	40(4)	30(3)	72(33)	0
Total		100(10)	100(10)	96(44)	57(4)

(20.00%) genes. The 5-year-old clam showed more resistance toward the *copA* (14%), *nccA* (14%), and *zntB* (14%) genes.

In addition to the co-resistance to the same class of antibiotics, resistance to cephalosporin (CFP, CEP, CZ) were significantly correlated with penicillins (AMP, AMC) ($p< 0.01$), tetracycline ($p < 0.001$), sulfanilamide (SXT) ($p< 0.01$) and quinolone (CIP) ($p< 0.01$). Aminoglycoside (GM) resistance phenotype is closely correlated with quinolone (CIP) resistance phenotype ($p < 0.001$). The bla_{SHV} gene was positively correlated with *aadA*, *ampR* and *cadD* gene ($p<0.01$). The *strA* gene was positively correlated with *sul1*($p<0.01$), *qnrS* ($p<0.01$) and *tetB* ($p<0.05$), and negatively correlated with *qyrA* ($p<0.05$). The *copA* was significantly correlated with *strB*, *ermC* and qnr_{VC457} ($p<0.01$). The heavy metal resistance genes *copB* and *nccA* were significantly correlated with the clindamycin resistance phenotype ($p<0.01$) (Figure 6).

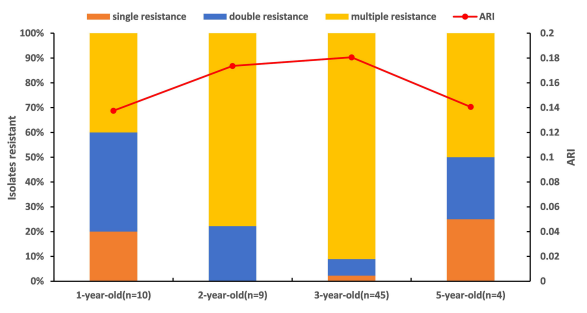

FIGURE 5
Prevalence of resistant *Vibrio* spp. and antibiotic resistance index (ARI) from clam *Meretrix meretrix* in different ages. Single resistance: resistance to one antibiotic; Double resistance: resistance to two antibiotics; Multiple resistance: resistance to three or more antibiotics.

Discussion

Temperature predicts *Vibrio* abundance quite well (Thompson et al., 2004). The prevalence of *V. parahaemolyticus*, *Vibrio vulnificus*, and *V. mimicus* in the environment positively correlated with temperature (León Robles et al., 2013). In this study, the temperature was higher in the summer (July and August), and lower in the spring (April) and autumn (November). The abundance of *Vibrio* in *Meretrix meretrix* in the summer was higher than in the spring and autumn. *Vibrio* was the dominant bacteria in the clam hepatopancreas in the summer, and there was a significant positive correlation between *Vibrio* abundance and temperature ($p<0.05$). Our results were consistent with a previous study demonstrating the increase in *Vibrio*

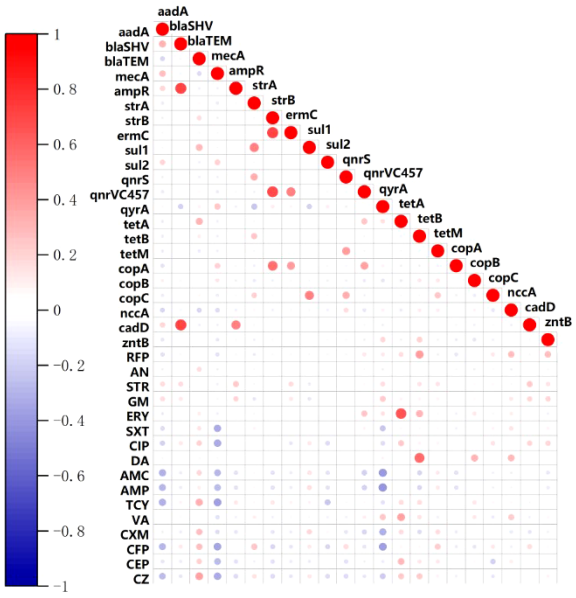

FIGURE 6
Correlation between the resistant phenotype and resistant genotype of *Vibrio* spp.

abundance upon an increase in the temperature within a certain temperature range (Cruz et al., 2016).

Some studies found the greater prevalence of *V. alginolyticus*, *V. cholerae*, *Vibrio communis*, and *V. parahemolyticus* among all the *Vibrio* spp. isolated from the clams (Yücel and Balci, 2010; Adebayo-Tayo et al., 2011; Amalina et al., 2019; Abdalla et al., 2022). However, our study indicated the predominance of *V. mediterranei* in the *Vibrio* spp. of the clams. The difference in the dominant *Vibrio* species may be due to different sites or locations of shellfish collection. *Vibrio* is an indigenous marine bacterium (Hsiao and Zhu, 2020), and not all *Vibrio* variants are pathogenic (Song et al., 2017). However, three other dominant pathogenic *Vibrio*, including *V. harveyi*, *V. algolyticus*, and *V. parahaemolyticus*, were also detected in this study. *V. parahaemolyticus* is the major *Vibrio* species causing human illness and has emerged as a severe global threat to human health through the consumption of raw or undercooked seafood (Yue et al., 2010; Yue et al., 2011; Silva et al., 2018; Park et al., 2019). *V. harveyi* is reported to be the primary pathogen of cultured prawns (Stalin and Srinivasan, 2016).

The antibiotic resistance of *Vibrio* in marine resources is a major global concern for human health (Yang et al., 2017; Silva et al., 2018). The current results showed that 73 *Vibrio* strains were resistant to 15 other antibiotics except for sulfamethoxazole-trimethoprim. This observation was consistent with a previous study (Abdalla et al., 2022). Moreover, clindamycin (76%), amikacin (63%), ampicillin (62%), rifampicin (62%), vancomycin (57%) and amoxicillin (50%) resistance were very prevalent among the *Vibrio* isolates in this study. High prevalence of resistances to ampicillin and rifampicin have also been reported in *Vibrio* isolated from many aquatic products in different regions of the world (Obaidat et al., 2017), which indicating the existence of intrinsic resistance to these antibiotics (Su and Chen, 2020).

ARI is usually used to analyze the prevalence of bacterial resistance in a given population at a specific sites (Mohanta and Goel, 2014). When ARI value >0.2,it means that the isolates are exposed to contamination where antibiotics are often used, and when ARI ≤0.2,it means that antibiotics are seldom or never used (Krumperman, 1983). The ARI value of *Vibrio* in *Meretrix meretrix* at all ages was less than 0.2, indicating that the antibiotic level in the meretrix was low. A higher ARI value is detected in the 2-year-old and 3-year-old clams compared to the other ages, indicating the 2-year-old and 3-year-old clams may be more susceptible to antibiotic contamination.

Due to the toxicity, non-biodegradability and bioaccumulation of heavy metals in the food chain, heavy metal pollution is considered as a serious threat to aquatic ecosystems and human health (Diagomanolin et al., 2004). Geligang is reported to have suffered from heavy metal pollution, including zinc, copper and cadmium (Zhang et al., 2016). In this study, our results showed that the heavy metals Cd^{2+}, Cu^{2+}, and Zn^{2+} were tolerated in the majority of the *Vibrio* isolates, which may be explained by the existence of these three heavy metal ions in Geligang. Moreover, the concentration of these three heavy metal ions in the clam may be higher due to the enrichment of the clam itself. About 70% of the *Vibrio* isolates with conjugative elements (ICEs) derived from Yangtze River Estuary displayed strong resistance to Hg (≥1 mM) and Cr (≥10 mM), and the heavy metal contamination is relatively serious in Yangtze River Estuary in China (Song et al., 2013). The tolerance to heavy metals was also found to be prevalent in the V. parahaemolyticus strains with more than two antibiotic resistance phenotypes (Kang et al., 2018), which is consistent with our results. Indeed, the co-resistance between antibiotic resistance and heavy metal resistance has been well confirmed in many studies (Zhao et al., 2012; Kang et al., 2018).

Data availability statement

The data presented in the study are deposited in the NCBI repository, accession number PRJNA901517.

Author contributions

JF: conceptualization. JS and YZ: experimental operation. JS, YZ and TH: manuscript writing. JF and JS: review and acquisition of funding. HM and TS: field sampling. YX and YJ: data analysis. All authors contributed to the article and approved the submitted version.

Funding

This work was supported by the Dalian High Level Talent Innovation Support Plan (2021RD04); Open Project of National Key Laboratory of Environmental Monitoring Quality Control for Environmental Protection (KF202209); the National Key R & D Program of China (Grant 2020 YFA0607601); Millions of Talent Projects of Liaoning Province, China.

Conflict of interest

The authors declare that the research was conducted in the absence of any commercial or financial relationships that could be construed as a potential conflict of interest.

Publisher's note

Supplementary material

The Supplementary Material for this article can be found online at: https://www.frontiersin.org/articles/10.3389/fmars.2022.1071371/full#supplementary-material

References

Abdalla, T., Al-Rumaithi, H., Osaili, T. M., Hasan, F., Obaid, R. S., Abushelaibi, A., et al. (2022). Prevalence, antibiotic-resistance, and growth profile of vibrio spp. isolated from fish and shellfish in subtropical-arid area. *Front. Microbiol.* 13. doi: 10.3389/fmicb.2022.861547

Adebayo-Tayo, B. C., Okonko, I. O., Esen, C. U., Odu, N. N., Onoh, C. C., and Igwiloh, N. J. P. (2011). Incidence of potentially pathogenic *Vibrio* spp. in fresh seafood from itu creek in uyo, akwa ibom state, Nigeria. *World Appl. Sci. J.* 15 (7), 985–991. doi: 10.1016/j.jip.2009.11.008

Alsalem, Z., Elhadi, N., Aljeldah, M., Alzahrani, F., and Nishibuchi, M. (2018). Characterization of *Vibrio* vulnificus isolated from the coastal areas in the Eastern province of Saudi Arabia. *J. Pure Appl. Microbiol.* 12, 1355–1364. doi: 10.22207/JPAM.12.3.38

Amalina, N. Z., Santha, S., Zulperi, D., Amal, M. N. A., Yusof, M. T., Zamri-Saad, M., et al. (2019). Prevalence, antimicrobial susceptibility and plasmid profiling of vibrio spp. isolated from cultured groupers in peninsular Malaysia. *BMC Microbiol.* 19, 251. doi: 10.1186/s12866-019-1624-2

CDC (2019a) *Vibrio species causing vibriosis–people at risk*. Available at: www.cdc.gov/vibrio/people-at-risk.html (Accessed October 15 2021).

CDC (2019b) *Vibrio species causing vibriosis–symptoms*. Available at: https://www.cdc.gov/vibrio/symptoms.html (Accessed October 15 2021).

Clinical Laboratory Standard Institute (2016). *Performance standards for antimicobial susceptibility testing: Seventeenth informational supplement M100-S17* (PA, USA: Wayne).

Cruz, C. D., Chycka, M., Hedderley, D., and Fletcher, G. C. (2016). Prevalence, characteristics and ecology of *Vibrio vulnificus* found in new Zealand shellfish. *J. Appl. Microbiol.* 120 (4), 1100–1107. doi: 10.1111/jam.13064

Diagomanolin, V., Farhang, M., Ghazi-Khansari, M., and Jafarzadeh, N. (2004). Heavy metals (Ni, cr, Cu) in the karoon waterway river, Iran. *Toxicol. Lett.* 151 (1), 63–68. doi: 10.1016/j.toxlet.2004.02.018

Economopoulou, A., Chochlakis, D., Almpan, M. A., Sandalakis, V., Maraki, S., Tselentis, Y., et al. (2017). Environmental investigation for the presence of *Vibrio* species following a case of severe gastroenteritis in a touristic island. *Environ. Sci. pollut. Res.* 24 (5), 4835–4840. doi: 10.1007/s11356-016-8231-7

Food and Agriculture Organization (2022). *The state of world fisheries and aquaculture 2022. towards blue Transformation0* (Rome: FAO).

Hsiao, A., and Zhu, J. (2020). Pathogenicity and virulence regulation of *Vibrio cholerae* at the interface of host-gut microbiome interactions. *Virulence* 11 (1), 1582–1599. doi: 10.1080/21505594.2020.1845039

Huang, Y., Du, P., Zhao, M., Liu, W., Du, Y., Diao, B., et al. (2017). Functional characterization and conditional regulation of the type VI secretion system in *Vibrio fluvialis*. *Front. Microbiol.* 8. doi: 10.3389/fmicb.2017.00528

Jiang, Y., Yao, L., Zhai, Y., and Wang, L. (2014). Studies on molecular mechanism of a multi-drug resistant *Vibrio parahaemolyticus* strain. *J Food Saf. &Quality* 5 (1), 77–82. doi: 10.19812/j.cnki.jfsq11-5956/ts.2014.01.014

Kamika, I., and Momba, M. N. B. (2013). Assessing the resistance and bioremediation ability of selected bacterial and protozoan species to heavy metals in metal-rich industrial wastewater. *BMC Microbiol.* 13, 28. doi: 10.1186/1471-2180-13-28

Kang, C. H., Shin, Y., Kim, W., Kim, Y., Song, K., Oh, E.-G., et al. (2016). Prevalence and antimicrobial susceptibility of *Vibrio parahaemolyticus* isolated from oysters in Korea. *Environ. Sci. pollut. Res.* 23 (1), 918–926. doi: 10.1007/s11356-015-5650-9

Kang, C. H., Shin, Y., Yu, H., Kim, S., and So, J. S. (2018). Antibiotic and heavy-metal resistance of *Vibrio parahaemolyticus* isolated from oysters in Korea. *Mar. pollut. Bull.* 135, 69–74. doi: 10.1016/j.marpolbul.2018.07.007

Kitaoka, M., Miyata, S. T., Unterweger, D., and Pukatzki, S. (2011). Antibiotic resistance mechanisms of *Vibrio cholerae*. *J. Med. Microbiol.* 60 (4), 397–407. doi: 10.1099/jmm.0.023051-0

Krumperman, P. H. (1983). Multiple antibiotic resistance indexing of escherichia coli to identify high-risk sources of fecal contamination of foods. *Appl. Environ. Microbiol.* 46 (1), 165–170. doi: 10.1128/aem.46.1.165-170.1983

León Robles, A., Acedo Félix, E., Gomez-Gil, B., Quiñones Ramírez, E. I., Nevárez-Martínez, M., and Noriega-Orozco, L. (2013). Relationship of aquatic environmental factors with the abundance of *Vibrio cholerae*, *Vibrio parahaemolyticus*, *Vibrio mimicus* and *Vibrio vulnificus* in the coastal area of guaymas, Sonora, Mexico. *J. Water Health* 11 (4), 700–712. doi: 10.2166/wh.2013.160

Letchumanan, V., Yin, W.-F., Lee, L.-H., and Chan, K.-G. (2015). Prevalence and antimicrobial susceptibility of *Vibrio parahaemolyticu* s isolated from retail shrimps in Malaysia. *Front. Microbiol.* 6. doi: 10.3389/fmicb.2015.00033

Liu, X. (2016). *Investigation on Antimicrobial Resistance and the Prevalence of qnrVC Gene in Vibrios from Mariculture Sources* (Shanghai: Shanghai Ocean University).

Liu, X., Sun, H., and Li, Y. (2014). Analysis on enterococcal clinical resistance and detection of new resistance gene vanM in enterococcus faecium. *J. Beihua University(Natural Science)* 15 (4), 482–485. doi: 10.11713/j.issn.1009-4882.2014.04.014

Li, M., Zhao, L., Ma, J., Zhao, N., Luo, J., Wang, C., et al. (2018). *Vibrio vulnificus* in aquariums is a novel threat to marine mammals and public health. *Transboundary Emerging Dis.* 65 (6), 1863–1871. doi: 10.1111/tbed.12967

Mala, E., Oberoi, A., and Alexander, V. S. (2014). *Vibrio* isolates from cases of acute diarrhea and their antimicrobial susceptibility pattern in a tertiary care hospital. *Int. J. Basic Appl. Sci.* 3 (1), 35–37. doi: 10.14419/ijbas.v3i1.1735

Manjusha, S., Sarita, G. B., Elyas, K. K., and Chandrasekaran, M. (2005). Multiple antibiotic resistances of *Vibrio* isolates from coastal and brackish water areas. *Am. J. Biochem. Biotechnol.* 1 (4), 193–198. doi: 10.3844/ajbbsp.2005.193.198

Ministry of Agriculture and Rural Affairs Fisheries Bureau, National Fisheries Technology Extension Center and China Society of Fisheries (2021). *China Fishery statistics yearbook* (Beijing: China Agriculture Press).

Miranda, C. D., Godoy, F. A., and Lee, M. R. (2018). Current status of the use of antibiotics and the antimicrobial resistance in the Chilean salmon farms. *Front. Microbiol.* 9. doi: 10.3389/fmicb.2018.01284

Moffitt, C. M., and Cajas-Cano, L. (2014). Blue growth: the 2014 FAO state of world fisheries and aquaculture. *Fisheries (Bethesda)* 39 (11), 552–553. doi: 10.1080/03632415.2014.966265

Mohanta, T., and Goel, S. (2014). Prevalence of antibiotic-resistant bacteria in three different aquatic environments over three seasons. *Environ. Monit. Assess.* 186 (8), 5089–5100. doi: 10.1007/s10661-014-3762-1

Obaidat, M. M., Salman, A. E. B., and Roess, A. A. (2017). Virulence and antibiotic resistance of vibrio parahaemolyticus isolates from seafood from three developing countries and of worldwide environmental, seafood, and clinical isolates from 2000 to 2017. *J. Food Prot.* 80 (12), 2060–2067. doi: 10.4315/0362-028X.JFP-17-156

Oliver, J. D. (2015). The biology of *Vibrio vulnificus*. *Microbiol. Spectr.* 3 (3), 1–10. doi: 10.1128/microbiolspec.VE-0001-2014

Park, Y. G., Lee, M. S., Lee, D. S., Lee, J. M., and Yim, M. J. (2018). Antibiotic resistance of symbiotic marine bacteria isolated from marine organisms in jeju island of south Korea. *J. Oceanogr. Mar. Res.* 6 (2), 181. doi: 10.4172/2572-3103.1000181

Park, K., Mok, J. S., Kwon, J. Y., Ryu, A. R., and Shim, K. B. (2019). Seasonal and spatial variation of pathogenic *Vibrio* species isolated from seawater and shellfish off the gyeongnam coast of Korea in 2013-2016. *Korean J. Fish. Aquat.Sci.* 52 (1), 27–34. doi: 5657/KFAS.2019.0027

Romalde, J. L., Diéguez, A. L., Lasa, A., and Balboa, S. (2014). New *Vibrio* species associated to molluscan microbiota: a review. *Front. Microbiol.* 4. doi: 10.3389/fmicb.2013.00413

Sambrook, J. (2001). *Molecular Cloning: A Laboratory Manual* (New York: Cold Spring Harbor Laboratory Press).

Silva, I. P., de Souza Carneiro, C., Saraiva, M. A. F., de Oliveira, T. A. S., de Sousa, O. V., and Evangelista-Barreto, N. S. (2018). Antimicrobial resistance and potential virulence of *Vibrio parahaemolyticus* isolated from water and bivalve mollusks from bahia, Brazil. *Mar. pollut. Bull.* 131, 757–762. doi: 10.1016/j.marpolbul.2018.05.007

Song, X., Ma, Y., Fu, J., Zhao, A., Guo, Z., Malakar, P. K., et al. (2017). Effect of temperature on pathogenic and non-pathogenic *Vibrio parahaemolyticus* biofilm formation. *Food Control* 73, 485–491. doi: 10.1016/j.foodcont.2016.08.041

Song, Y. Z., Yu, P., Li, B. L., Pan, Y. J., Zhang, X. J., Cong, J., et al. (2013). The mosaic accessory gene structures of the SXT/R391-like integrative and conjugative elements derived from *Vibrio* spp. isolated from aquatic products and environment in the Yangtze river estuary, China. *BMC Microbiol.* 13, 214. doi: 10.1186/1471-2180-13-214

Stalin, N., and Srinivasan, P. (2016). Molecular characterization of antibiotic resistant *Vibrio harveyi* isolated from shrimp aquaculture environment in the south east coast of India. *Microb. Pathogen.* 97, 110–118. doi: 10.1016/j.micpath.2016.05.021

Su, C. L., and Chen, L. M. (2020). Virulence, resistance, and genetic diversity of vibrio parahaemolyticus recovered from commonly consumed aquatic products in shanghai, China. *Mar. pollut. Bull.* 160, 111554. doi: 10.1016/j.marpolbul.2020.111554

Sujeewa, A. K. W., Norrakiah, A. S., and Laina, M. (2009). Prevalence of toxic genes of *Vibrio parahaemolyticus* in shrimps (Penaeus monodon) and culture environment. *Int. Food Res. J.* 16 (1), 89–95. doi: 10.20431/2349-0365.0406003

Thompson, J. R., Randa, M. A., Marcelino, L. A., Tomita-Mitchell, A., Lim, E., and Polz, M. F. (2004). Diversity and dynamics of a north Atlantic coastal *Vibrio* community. *Appl. Environ. Microbiol.* 70 (7), 4103–4110. doi: 10.1128/AEM.70.7.4103-4110.2004

Wu, L., Liao, J., Pang, M., Bao, H., Zhou, Y., Sun, L., et al. (2019). Virulence and antimicrobial resistance of *Vibrio harveyi* in large yellow croaker. *J. Food Saf. Qual.* 10 (8), 2111–2119. doi: 10.3969/j.issn.2095-0381.2019.08.005

Yang, S., Deng, W., Liu, S., Yu, X., Mustafa, G. R., Chen, S., et al. (2020). Presence of heavy metal resistance genes in escherichia coli and salmonella isolates and analysis of resistance gene structure in e. coli E308. *J. Global Antimicrob. Resist.* 21, 420–426. doi: 10.1016/j.jgar.2020.01.009

Yang, J. H., Mok, J. S., Jung, Y. J., Lee, K. J., Kwon, J. Y., Park, K., et al. (2017). Distribution and antimicrobial susceptibility of *Vibrio* species associated with zooplankton in coastal area of Korea. *Mar. pollut. Bull.* 125 (1-2), 39–44. doi: 10.1016/j.marpolbul.2018.05.007

Yücel, N., and Balci, Ş. (2010). Prevalence of listeria, aeromonas, and *Vibrio* species in fish used for human consumption in Turkey. *J. Food Prot.* 73 (2), 380–384. doi: 10.4315/0362-028X-73.2.380

Yue, X., Liu, B., and Sun, L. (2011). Isolation and characterization of a virulent *Vibrio* spp. bacterium from clams (Meretrix meretrix) with mass mortality. *J. Invertebr. Pathol.* 106 (2), 242–249. doi: 10.1016/j.jip.2010.10.006

Yue, X., Liu, B., Xiang, J., and Jia, J. (2010). Identification and characterization of the pathogenic effect of a *Vibrio parahaemolyticus*-related bacterium isolated from clam meretrix meretrix with mass mortality. *J. Invertebr. Pathol.* 103 (2), 109–115. doi: 10.1016/j.jip.2009.11.008

Zago, V., Zambon, M., Civettini, M., Zaltum, O., and Manfrin, A. (2017). Virulence-associated factors in *Vibrio cholerae* non-O1/non-O139 and v. mimicus strains isolated in ornamental fish species. *J. Fish. Dis.* 40 (12), 1857–1868. doi: 10.1111/jfd.12659

Zhang, A., Shao, S., Zhao, K., and Li, J. (2016). Nutritional composition and edible safety analysis of two estuarine bivalve clams,Meretrix meretrix and mactra veneriformis in shuangtaizi estuary. *J. Fish. China* 40 (9), 1497–1504. doi: 10.11964/jfc.20160610422

Zhao, S., Feng, C. H., Quan, W. M., Chen, X. F., Niu, J. F., and Shen, Z. Y. (2012). Role of living environments in the accumulation characteristics of heavy metals in fishes and crabs in the Yangtze river estuary, China. *Mar. pollut. Bull.* 64 (6), 1163–1171. doi: 10.1016/j.marpolbul.2012.03.023

frontiers | Frontiers in Marine Science

TYPE Brief Research Report
PUBLISHED 04 January 2023
DOI 10.3389/fmars.2022.1076097

OPEN ACCESS

EDITED BY
Songzhe Fu,
Dalian Ocean University, China

REVIEWED BY
Qiuying Han,
Hainan Tropical Ocean University, China
Liu Guangxin,
South China Sea Fisheries Research Institute (CAFS), China

*CORRESPONDENCE
Xiaoping Huang
xphuang@scsio.ac.cn

SPECIALTY SECTION
This article was submitted to Marine Fisheries, Aquaculture and Living Resources, a section of the journal Frontiers in Marine Science

RECEIVED 21 October 2022
ACCEPTED 07 December 2022
PUBLISHED 04 January 2023

CITATION
Liu S, Wu Y, Luo H, Ren Y, Jiang Z, Zhang X, Fang Y, Liang J and Huang X (2023) Seagrass canopy structure mediates putative bacterial pathogen removal potential.
Front. Mar. Sci. 9:1076097.
doi: 10.3389/fmars.2022.1076097

Seagrass canopy structure mediates putative bacterial pathogen removal potential

Songlin Liu[1,2,3,4], Yunchao Wu[1,2,3,4], Hongxue Luo[1,2,3,4,5], Yuzheng Ren[1,2,3,4,5], Zhijian Jiang[1,2,3,4,5], Xia Zhang[1,2,3,4], Yang Fang[1,2,3,4,5], Jiening Liang[1,2,3,4,5] and Xiaoping Huang[1,2,3,4,5]*

[1]Key Laboratory of Tropical Marine Bio-resources and Ecology, South China Sea Institute of Oceanology, Chinese Academy of Sciences, Guangzhou, China, [2]Sanya Institute of Ocean Eco-Environmental Engineering, Sanya, China, [3]Innovation Academy of South China Sea Ecology and Environmental Engineering, Chinese Academy of Sciences, Guangzhou, China, [4]Guangdong Provincial Key Laboratory of Applied Marine Biology, South China Sea Institute of Oceanology, Chinese Academy of Sciences, Guangzhou, China, [5]University of Chinese Academy of Sciences, Beijing, China

Bacterial pathogen removal function in seagrass meadows is gaining attention worldwide, with enhancing particle sedimentation as the main potential mechanism. Unfortunately, seagrass meadows are declining to patchiness and fragmentation due to anthropogenic activities and global climate change. However, the effects of seagrass decline on bacterial pathogen removal potential are poorly understood, limiting our ability to understand coastal-living humans and marine organisms that suffered pressure from diseases and other health-related effects in response to seagrass decline. Here we investigated abundance of putative bacterial pathogens (including *Vibrio* spp., *Salmonella* spp., *Staphylococcus* spp., and *Enterococcus* spp.) in trapped particles under different canopy structures of *Enhalus acoroides* patches in South China Sea. The abundance of *Vibrio* spp., *Salmonella* spp., and *Staphylococcus* spp. trapped particles, respectively, was observed much greater in seagrass patches with high density and height than other patches, and significantly positive correlations with seagrass density and height were observed. This was mainly ascribed to seagrass patches of high density and height being able to trap more particles. Surprisingly, however, the *Enterococcus* spp. abundance showed negative correlations with density and area. *Enterococcus* spp. is generally inhibited in well-oxygenated environments, of which the microenvironment of dissolved oxygen might be mediated by seagrass density and area. Overall, this research suggests that the potential of removal of putative bacterial pathogen was inhibited in fragmented seagrass meadow; therefore, coastal-living humans and marine organisms might suffer from an increasing risk of diseases due to the decline of seagrass meadows.

KEYWORDS

seagrass meadows, fragmentation, canopy structure, pathogen, trapped particle

Introduction

About 40% of the world's population inhabit a narrow coastal band that takes up 7% of the Earth's land area (McGranahan et al., 2007). At a global scale, more than 80% of domestic wastewater is discharged into rivers or ocean without any treatment (Programme, U.N.W.W.A 2017), thus introducing bacterial pathogens of human and marine organisms to coastal waters (Stewart et al., 2008; Perkins et al., 2014). Coastal-living humans can suffer diseases and other health-related effects when exposed to bacterial pathogens in the ocean (Graciaa et al., 2018; Klohmann and Padilla-Gamiño, 2022). Seagrass meadows, mainly distributed along the coastal areas, are recently highlighted for reducing seawater bacterial pathogens capable of causing diseases in humans and marine organisms (Lamb et al., 2017). Although there is little information about the underlying mechanisms of seagrass meadows for removing putative bacterial pathogens, it is likely due to the mechanically trapped particles (Guan et al., 2019; Deng et al., 2021; Klohmann and Padilla-Gamiño, 2022). Therefore, seagrass meadows can help decrease bacterial pathogen pressure and improve human and marine organism health.

Unfortunately, human activities and global climate change have led to seagrass meadows' worldwide decline at 7% of the annual rate (Waycott et al., 2009). Seagrass decline can result in continuously changing seagrass meadows to patchiness and fragmentation (Montefalcone et al., 2010; Evans et al., 2018). In different patches, there were always observed variations of seagrass canopy structure, like meadow area, seagrass shoot density, and height (Ramage and Schiel, 1999; McCloskey and Unsworth, 2015)—for example, the shoot density and shoot height of a disturbed and patchy intertidal *Zostera marina* seagrass meadow in Porthdinllaen, North Wales ranged from 278.4 to 2,321.6 shoots m^{-2} and 17.3 to 35.4 cm, respectively (McCloskey and Unsworth, 2015). Changes of seagrass canopy structure can significantly influence the potential of trapped seawater particles (Gacia et al., 2003). It has been reported that longer and wider leaves of *Enhalus acoroides* can enhance more particle deposition in comparison to *Thalassia hemprichii* (Komatsu et al., 2004; Deng et al., 2021). Similarly, Barcelona et al. (2021) found that particles trapped by the blades of seagrass in the whole canopy increased with canopy density. Therefore, changes of seagrass canopy structure associated with trapped particle potential may influence the removal of seawater bacterial pathogens. However, empirical evidence of seagrass canopy structure influencing bacterial pathogen removal potential is otherwise rare.

In this study, we investigated the putative bacterial pathogen abundances (including *Vibrio* spp., *Salmonella* spp., *Staphylococcus* spp., and *Enterococcus* spp.) in the trapped particles of different canopy structures of *E. acoroides* patches in Li'an Bay of South China Sea, which are influenced by aquaculture and human wastewater discharge along the bay's shoreline (Cui et al., 2021). The results of this study will help reveal the effects of seagrass decline on the removal potential of putative bacterial pathogen as well as provide a scientific basis for improving the management of seagrass meadow protection.

Materials and methods

Study area and sampling site setting

This study was conducted in Li'an Bay (18°25′30″ N, 109°2′30″ E) of Hainan Island, South China Sea, which is a nearly enclosed bay with *E. acoroides* as the dominant seagrass distributed in shallow coastal waters (Huang et al., 2006). Dense populations and shrimp pond cultures are distributed around the bay's shoreline, and wastewater is discharged to coastal waters (Cui et al., 2021). The continuous seagrass meadows declined to patches or fragments under human pressure, presenting obvious heterogeneity in seagrass canopy structure. During August 2019, 20 sampling sites (S1–S20) of different *E. acoroides* patches were set in the northwest area of this bay. At each meadow patch, we measured the meadow area, average seagrass shoot density, and height, which represent the seagrass canopy structure heterogeneity.

Sample collection and analysis

One to three water column particle deposition traps (PVC centrifuge tubes 10 cm in height and 20 cm in diameter) were set under each patch within *E. acoroides* seagrass meadow (Deng et al., 2021). Small patches were set with one trap, while big patches were set with no more than three traps. The traps were retrieved after a deployment of 2 days. Once collected, all the particles were stored at 4°C for subsequent putative bacterial pathogen abundance analysis within 2 to 3 h.

The selective medium Slanetz–Bartley (Hopebio, China; Moaddab and Töreci, 2000), thiosulphate–citrate–bile salt sucrose agar (BD, USA; Uchiyama, 2000), CHROMagar Salmonella (CHROMagar, France; Webb et al., 2009), and CHROMagar Staphylococcus (CHROMagar, France; Cao et al., 2015) were respectively used to determine the abundance of *Enterococcus* spp., *Vibrio* spp., *Salmonella* spp., and *Staphylococcus* spp., in trapped particles. Briefly, 5 g of trapped particles was added to 50 ml sterilized 0.85% NaCl. The mix was vortexed for 2 min and then ice-bathed for 2 min, repeating the procedure three times and then resting for 5 min. Then, the original supernatant was directly screened on the four selective agars with 100 μl/plate. At the same time, 10 ml of the original supernatant was filtered onto a 0.45-μm polyethersulfone membrane filter (Supor-200, Pall), and the filter was then placed on the four selective agars with one

filter/plate. For the selection of *Enterococcus* spp., the plates were successively incubated at 37.0°C for around 4 h and then at 44°C for around 44 h. For the selection of *Vibrio* spp., *Salmonella* spp., and *Staphylococcus* spp., the plates were incubated at 37.0°C for 24 h. After incubation, the clones were counted. The abundance of the bacteria in sediment (cfu g^{-1} DW) was calculated based on the dilution folds and the wet weight/dry weight conversion.

Data analysis

Data analysis was carried out using PRIMER v6 with PERMANOVA+ add-on and Python 3.8.7. First, seagrass canopy metrics data was normalized (zero mean normalization), and then triangular resemblance matrix was created by analyzing the Bray–Curtis similarity between the sampling sites. Principal component analysis (PCA) plots were used to provide explanation of seagrass canopy structure linked to the driving factors, with the sampling sites divided into different groups. Second, the relationships between seagrass canopy metrics (area, seagrass shoot density, and height) and the putative bacterial pathogen abundance data were evaluated by distance-based redundancy analyses (db-RDA). A one-way multifactorial permutational analysis of variance was subsequently performed to determine the statistically significant differences among the groups divided by PCA. Furthermore, Pearson correlation analysis was conducted between seagrass canopy metrics and putative bacterial pathogens. All main and interaction effects with p <0.05 were considered statistically significant.

Results

Details on the patch variables from the 20 sites are presented in Table 1. A PCA showed first two principal components (PC) that explained 83% variation of all seagrass patch canopy structures (Figure 1). PC1 showed a strong correlation with density (r = 0.692) and height (r = 0.686), while PC2 was observed to have a positive correlation with area (r = 0.974) (Figure 1). All the sampling seagrass patches can be divided into four groups by the two PCs (Figure 1). S1, S2, and S3 patches had a small area, respectively, and those with low density and height were marked as the SA+LDH group, while S5, S6, and S8 had a large area, respectively, but with low density and height and thus

TABLE 1 Seagrass canopy metrics for the 20 sampling sites.

Site	Density (shoots m^{-2})	Height (cm)	Area (m^2)	Group
S1	64	29.9	0.125	SA+LDH
S2	96	20.8	0.5	SA+LDH
S3	112	17.97	0.4	SA+LDH
S4	144	63.7	13	SA+HDH
S5	160	21.6	40	LA+LDH
S6	160	8.57	40	LA+LDH
S7	176	47.77	60	LA+HDH
S8	192	16.43	40	LA+LDH
S9	224	25.33	5	SA+HDH
S10	224	55.2	8	SA+HDH
S11	240	44.17	2	SA+HDH
S12	240	38.9	2	SA+HDH
S13	256	26.5	2.2	SA+HDH
S14	256	20.5	8	SA+HDH
S15	256	49.7	4	SA+HDH
S16	256	52.23	60	LA+HDH
S17	272	43.27	1.5	SA+HDH
S18	304	52.83	13	SA+HDH
S19	320	50.97	60	LA+HDH
S20	352	54.7	8	SA+HDH

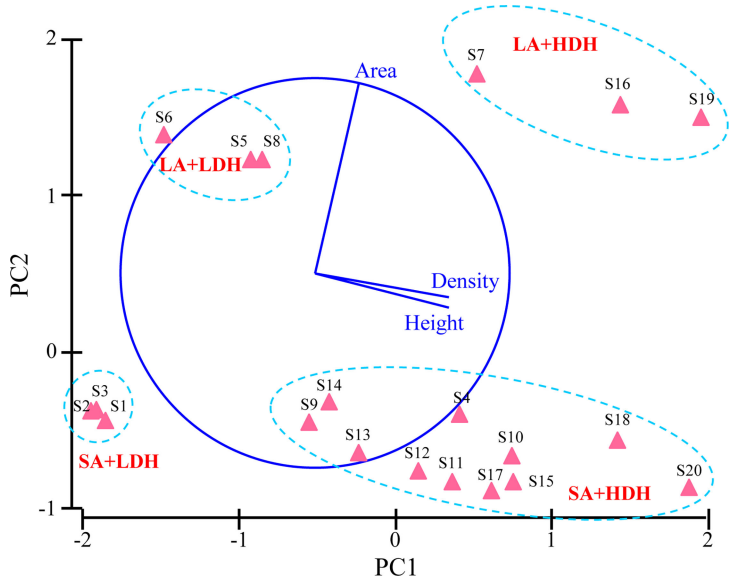

FIGURE 1
Principal component analysis (PCA) depicting the extent of differences in seagrass canopy structure among all sampling patches. PC1 = 50.5% variation and PC2 = 32.4% variation.

marked as the LA+LDH group (Figure 1 and Table 1). Furthermore, S7, S16, and S19 had a large area and high density and height, thus named as the LA+HDH group, and the other sampling sites were of relatively high density and height but with a small area, thus named as the SA+HDH group (Figure 1 and Table 1).

The average abundance of *Vibrio* spp., *Salmonella* spp., *Staphylococcus* spp., and *Enterococcus* spp. in the trapped particles beneath the *E. acoroides* ranged from 5,987.67 to 36,976.27, 120.44 to 657.18, 377.11 to 673.69, and 267.41 to 1,540.89 cfu g^{-1} DW, respectively, with the average abundance of all sampling patches being 18,272.25, 333.57, 529.12, and 550.33 cfu g^{-1} DW, respectively. There was a significant effect of seagrass canopy structure on the putative bacterial pathogen communities in the trapped particles (pseudo-F = 7.2746, P-$perm$ = 0.001). The abundance of *Vibrio* spp., *Salmonella* spp., and *Staphylococcus* spp. was observed to be generally higher in groups of LA+HDH and SA+HDH than in other groups, while that of *Enterococcus* spp. showed an opposite trend. The db-RDA analyses of the four putative bacterial pathogens' data explained 64.9% of the variation in the first two axes (Figure 2). The db-RDA analyses confirmed the clear separation of putative bacterial pathogen communities under the four groups' patches according to seagrass canopy metrics. Db-RDA1 generally separated the putative bacterial pathogen communities of high-density-and-height-canopy sites from that of low-density-and-height-canopy sites, while db-RDA2 separated the large-area sites from small-area sites (Figure 2). There were strong positive correlations between area and db-RDA2 (r = 0.940) and strong negative correlations between density (r = -0.781), height (r = -0.551), and db-RDA1, respectively.

Pearson correlation analysis was further conducted for the correlation between each putative bacterial pathogen with each seagrass canopy metric. The abundance of *Vibrio* spp. and *Staphylococcus* spp., respectively, was observed to have significantly positive correlations with density and height, while the abundance of *Salmonella* spp. was only shown to have a significantly positive correlation with density (Figure 3). In contrast, *Enterococcus* spp. abundance was significantly negatively correlated with density and area (Figure 3).

Discussion

The seagrass meadows of Li'an have shown obvious fragmentation and patchiness, of which the smallest patch was only 0.125 m^2 and the lowest *E. acoroides* density was 64 shoots m^{-2}. Human physical disturbance, including repeated clam digging and fishing, overload of aquaculture activities, and nutrient loading induced by wastewater discharge were the main reason for the seagrass decline and fragmentation of seagrass meadows in Li'an (Yu et al., 2019; Cui et al., 2021). Therefore, anthropogenic activities led to seagrass canopy structure heterogeneity within a fine-scale seagrass meadow. Anthropogenic activities induced the wastewater discharge with input of abundant particles associated with putative bacterial pathogens to seagrass meadows (Ghaderpour et al., 2014; Perkins et al., 2014). In this study, the reported *Salmonella*

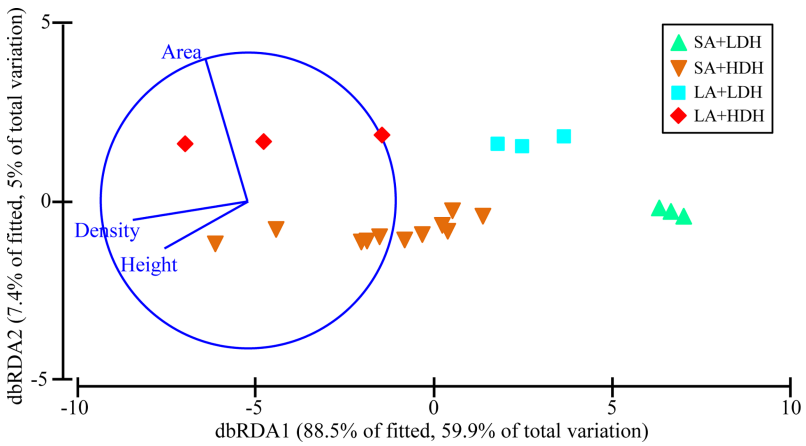

FIGURE 2
Distance-based redundancy analysis (db-RDA) ordination of putative bacterial pathogen data fitted to seagrass canopy structure variables. The plot represents a db-RDA ordination based upon the Bray–Curtis distance of all the sampling sites.

FIGURE 3
Relationship between four putative bacterial pathogens and three seagrass canopy metrics. Purple represents a negative correlation between variables, and red represents a positive correlation (*p<0.05, **p<0.01).

spp., *Staphylococcus* spp., and *Enterococcus* spp. abundance of trapped particles in coastal sediments was in the range of abundance values reported by previous studies (Craig et al., 2002; Bharathi and Nair, 2005; Perkins et al., 2014). However, the abundance of *Vibrio* spp. in this study was observed to be much higher than that previously reported in less human-impacted coastal areas (Comeau and Suttle, 2007; Perkins et al., 2014). The high abundance of *Vibrio* spp. in this study area should originate from coastal aquaculture wastewater discharge (Cui et al., 2021), suggesting that the seagrass meadows of this study were significantly influenced by coastal aquaculture as well.

The putative bacterial pathogen abundance and communities of trapped particles were observed to be significantly different among the four types of seagrass patches, mainly driven by shoot density and height. It has been reported that physical collisions between the particles and the leaves retard water flow by the seagrass canopy, which is the main driving force for particle trapping within seagrass meadows (Komatsu et al., 2004; Hendriks et al., 2008). The high density and height of seagrass

canopy can retard water flow more efficiently and elevate the possibility of physical collision, thereby trapping more particles (Gacia et al., 2003; Komatsu et al., 2004; Barcelona et al., 2021). Deng et al. (2021) reported that a higher daily particle deposition rate was observed under *E. acoroides* stands than under *T. hemprichii* stands within the fine-scale seagrass meadows, which is mainly attributed to the higher canopy of *E. acoroides* than that of *T. hemprichii*. Similarly, seawater particles, especially the fine particles, trapped by the seagrass leaves in the whole canopy increased with seagrass density (Barcelona et al., 2021). Furthermore, fine particles are associated with a higher abundance of putative bacterial pathogens in comparison with coarser particles (Maugeri et al., 2004; Lyons et al., 2007). Therefore, the abundance of trapped particles of *Vibrio* spp., *Salmonella* spp., and *Staphylococcus* spp., respectively, was generally observed to be much greater under high-density and tall-height seagrass patches in this study. Additionally, *Vibrio* spp., *Salmonella* spp., and *Staphylococcus* spp. were generally observed to have significantly positive correlations with seagrass density and height, which supported our assumption as well. In contrast to our expectation, area can only explain less than 5% variations of the putative bacterial pathogen abundance of different patches, and the abundance of *Vibrio* spp., *Salmonella* spp., and *Staphylococcus* spp., respectively, was shown to have no significant correlations with area. Navarrete-Fernández et al. (2022) reported that most trapped particles mainly accumulated along the outer and the inner edge of the meadow or just penetrate the few meters of the meadow. We assumed in this study that the trapped particles accumulated along the edge of seagrass meadows, which supported that the seagrass patch area size has less impact on particle trapping.

Interestingly, the abundance of *Enterococcus* spp. was observed to have negative correlations with density and area. *Enterococcus* spp. is consistently present and, being facultative anaerobic bacteria (Fisher and Phillips, 2009), it has been reported to be inhibited in well-oxygenated environments due to direct and indirect photodissociation effects (Curtis et al., 1992; Sassoubre et al., 2012). The concentration of dissolved oxygen in seawater in a large-area seagrass patch was 10–20% higher than in a small-area seagrass patch in the meadows of this study (unpublished data). Therefore, a high-density and large-area seagrass patch should release more oxygen into the seawater within a fine scale due to photosynthesis and consequently result in the abundance of *Enterococcus* spp. to decrease in this study. However, we can only speculate the potential effects of oxygen on the putative bacterial pathogen in this study. For a future study, we recommend the research effects of microenvironment variations within seagrass meadows on putative bacterial pathogen removal potential. Such research will help reveal the new mechanism for removing putative bacterial pathogen within seagrass meadows.

At a global scale, seagrass meadows are declining and become fragmentated. Given the decrease in the removal of putative bacterial pathogen potential in fragmented seagrass meadows, it could be argued that seagrass decline would lead to coastal-living humans and marine organisms suffering from high-risk diseases. Therefore, we suggest the recovery and protection of the declining seagrass meadows worldwide, which have important implications for human and marine organism health protection (Klohmann and Padilla-Gamiño, 2022).

Conclusion

We found that high-density and tall seagrass patches can trap a greater abundance of putative bacterial pathogens of *Vibrio* spp., *Salmonella* spp., and *Staphylococcus* spp. in water columns. These findings imply that seagrass decline can decrease the ecological function of putative bacterial pathogen removal potential. What is unknown, however, is that the abundance of trapped particles of *Enterococcus* spp. was observed to have negative correlations with density and area, which might be affected by dissolved oxygen variations. Further work is needed to conduct an evaluation of the putative bacterial pathogen changes in response to microenvironment variations within seagrass meadows.

Data availability statement

The raw data supporting the conclusions of this article will be made available by the authors, without undue reservation.

Author contributions

SL: conceptualization, methodology, and writing—original draft. YW: investigation, methodology, and data curation. HL: Investigation and validation. YR: formal analysis and software. ZJ: project administration and investigation. XZ: resources and data curation. YF: methodology and data curation. JL: formal analysis. XH: supervision, writing—review and editing, and funding acquisition. All authors contributed to the article and approved the submitted version.

Funding

This work was supported by the National Key Research and Development Program of China (2022YFF0802201), the Key Research and Development Project of Hainan (ZDYF2020180 and ZDYF2021SHFZ254), the National Natural Science Foundation of China (42176155, U1901221, and 41730529), and the Innovation Academy of South China Sea Ecology and

Environmental Engineering, Chinese Academy of Sciences (ISEE2021PY06 and ISEE2021ZD03).

Conflict of interest

The authors declare that the research was conducted in the absence of any commercial or financial relationships that could be construed as a potential conflict of interest.

Publisher's note

References

Barcelona, A., Oldham, C., Colomer, J., Garcia-Orellana, J., and Serra, T. (2021). Particle capture by seagrass canopies under an oscillatory flow. *Coast. Eng.* 169, 103972. doi: 10.1016/j.coastaleng.2021.103972

Bharathi, P. L., and Nair, S. (2005). Rise of the dormant: simulated disturbance improves culturable abundance, diversity, and functions of deep-sea bacteria of central Indian ocean basin. *Mar. Georesources Geotechnology* 23 (4), 419–428. doi: 10.1080/10641190500446805

Cao, J. P., Han, D., and Wang, J. (2015). A comparative study on quantitative detection of staphylococcus aureus in food. *J. Anhui Agric. Sci* 43 (8), 242-243+245. doi: 10.13989/j.cnki.0517-6611.2015.08.092

Comeau, A. M., and Suttle, C. A. (2007). Distribution, genetic richness and phage sensitivity of vibrio spp. from coastal British Columbia. *Environ. Microbiol.* 9 (7), 1790–1800. doi: 10.1111/j.1462-2920.2007.01299.x

Craig, D., Fallowfield, H. J., and Cromar, N. (2002). Enumeration of faecal coliforms from recreational coastal sites: evaluation of techniques for the separation of bacteria from sediments. *J. Appl. Microbiol.* 93 (4), 557–565. doi: 10.1046/j.1365-2672.2002.01730.x

Cui, L., Jiang, Z., Huang, X., Chen, Q., Wu, Y., Liu, S., et al. (2021). Eutrophication reduces seagrass contribution to coastal food webs. *Ecosphere* 12 (6), e03626. doi:

Curtis, T. P., Mara, D. D., and Silva, S. A. (1992). Influence of pH, oxygen, and humic substances on ability of sunlight to damage fecal coliforms in waste stabilization pond water. *Appl. Environ. Microbiol.* 58 (4), 1335–1343. doi: 10.1128/aem.58.4.1335-1343.1992

Deng, Y., Liu, S., Feng, J., Wu, Y., and Mao, C. (2021). What drives putative bacterial pathogens removal within seagrass meadows? *Mar. Pollut. Bull.* 166, 112229. doi: 10.1016/j.marpolbul.2021.112229

Evans, S. M., Griffin, K. J., Blick, R. A., Poore, A. G., and Vergés, A. (2018). Seagrass on the brink: Decline of threatened seagrass posidonia australis continues following protection. *PloS One* 13 (4), e0190370. doi: 10.1371/journal.pone.0190370

Fisher, K., and Phillips, C. (2009). The ecology, epidemiology and virulence of enterococcus. *Microbiology* 155 (6), 1749–1757. doi: 10.1099/mic.0.026385-0

Gacia, E., Duarte, C. M., Marbà, N., Terrados, J., Kennedy, H., Fortes, M. D., et al. (2003). Sediment deposition and production in SE-Asia seagrass meadows. *Estuar. Coast. Shelf Sci.* 56 (5), 909–919. doi: 10.1016/S0272-7714(02)00286-X

Ghaderpour, A., Nasori, K. N. M., Chew, L. L., Chong, V. C., Thong, K. L., and Chai, L. C. (2014). Detection of multiple potentially pathogenic bacteria in matang mangrove estuaries, Malaysia. *Mar. Pollut. Bull.* 83 (1), 324–330. doi: 10.1016/j.marpolbul.2014.04.029

Graciaa, D. S., Cope, J. R., Roberts, V. A., Cikesh, B. L., Kahler, A. M., Vigar, M., et al. (2018). Outbreaks associated with untreated recreational water–united states 2000–2014. *MMWR Morb Mortal Wkly Rep.* doi: 10.15585/mmwr.mm6725a1

Guan, C., Saha, M., and Weinberger, F. (2019). Chemical defence of a seagrass against microfoulers and its seasonal dynamics. *Appl. Sci.* 9 (6), 1258. doi: 10.3390/app9061258

Hendriks, I. E., Sintes, T., Bouma, T. J., and Duarte, C. M. (2008). Experimental assessment and modeling evaluation of the effects of the seagrass Posidonia oceanica on flow and particle trapping. *Mar. Ecol. Prog. Ser.* 356, 163–173. doi: 10.3354/meps07316

Huang, X. P., Huang, L. M., Li, Y. H., Xu, Z. Z., Fong, C. W., Huang, D. J., et al. (2006). Main seagrass beds and threats to their habitats in the coastal sea of south China. *Chin. Sci. Bull.* 51, 136–142. doi: 10.1007/s11434-006-9136-5

Klohmann, C., and Padilla-Gamiño, J. L. (2022). Pathogen filtration: An untapped ecosystem service. *Front. Mar. Sci.* 1226. doi: 10.3389/fmars.2022.921451

Komatsu, T., Umezawa, Y., Nakakoka, M., Supanwanid, C., and Kanamoto, Z. (2004). Water flow and sediment in Enhalus acoroides and other seagrass beds in the Andaman Sea, off khao bae Na, Thailand. *Coast. Mari. Sci.* 29 (1), 63–68 doi: 10.15083/00040824

Lamb, J. B., van de Water, J. A., Bourne, D. G., Altier, C., Hein, M. Y., Fiorenza, E. A., et al. (2017). Seagrass ecosystems reduce exposure to bacterial pathogens of humans, fishes, and invertebrates. *Science* 355 (6326), 731–733. doi: 10.1126/science.aal1956

Lyons, M. M., Lau, Y.-T., Carden, W. E., Ward, J. E., Roberts, S. B., Smolowitz, R., et al. (2007). Characteristics of marine aggregates in shallow-water ecosystems: implications for disease ecology. *EcoHealth* 4 (4), 406–420. doi: 10.1007/s10393-007-0134-0

Maugeri, T., Carbone, M., Fera, M., Irrera, G., and Gugliandolo, C. (2004). Distribution of potentially pathogenic bacteria as free living and plankton associated in a marine coastal zone. *J. Appl. Microbiol.* 97 (2), 354–361. doi: 10.1111/j.1365-2672.2004.02303.x

McCloskey, R. M., and Unsworth, R. K. (2015). Decreasing seagrass density negatively influences associated fauna. *PeerJ* 3, e1053. doi: 10.7717/peerj.1053

McGranahan, G., Balk, D., and Anderson, B. (2007). The rising tide: assessing the risks of climate change and human settlements in low elevation coastal zones. *Environ. urbanization* 19 (1), 17–37. doi: 10.1177/0956247807076960

Moaddab, S. R., and Töreci, K. (2000). Species level identification and investigation of resistance to vancomycin and some other antibiotics in enterococcus strains. *Türk Mikrobiyol Cem Derg* 30, 77–84.

Montefalcone, M., Parravicini, V., Vacchi, M., Albertelli, G., Ferrari, M., Morri, C., et al. (2010). Human influence on seagrass habitat fragmentation in NW Mediterranean Sea. *Estuarine Coast. Shelf Sci.* 86 (2), 292–298. doi: 10.1016/j.ecss.2009.11.018

Navarrete-Fernández, T., Bermejo, R., Hernández, I., Deidun, A., Andreu-Cazenave, M., and Cózar, A. (2022). The role of seagrass meadows in the coastal trapping of litter. *Mar. Pollut. Bull.* 174, 113299. doi: 10.1016/j.marpolbul.2021.113299

Perkins, T. L., Clements, K., Baas, J. H., Jago, C. F., Jones, D. L., Malham, S. K., et al. (2014). Sediment composition influences spatial variation in the abundance of human pathogen indicator bacteria within an estuarine environment. *PloS One* 9 (11), e112951. doi: 10.1371/journal.pone.0112951

Programme, U.N.W.W.A (2017). *"the untapped resource, the united nations world water development report"* (Paris, France: UNESCO World Water Assessment Programme).

Ramage, D. L., and Schiel, D. R. (1999). Patch dynamics and response to disturbance of the seagrass Zostera novazelandica on intertidal platforms in southern new Zealand. *Mar. Ecol. Prog. Ser.* 189, 275–288. doi: 10.3354/MEPS189275

Sassoubre, L. M., Nelson, K. L., and Boehm, A. B. (2012). Mechanisms for photoinactivation of enterococcus faecalis in seawater. *Appl. Environ. Microbiol.* 78 (21), 7776–7785. doi: 10.1128/AEM.00913-14

Stewart, J. R., Gast, R. J., Fujioka, R. S., Solo-Gabriele, H. M., Meschke, J. S., Amaral-Zettler, L. A., et al. (2008). The coastal environment and human health: microbial indicators, pathogens, sentinels and reservoirs. *Environ. Health* 7 (2), 1–14. doi: 10.1186/1476-069X-7-S2-S3

Uchiyama, H. (2000). Distribution of vibrio species isolated from aquatic environments with TCBS agar. *Environ. Health Prev. Med.* 4 (4), 199–204. doi: 10.1007/BF02931258

Waycott, M., Duarte, C. M., Carruthers, T. J., Orth, R. J., Dennison, W. C., Olyarnik, S., et al. (2009). Accelerating loss of seagrasses across the globe threatens coastal ecosystems. *Proc. Natl. Acad. Sci.* 106 (30), 12377–12381. doi: 10.1073/pnas.0905620106

Webb, K., Ritter, V., and Hammack, T. (2009). CHROMagar salmonella detection test kit. *J. AOAC Int.* 92 (6), 1906–1909. doi: 10.1093/jaoac/92.6.1906

Yu, S., Wu, Y., Serrao, E. A., Zhang, J., Jiang, Z., Huang, C., et al. (2019). Fine-scale genetic structure and flowering output of the seagrass Enhalus acoroides undergoing disturbance. *Ecol. Evol.* 9 (9), 5186–5195. doi: 10.1002/ece3.5106

frontiers | Frontiers in Marine Science

TYPE Original Research
PUBLISHED 12 January 2023
DOI 10.3389/fmars.2022.1088176

OPEN ACCESS

EDITED BY
Yiqin Deng,
South China Sea Fisheries Research Institute (CAFS), China

REVIEWED BY
Shaowu Li,
Heilongjiang River Fisheries Research Institute (CAFS), China
Mao Lin,
Jimei University, China

*CORRESPONDENCE
Yuting Deng
dengyt@prfri.ac.cn

†These authors have contributed equally to this work and share first authorship

SPECIALTY SECTION
This article was submitted to Marine Fisheries, Aquaculture and Living Resources, a section of the journal Frontiers in Marine Science

RECEIVED 03 November 2022
ACCEPTED 15 December 2022
PUBLISHED 12 January 2023

CITATION
Lin X, Tan A, Deng Y, Liu W, Zhao F and Huang Z (2023) High occurrence of antibiotic resistance genes in intensive aquaculture of hybrid snakehead fish.
Front. Mar. Sci. 9:1088176.
doi: 10.3389/fmars.2022.1088176

High occurrence of antibiotic resistance genes in intensive aquaculture of hybrid snakehead fish

Xiaojing Lin[1,2†], Aiping Tan[1†], Yuting Deng[1,3*], Wenwen Liu[1,2], Fei Zhao[1] and Zhibin Huang[1]

[1]Key Laboratory of Fishery Drug Development of Ministry of Agriculture and Rural Affairs, Key Laboratory of Provincial Key Laboratory of Aquatic Animal Immunology and Sustainable Aquaculture, Pearl River Fisheries Research Institute, Chinese Academy of Fishery Sciences, Guangzhou, China, [2]College of Fisheries and Life Science, Shanghai Ocean University, Shanghai, China, [3]Key Laboratory of Control of Quality and Safety for Aquatic Products of Ministry of Agriculture and Rural Affairs, Chinese Academy of Fishery Sciences, Beijing, China

The increasing abundance of antibiotic resistance genes (ARGs), which are regarded as new pollutants, has raised public health concern. The use of antibiotics in aquaculture has promoted the evolution and spread of ARGs. The occurrence and abundance of ARGs in aquaculture has attracted extensive attention. However, the distribution and transmission of ARGs in aquaculture require further study. This study analyzed water and sediment from intensive culture of hybrid snakehead fish farm in Zhongshan, South China. Twenty-two types of ARGs were detected in all environmental samples. The relative abundance of sulfonamide resistance genes (*sul1* and *sul2*) was the highest, ranging from 3.37×10^{-2} to 8.53×10^{0} copies/16S rRNA gene. High occurrence of quinolones, phenicols, tetracycline resistance genes, and class 1 integrase gene (*intI1*) was also observed in pond water samples. This implies that pond water is one of the main reservoirs and origins of ARGs in the aquatic environment. *Proteobacteria* was the most abundant phylum in all the environmental samples, and its relative abundance ranged from 24.05% to 41.84%. Network and canonical correspondence analyses showed that a high abundance of ARGs (*int1*, *sul1*, *sul2*, *qacEΔ1*, *aac6*, and *oqxA*) was positively correlated with *Proteobacteria*, *Cyanobacteria*, and *Bacteroidetes*, and the abundance of *Proteobacteria*, *Actinobacteria*, and *Patescibacteria* was positively correlated with environmental factors (sulfide, nitrite nitrogen, pH, free chlorine, and ammonia nitrogen). These findings demonstrate the prevalence and persistence of ARGs in intensive fish farming in southern China. This suggests that ARG levels and microbiological community composition in aquaculture should be conventionally determined to assess potential risks to public health.

KEYWORDS

antibiotic resistance genes (ARGs), bacterial community, snakehead fish, public health, intensive aquaculture

Introduction

The hybrid snakehead fish (*Channa maculate* ♀ × *C. argus* ♂) is an important commercial fish with high market value in Chinese aquaculture. The production of hybrid snakehead fish has increasingly developed towards intensive and high-density aquaculture in China with the continual improvement of aquaculture technology (Liu et al., 2017). In the past ten years, rough culture has changed to a modern refined aquaculture mode by increasing the stocking density and feeding compounds or providing complete feed to sustain the rapid growth of this industry. However, negative effects related to nutrient discharge may cause eutrophication, deterioration of water quality, and other potential environmental risks (Liu et al., 2014). High-stock density aquaculture involves the rearing of fish in congested and stressful environments. These fishes are more susceptible to bacterial infections, resulting in significant production losses. Antibiotics have been widely used to reduce disease burden in China since the 1980s because of their low cost, convenience of use, and remarkable curative effects. Antibiotics are extensively used as therapeutic drugs for humans, livestock, aquaculture, and as feed additives in farming (Su et al., 2018a). Several studies have reported that improper use of antibiotics in aquaculture exerts selection pressure on the natural bacterial population and enhances their ability to produce antibiotic-resistant bacteria or antibiotic resistance genes (ARGs) in aquatic environments (Hossain et al., 2022).

ARGs are defined as a new type of environmental pollutants because of their persistence and easy diffusivity. This has become the biggest challenge to human health in the 21st century (Berendonk et al., 2015). Antibiotic resistance genes are key factors in the development of bacterial drug resistance. They are enriched in medical wastewater, riverbed sludge, pig farm soil, and drinking water treatment systems. They can be horizontally transferred through mobile genetic elements (MGEs) (Gao et al., 2012; Li et al., 2015; Zhou et al., 2017; Hu et al., 2018; Su et al., 2018b). Moreover, foodborne pathogens that carry ARGs pose a potential threat to human health when they enter the food chain (Zhao et al., 2018). The aquatic ecosystem is an enrichment pool for many types of ARGs, and the pollution of the system by exogenous antibiotics is an important factor that results in the enrichment and diffusion of ARGs (Allen et al., 2010). Several studies have also reported the high presence of antibiotics in the environment, including sulfonamides, tetracyclines, quinolones, and the most frequently detected antibiotic resistance genes along with their respective antibiotic classes are sulfonamides (*sul1* and *sul2*), tetracyclines (*tetA*, *tetB*, *tetK*, and *tetM*), and quinolones (*qnrA*, *qnrB*, and *qnrS*) (Zhou et al., 2017; Hu et al., 2018).

Aquaculture is considered to be a "genetic hotspot" for the transmission of resistance genes. Several ARGs have been detected in aquaculture environments and farming organisms in China, India, Finland, Nigeria, and Chile (Su et al., 2017). Antibiotic-resistant genes are widely distributed in aquaculture environments and in aquatic animals (aquatic products). It has been speculated that the use of antibiotics in aquaculture may promote the enrichment and migration of ARGs in the environment and animals. Nutrients have been suggested to directly or indirectly promote ARGs dissemination (Ning et al., 2022). Environmental factors such as total phosphorus and total nitrogen affect the abundance and diversity of ARGs in shrimp and fishponds (Su et al., 2017). Furthermore, bacterial communities in different aquaculture modes affect the distribution and abundance of ARGs (Huang et al., 2017; Wang et al., 2022). These findings indicated that antibiotic use and environmental factors affect the occurrence and distribution of ARGs.

Hybrid snakehead fish farming is a typical example of intensive aquaculture, which may result in a series of negative effects including the production of large amounts of antibiotic-resistant bacteria and ARGs pollution. This study evaluated the risk of ARGs in intensive aquaculture by quantitatively analyzing 22 typical ARGs in the breeding environment of hybrid snakehead fish using real-time quantitative PCR (RT-qPCR). In addition, the correlation between bacterial communities at different culture stages, ARG abundance, and environmental factors was elucidated, and co-occurrence patterns between ARGs and bacterial taxa were identified. This study provides information on antibiotic resistance in intensive aquaculture and advances the development of a healthy, green, and sustainable freshwater aquaculture industry.

Materials and methods

Sample collection

The hybrid snakehead fish farm (22.602° N, 113.503° E) selected for this study is located in Zhongshan, Guangdong Province, China. This farm has over 70 mud ponds with a total feeding area of 50 ha. Each pond has an area of approximately 0.4–0.6 ha with a depth of approximately 1.8–2.5 m. Three ponds at the sampling sites (ponds A, B, and C) were selected for this study. The seasons in Guangdong Province allowed three different fish harvests. The first crop of hybrid fish involved stocking fingerlings before May and harvesting in November of the same year with a rearing period of no more than six months. The stocking density of the fingerlings was 10 thousand per ha (1,500 fish/kg), and the harvest size of the adult fish was usually 500–750 g. Different antibiotics, including florfenicol, doxycycline, sulfonamides, and enrofloxacin, have been used as therapeutic and prophylactic agents against bacterial infections because of their high stock density. Oral administration is usually mixed with feed; the usage limits for

sulfonamides, florfenicol, doxycycline, and enrofloxacin are 100-200 mg/kg BW, 10-15 mg/kg BW, 20-50 mg/kg BW, and 2500 mg/kg feed, respectively (Liu et al., 2017).

Sediment and water samples were collected in June (fingerlings, X), September (rearing, Y), and November (harvesting, Z) 2020. The rearing and harvesting periods corresponded to rapid growth and upcoming sales, respectively. Five hundred milliliters of water samples (500 mL) were collected from the four corners of each pond (10–15 cm below the surface) using a stainless-steel sampler. Samples from each pond were then completely mixed and transferred to sterile polyethylene bottles to avoid differences in heterogeneity caused by single sampling. Sediment samples (500 g with four replicates of each sample) were collected from 0-10 cm depth using a grab sampler and then mixed thoroughly in sterile polyethylene bottles. All samples were stored in a portable refrigerator and transported to the laboratory for pre-treatment within 24 h.

Total DNA extraction

Each sample was subsequently divided into two equal parts, which were used for the quantitative PCR analysis and high-throughput sequencing of the bacterial community. Water samples (0.5–1 L) were filtered through a 0.22-μm micro-pore membrane (Pall, Michigan, USA) using vacuum filtration for DNA extraction. The membranes were aseptically stored at -80° C for DNA extraction using the PowerSoil DNA isolation kit (Qiagen Biotech, Germany) according to the manufacturer's instructions. The sediment samples were lyophilized, ground, and sieved through an 80-mesh screen. Approximately 0.25 g of each sediment sample was used for DNA extraction using the PowerSoil DNA isolation kit (Qiagen Biotech, Germany) according to the manufacturer's protocol. The DNA concentration and purity were monitored using 1% agarose gels and an ultramicro ultraviolet spectrophotometer (Gene Company Limited, China).

Gene identification and quantification

The 21 most common target ARGs in the water and sediment samples were quantified using quantitative PCR. These included three sulfonamide resistance genes (*sul1*, *sul2*, and *sul3*), four tetracycline resistance genes (*tetA*, *tetB*, *tetM*, and *tetW*), six quinolone resistance genes (*qnrA*, *qnrB*, *qnrC*, *qnrS*, *oqxA*, and *aac(6)-Ib-cr*), three β-lactams ($bla_{\text{CTX-M}}$, bla_{SHV}, and bla_{TEM}), three phenicol resistance genes (*fexA*, *floR*, and *cmlA*), two macrolide resistance genes (*mefA* and *ermB*), together with a class 1 integron integrase gene (*intI1*), a quaternary ammonium compound resistance gene (*qacEΔ1*), and 16S rRNA gene. Table S1 lists the annealing temperatures, specific primers, and expected amplicon sizes of target genes. Calibration standard curves for positive controls and quantification were constructed using plasmid DNA (cloned ARGs) extracted from *Escherichia coli* DH5α, as previously described (Li et al., 2015). All qPCR assays were performed on a QuantStudio 6 Flex Real-Time Fluorescence PCR instrument (Applied Biosystems, USA) equipped with real-time PCR-based gene expression profiling. Quantitative PCR was performed using TB Green® Premix Ex Taq™ (Takara), according to the manufacturer's instructions. Each reaction was performed in triplicate. The standard curve for each qPCR assay consisted of a 10-fold dilution series from 0.5×10^9 copies·mL^{-1} to 0.5×10^3 copies·mL^{-1}. The amplification efficiencies ranged from 78.918% to 104.98%, and the R^2 values were between 0.982 and 1.000 for all the standard curves. The abundance of ARGs was determined as the copy number per milliliter of the water sample or the copy number per gram of the sediment sample (dry weight). Relative copy number of the resistance gene (relative abundance gene) = copy number of resistance gene/ copy number of the 16S rRNA gene.

Analysis of environmental factors

Dissolved oxygen (DO), water temperature (WT), pH, ammonia nitrogen (NH_3-N), nitrite nitrogen (NO_2-N), sulfide (SO_4), phosphate (PO_4), free chlorine (Cl), copper (Cu), chromium (Cr), total iron (Fe), total alkalinity (TOA), and total hardness (TOH) of the water samples were determined using a water quality detector (Octadem W-II, USA).

Bacterial community analysis

High-throughput sequencing of the bacterial community was performed using an Illumina HiseqTM 2500/4000 by Gene Denovo Biotechnology Co., Ltd. (Guangzhou, China) to further analyze the microbial community composition of the environmental samples. Specific primers (341F, CCTACGGGN GGCWGCAG; 806R, GGACTACHVGGGTATCTAAT) were used to amplify the V3 - V4 regions of 16S rRNA gene. PCR products (466 bp) were recorded to construct a library of amplicons, and amplicon sequencing was performed on an OmicSmart platform (Illumina, USA). The original sequencing data contained a large amount of low-quality data or data without biological significance (such as chimeras) owing to PCR and sequencing errors. Therefore, strict quality control was performed in multiple data processing processes, including read utilization, tag splicing, and operational statistical unit (OTU) clustering, to ensure the statistical reliability and biological effectiveness of subsequent analyses. The sequences date reported in this study was archived in Sequence Read Archive (SRA) with the accession number PRJNA907527.

Statistical analysis

The copy numbers calculated by qPCR were defined as absolute gene abundance. A heatmap showing the natural logarithm-transformed values of normalized ARG copies was constructed using GraphPad Prism 7 (San Diego, CA, USA). Bacterial community data, including taxonomic composition, community comparison, and diversity indices (Shannon, Simpson, Chao1, and ACE), were obtained using Omicsmart (http://www.omicsmart.com). Principal coordinate analysis (PCoA) was used to compare and visualize the differences in the abundance of ARGs and microbial communities based on a Jaccard distance matrix. Visualizing the network topology in Gephi (0.9.2) using the Fruchterman-Reingold algorithm. Canonical correspondence analysis (CCA) was performed using the R language vegan package to compare the bacterial communities and environmental variables. Statistical analyses were performed using SPSS (version 25.0; IBM Corp., Armonk, NY, USA). The evaluations were based on a significance level of 5%. Statistical significance was set at $P < 0.05$.

Results

Prevalence of ARGs in a hybrid snakehead fish farm

The abundance of twenty-two resistance genes, *intI1* and 16S rRNA gene, was investigated to analyze the distribution of ARGs in hybrid snakehead fish farms. A significantly higher abundance of ARGs (sulfonamides, quinolones, and phenicols) was detected in water samples than in sediment samples (Figure 1). The absolute abundances of sulfonamides, quinolones, and phenolics in the water samples were 1.61×10^{2}–2.34×10^{9}, 2.90×10^{3}–4.64×10^{7} and 1.48×10^{2}–2.97×10^{7} copies·mL^{-1}, respectively. The absolute abundances of sulfonamides, quinolones, and phenols in the sediment samples were 2.26×10^{2}–7.77×10^{8}, 1.20×10^{3}–1.38×10^{7} and 2.93×10^{2}–1.71×10^{7} copies·g^{-1}, respectively. The most abundant antibiotic resistance genes were sulfonamide resistance genes (*sul1* and *sul2*) in the snakehead fish farm, with a total abundance of 7.36×10^{6}–2.34×10^{9} copies·mL^{-1} (copies·g^{-1}) in all samples. Quinolones, tetracycline, and phenicol resistance genes were also abundant on the aquatic farm, with a total abundance of 1.20×10^{3}–4.64×10^{7} copies·mL^{-1} (copies·g^{-1}), 5.83×10^{0}–5.00×10^{6} copies·mL^{-1} (copies·g^{-1}), and 1.48×10^{2}–2.97×10^{7} copies·mL^{-1} (copies·g^{-1}), respectively. β-lactam resistance genes ($bla_{\text{CTX-M}}$ and bla_{SHV}) showed the lowest absolute abundance compared with the other types of ARGs. The total absolute abundance of β-lactam resistance genes was 1.78×10^{-2} to 1.76×10^{5} copies·mL^{-1} (copies·g^{-1}) (Table S2). The absolute abundance of *qacEΔ1* ranged from 2.51×10^{4} to 6.60×10^{5} copies·mL^{-1} (copies·g^{-1}). The abundance of ARGs did not differ significantly during the fingerling, rearing, and harvesting stages (Figure 1). Pearson's test showed that there was a prominent correlation between *intI1* and eight ARGs: *sul1*, *sul2*, *aac6*, *qnrA*, *tetM*, *ermB*, $bla_{\text{CTX-M}}$, and *qacEΔ1* ($r > 0.5$, $P < 0.05$).

The copy numbers of ARGs were normalized to the corresponding copy numbers of 16S rRNA gene to calculate the relative abundance of ARGs (Figure 2). The relative

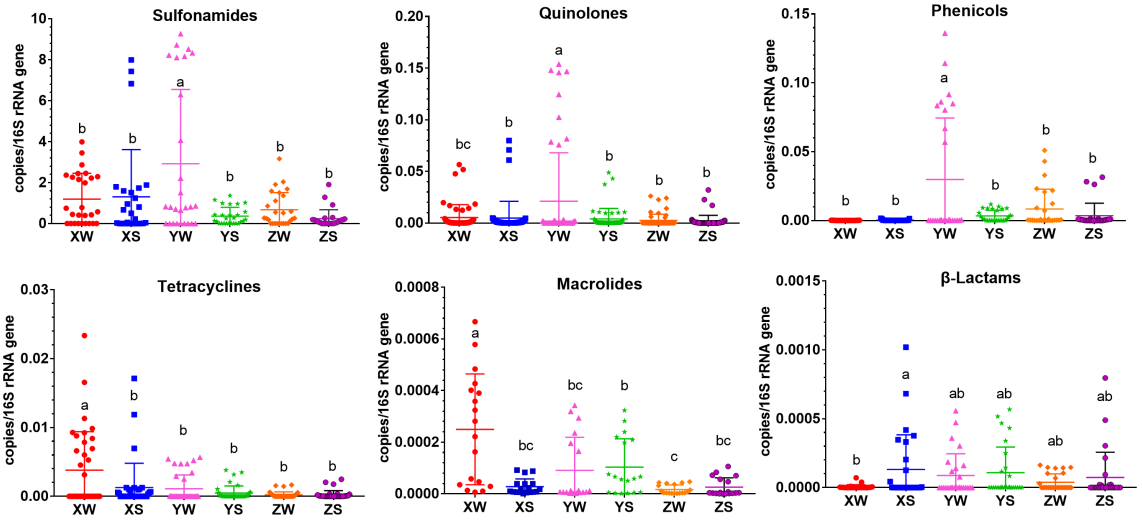

FIGURE 1
Distribution of different classes of ARGs in the water and sediment samples. X, Y, and Z indicate the fingerling, rearing, and harvesting stages, respectively, and S and W indicate the pond water and sediment samples, respectively. a,b and c indicate different significance at $P < 0.05$.

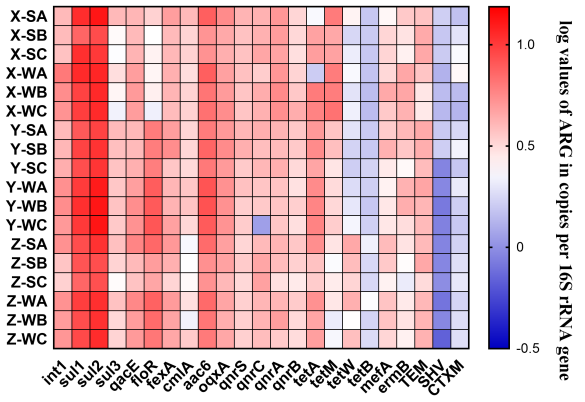

FIGURE 2
Heat map of the relative abundance of ARGs in each sample. X, Y, and Z indicate the fingerling, rearing, and harvesting stages, respectively; S and W indicate pond water and sediment samples, respectively; and A, B, and C indicate three different ponds.

abundance of sulfonamide resistance gene *sul2* from the water sample was the highest ($8.53 \times 10^{0} \pm 2.73 \times 10^{-1}$ copies/16S rRNA genes), followed by *sul1* from the water sample ($2.38 \times 10^{0} \pm 2.27 \times 10^{0}$ copies/16S rRNA genes). The following ARGs had lower relative copies/16S rRNA genes: *tetW* (6.07×10^{-8}–1.40×10^{-4}), *tetB* (5.65×10^{-6}–3.12×10^{-4}), *ermB* (3.80×10^{-7}–2.01×10^{-4}), bla_{TEM} (5.67×10^{-6}–1.08×10^{-4}), $bla_{\mathrm{CTX\text{-}M}}$ (8.10×10^{-8}–1.98×10^{-6}), and bla_{SHV} (8.99×10^{-11}–1.32×10^{-7}). The lowest concentration of ARGs was for $bla_{\mathrm{CTX\text{-}M}}$ (copies/16S rRNA genes). The relative abundance of each resistance gene is shown in Table S3.

Environmental factors in pond water samples

Overall, the pH value and concentrations of ammonia nitrogen, phosphate, and total alkalinity were significantly different among the three culture stages, whereas the concentrations of dissolved oxygen, nitrite nitrogen, sulfide, free chlorine, copper, chromium, total iron, total hardness, and water temperature were not significantly different (Figure 3). Most of these parameters were within the acceptable ranges except for ammonia nitrogen, which ranged from 0.036 to 5.65 $mg{\cdot}L^{-1}$ (acceptable ranges ≤4.0 $mg{\cdot}L^{-1}$) (Liu Q et al., 2014). The pH was maintained between 6.27 and 7.51, which was slightly lower during the harvesting stage. The temperature was maintained between 28°C and 31°C. The concentration of nitrite nitrogen ranged from 0.176 to 0.55 $mg{\cdot}L^{-1}$. High concentration of dissolved oxygen was determined from the surface water (10.49–17.83 $mg{\cdot}L^{-1}$), while low concentrations of sulfide, phosphate, free chlorine, copper and total iron were detected during fingerlings to the harvesting stage. The details of the environmental factors are listed in Table S4.

Bacterial community in water samples and sediment samples

Eighteen libraries of bacterial 16S rRNA genes from pond environmental samples were sequenced using the Illumina high-throughput sequencing platform to explore the shift in bacterial communities during snakehead fish culture. After assembly and filtration, the samples had an average of 116,921.93 ± 132 and 116,907.93 ± 137 clean tags in the sediment and water samples, respectively. The α-diversity indices of the microbial communities in the sediment and water of the fish culture ponds are shown in Figure 4 and Table S5. The Shannon, Simpson, Chao1, and ACE indices considered both the species richness and relative abundance distribution. Greater population richness and more diverse bacterial communities were observed in the sediment samples than in the water samples from the snakehead fish farm (Figure 4). Population richness was abundant in the sediment samples during the fingerling and harvesting stages, but was slightly lower during the rearing stage.

Proteobacteria and *Cyanobacteria* were the most abundant phyla in water sample and sediment samples, with relative abundances ranging from 38.77% to 44.92% (Figure 5). The second most abundant phylum in water samples was *Cyanobacteria*, followed by *Planctomycetes*, *Bacteroidetes*, *Chloroflexi*, *Actinobacteria*, and *Verrucomicrobia*. The second-most dominant phylum in the sediment samples was *Chloroflexi*, followed by *Actinobacteria*, *Planctomycetes*, *Acidobacteria*, *Verrucomicrobia*, *Bacteroidetes*, and *Gemmatimonadetes*. Although the bacterial community structures were different between the environmental samples in the three ponds, the most abundant phyla (*Cyanobacteria*, *Proteobacteria*, *Bacteroidetes*, *Actinobacteria*, and *Chloroflexi*) were similar in the environmental samples, with total relative abundances of 49.22% and 85.12% (Table S6).

Bacteria from water or sediment samples of fingerling, rearing, and harvesting stages clustered together in the principal coordinate analysis plot based on the Jaccard similarity index (OTUs presence and absence). However, the presence and abundance of bacterial communities differed between the water and sediment samples at the family level (Figure 6 and Table S7). In addition, the different colored nodes in Figure 6 represent samples from different breeding stages, implying that the microbial community structure greatly changed at different breeding stages.

Correlations among bacterial community, ARGs, and environmental factors

Network analysis and CCA were performed to further explore the relationship between the bacterial community in

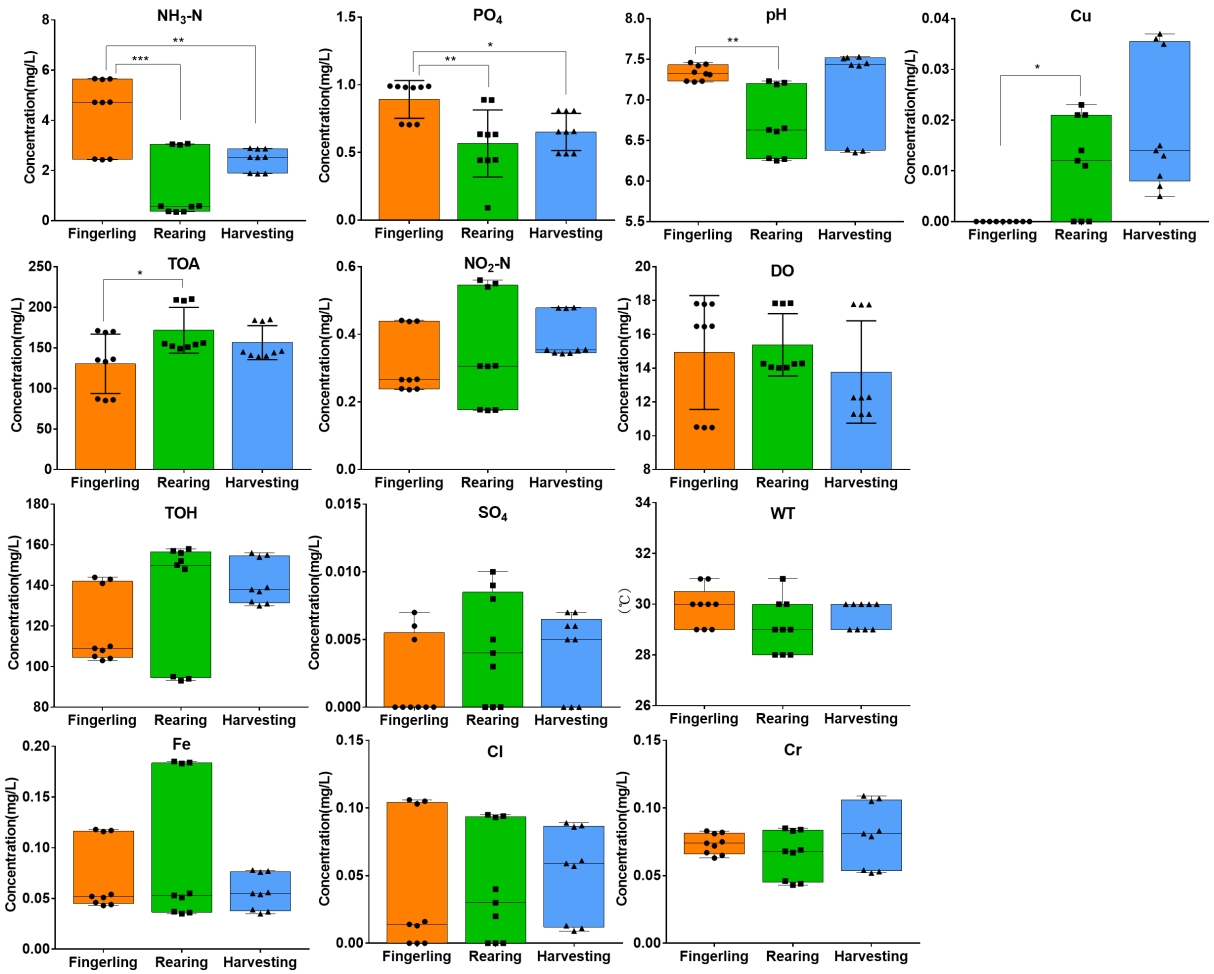

FIGURE 3
Concentrations of NH_3-N, PO_4, Cu, TOA, NO_2-N, DO, TOH, SO_4, Fe, Cl, and Cr and values of water temperature and pH in the water samples. *, $P < 0.05$; **, $P < 0.01$; ***, $P < 0.001$.

the sediment and water samples, environmental factors, and ARG abundance in hybrid snakehead fish farms (Figures 7A, B). Network analysis showed that the co-occurrence patterns between the bacterial community and ARGs consisted of 41 nodes and 96 edges (Figure 7A). The modularity index was 0.448, suggesting that the network had a modular structure. *Proteobacteria*, *Cyanobacteria*, *Bacteroidetes*, *Actinobacteria*, and *Verrucomicrobia* were strongly correlated with ten ARG subtypes (*intI1*, *sul2*, *sul1*, *aac6*, *cmlA*, *ermB*, *tetA*, *qacEΔ1*, *qnrA*, and *qnrS*) (Figure 7A). This suggested that the spread of ARGs in aquaculture is significantly affected by the proliferation of environmental microorganisms.

The correlation between the target environmental factors and bacteria at the phylum level in fishpond water samples was determined using CCA (Figure 7B). At the phylum level, CCA1 and CCA2 explained 66.69% and 13.18% of total variance, respectively. *Proteobacteria*, *Actinobacteria*, *Patescibacteria*, *Fusobacteria*, *Rokubacteria*, *Chloroflexi*, and *Planctomycetes* were positively correlated with sulfide, nitrite nitrogen, pH, free chlorine, and ammonia nitrogen. In addition, copper and dissolved oxygen levels were positively correlated with *Firmicutes*, *Cyanobacteria*, *Tenericutes*, *Verrucomicrobia*, *Fusobacteria*, and *Chloroflexi*.

Discussion

Diversity and abundance of ARGs in the hybrid snakehead fish farm

Twenty-one target ARGs and two integron-related genes (*intI1* and *qacEΔ1*) were detected in environmental samples from the hybrid snakehead fish culture system at the three breeding stages. Consistent with previous studies, these results

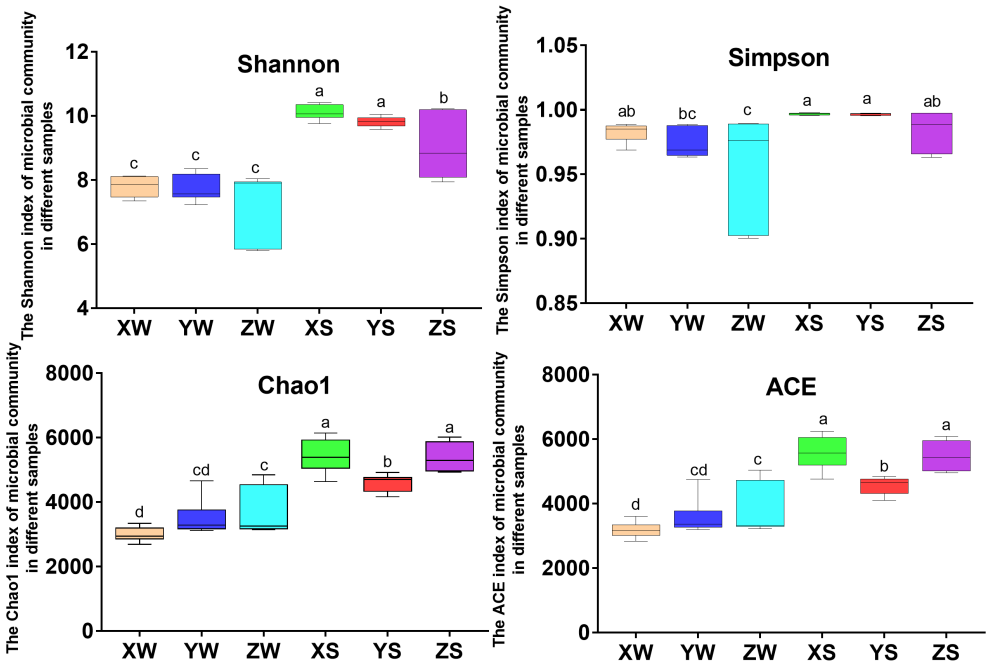

FIGURE 4
Differences and temporal trends of α-diversity indices between water and sediment samples in the hybrid snakehead fish culture system. X, Y, and Z indicate the fingerling, rearing, and harvesting stages, respectively, and S and W indicate the pond water and sediment samples, respectively. a,b and c indicate different significance at $P < 0.05$.

indicated the persistence of ARGs in aquaculture environments. (Shen et al., 2020; Suyamud et al., 2021). The high abundance of sulfonamide, tetracycline, quinolone, and phenicol resistance genes suggests that these bacteria may confer resistance to the most commonly used antibiotics in hybrid snakehead fish culture systems. Sulfonamide resistance genes (*sul1* and *sul2*) were detected in high absolute abundance, followed by *floR*, *aac6*, and *tetA*. Coincidentally, sulfonamide and tetracycline resistance genes frequently occur in river environments and are accompanied by the presence of integrons (Kumar et al., 2020; Dong et al., 2022). Similarly, the ARG subtypes mentioned above have the highest abundance in sediment and water samples from shrimp and fishponds (Huang et al., 2017; Cheng et al., 2021). For instance, the abundance of the

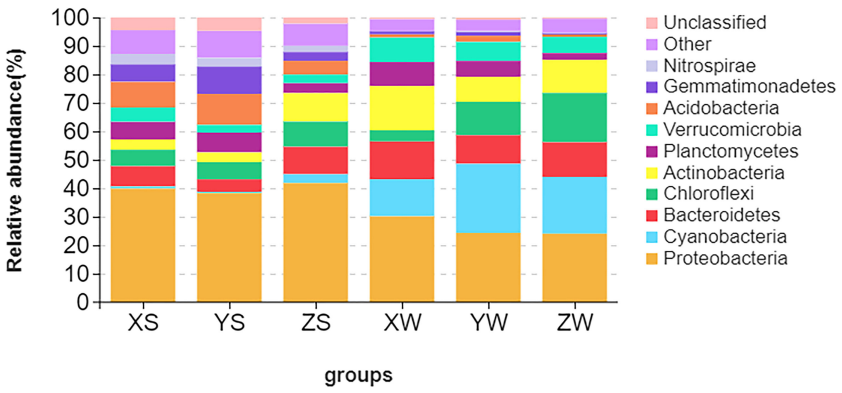

FIGURE 5
Relative abundance of the top 10 phyla in the water and sediment samples. X, Y, and Z indicate the fingerling, rearing, and harvesting stages, respectively, and S and W indicate the pond water and sediment samples, respectively.

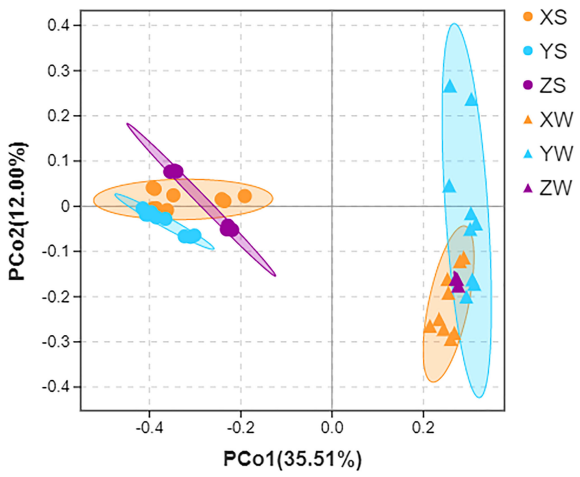

FIGURE 6
Principal coordinate analysis (PCoA) of Jaccard dissimilarity in water and sediment samples. X, Y, and Z indicate the fingerling, rearing, and harvesting stages, respectively, and S and W indicate the pond water and sediment samples, respectively.

tetracycline resistance gene *tetA*(10^6–10^9 copies·mL^{-1}) was the highest in sediment and water samples from freshwater fish farms (Huang et al., 2017). Concentrations of the sulfonamide resistance gene *sul1* and tetracycline resistance gene *tetW* were the highest in 15 sediment samples collected from five Chinese provinces (Cheng et al., 2021). In addition, the quinolone resistance gene *qnrB* is abundant in six freshwater ponds (Wang et al., 2022). Integrons play an important role in the emergence and horizontal transfer of ARGs among bacteria and are the main transmissible vectors commonly found in different environments (Wang et al., 2019). The relatively high abundance of *intI1* in the hybrid snakehead fish farm suggests potentially high mobility of ARGs. We also found a significant correlation between *intI1* and eight resistance genes ($r > 0.5$, $P < 0.05$). The abundances of ARGs and *intI1* measured in this study were comparable to those reported in other natural water bodies and aquaculture environments (Wang et al., 2019).

Several studies have confirmed the prevalence of ARGs in hospitals, pharmaceutical manufacturers, livestock farms, wastewater treatment plants, and rivers (Gao et al., 2012; Li et al., 2015; Zhou et al., 2017; Hu et al., 2018; Su et al., 2018a). Overuse of various antibacterial agents in humans and veterinarians, agriculture, and aquaculture has led to the emergence of antibiotic-resistant pathogens (Pham et al., 2018; Li et al., 2022). Water from nearby rivers brings polluting compounds from agricultural and domestic wastewater into aquaculture systems. In contrast, untreated aquaculture wastewater is pumped into rivers. High-density aquaculture involves rearing hybrid snakehead fishes in congested and stressful environments. The pond water is hardly exchanged, which allows antibiotics to impose selective pressure on bacteria. Our study demonstrated high ARGs and *intI1* copy numbers in pond water samples. This implies that one of the main reservoirs and sources of ARG in the surrounding aquatic environment is the pond water.

The abundance of ARGs varies temporally during different seasons and breeding stages in aquaculture (Zhang et al., 2021; Zhou et al., 2022). A higher mean abundance of ARGs in aquaculture sediments was observed in autumn and winter, whereas the mean abundance of ARGs decreased significantly in spring and summer (Xu et al., 2022). A comparison of the different breeding stages of grass carp ponds showed that the relative abundance of *sul2* in the harvesting and rearing culture stages was significantly higher than that in the larval culture stage, whereas the abundances of *cfr* and *tetQ* were significantly higher in the larval culture stage (Zhou et al., 2022). This study found that the abundance of ARGs did not differ significantly during the fingerling, rearing, or harvesting stages. Notably, the differential abundance of different ARG subtypes belonging to the same class of resistance genes may be irregularly expressed in aquaculture according to different culture systems, geographical locations, or drug usage.

Correlations between ARGs and microbial community structure

The relationship between ARGs and microbial communities was comprehensively explored by analyzing 22 resistance genes, *intI1*, and identifying bacteria at the phylum level, based on previous studies (Su et al., 2018b; Han et al., 2022). Despite the presence of various ARGs in aquaculture environments, microorganisms are considered the main vectors and determinants of ARG distribution and transmission (Wang et al., 2019). Antibiotic resistance genes mainly exist in bacterial genomes and may be transmitted through mobile genetic elements, including plasmids, integrons, transposons, and insertion sequences (Suyamud et al., 2021). *Proteobacteria* is the predominant phylum in Litopenaeus vannamei pond water, followed by *Bacteroides* (Zheng et al., 2016). *Proteobacteria* is also the most abundant phylum in water and sediment samples from different natural environments, followed by *Actinobacteria*, *Bacteroidetes*, *Chloroflexi*, and *Cyanobacteria* (Fang et al., 2019). This study found that *Proteobacteria* and *Cyanobacteria* were the two predominant phyla in water samples from snakehead fish aquaculture, which is similar to the dominant bacterial phyla found in previous studies on fish ponds (Su et al., 2017; Klase et al., 2019). The present results indicate that the microbiota structure at the family or genus level significantly changed at different breeding stages despite the similar abundance of the predominant bacterial phyla. There are differences in breeding patterns and seasonal changes in the bacterial composition of different ponds (Xu et al., 2020). We also found that the presence and abundance of bacterial communities differed between water and sediment samples at the family level. These results may be attributed to differences in aquaculture patterns and regional differences.

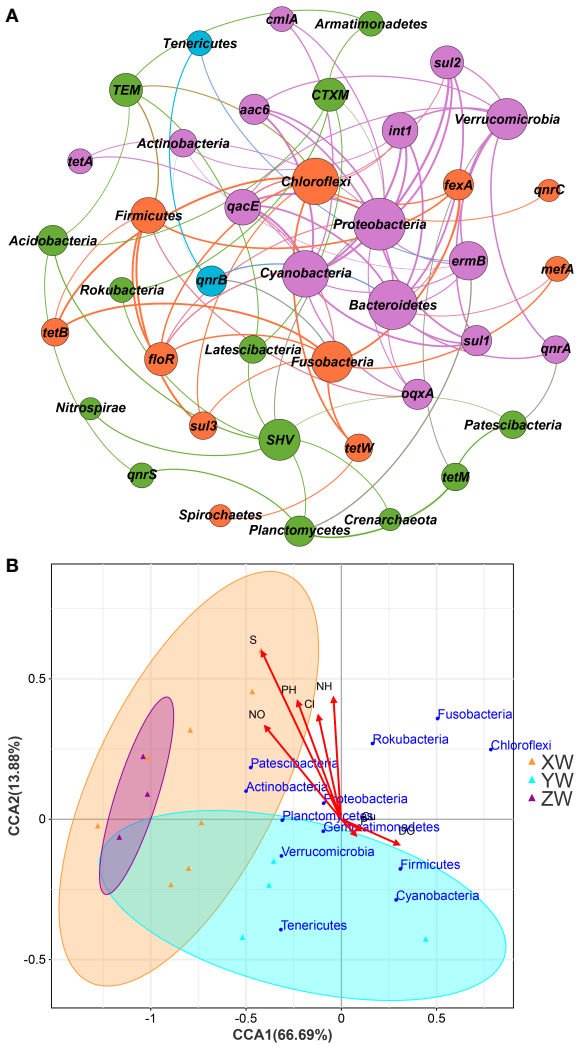

FIGURE 7
Correlations among the bacterial community, ARGs, and environmental factors. **(A)** Network analysis of ARGs and bacterial communities at the phylum level in the pond water. The linkage between the nodes indicates a correlation between the two factors, and the size of the node is proportional to the number of connections. At the same time, the thickness of the line was proportional to the correlation between the factors. **(B)** Canonical correspondence analysis of the environmental factors and bacterial communities at the phylum level.

Network analysis was performed to further analyze the co-occurrence of ARGs and dominant bacteria at the phylum level in the pond water and sediment samples. *Proteobacteria*, *Cyanobacteria*, *Bacteroidetes*, *Actinobacteria*, and *Verrucomicrobia* were strongly correlated with ten ARG subtypes (*sul1*, *sul2*, *aac6*, *cmlA*, *ermB*, *tetA*, *qacE*, *qnrA*, and *qnrS*) and *intI1*. This implies that these predominant bacteria may be responsible for the increased abundance of ARGs in the snakehead fish farms. Some *Firmicutes* bacterial taxa are major potential hosts of ARGs, which strongly co-occur with *sul1*, *qnrS*, *tetM*, and *intl1* genes (Cheng et al., 2021). Meanwhile, the sulfonamide resistance gene *sul1* and tetracycline resistance genes (*tetW* and *tetG*) are mainly associated with *Actinomyces*, *Proteobacteria*, and *Actinomycetes*. Among these, *Proteobacteria* have a high potential for hosting the sulfonamide resistance gene (Shen et al., 2020). These results indicate that changes in bacterial composition may lead to significant and strong correlation differences between ARG and predicted carrier bacteria in different environments.

Relationship between environmental factors and the bacterial community

The distribution of ARG and their potential carrier microorganisms is greatly affected by environmental factors such as nutrients and pollutants in water (Zhao et al., 2021; Ning et al.,

2022). Changes in environmental factors, such as organic matter level, total nitrogen, temperature, and heavy metals, promote the transfer of bacterial communities and reproduction of ARG in aquatic environments (Xu et al., 2022). The present study found a significant correlation between the environmental factors of water and the bacterial communities in ponds. *Proteobacteria*, *Actinobacteria*, and *Patescibacteria* were positively correlated with sulfide, nitrite nitrogen, pH, free chlorine, and ammonia nitrogen concentrations. Ammonia nitrogen, nitrite nitrogen, and pH are important parameters for fish culture. Most fish species do well within a pH range of 6.5–9.5. Chronic pH levels below 6.5 may reduce fish reproduction and are associated with fish die-offs. The nitrate levels in pond water are also a major concern in fish culture. Exceedingly high nitrate-nitrogen and ammonia concentrations are health hazards. Most of these parameters, except for ammonia nitrogen, were within the acceptable range for snakehead fish cultures. This may be attributed to the high-density culture of fish and excessive feed in the pond. Long rearing times induce the accumulation of feeding residues that affect the levels of nitrogenous compounds (Chen et al., 2018), and prolonged exposure to nitrogenous compounds may result in immunological responses within fishponds. At the same time, heavy metal pollution causes the deterioration of water quality, which affects the ecological stability of flora in the water environment (Ai et al., 2022). Other pollutants with significant antibacterial activity can select antibiotic resistance genes, such as heavy metals (He et al., 2017), pesticides (Anjum and Krakat, 2016), and disinfectants (Chaturvedi et al., 2021). In addition, antibiotic resistance can be triggered and catalyzed by metal-driven co-selection, an indirect selection process with physiological and genetic consequences (Ai et al., 2022). In contrast, this study only detected low metal concentrations in pond water and their levels were not significantly correlated with the bacterial community. However, multiple factors in snakehead fish cultures with high stock densities pose a high potential risk of increasing antibiotic resistance in aquaculture. Controlling bacterial diseases in fish cultures has become more difficult because of the emergence of ARGs, especially those caused by multidrug-resistant bacteria.

Conclusion

This study showed an increased occurrence of sulfonamides, tetracyclines, quinolones, and phenicol resistance genes in pond water and sediments of the hybrid snakehead fish farm. Some bacterial taxa from the phyla *Proteobacteria*, *Cyanobacteria*, *Bacteroidetes*, *Actinobacteria*, and *Verrucomicrobia* may be major potential hosts of ARGs in this aquatic farm. In addition, the congested and stressful environment of snakehead fish cultures may cause pollution problems with negative effects on the propagation of resistant bacteria that drive the occurrence of ARGs. More attention should be paid to the better feeding and management of fish cultures. Moreover, the elimination of ARGs in wastewater from aquaculture environments should be considered to reduce the pollutants discharged into the natural environment. The levels of antibiotic resistance genes and microbial community composition in aquaculture should be tested regularly to assess potential risks to public health.

Data availability statement

The raw sequencing date generated from this study have been deposited in NCBI SRA (http://www.ncbi.nlm.nih.gov/sra) under the accession number PRJNA907527.

Author contributions

XL and YD played an important role in this study. XL and AT completed a part of the experiment. FZ and WL performed the data analysis. XL wrote the first draft of the manuscript. AT has edited the final version of the manuscript. YD and ZH reviewed and edited the manuscript. All authors contributed to the article and approved the submitted version.

Funding

This work was supported by Guangdong Natural Science Foundation (No.2020A1515011584) and Central Public-interest Scientific Institution Basal Research Fund, CAFS (2022GH04, 2021SJ-XT3, 2020TD45).

Conflict of interest

The authors declare that the research was conducted in the absence of any commercial or financial relationships that could be construed as a potential conflict of interest.

Publisher's note

Supplementary material

The Supplementary Material for this article can be found online at: https://www.frontiersin.org/articles/10.3389/fmars.2022.1088176/full#supplementary-material

References

Ai, L., Ma, B., Shao, S., Zhang, L., and Zhang, L. (2022). Heavy metals in Chinese freshwater fish: Levels, regional distribution, sources and health risk assessment. *Sci. Total Environ.* 853, 158455. doi: 10.1016/j.scitotenv.2022.158455

Allen, H. K., Donato, J., Wang, H. H., Cloud-Hansen, K. A., Davies, J., and Handelsman, J. (2010). Call of the wild: Antibiotic resistance genes in natural environments. *Nat. Rev. Microbio.* 8 (4), 251–259. doi: 10.1038/nrmicro2312

Anjum, R., and Krakat, N. (2016). Detection of multiple substances, biofilm formation, and conjugative transfer of b. cereus from contaminated soils. *Curr. Microbio.* 72 (3), 321–328. doi: 10.1007/s00284-015-0952-1

Berendonk, T. U., Manaia, C. M., Merlin, C., Fatta-Kassinos, D., Cytryn, E., Bürgmann, H., et al. (2015). Tackling antibiotic resistance: The environmental framework. *Nat. Rev. Microbiol.* 13 (5), 310–317. doi: 10.1038/nrmicro3439

Chaturvedi, P., Shukla, P., Giri, B. S., Chowdhary, P., Chandra, R., Gupta, P., et al. (2021). Prevalence and hazardous impact of pharmaceutical and personal care products and antibiotics in environment: A review on emerging contaminants. *Environ. Res.* 194, 110664. doi: 10.1016/j.envres.2020.110664

Cheng, X., Lu, Y., Song, Y., Zhang, R., ShangGuan, X., Xu, H. Z., et al. (2021). Analysis of antibiotic resistance genes, environmental factors, and microbial community from aquaculture farms in five provinces, china. *Front. Microbio.* 12. doi: 10.3389/fmicb.2021.679805

Chen, B., Lin, L., Fang, L., Yang, Y., Chen, E., Yuan, K., et al. (2018). Complex pollution of antibiotic resistance genes due to beta-lactam and aminoglycoside use in aquaculture farming. *Water Res.* 134, 200–208. doi: 10.1016/j.watres.2018.02.003

Dong, J., Yan, D., Mo, K., Chen, Q., Zhang, J., Chen, Y. C., et al. (2022). Antibiotics along an alpine river and in the receiving lake with a catchment dominated by grazing husbandry. *J. Environ. Sci.* 115, 374–382. doi: 10.1016/j.jes.2021.08.007

Fang, H., Huang, K., Yu, J., Ding, C., Wang, Z., Zhao, C., et al. (2019). Metagenomic analysis of bacterial communities and antibiotic resistance genes in the eriocheir sinensis freshwater aquaculture environment. *Chemosphere.* 224, 202–211. doi: 10.1016/j.chemosphere.2019.02.068

Gao, P., Munir, M., and Xagoraraki, I. (2012). Correlation of tetracycline and sulfonamide antibiotics with corresponding resistance genes and resistant bacteria in a conventional municipal wastewater treatment plant. *Sci. Total Environ.* 421-422, 173–183. doi: 10.1016/j.scitotenv.2012.01.061

Han, Y., Hu, Y., Wen, H., Wu, J., Liu, Y., Zhang, Y. C., et al. (2022). Occurrence and driving mechanism of antibiotic resistance genes in marine recreational water around qinhuangdao, China. *Fron Mar. Sci.* 9. doi: 10.3389/fmars.2022.976438

He, X., Xu, Y., Chen, J., Ling, J., Li, Y., Huang, L., et al. (2017). Evolution of corresponding resistance genes in the water of fish tanks with multiple stresses of antibiotics and heavy metals. *Water Res.* 124, 39–48. doi: 10.1016/j.watres.2017.07.048

Hossain, A., Habibullah-Al-Mamun, M., Nagano, I., Masunaga, S., and Kitazawa, D. (2022). Antibiotics, antibiotic-resistant bacteria, and resistance genes in aquaculture: Risks, current concern, and future thinking. *Environ. Sci. pollut. Res. Int.* 299 (8), 11054–11075. doi: 10.1007/s11356-021-17825-4

Huang, L., Xu, Y., Xu, J., Ling, J., Chen, J., Zhou., J. L., et al. (2017). Antibiotic resistance genes (ARGs) in duck and fish production ponds with integrated or non-integrated mode. *Chemosphere.* 168, 1107–1114. doi: 10.1016/j.chemosphere.2016.10.096

Hu, J., Zhao, F., Zhang, X., Li, K., Li, C., Ye, L., et al. (2018). Metagenomic profiling of ARGs in airborne particulate matters during a severe smog event. *Sci. Total Environ.* 615, 1332–1340. doi: 10.1016/j.scitotenv.2017.09.222

Klase, G., Lee, S., Liang, S., Kim, J., Zo, Y. G., and Lee, J. (2019). The microbiome and antibiotic resistance in integrated fish farm water: Implications of environmental public health. *Sci. Total Environ.* 649, 1491–1501. doi: 10.1016/j.scitotenv.2018.08.288

Kumar, M., Sulfikar,, Chaminda, T., Patel, A. K., Sewwandi, H., and Mazumder, P. (2020). Prevalence of antibiotic resistance in the tropical rivers of Sri Lanka and India. *Environ. Res.* 188, 109765. doi: 10.1016/j.envres.2020.109765

Li, J., Cheng, W., Xu, L., Strong, P. J., and Chen, H. (2015). Antibiotic-resistant genes and antibiotic-resistant bacteria in the effluent of urban residential areas, hospitals, and a municipal wastewater treatment plant system. environ. *Sci. pollut. Res.* 22 (6), 4587–4596. doi: 10.1007/s11356-014-3665-2

Li, S., Ondon, B. S., Ho, S. H., Jiang, J., and Li, F. (2022). Antibiotic resistant bacteria and genes in wastewater treatment plants: From occurrence to treatment strategies. *Sci. Total Environ.* 838 (Pt 4), 156544. doi: 10.1016/j.scitotenv.2022.156544

Liu, Q., Lai, Z., Yang, W., Gao, Y., and Wang, C. (2014). Assessment of water quality of intensive ponds in the pearl river delta region. *South China Fisheries Sci.* 10, 36–43. doi: 10.3969/j.issn.2095–0780.2014.06.005

Liu, X., Steele, J. C., and Meng, X. (2017). Usage, residue, and human health risk of antibiotics in Chinese aquaculture: A review. *Environ. Pollution.* 223, 161–169. doi: 10.1016/j.envpol.2017.01.003

Ning, K., Ji, L., Zhang, L., Zhu, X., Wei, H., and Wang, Z. (2022). Is rice-crayfish co-culture a better aquaculture model: From the perspective of antibiotic resistome profiles. *Environ. pollut.* 2929 (Pt B), 118450. doi: 10.1016/j.envpol.2021.118450

Pham, T., Rossi, P., Dinh, H., Pham, N., Tran, P. A., Ho, T., et al. (2018). Analysis of antibiotic multi-resistant bacteria and resistance genes in the effluent of an intensive shrimp farm (Long an, Vietnam). *J. Environ. Manage.* 214, 149–156. doi: 10.1016/j.jenvman.2018.02.089

Shen, X. X., Jin, G. Q., Zhao, Y. Z., and Shao, X. H. (2020). Prevalence and distribution analysis of antibiotic resistance genes in a large-scale aquaculture environment. *Sci. Total Environ.* 711, 134626. doi: 10.1016/j.scitotenv.2019.134626

Su, H., Hu, X., Xu, Y., Xu, W., Huang, X., Wen, G., et al. (2018a). Persistence and spatial variation of antibiotic resistance genes and bacterial populations change in reared shrimp in south China. *Environ. Int.* 119, 327–333. doi: 10.1016/j.envint.2018.07.007

Su, H., Liu, S., Hu, X., Xu, X., Xu, W., Xu, Y., et al. (2017). Occurrence and temporal variation of antibiotic resistance genes (ARGs) in shrimp aquaculture: ARGs dissemination from farming source to reared organisms. *Sci. Total Environ.* 607-608, 357–366. doi: 10.1016/j.scitotenv.2017.07.040

Su, H., Liu, Y., Pan, C., Chen, J., He, L., Ying, G. G., et al. (2018b). Persistence of antibiotic resistance genes and bacterial community changes in drinking water treatment system: from drinking water source to tap water. *Sci. Total Environ.* 616-617, 453–461. doi: 10.1016/j.scitotenv.2017.10.318

Suyamud, B., Lohwacharin, J., Yang, Y., and Sharma, V. K. (2021). Antibiotic resistant bacteria and genes in shrimp aquaculture water: identification and removal by ferrate(VI). *J. Hazard Mater.* 420, 126572. doi: 10.1016/j.jhazmat.2021.126572

Wang, J. H., Lu, J., Wu, J., Zhang, Y., and Zhang, C. (2019). Proliferation of antibiotic resistance genes in coastal recirculating mariculture system. *Environ. pollut.* 248, 462–470. doi: 10.1016/j.envpol.2019.02.062

Wang, Q., Mao, C., Lei, L., Yan, B., Yuan, J., Guo, Y. Y., et al. (2022). Antibiotic resistance genes and their links with bacteria and environmental factors in three predominant freshwater aquaculture modes. *Ecotoxicol Environ. Saf.* 241, 113832. doi: 10.1016/j.ecoenv.2022.113832

Xu, M., Huang, X. H., Shen, X. X., Chen, H. Q., Li, C., Jin, G. Q., et al. (2022). Metagenomic insights into the spatiotemporal responses of antibiotic resistance genes and microbial communities in aquaculture sediments. *Chemosphere.* 307 (Pt 1), 135596. doi: 10.1016/j.chemosphere.2022.135596

Xu, C., Lv, Z., Shen, Y., Liu, D., Fu, Y., Zhou, L., et al. (2020). Metagenomic insights into differences in environmental resistome profiles between integrated and monoculture aquaculture farms in China. *Environ. Int.* 144, 106005. doi: 10.1016/j.envint.2020.106005

Zhang, R., Kang, Y., Zhang, R., Han, M., Zeng, W., Wang, Y. H., et al. (2021). Occurrence, source, and the fate of antibiotics in mariculture ponds near the maowei Sea, south China: storm caused the increase of antibiotics usage. *Sci. Total Environ.* 752, 141882. doi: 10.1016/j.scitotenv.2020.141882

Zhao, X., Su, H., Xu, W., Hu, X., Xu, Y., Wen, G. L., et al. (2021). Removal of antibiotic resistance genes and inactivation of antibiotic-resistant bacteria by oxidative treatments. *Sci. Total Environ.* 778, 146348. doi: 10.1016/j.scitotenv.2021.146348

Zhao, W., Wang, B., and Yu, G. (2018). Antibiotic resistance genes in China: occurrence, risk, and correlation among different parameters. *Environ. Sci. pollut. Res.* 25 (22), 21467–21482. doi: 10.1007/s11356-018-2507-z

Zheng, Y. F., Min, Y., Yan, L., Ying, S., Tao, X., Yu, M. C., et al. (2016). Comparison of cultivable bacterial communities associated with pacific white shrimp (litopenaeus vannamei) larvae at different health statuses and growth stages. *Aquaculture* 451, 163169. doi: 10.1016/j.aquaculture.2015.09020

Zhou, Y., Niu, L., Zhu, S., Lu, H., and Liu, W. (2017). Occurrence, abundance, and distribution of sulfonamide and tetracycline resistance genes in agricultural soils across China. *Sci. Total Environ.* 599-600, 1977–1983. doi: 10.1016/j.scitotenv.2017.05.152

Zhou, A., Xie, S., Tang, H., Zhang, L., Zhang, Y., Zuo, Z. H., et al. (2022). The dynamic of the potential pathogenic bacteria, antibiotic-resistant bacteria, and antibiotic resistance genes in the water at different growth stages of grass carp pond. *Environ. Sci. pollut. Res. Int.* 29 (16), 23806–23822. doi: 10.1007/s11356-021-17578-0

frontiers | Frontiers in Marine Science

TYPE Brief Research Report
PUBLISHED 13 February 2023
DOI 10.3389/fmars.2023.1083714

OPEN ACCESS

EDITED BY
Francisco Vargas-Albores,
National Council of Science and Technology (CONACYT), Mexico

REVIEWED BY
Javier Santander,
Memorial University of Newfoundland, Canada
Biswajit Maiti,
Nitte University, India

*CORRESPONDENCE
Yiqin Deng
yiqindd@126.com
Juan Feng
juanfeng@scsfri.ac.cn

SPECIALTY SECTION
This article was submitted to Marine Fisheries, Aquaculture and Living Resources, a section of the journal Frontiers in Marine Science

RECEIVED 29 October 2022
ACCEPTED 30 January 2023
PUBLISHED 13 February 2023

CITATION
Deng Y, Gao S, Xu L, Cheng C, Ma H and Feng J (2023) First insight into how stress exposure triggers *Vibrio harveyi* recipient successful conjugation.
Front. Mar. Sci. 10:1083714.
doi: 10.3389/fmars.2023.1083714

First insight into how stress exposure triggers *Vibrio harveyi* recipient successful conjugation

Yiqin Deng*, Si'ao Gao, Liwen Xu, Changhong Cheng, Hongling Ma and Juan Feng*

Key Laboratory of South China Sea Fishery Resources Exploitation and Utilization, Ministry of Agriculture and Rural Affairs, South China Sea Fisheries Research Institute, Chinese Academy of Fishery Sciences, Guangzhou, China

Conjugation is the most common horizontal gene transfer (HGT) process that can be affected by environmental change and promote bacterial virulence and drug resistance. However, it is unknown whether environmental changes can influence the conjugation ability of the marine fish pathogen *Vibrio harveyi*, thereby affecting its pathogenicity and drug resistance. This study systematically analyzes the effect of environmental stress on the ability of *V. harveyi* to obtain shuttle plasmids from *Escherichia coli* during conjugation. The results indicate that *V. harveyi* cannot receive shuttle plasmid pMMB207 without exposure to stress. However, certain stress exposure (37–46°C, 4%–16% ethanol, 0.14–0.56 mM SDS, 0.04~0.05 M NaOH, and 0.012–0.024 M HCl for 5–60 minutes) in the log phase of *V. harveyi* before conjugation successfully induces the fertility of the *V. harveyi* recipient in intergeneric mating with *E. coli*. In particular, ethanol and heat stress showed strong induction with up to 2.5×10^5 and 5.3×10^3 transconjugants when exposed to 16% ethanol for 10 minutes and 40°C for 60 minutes, respectively. Additionally, appropriate levels of NaOH (0.05 M, 10 minutes), SDS (0.42 mM, 5 minutes), and HCl (0.024 M, 5 minutes) lead to 2.3×10^3, 4.5×10^2, and 1.8×10^2 transconjugants, respectively. These results will help establish homologous recombination gene knockout technology and greatly advance molecular theoretical research on *V. harveyi*. They will also support the establishment of disease prevention and control strategies based on the interruption of the HGT process by environmental regulation.

KEYWORDS

***Vibrio harveyi*, stress exposure, horizontal gene transfer, induced fertility, environmental regulation**

1 Introduction

About 1.6%–32.6% of genes in each microbial genome are obtained through horizontal gene transfer (HGT), which has become the most important driving force in the evolution of prokaryotes, affecting prokaryotic pathogenicity, drug resistance, metabolism, and so on (Koonin et al., 2001; Thomas and Nielsen, 2005). HGT mainly occurs in prokaryotes through three processes: transformation, transduction, and conjugation. Conjugation transfer is the

most likely HGT mode with the highest transfer efficiency in the environment due to the wide range of transferred genes, the lack of a requirement for homology and recombination, and the ability to cross species (Koonin et al., 2001).

Conjugation is a DNA exchange process that forms a "junction bridge" through the contact fusion of the cell membranes of the donor and recipient bacteria. Single-strand plasmids are transported across the cell membrane into recipient cells through the junction bridge, and complementary chains are synthesized to form new plasmid molecules (Thomas and Nielsen, 2005). As a result, conjugation requires the joint participation of the donor bacteria, recipient bacteria, and plasmid. Certain environmental stress can affect bacterial cell membrane status and immune systems, including restriction-modification (R-M) and clustered regu¬larly interspaced short palindromic repeat-associated protein (CRISPR) systems, thus affecting the conjugation efficiency and stability of foreign plasmids in recipient bacteria cells (Schäfer et al., 1994). For example, heat treatment at 50 °C for 20 minutes can inhibit the R-M system of *Salmonella typhimurium*, thus increasing its fertility in intergeneric mating with *Escherichia coli* by approximately 200 folds and enhancing the stability of hybrid recombinants (Mojica-a and Middleton, 1971). Additionally, exposure to 4%–20% ethanol for nine minutes increases the fertility of *Corynebacterium glutamicum* crosses with *E. coli* by up to 10^4 folds, probably by affecting the cytoplasmic membrane fluidity (Schäfer et al., 1994).

In recent years, *Vibrio harveyi* has become the most dominant Vibrio pathogenic bacteria of marine fish in the South China Sea, causing massive economic losses to the aquaculture industry (Deng et al., 2020a; Deng et al., 2020b). It is reported that *V. harveyi* can obtain foreign DNA through HGT, increasing its pathogenicity and drug resistance, the complexity and variability of Vibrio disease prevention and control, and posing a significant threat to breeding and food safety (Ruwandeepika et al., 2010; Deng et al., 2019; Deng et al., 2020b). In addition, the temperature rise caused by global warming and the environmental pollution caused by human activities can seriously affect the sustainable development of aquaculture (Khoshnevis Yazdi and Shakouri, 2010; Zhou et al., 2021). However, it is unknown whether the environmental changes affect the HGT of *V. harveyi*, thus impacting their pathogenicity and drug resistance. Furthermore, it was found that the laboratory conjugation transfer efficiency of *V. harveyi* is extremely low and normally unsuccessful. This precludes the use of conjugation to transfer suicide plasmids from the donor bacteria to the recipient bacteria in order to carry out in-frame gene mutations, seriously limiting research into the regulation of virulence and drug resistance in *V. harveyi*.

In this study, we investigated the effects of different environmental stresses (heat, ethanol, SDS, acid, alkali, and salinity) on the conjugation efficiency of *V. harveyi* recipient crosses with *E. coli*. This will provide new insights into the mechanisms of pathogenicity and drug resistance in *V. harveyi*, in addition to an important scientific foundation for in-frame deletions and will establish strategies for preventing and controlling outbreaks of *V. harveyi* disease based on the blocking of the conjugation transfer process.

2 Materials and methods

2.1 Bacterial strains and growth conditions

The bacterial strains and plasmids used in this study are listed in Table 1. The conjugative receptor strain *V. harveyi* 345 was isolated from a diseased pearl gentian grouper with multi-drug resistance and a median lethal dose of 9.83×10^5 CFU·g^{-1} (Deng et al., 2019). It was cultured in Luria–Bertani (LB) broth with 2% additional NaCl (LBS) at 28°C. The mobilizable shuttle plasmid pMMB207 (Figure S1) is chloramphenicol (Cm) resistant and can be transferred *via* conjugation from *E. coli* to a variety of bacteria including *Aeromonas hydrophila*, *V. alginolyticus*, *V. campbellii*, *V anguillarum*, and *V. parahaemolyticus* (Zhang, 2012; Pang, 2015; Liu et al., 2017; Li et al., 2022). The conjugative donor strain, *E. coli* GEB883-pMMB207, was the GEB883 strain with pMMB207. It was cultured in LB with 20 μg/ml Cm and 0.3 mM diaminopimelate (DAP) at 37°C.

2.2 Conjugation assay

V. harveyi 345 was inoculated into an LBS liquid medium and cultured overnight at 28°C with 200 rpm shaking, then diluted 300 times and cultured under the same conditions until the early log phase (OD600nm = 0.5–1.0). The *E. coli* GEB883-pMMB207 was inoculated into LB liquid medium with 20 μg/ml Cm and 0.3 mM DAP at 37°C with 200 rpm shaking, then the overnight culture was diluted 100 times and cultured under the same conditions until the early log phase (OD600nm = 0.5–1.0).

TABLE 1 The bacterial strains and plasmids used in this study.

Strains or plasmids	Relevant characteristics	Sources
Bacterial strains		
V. harveyi 345	*V. harveyi* 345: isolated from diseased grouper kidney off the South China Sea coast	(Deng et al., 2019)
E. coli GEB883	Ery^r, Tet^r,WT*E.coli* K12 Δ*dapA::erm pir RP4*-2 Δ*recAgyrA462*, *zei298::Tn10*	(Nguyen et al., 2018)
Plasmids		
pMMB207	Cm^r; Prokaryotic cell expression vector plasmid; Tac-Promoter; stable expression	(Liu et al., 2017)

The early log phase recipient bacterial cells of *V. harveyi* 345 were exposed to different stress (31–46°C for 15–60 minutes, 4%–16% ethanol for 5–30 minutes, 0.14–0.56 mM SDS for 5–30 minutes, 0.01–0.05 M NaOH for 5–20 minutes, 0.012–0.06 M HCl for 5–30 minutes), and then washed with 3% NaCl for appropriate times (temperature: did not wash, ethanol: washed three times, SDS: washed four times, NaOH: washed two times, and HCl: washed two times) according to the stress conditions. For each stress condition, 500 µL recipient bacterial cells were used to do stress exposure, and then the 500 µL stress-exposed recipient bacterial cells were mixed with 500 µL early log phase donor bacterial cells of *E. coli* GEB883-pMMB207. In addition, for salinity stress, an overnight culture of *V. harveyi* 345 was diluted 300 times in LB liquid medium with a final NaCl concentration of 0.5%, 1.0%, 1.5%, and 4.0% and cultured until the early log phase (OD600nm = 0.5–1.0). Then, 500 µL early log phase recipient bacterial cells were mixed with 500 µL early log phase donor bacterial cells. The mixture was centrifugated at 8,000 g for two minutes at room temperature. After removing the supernatant, the precipitation was suspended with 50 µL of 3% NaCl and seeded onto an LBS plate with DAP (0.3 mM). The plate was dried and conjugated for 16 hours at 28°C. The conjunctive plaques were then scraped and re-suspended in 1 mL 3% NaCl and washed once with 3% NaCl. The bacterial suspension was screened on LBS plates with Cm (34 µg/mL) at an appropriate dilution and incubated for 16 hours at 28°C. Firstly, three to four transconjugant candidates of each condition were selected to do PCR verification with the specific primers pMMB207-F (5'-ctactgagcgctgccgcaca-3') and pMMB207-R (5'-tcgttttatttgatgcctggcag-3') with a target band of 1877 bp. The PCR action was checked by 1% agarose gel electrophoresis. Then, the number of transconjugants was counted and compared under different stress conditions. The early log phase recipient *V. harveyi* 345 without exposure to stress (28°C, 3% NaCl, 0% ethanol, 0 mM SDS, 0 M NaOH, or 0 M HCl) was used as the control, and the experiment was conducted three times.

3 Results

Without exposure to stress, the shuttle plasmid pMMB207 cannot be transferred to *V. harveyi* by conjugation. However, this plasmid's intergeneric transfer could be optimized by exposing the *V. harveyi* recipient cells to stress before mating. Compared with untreated controls, fertility was obtained when bacterial cells were exposed to various treatments, including high temperatures, small alcohols (ethanol), detergents (SDS), and pH shifts (Figure 1).

Generally, ethanol has the largest effect on transconjugation, leading to as many as 2.5×10^5 transconjugants, followed by temperature (5.3×10^3), NaOH (2.3×10^3), SDS (4.5×10^2), and HCl (1.8×10^2) (Figure 2). No transconjugants grew in the absence of heat shock (28°C) or when recipient cells of *V. harveyi* 345 were heat shocked for 15–60 minutes at 31 and 34°C (Figure 2A). When the recipient cells were heat treated for 30 minutes at 37°C, pMMB207 was successfully transferred into *V. harveyi*, and 24 transconjugants grew. *V. harveyi* has a high mating ability when exposed to 40°C for 30–60 minutes, 43°C for 15–60 minutes, and 46°C for 15 minutes (Figure 2A). When exposed to 40°C, the mating ability increased with the extension of processing time (Figure 2A). However, the mating ability decreased as the processing time increased when exposed to 43 and 46°C (Figure 2A). When treated with 4% ethanol for 15 minutes, *V. harveyi* successfully incorporated the shuttle plasmid pMMB207 (Figure 2B). Relatively high fertility was induced by 4%–8% ethanol for 5–30 min and 12% ethanol for 5–10 minutes, which led to 1,970–4,500 transconjugants (Figure 2B). Additionally, optimal fertility was induced by stress conditions of 12% ethanol for 20–30 minutes and 16% ethanol for 5–10 minutes, which led to 44,770–249,770 transconjugants (Figure 2B). Figure 2C illustrates that exposure to a low concentration of 0.14 mM SDS detergent increased the fertility of *V. harveyi* as the incubation time increased. However, the opposite trend occurred when exposed to high concentrations of SDS (0.42 and 0.56 mM), and no transconjugants were obtained when exposed for 20–30 minutes. When treated with a medium concentration of 0.28 mM SDS, the transconjugants increased at first (5–20 minutes), then sharply decreased (30 minutes). Acid (HCl) and alkali (NaOH) treatments aided *V. harveyi* to receive the shuttle plasmid pMMB207 from *E. coli via* conjugation, especially when *V. harveyi* was treated with 0.04–0.05 M NaOH for 5–20 minutes, yielding up to 2,300 transconjugants, and when treated with 0.012-0.024 M HCl for 5–30 minutes, generating up to 180 transconjugants (Figures 2D, E). However, *V. harveyi* nearly failed to mate with *E. coli* when treated with 0.01–0.03 M NaOH and 0.036–0.06 M HCl (Figures 2D, E). Furthermore, when the overnight culture of *V. harveyi* 345 was diluted and cultured in LB liquid medium with different NaCl concentrations (0.5%, 1.0%, 1.5%, and 4.0%), no transconjugants were obtained (data not shown). Additionally, 252 transconjugant candidates were selected for PCR verification (Figure S2). Finally, 244 candidates met the target bands with an effective proportion of 96.83%, which confirms the effectiveness of the results.

4 Discussion

Here, we systematically studied the efficiency of foreign plasmid conjugation transfer into *V. harveyi* after exposure to different stresses and found that certain stress exposures, such as temperature, acid, alkali, SDS, and ethanol, can significantly improve the fertility of *V. harveyi* recipients in intergeneric mating with *E. coli*. This partly verifies our conjecture that warmer temperatures and antibiotic pollution could probably enhance bacterial antibiotic resistance and bacterial infection by promoting the HGT of virulence genes and antibiotic resistance genes, thus increasing the complexity and diversity of disease control (Deng et al., 2020a; Deng et al., 2020b; Deng et al., 2020c). Therefore, the results of this study have important theoretical significance for establishing disease prevention and control strategies by interrupting the HGT process with environmental regulation.

The state of the recipient cell membrane is a crucial factor affecting the formation of the junction bridge, thereby affecting conjugation transfer (Thomas and Nielsen, 2005). Genco and Clark (1988) reported that the outer membrane protein OmpA of the receptor bacteria can stabilize the junction bridge with the donor bacteria and promote the fertility of *E. coli*, *S. typhimurium*, and *Neisseria cinerea*. Sherburne and Taylor (1997) found that the deletion of lipid A synthesis genes *rfaD* and *rfaE* in *S. typhimurium* contributes to the truncation of lipid A, the reduction of porin by more than 90%, the change of cell membrane permeability, and the

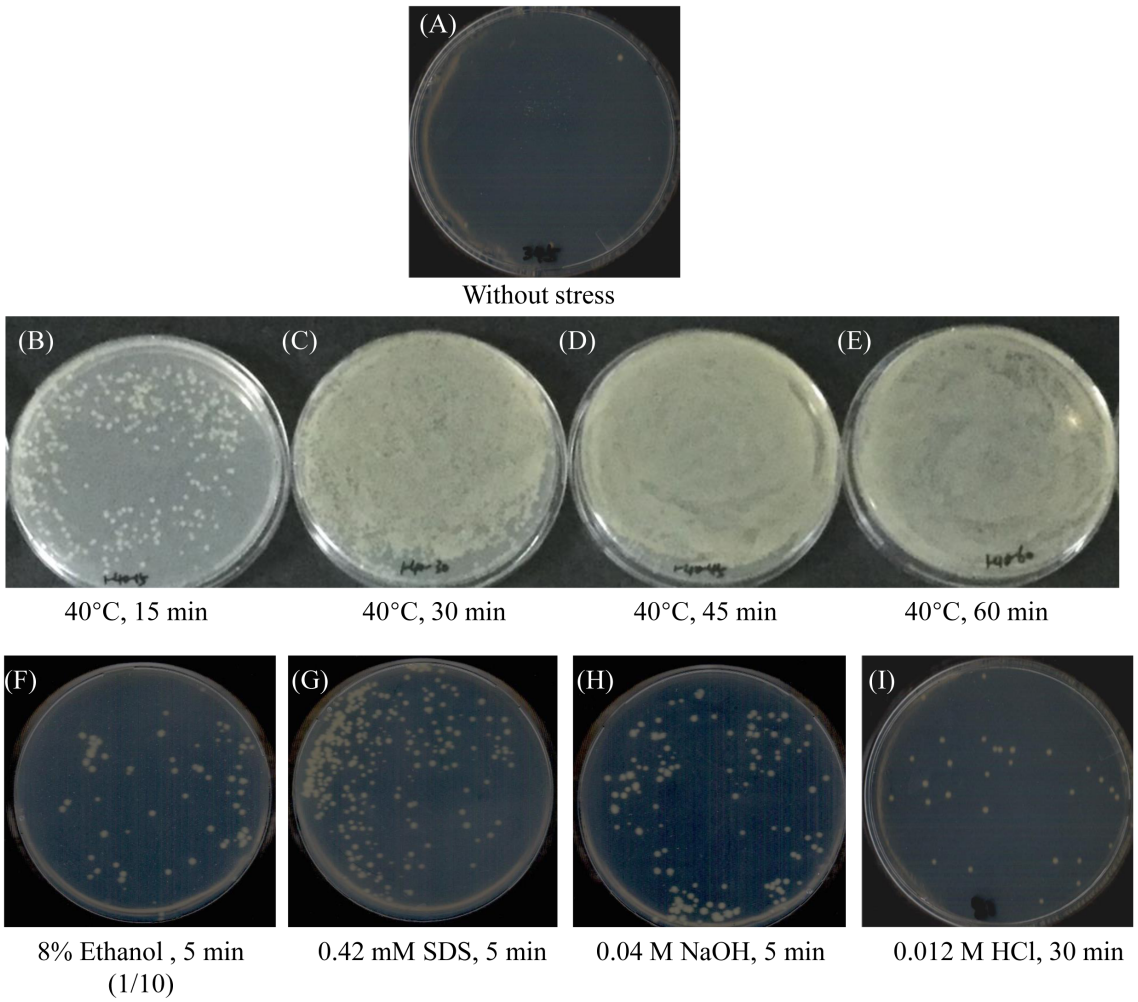

FIGURE 1
The growth of transconjugants with indicated stress on LBS plates containing 34 μg/mL Cm. **(A)** Without stress, no transconjugant growth. **(B–E)** Exposure to 40°C for 15, 30, 45, and 60 minutes, respectively. The conjunctive plaques were suspended in 100 μL of 3% NaCl and screened on LBS plates with 34 μg/mL Cm. **(F)** Exposure to 8% ethanol for 5 minutes. The conjunctive plaques were suspended in 1 mL of 3% NaCl and 100 μL of the suspension was screened on LBS plates with 34 μg/mL Cm. **(G–I)** Exposure to 0.42 mM SDS for 5 minutes, 0.04 M NaOH for 5 minutes, and 0.012 M HCl for 30 minutes, respectively. The conjunctive plaques were finally suspended in 100 μL of 3% NaCl and screened on LBS plates with 34 μg/mL Cm.

reduction of conjugation efficiency by 10–100 folds. Furthermore, successfully escaping the splicing effect of sequence-specific restriction endonucleases in the host cell immune system (R-M system, CRISPR, *etc*.) is another barricade to the success of conjugation transfer (Hickey and Hirshfield, 1990).

Heat stress can change the permeability of bacterial cell membranes (Panja et al., 2008). During DNA transformation, a heat pulse (0→42°C) can release lipids, denature membrane proteins, considerably lower cellular outer membrane fluidity, and consequently form pores on cell surfaces, allowing the DNA to cross the outer membrane barrier (Panja et al., 2008). Furthermore, Mojica-a and Middleton (1971) found that exposure to 50 °C for 20 minutes can increase the fertility of *S. typhimurium* by nearly 200 folds by inactivating its R-M system. Ethanol treatment, like heat, leads to changes in protein composition and an increased ratio of saturated to unsaturated fatty acids in the cytoplasmic membrane (Piper, 1995). Protein denaturation and fatty acid profile changes in the cell can occur as a consequence of exposure to pH shifts or detergents (Hickey and Hirshfield, 1990; Adamowicz et al., 1991; Bhuyan, 2010). Therefore, exposure to temperature, ethanol, SDS, acid, and alkali induces the fertility of *V. harveyi* recipients, probably by increasing its membrane permeability and/or inactivating the immune system. Furthermore, a lower temperature or concentration of stress cannot effectively change the cell membrane and immune system, whereas a higher temperature or concentration of stress is probably lethal to the cells and thus cannot induce the fertility of the recipients (Schäfer et al., 1994).

It should be pointed out that in the process of homologous recombination gene knockout mediated by suicide plasmid of pathogenic bacteria such as Vibrio (Val et al., 2012), conjugation transfers the recombinant suicide plasmid from the donor bacteria to the recipient bacteria and plays a key role in the success of gene knockout. However, due to the extremely low efficiency of *V. harveyi* fertility, or even *V. harveyi* that cannot be conjugated, there is no effective mutation system to study its pathogenesis and drug resistance. Based on our research, a breakthrough to improve the conjugation efficiency of *V. harveyi* has occurred, and we have already

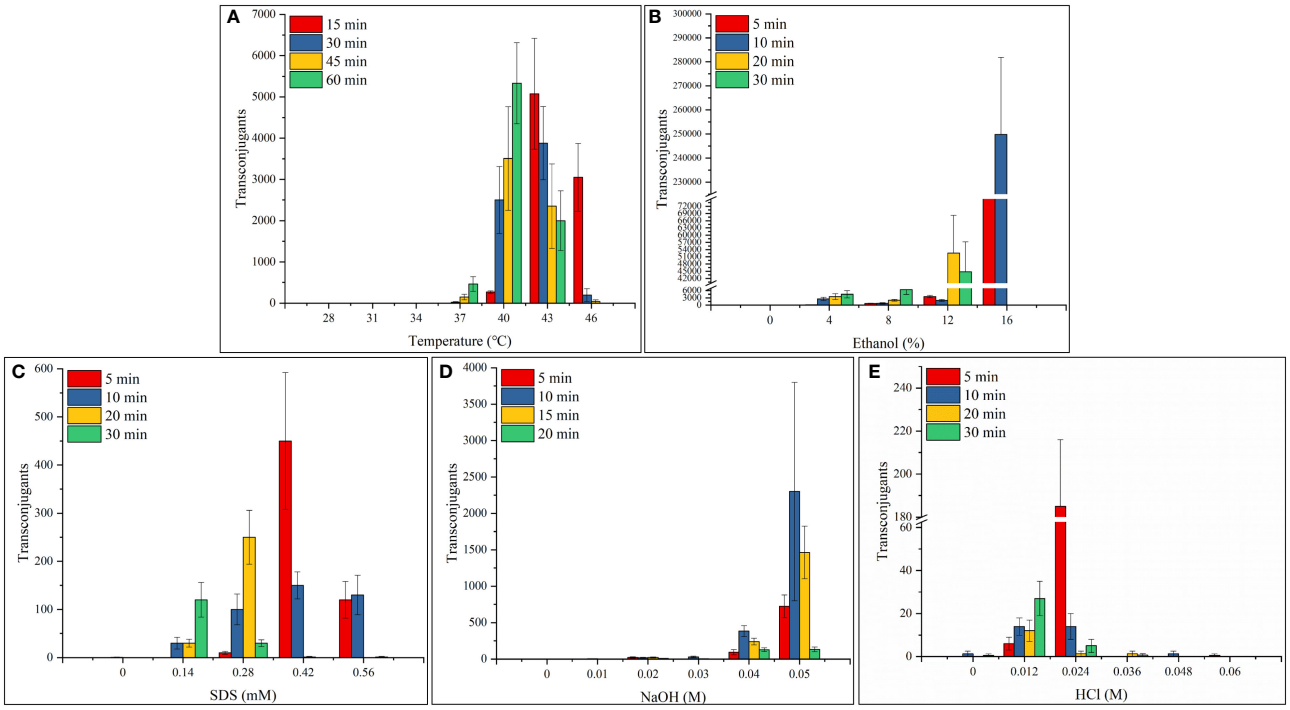

FIGURE 2
The induced interspecific mating ability of *V. harveyi* with exogenous stress. **(A)** Exposure to 31–46°C for 15–60 minutes; exposure to 28°C was used as the control. **(B)** Exposure to 4%–16% ethanol for 5–30 minutes. **(C)** Exposure to 0.14–0.56 mM SDS for 5–30 minutes. **(D)** Exposure to 0.01–0.05 M NaOH for 5–20 minutes. **(E)** Exposure to 0.012–0.06 M HCl for 5–30 minutes. Values are mean ± standard error of the mean (n = 3).

established homologous recombination gene knockout technology based on heat shock, ethanol, SDS, acid, and alkali stimulation, which has greatly promoted the research into the molecular mechanism of *V. harveyi* (Deng et al., 2017a; Deng et al., 2017b; Zhang et al., 2021).

To summarize, environmental changes affect the acquisition of foreign plasmids by *V. harveyi* recipients, thus affecting the evolution of bacterial virulence and drug resistance. Changes in the fertility of *V. harveyi* occur by affecting the status of the cell membrane and the activities of the immune system, but the specific mechanism needs to be further studied. In the future, we propose to conduct research in the following three areas: (1) how environmental stress regulates the conjugation of *V. harveyi* to obtain foreign plasmids at the cellular and molecular levels; (2) the regulation of environmental changes on the fertility of more *V. harveyi* strains and other typical aquaculture pathogens, including *Vibrio*, *Aeromonas*, and *Edwardsiella*; and (3) the regulation of environmental changes on the efficiency of other ori-plasmid conjugation transfer into typical aquaculture pathogens. In doing so, we will develop disease prevention and control strategies based on environmental regulation to block the HGT process.

Data availability statement

The raw data supporting the conclusions of this article will be made available by the authors, without undue reservation.

Author contributions

YD contributed to conception and design of the study, wrote the first draft of the manuscript. SG and HM conducted the experiment. LX performed the statistical analysis. CC wrote sections of the manuscript. JF supervised the study. All authors contributed to manuscript revision, read, and approved the submitted version.

Funding

This work was supported by the Central Public-Interest Scientific Institution Basal Research Fund, CAFS (2022GH03), the Guangzhou Science and Technology Program (202201010162), the National Natural Science Foundation of China (NSFC) (31902415), the Central Public-Interest Scientific Institution Basal Research Fund, the South China Sea Fisheries Research Institute, CAFS (2021SD15), the Natural Science Fund of Guangdong (2019A1515011833), and the China Agriculture Research System (CARS-48).

Acknowledgments

We would like to thank International Science Editing (http://www.internationalscienceediting.com) for editing this manuscript.

Conflict of interest

The authors declare that the research was conducted in the absence of any commercial or financial relationships that could be construed as a potential conflict of interest.

Publisher's note

All claims expressed in this article are solely those of the authors and do not necessarily represent those of their affiliated organizations, or those of the publisher, the editors and the reviewers. Any product that may be evaluated in this article, or claim that may be made by its manufacturer, is not guaranteed or endorsed by the publisher.

Supplementary material

The Supplementary Material for this article can be found online at: https://www.frontiersin.org/articles/10.3389/fmars.2023.1083714/full#supplementary-material

References

Adamowicz, M., Kelley, P. M., and Nickerson, K. W. (1991). Detergent (sodium dodecyl sulfate) shock proteins in *Escherichia coli*. *J. bacteriology* 173 (1), 229–233. doi: 10.1128/jb.173.1.229-233.1991

Bhuyan, A. K. (2010). On the mechanism of SDS-induced protein denaturation. *Biopolymers: Original Res. Biomolecules* 93 (2), 186–199. doi: 10.1002/bip.21318

Deng, Y. Q., Feng, J., Bei, L., and Su, Y. L. (2017b). *A thermal shock-based vibrio harveyi homologous recombinant gene knockout method*, Chinese patent: CN107904228B2022.09.06. Available at: http://www2.soopat.com/Patent/201711295414?lx=FMSQ.

Deng, Y. Q., Wu, J. J., Feng, J., and Su, Y. L. (2017a). *Method for improve genetic transformation of Vibrio harveyi*, Chinese patent: CN108165571B2022.06.24. Available at: http://www2.soopat.com/Patent/201711293764.

Deng, Y. Q., Xu, L. W., Chen, H. X., Liu, S. L., Guo, Z. X., Cheng, C. H., et al. (2020a). Prevalence, virulence genes, and antimicrobial resistance of vibrio species isolated from diseased marine fish in south China. *Sci. Rep.* 10 (1), 1–8. doi: 10.1038/s41598-020-71288-0

Deng, Y. Q., Xu, L. W., Liu, S. L., Wang, Q., Guo, Z. X., Chen, C., et al. (2020b). What drives changes in the virulence and antibiotic resistance of *Vibrio harveyi* in the south China Sea? *J. fish Dis.* 43 (8), 853–862. doi: 10.1111/jfd.13197

Deng, Y. Q., Xu, H. D., Su, Y. L., Liu, S. L., Xu, L. W., Guo, Z. X., et al. (2019). Horizontal gene transfer contributes to virulence and antibiotic resistance of *Vibrio harveyi* 345 based on complete genome sequence analysis. *BMC Genomics* 20 (1), 1–19. doi: 10.1186/s12864-019-6137-8

Deng, Y. Q., Xu, L. W., Zhang, Y. Q., Guo, Z. X., and Feng, J. (2020c). Analysis of virulence genes and antibiotic resistance of *Photobacterium damselae* isolated from marine fishes in coastal south China. *Acta Microbiologica Sin.* 2020, 60(11). doi: 10.13343/j.cnki.wsxb.20200129

Genco, C. A., and Clark, V. L. (1988). Role of outer-membrane proteins and lipopolysaccharide in conjugation between *Neisseria gonorrhoeae* and *Neisseria cinerea*. *Microbiology* 134 (12), 3285–3294. doi: 10.1099/00221287-134-12-3285

Hickey, E. W., and Hirshfield, I. N. (1990). Low-pH-induced effects on patterns of protein synthesis and on internal pH in *Escherichia coli* and *Salmonella typhimurium*. *Appl. Environ. Microbiol.* 56 (4), 1038–1045. doi: 10.1128/aem.56.4.1038-1045.1990

Khoshnevis Yazdi, S., and Shakouri, B. (2010). The effects of climate change on aquaculture. *Int. J. Environ. Sci. Dev.* 1 (5), 378. doi: 10.7763/IJESD.2010.V1.73

Koonin, E. V., Makarova, K. S., and Aravind, L. (2001). Horizontal gene transfer in prokaryotes: quantification and classification. *Annu. Rev. Microbiol.* 55 (1), 709–742. doi: 10.1146/annurev.micro.55.1.709

Li, W. J., Xue, T. Y., Lian, L. L., Ren, J. L., Tang, F., Xue, F., et al. (2022). *vcrV* gene affects translocation of T3SS1 effector protein and biological characteristics of *Vibrio parahaemolyticus*. *Microbiol. China* 49 (5), 1608–1618. doi: 10.13344/j.microbiol.china.211147

Liu, J. X., Zhao, Z., Deng, Y. Q., Shi, Y., Liu, Y. P., Wu, C., et al. (2017). Complete genome sequence of *Vibrio campbellii* LMB 29 isolated from red drum with four native megaplasmids. *Front. Microbiol.* 8, 2035. doi: 10.3389/fmicb.2017.02035

Mojica-a, T., and Middleton, R. B. (1971). Fertility of *Salmonella typhimurium* crosses with *Escherichia coli*. *J. Bacteriology* 108 (3), 1161–1167. doi: 10.1128/jb.108.3.1161-1167.1971

Nguyen, A. N., Disconzi, E., Charrière, G. M., Destoumieux-Garzón, D., Bouloc, P., Le Roux, F., et al. (2018). *csrB* gene duplication drives the evolution of redundant regulatory pathways controlling expression of the major toxic secreted metalloproteases in *Vibrio tasmaniensis* lgp32. *MSphere* 3 (6), e00582–e00518. doi: 10.1128/mSphere.00582-18

Pang, M. D. (2015). *Study on genomic characteristics and virulence related genes of aeromonas hydrophila epidemic strains* (Nanjing: Agricultural University).

Panja, S., Aich, P., Jana, B., and Basu, T. (2008). How does plasmid DNA penetrate cell membranes in artificial transformation process of *Escherichia coli*? *Mol. membrane Biol.* 25 (5), 411–422. doi: 10.1080/09687680802187765

Piper, P. W. (1995). The heat shock and ethanol stress responses of yeast exhibit extensive similarity and functional overlap. *FEMS Microbiol. Lett.* 134 (2-3), 121–127. doi: 10.1111/j.1574-6968.1995.tb07925.x

Ruwandeepika, H. A. D., Defoirdt, T., Bhowmick, P. P., Shekar, M., Bossier, P., and Karunasagar, I. (2010). Presence of typical and atypical virulence genes in vibrio isolates belonging to the *Harveyi* clade. *J. Appl. Microbiol.* 109 (3), 888–899. doi: 10.1111/j.1365-2672.2010.04715.x

Schäfer, A., Kalinowski, J., and Pühler, A. (1994). Increased fertility of *Corynebacterium glutamicum* recipients in intergeneric matings with *Escherichia coli* after stress exposure. *Appl. Environ. Microbiol.* 60 (2), 756–759. doi: 10.1128/aem.60.2.756-759.1994

Sherburne, C., and Taylor, D. E. (1997). Effect of lipopolysaccharide mutations on recipient ability of *Salmonella typhimurium* for incompatibility group h plasmids. *J. Bacteriology* 179 (3), 952–955. doi: 10.1128/jb.179.3.952-955.1997

Thomas, C. M., and Nielsen, K. M. (2005). Mechanisms of, and barriers to, horizontal gene transfer between bacteria. *Nat. Rev. Microbiol.* 3 (9), 711–721. doi: 10.1038/nrmicro1234

Val, M. E., Skovgaard, O., Ducos-Galand, M., Bland, M. J., and Mazel, D. (2012). Genome engineering in *Vibrio cholerae*: a feasible approach to address biological issues. *PloS Genet.* 8 (1), e1002472. doi: 10.1371/journal.pgen.1002472

Zhang, Y. F. (2012). *Identification and functional study of spermidine binding protein gene of vibrio anguillarum* (Qingdao University of Science and Technology). Available at: https://kns.cnki.net/KCMS/detail/detail.aspx?dbcode=CMFD&filename=1013160574.nh.

Zhang, Y. Q., Deng, Y. Q., Feng, J., Guo, Z. X., Mao, C., Chen, H. X., et al. (2021). CqsA inhibits the virulence of *Vibrio harveyi* to the pearl gentian grouper (♀ *Epinephelus fuscoguttatus*×♂ epinephelus lanceolatus). *Aquaculture* 535, 736346. doi: 10.1016/j.aquaculture.2021.736346

Zhou, A. G., Zhang, Y., Xie, S. L., Chen, Y. L., Li, X., Wang, J., et al. (2021). Microplastics and their potential effects on the aquaculture systems: a critical review. *Rev. Aquaculture* 13 (1), 719–733. doi: 10.1111/raq.12496

frontiers | Frontiers in Marine Science

TYPE Original Research
PUBLISHED 12 May 2023
DOI 10.3389/fmars.2023.1139713

OPEN ACCESS

EDITED BY
Yiqin Deng,
Chinese Academy of Fishery Sciences (CAFS), China

REVIEWED BY
Ravi Raghavbhai Sonani,
University of Virginia, United States
Biao Jiang,
Zhongkai University of Agriculture and Engineering, China

*CORRESPONDENCE
Qian Zhang
qianzhang@dlou.edu.cn
Junxin Zhang
junxin_zhang@dlou.edu.cn

RECEIVED 07 January 2023
ACCEPTED 28 April 2023
PUBLISHED 12 May 2023

CITATION
Zhang W, Huang R, Zhang T, Wang B, Li N, Sun Y, Ma H, Zhang Q, Zhang J and Liu Y (2023) Study on the inactivation and reactivation mechanism of pathogenic bacteria in aquaculture by UVC-LED. *Front. Mar. Sci.* 10:1139713. doi: 10.3389/fmars.2023.1139713

Study on the inactivation and reactivation mechanism of pathogenic bacteria in aquaculture by UVC-LED

Weixiao Zhang[1,2], Ruipin Huang[1,2], Tao Zhang[1,2], Baolong Wang[1,2], Na Li[1,2], Yan Sun[1,2], He Ma[1,2], Qian Zhang[1,2]*, Junxin Zhang[1]* and Ying Liu[2,3]

[1]College of Marine Science and Environment, Dalian Ocean University, Dalian, China, [2]Key Laboratory of Environment Controlled Aquaculture, Ministry of Education, Dalian Ocean University, Dalian, China, [3]College of Biosystems Engineering and Food Science, Zhejiang University, Hangzhou, China

Ultraviolet disinfection is an important method for controlling the large-scale outbreaks of diseases in aquaculture. As a novel and promising light source, ultraviolet light-emitting diode (UV-LED) has the advantages of safety, high efficiency and no environmental pollution risks. However, it remains unclear whether UV-LEDs can replace traditional UV light sources for aquaculture water treatment processes. Present study aimed to investigate the efficacy of UVC-LEDs (265 nm) on pathogenic bacteria, specifically *Aeromonas salmonicida* and *Escherichia coli*. The effects of UVC-LED dose, light conditions, and temperature on bacterial reactivation were also investigated. The results showed that exposure to UVC-LED effectively inactivated both types of bacteria. To achieve 4.5-log inactivation of *A. salmonicida* and *E. coli*, 24 mJ/cm^2 and 28 mJ/cm^2 UVC-LED irradiation were required, and the inactivation rate increased with increasing UVC-LED fluence. Both *A. salmonicida* and *E. coli* were revived after UVC-LED disinfection, and photoreactivation was significantly higher than dark reactivation. Bacterial reactivation rate due to high-dose UVC-LED treatment was significantly lower than that of low-dose. After 72 h of reactivation, photoreactivation and dark reactivation rates were 1 ± 0.4% and 2.2 ± 0.2%for *A. salmonicida*, and 0.02% and 0% for *E. coli*, respectively. Besides, the photoreactivation rates for the two bacteria exhibited different correlations with temperature. The highest photoreactivation rate for *A. salmonicida* was 68.7 ± 4% at 20°C, while the highest photoreactivation rate for *E. coli* was 53.98 ± 2.9% at 15°C for 48 h. This study reveals the rapid and efficient inactivation of bacteria by UVC-LED, and elucidates the mechanism and influencing factors for inactivation and reactivation by UVC-LED. The study also highlights that adequate UVC-LED irradiation and avoidance of visible light after UVC-LED disinfection can effectively inhibit bacterial reactivation. Our findings form a reference for the design and operation of UV disinfection in aquaculture.

KEYWORDS

UVC-LED, aquaculture, bacteria disinfection, photoreactivation, dark repair

1 Introduction

Due to the rapid development of aquaculture industries, the pressure on the treatment of aquaculture wastewater discharge has been increased. The direct discharge of aquaculture wastewater water containing a large amount of residual bait feces and bacterial viruses will lead to water environmental pollution, which enhances the necessity and urgency of aquaculture wastewater treatment. (Wang et al., 2022). Without effective treatment, excrements from culture organisms as well as residues of chemicals and feeds in aquaculture wastewater leads to increases in nitrogen, phosphorus, and other nutrients, bacterial proliferation, as well as disease outbreaks, which severely affects aquaculture development (Hu et al., 2019; Shu et al., 2022). In 2021, the pollution area of aquaculture reached 58.98 km^2 in China, which caused the death of aquaculture animals (1.01×10^7 kg), economic losses of more than 20 million dollars and the proliferation of bacteria and viruses (China Fisher Statistical Yearbook, 2022). Therefore, there is a need to develop an effective and safe disinfection technology for removal of pathogenic microorganisms and pollutants in aquaculture.

In traditional wastewater treatment, chlorine, ozone and UV disinfection are the most commonly used methods for disinfection. Mechanistically, chlorine and ozone produce strong oxidizing substances to destroy cell membranes, remove pathogenic bacteria and decompose organic matter from wastewater (Deborde and Von Gunten, 2008; Lee and Von Gunten, 2016; Li et al., 2017b). As chemical disinfectants, addition of chlorine and ozone to water produces by-products and residues that threaten the safety of aquatic animals. Ultraviolet (UV) disinfection is associated with the absence of harmful by-products, high sterilization efficiencies, simplified operation and convenient management among others (Zheng et al., 2011). Reducing the use of chemical inputs in the breeding process meets the requirements for green aquaculture in China. Instead of chemical addition, UV sterilization is becoming common in water treatment and aquaculture (Guo et al., 2009b). The UVC wavelengths between 240-280 nm have the best disinfectant effects on bacteria, especially at 253.7 nm, since the maximum absorbance of DNA and protein for most microorganisms is around 260 nm and below 280 nm, respectively (Beck et al., 2017). The low-pressure (LP: 254 nm) and medium-pressure (MP: 240-580 nm) mercury lamps have been widely used in drinking water and sewage treatment plants (Oguma et al., 2004). UVC directly affects DNA by disrupting its transcription and replication processes, causing damage to the double-stranded DNA structure and forming cyclobutane pyrimidine dimers. Since they are mercury-free, have flexible wavelengths, compactness and low energy consumption, ultraviolet light-emitting diodes (UV-LED) are novel and reliable UV light sources to replace the traditional mercury lamps (Shen et al., 2020). It has been reported that UVC-LED has a great effect in the disinfection process of recirculation aquaculture systems (Moreno-Andrés et al., 2020). In the study of Nyhan et al., the inactivation efficiency of traditional light source and UVC-LED on *Escherichia coli*, *Bacillus subtilis*, *Salmonella Typhimurium* and *Listeria monocytogenes* were compared. It was found that the disinfection effectiveness of UVC-LED on bacteria is either equal to or superior to that of low pressure mercury lamps (Nyhan et al., 2021). At 275 nm, UVC-LED has a better inactivation efficiency on *E. coli*, than 253.7 nm LP-UV, indicating that UVC-LED has better disinfection effects (Green et al., 2018). Nevertheless, there is no fundamental distinction between traditional mercury lamps and UVC-LEDs, as traditional mercury lamps also emit the UV wavelength which is absorbed by DNA. It has also been reported that UVC-LEDs at 265 nm have higher antibacterial efficacies than LP-UV, but are limited by the higher costs of disinfection temporarily. (Chatterley and Linden, 2010). The majority of UVC disinfection devices are designed as pipeline systems, which allows optical path of UVC can be controlled and ensure the efficiency of disinfection. Moreover, physical filtration often set prior to UVC treatment to remove suspended solids and particulate matter in the process of wastewater disinfection, which helps to enhance the effectiveness of subsequent UVC treatment.

After UV irradiation, some bacteria can repair their damaged DNA *via* photoreactivation and dark repair. It is necessary to focus on the variations of reactivation and influencing factors of bacteria after UV irradiation. Dark repair is a multistep process, where damaged or abnormal DNA bases are removed by base excision repair (BER) and nucleotide excision repair (NER) subpathways (Nyangaresi et al., 2018). Photoreactivation is a highly specific process for damaged DNA repair. Photolyase absorbs energy from visible light and participates in bacterial reactivation (Ramírez et al., 2021). Besides, photoreactivation is affected by repair time and UV radiation dose among others. It was found that the amount of *E. coli* increased as the reactivation duration extended, and the photoreactivation was positively correlated with the duration of recovery, since light provides energy for photolytic enzymes involved in repairing DNA damage (Locas et al., 2008). Since photoreactivation is a photochemical reaction, its rate is greatly affected by temperature. Photoreactivation rate has been shown to increase with increasing temperature (Kelner, 1949). However, in another study, after UV irradiation, the photoreactivation rate of *E. coli* rapidly decreased with increasing temperature and the highest photoreactivation rate appeared at 10°C. Current studies on temperature are focused on *E. coli*, with studies on aquatic pathogens being few. Therefore, there is a need to elucidate on bacterial reactivation in aquaculture wastewater after ultraviolet disinfection.

We investigated the feasibility of UVC-LED as novel light sources for bacterial disinfection in aquaculture, and focused on the reactivated effects and influencing factors of bacterial after UV irradiation. Two common gram-negative bacteria (*E. coli* and *A. salmonicida*) in aquaculture were inactivated by UVC-LED at an emission wavelength of 265 nm. The effects of UVC-LED dose, light conditions and temperature on bacterial reactivation were further investigated, the mechanisms and influencing factors of inactivation and reactivation supported the application of UVC-LED and operation of UV disinfection processes in aquaculture.

2 Materials and methods

2.1 Microbial cultivation

To clarify the potential application of UVC-LED disinfection in aquaculture, *Aeromonas salmonicida* (*A. salmonicida*) and *Escherichia coli* ATCC 8099 (*E. coli*) were selected as the

representatives of common pathogens in aquaculture. *A. salmonicida* is a prevalent pathogenic bacterium that can cause significant economic losses in fish diseases (Coscelli et al., 2015), whereas Escherichia coli is often utilized as a model bacterium for the safety evaluation (Okeke et al., 2011). The strain *A. salmonicida* was granted by Professor Feng (Institute of Microbiology, Chinese Academy of Sciences) which was inoculated in Luria-Bertani (LB) medium and incubated in the shaker incubator at 28°C, 120 r/min for 48 h. *E. coli* was purchased from Guangdong Huankai Microbial Technology Company, the strain was inoculated in Luria-Bertani (LB) medium and incubated in a shaker incubator at 37°C for 24 h. The cells were collected by centrifugation (6000 rpm, 5 min and 4°C) and suspended in sterile phosphate buffered saline (PBS, 0.1 M) to yield a concentration of approximately 10^7-10^8 CFU/mL. Enumeration was performed by the spread plate method, 50 µL serially diluted samples were spread on agar plates in triplicate and incubated at the corresponding culture temperature. The colonies on the plates between10-300 were counted and calculated as CFU/mL.

2.2 UVC-LEDs and experimental setup

UVC-LED devices (peak wavelength at 265 nm, Shenzhen Fluence Technology PLC) were applied as the light source in present study. Twenty-five UVC-LED lamps were connected and fixed on a circular board (40 mm diameter, 12.6 cm^2 area). A metal radiating fin was installed above the circular board to protect the UVC-LED from overheating and magnetic stirrer was used to mix the solution during the experiment. The average UVC-LED irradiance was 0.20 mW/cm^2 during all experiments. Light intensity was adjusted by changing the current of the DC power supply and measured by digital handheld optical power and energy meter console (PM100D, THORLABS) with a probe (S120VC). The irradiation device (a) and the UVC-LED spectrogram (b) were illustrated in Figure 1

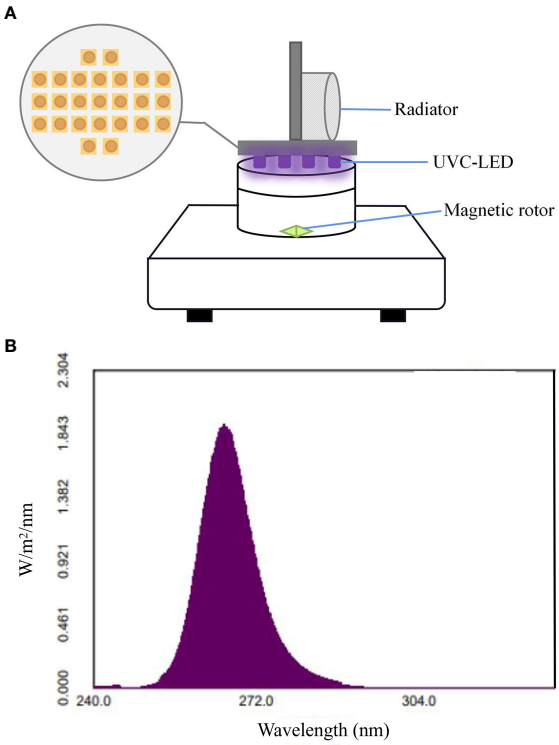

FIGURE 1
(A) The UVC-LED inactivation system and **(B)** emission spectra.

2.3 Irradiation experiment

Taken 20 mL of the above diluted bacterial solution was placed in the petri dish (60 mm diameter, 15 mm height) and irradiated at 20 mm from UVC-LED. Before irradiation, the UVC-LED modules were preheated and reached the stable emission stage. A cylindrical device was used to cover the outside of the ultraviolet device to ensure that the UV beam remains parallel. During the whole experimental process, the shading curtain was used to avoid the interference of other surrounding light. The disinfection effects on *A. salmonicida* and *E. coli* under the treatment of different UVC-LED dosages were compared by changing the exposure duration. The UVC-LED treatment duration were set as 0, 20, 40, 60, 80, 100, 120, 140, 160 and 180 s. The UVC-LED treatment dosages were set as 0, 4, 8, 12, 16, 20, 24, 28, 32 and 36 mJ/cm^2, respectively. After UVC-LED treatment, 1 mL sample was taken immediately and diluted to a series of gradients for the enumeration. Agar plating method is a commonly used technique for bacterial counting, and it is also widely employed in the evaluation of disinfection efficacy. The inactivation efficiency of bacteria was analyzed by calculating log inactivation using Eq. (1) (Lu et al., 2021).

$$\text{Log inactivation} = \text{Log}(N_0/N) = k \times D \quad (1)$$

in which, N_0 and N were the colony counts (CFU/mL) before and immediately after disinfection, k was the UV inactivation rate constant (cm^2/mJ), and D was the dosage of UV treatment received by the bacteria (mJ/cm^2).

2.4 Photoreactivation and dark reactivation

According to the above experiment results, the inactivation of 3-log and 5-log of *A. salmonicida* and *E. coli* were selected for photoreactivation and dark repair experiments. Thus, UVC-LED irradiation at 12 mJ/cm^2, 24 mJ/cm^2 for *A. salmonicida*, and 20 mJ/cm^2, 36 mJ/cm^2 for *E. coli* were used. As described above, 30 mL of microbial suspension was prepared before UVC-LED irradiation, half of the microbial suspension was taken as the control group and the rest was placed in a petri dish for UVC-LED irradiation. Take 5 mL irradiated samples into sterile centrifuge tubes and transferred them to a light incubator (Temperature: 25 ± 0.5°C; Light intensity: 93.8 µmol/m^2/s) for photoreactivation and dark reactivation. Dark reactivation samples were taken into tubes covered with aluminum foil to avoid light exposure. Samples were taken at 0, 12, 24, 48 and 72 h for enumeration, respectively. Agar plating methods were used to enumerate these microorganisms in suspension. The rate of photoreactivation and dark repair was quantified using Eq. (2) (Lindenauer and Darby, 1994).

$$\text{Rate of reactivation}\,(\%) = (N_t - N)/(N_0 - N) \times 100\,\% \quad (2)$$

in which, N_t is the concentration of microorganisms after photoreactivation/dark repair for a period of time, t (h) (CFU/mL). N_0 and N were the colony counts (CFU/mL) before and immediately after disinfection.

To indicate the regrowth potential of bacteria after irradiation and reactivation, the growth ratio was expressed as Eq. (3) (Kashimada et al., 1996).

$$\text{Growth rate}\,(\%) = N_T/N_0 \times 100\,\% \quad (3)$$

in which, N_0 is the colony count (CFU/mL) before UVC-LED irradiation, N_T is the concentration of microorganisms after photoreactivation/dark repair for 72 h.

2.5 Impact of temperature on bacterial photoreactivation

To investigate the effects of different temperatures on the photoreactivation of the irradiated bacteria, 15°C, 20°C, 25°C were set up to simulate actual culture temperature in aquaculture (Wan et al., 2022). Using water bath devices to control the stability of temperature and monitor temperature variations in real-time. The temperature control devices were preheated at least 20 min before the experiment to remain the water temperature stable. *A. salmonicida* and *E. coli* were irradiated by UVC-LED at 12 mJ/cm^2 and 20 mJ/cm^2, respectively. Then the irradiated samples were immediately floated in water bath devices and made sure the bacterial suspension was in the centrifuge tube below the water surface. Sampling and counting are the same as described above. The rate of photoreactivation at different temperatures was quantified using Eq. (2).

2.6 Statistical analysis

All experiments were conducted in triplicates, and the results were expressed as mean ± standard deviation. One-way ANOVA was performed with SPSS 21.0 software, and the results were considered statistically significant when $p< 0.05$. Pearson correlation analysis was performed to display the correlations between UV fluence, repair mode, repair time, temperature and reactivation rate. Significant correlations were considered when $p< 0.05$, and highly significant correlations were considered when $p< 0.01$.

3 Results

3.1 UVC-LED inactivation of *A. salmonicida* and *E. coli*

Inactivation of *A. salmonicida* and *E. coli* at different UVC-LED irradiation fluences are shown in Figure 2. At 12 mJ/cm^2, UVC-LED irradiation yielded a 2.83-log inactivation of *A. salmonicida*, while completely inactivation (4-log reduction) was achieved at 24 mJ/cm^2 with the bacteria entering the non-culturable state. Inactivation of *A. salmonicida* stopped increasing as the UVC-LED irradiation fluence increased. For *E. coli*, 20 mJ/cm^2 was able to yield a 3-log inactivation, while 28 mJ/cm^2 UVC-LED was required to obtain a 4.4-log inactivation. A 36 mJ/cm^2 treatment was able to yield about 5-log

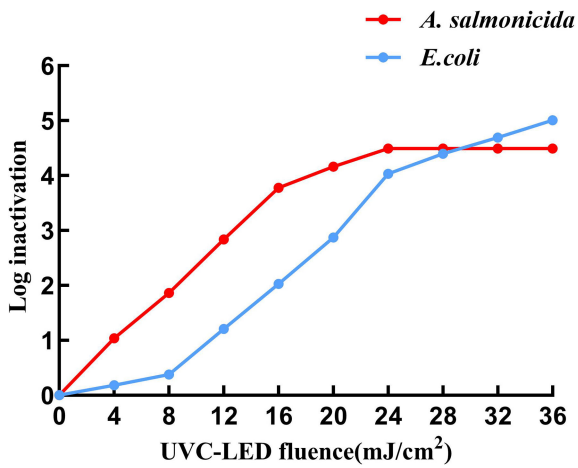

FIGURE 2
Inactivation of *A. salmonicida* and *E. coli* by UVC-LED at different fluences.

inactivation of *E. coli*, but they were still culturable. Even though the inactivation curves of the two bacteria were comparable, the inactivation rates slowed down when UVC-LED irradiation exceeded a certain fluence. The inactivation rate constant for *A. salmonicida* increased (k_d=0.24) when the UVC-LED irradiation fluence was less than 16 mJ/cm^2, and the inactivation rate (k_d=0.04) decreased significantly when the fluence of UVC-LED treatment was higher than 16 mJ/cm^2. When UVC-LED fluence exceeded 24 mJ/cm^2, *A. salmonicida* was no longer culturable (k_d= 0). In contrast, a shoulder effect was observed in *E. coli* inactivation when UVC-LED irradiation was less than 8 mJ/cm^2 (k_d=0.05). The inactivation rate for *E. coli* (k_d=0.23) improved with increasing UVC-LED irradiation fluence at the range of 8-24 mJ/cm^2, while it decreased (k_d=0.08) when UVC-LED irradiation was above 24 mJ/cm^2. These results indicate that a tailing stage might exist in bacterial inactivation when UVC-LED treatment exceeds a certain fluence, which may be attributed to self-aggregation caused by UV irradiation, leading to changes in bacterial surface properties (Kollu and Ormeci, 2015). Similar phenomena were also found in inactivation of isolated *Bacillus subtilis* spores by a low-pressure mercury lamp (253.7 nm) (Mamane-Gravetz and Linden, 2005).

3.2 Impact of UVC-LED fluences on photoreactivation

After UVC-LED inactivation, microorganisms can be repaired *via* different reactivation mechanisms, and the photoreactivation was significantly correlated with UVC-LED fluences. To assess the differences between sublethal and complete inactivation of bacteria, the inactivation of 3-log and 5-log of *A. salmonicida* and *E. coli* were selected for photoreactivation and dark repair. Based on this, UVC-LED at 12 mJ/cm^2 and 24 mJ/cm^2 or 20 mJ/cm^2 and 36 mJ/cm^2 were used for *A. salmonicida* and *E. coli* inactivation. Both irradiated *A. salmonicida* and irradiated *E. coli* exhibited obvious photoreactivations. The reactivation rate was positive correlated with reactivation duration and significantly negative correlated with

UVC-LED irradiation fluence ($p< 0.05$) both for *A. salmonicida* and *E. coli*. The higher the applied fluence of UVC-LED, the less the photoreactivation rate (Figure 3). Generally, after 12 mJ/cm^2 or 20 mJ/cm^2 UVC-LED irradiation, photoreactivation rates for both *A. salmonicida* and *E. coli* increased first, and then decreased with increasing reactivation time, but they were difficult to be revived after high fluence UVC-LED irradiation (24 mJ/cm^2 or 36 mJ/cm^2). After 12 mJ/cm^2 and 24 mJ/cm^2 UVC-LED irradiation, the *A. salmonicida* concentrations were 3×10^4 CFU/mL and 4.83×10^3 CFU/mL, respectively. The reactivation rates and bacterial concentrations were maximum after 48 h of reactivation (Figure 3A). Therefore, UVC-LED irradiation reduced the culturability of *A. salmonicida*. Compared to *A. salmonicida*, the photoreactivation rate for irradiated *E. coli* was relatively low, and after UVC-LED irradiations of 20 mJ/cm^2 and 36 mJ/cm^2, the concentrations of *E. coli* were 1.29×10^6 CFU/mL and 1.06×10^7 CFU/mL, respectively. After photoreactivation for 72 h in 36 mJ/cm^2 UVC-LED irradiation group, the highest photoreactivation rate and bacterial concentration for *E. coli* were 0.02% and 1.44×10^5 CFU/mL, respectively (Figure 3B).

3.3 Impact of UVC-LED fluences on dark repair

Apart from photoreactivation, microorganisms can also be repaired in dark conditions. In Figure 4, dark reactivations of *A. salmonicida* and *E. coli* differed from photoreactivation. The dark reactivation rate of *A. salmonicida* was extremely low, and the bacterial concentration continued to decrease at the early stage of dark reactivation. Only 0.8 ± 0.63% and 2.2 ± 0.24% of *A. salmonicida* had reactivated after revival for 72 h in 12 mJ/cm^2 and 24 mJ/cm^2 UVC-LED irradiated group, respectively. Therefore, higher fluences of UVC-LED irradiation and longer reactivation times improved the dark repair capacity of *A. salmonicida*. The dark reactivation rate at 72 h was higher than that at 48 h, and extended dark might contribute to *A. salmonicida* reactivation (Figure 4A). Compared to *A. salmonicida*, *E. coli* exhibited a different consistency with regards to dark repair and photoactivation of *E. coli*. The dark reactivation rate of *E. coli* increased with increasing reactivation time, and was delayed with a high dose of UVC-LED irradiation. After 20 mJ/cm^2 UVC-LED irradiation, there were 1.99×10^6 CFU/mL of *E. coli* in dark reactivation for 48 h and the dark repair rate reached a maximum of 0.13 ± 0.01%. There was no dark reactivation of *E. coli* after 36 mJ/cm^2 UVC-LED irradiation (Figure 4B). The dark reactivation rate of bacterial reactivation in the water sample reduced with increasing UVC-LED fluence, consistent with findings from other studies (Nebot Sanz et al., 2007). Thus, a higher fluence of UVC-LED irradiation might cause serious bacterial damage, leading to a loss of reactivation capacity.

Both strains showed better growth rates in light and dark conditions without UVC-LED irradiation. The growth rate of unirradiated *E. coli* under light conditions was 154.55 ± 6.94% while that of *A. salmonicida* under dark conditions was 2318.8 ± 227.8%, respectively (Figure 5). We postulated that reactivated light might inhibit bacterial growth when the cellular structure of *A. salmonicida* had not been destroyed by UV irradiation. The fluence of UVC-LED irradiation significantly affected *A. salmonicida* growth, which was enhanced by 12 mJ/cm^2 UVC-LED irradiation (achieved a growth rate of 192.8 ± 35.9%) while it was inhibited after 24 mJ/cm^2 UVC-LED irradiation (a growth rate of only 1 ± 0.4%). However, under both conditions of photoreactivation and dark reactivation, the growth rates of *E. coli* after UVC-LED irradiation were very low. Differences in outcomes between the two strains indicate differences in reactivation mechanisms of *E. coli* and *A. salmonicida*.

3.4 Effects of temperature on photoreactivation

From the above findings, photoreactivation was the main pathway for reactivation for *A. salmonicida* and *E. coli* after UVC-LED irradiation. Photoreactivation is a photochemical

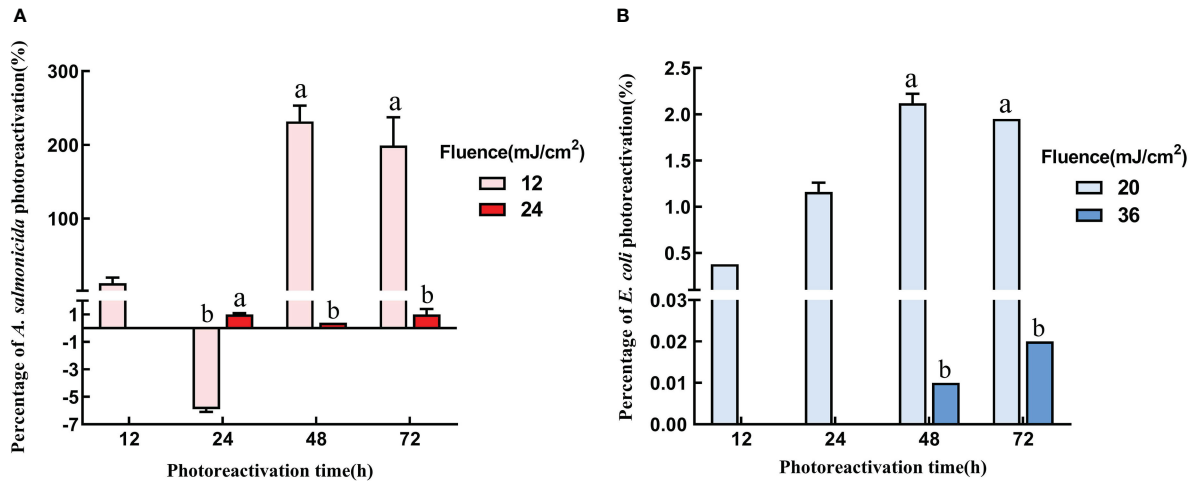

FIGURE 3
Photoreactivation with different UVC fluence **(A)** *A salmonicida*; **(B)** *E coli*). Note: Different lowercase letters in the figure indicate that bacterial reactivation is significantly different under different conditions. ($p< 0.05$).

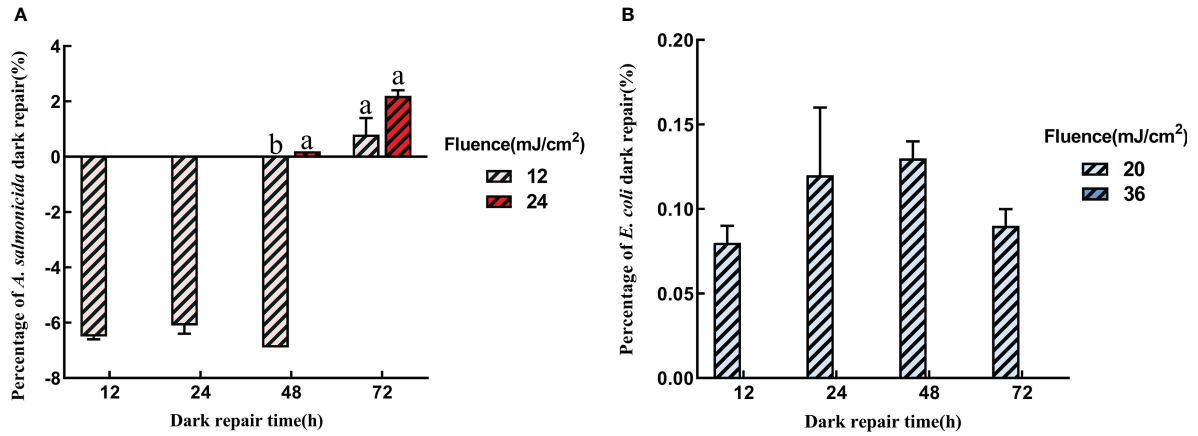

FIGURE 4
Dark repair with different UVC fluence **(A)** *A salmonicida*; **(B)** *E coli*). Different lowercase letters in the figure indicate that bacterial reactivation is significantly different under different conditions. ($p< 0.05$).

reaction that maybe be affected by reactivation temperatures. Temperature gradients were established considering the water temperature variations in different seasons during mariculture, as well as the temperature tolerance of the cultured organisms, to clarify whether different culture temperatures will have an impact on bacterial inactivation. The common aquaculture temperatures (15°C, 20°C, 25°C) were selected to investigate the effects of temperature on bacterial photoreactivation.

Photoreactivation of *A. salmonicida* exhibited the same trend under different reactivation durations and temperatures (Figure 6A). The photoreactivation rate of *A. salmonicida* increased with increasing temperature and prolongation of resurrection duration. The highest photoreactivation rates of 9.7 ± 2.5%, 68.7 ± 4% and 67.1 ± 10% at 15°C, 20°C, 25°C were achieved when UVC-LED irradiated *A. salmonicida* had been cultured for 72 h. The photoreactivation capacity of *A. salmonicida* at 15°C was significantly lower than those at 20°C and 25°C ($p< 0.05$), and after 72 h of photoreactivation, the bacterial concentrations were 2.02×10^7 CFU/mL, 1.42×10^8 CFU/mL and 1.39×10^8 CFU/mL, respectively. Therefore, higher temperatures were better for *A. salmonicida* photoreactivation, and the photoreactivation rate increased with time. On the contrary, the photoreactivation rate for *E. coli* decreased with increasing temperature, and the order of temperature effects on *E. coli* photoreactivation was 15°C >20°C >25°C. Under the three temperature conditions, *E. coli* reactivation reached the maximum value after culture for 48 h, which were 9.13×10^7 CFU/mL, 6.60×10^7 CFU/mL and 7.73×10^6 CFU/mL, respectively (Figure 6B). Therefore, the variation in temperature and repair rate between the two bacteria highlights the importance of considering the impact of temperature during UVC-LED disinfection

3.5 Correlations

To reveal the critical factors affecting bacterial inactivation and reactivation, correlation analyses of UVC-LED fluence, repair mode, repair time, temperature and reactivation rate were performed. Reactivation rates of the two bacteria were negatively correlated with UVC-LED fluence, and positively correlated with

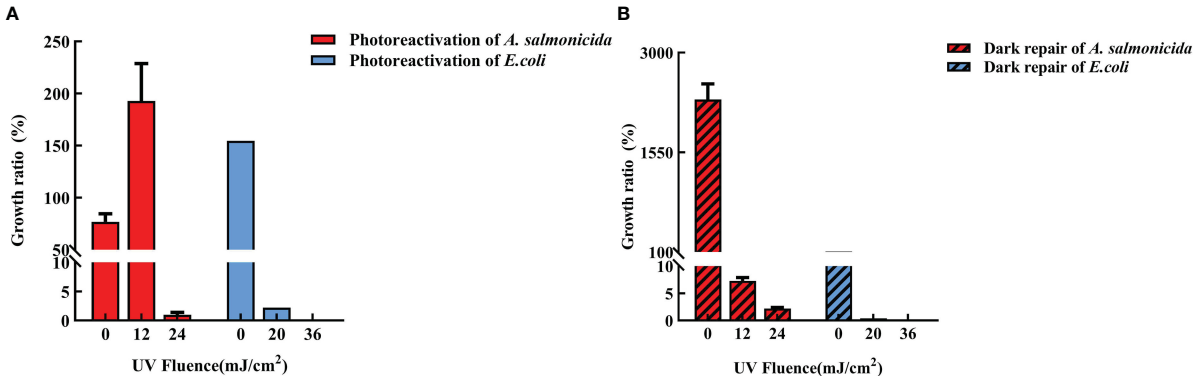

FIGURE 5
Growth rate after UVC-LED irradiation (**A**: photoreactivation; **B**: dark reactivation).

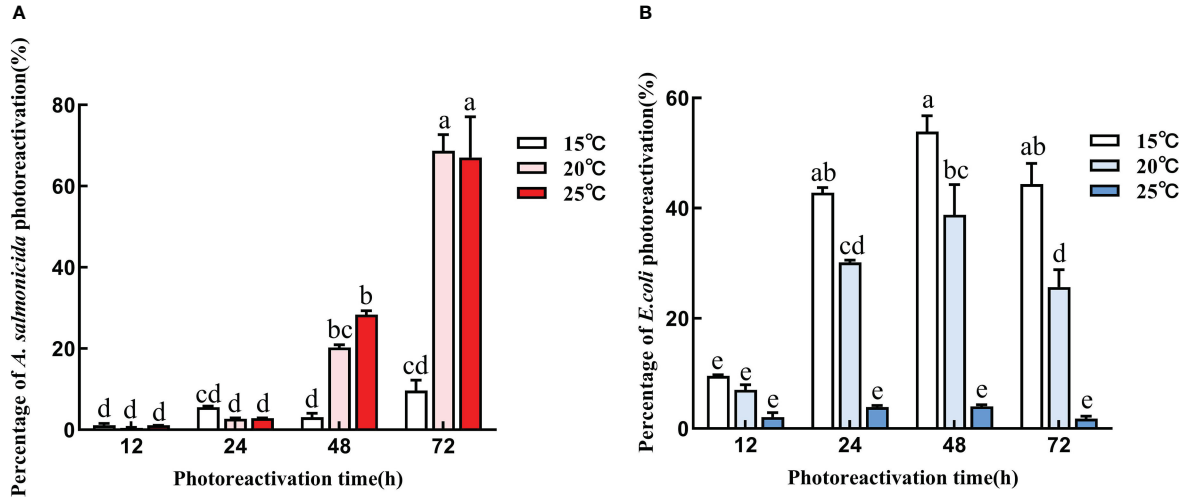

FIGURE 6
Photoreactivation with different temperature conditions **(A)** *A salmonicida*; **(B)** *E coli*). Note: Different lowercase letters in the figure indicate that bacterial reactivation is significantly different under different conditions. ($p < 0.05$).

repair time (Figure 7). Inactivations of *A. salmonicida* and *E. coli* gradually increased with increasing UVC-LED fluence, and both photoreactivation as well as dark repair rates significantly increased with increasing repair time. Temperature was negatively correlated with repair methods, therefore, more attention should be paid to temperature and light after UVC-LED treatment in aquaculture. The repair rate of *A. salmonicida* was significantly correlated with repair methods and temperature (Figure 7A). The photoreactivation rate of *A. salmonicida* increased with increasing temperature, and the reactivation rate at 25°C was significantly higher than that at 15°C. The repair rate of *E. coli* showed opposite correlations with repair methods and temperature. Under dark repair, *E. coli* was easier to repair, compared with *A. salmonicida* (Figure 7B). Therefore, reactivation varied with bacterial species and various reactivated conditions.

4 Discussion

4.1 Factors affecting bacterial inactivation

Ultraviolet, which can directly act on DNA, has significant inactivation effects on bacteria. In this study, similar disinfection trends for the two bacteria were observed after UVC-LED irradiation, and the inactivation rate increased with increasing UVC-LED fluence. Compared with *A. salmonicida*, the inactivation curve of *E. coli* had a shoulder effect and a tailing stage. Deficient *E. coli* inactivation was achieved at low UVC irradiations, consistent with a previous study (Hijnen et al., 2006). Bowker et al. also found that when the fluence of 255 nm UVC-LED less than 6.3 mJ/cm^2, the inactivation of *E.coli* was less than 1 log (Bowker et al., 2011; Masjoudi et al., 2021). The shoulder effects that occurred in light-induced inactivation can be

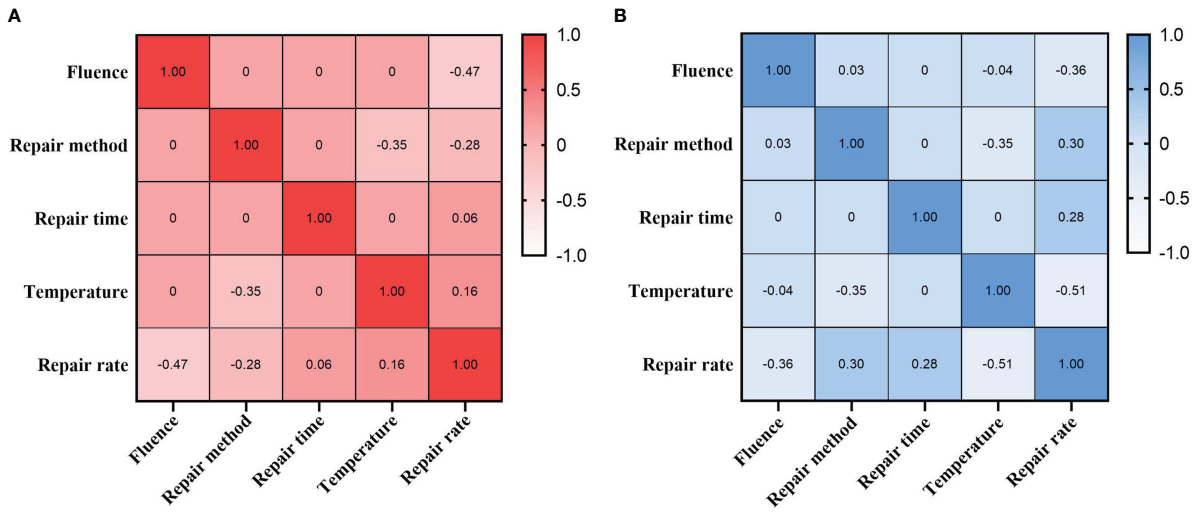

FIGURE 7
Correlations between UV fluence, repair method, repair time, temperature and repair rate **(A)** *A salmonicida*; **(B)** *E coli*).

explained by biological processes rather than photochemical reactions in cells that are attributed to photoreactivation and dark reactivation (Serna-Galvis et al., 2019; Song et al., 2019). The tailing stage refers to self-aggregation of bacteria when UVC irradiation reaches a certain dose (Kollu and Ormeci, 2015). The UVC-LED wavelength also played a vital role in sterilization (Jeong and Ha, 2019). UVC-LED at 254 nm resulted in 5-log inactivation of *E. coli* at about 27 mJ/cm^2 (Zhou et al., 2017), and inactivation of *E. coli* reached 6-log at 0.7 mJ/cm^2 by 266 nm UVC-LED (Kim et al., 2016), inactivation of *E. coli* reached 5-log at about 18 mJ/cm^2 by 280 nm UVC-LED (Li et al., 2017a). Therefore, 265 nm UV wavelength has the strongest sterilization efficiency. Even under the same wavelength of UV radiation, there were significant differences in inactivation efficiencies. In the study by Song et al. (2019), 5-log inactivation of *E. coli* required 7 mJ/cm^2 irradiation by 265 nm UVC-LED, while 36 mJ/cm^2 was required to achieve the same effect in this study, which may be associated with initial bacterial concentration. In this study, the initial concentration of *E. coli* was 1.69×10^8 CFU/mL, while the initial concentration in the study by Song et al. was 10^6 CFU/mL (2019). These results imply that the number of bacteria directly affects the irradiation of UVC absorbed by bacteria, which leads to different sterilization effects. At 265 nm, UVC-LED exerted excellent inactivation effects on the two bacteria. Due to the lack of a thick peptidoglycan layer, the gram-negative bacteria (*A. salmonicida* and *E. coli*) were highly sensitive to UV. The gram-negative bacteria has been shown to be more sensitive to UVC irradiation than gram-positive bacteria, which has a thicker peptidoglycan layer (Rohde, 2019). In the study, 4.6 mJ/cm^2 was required for *E. faecalis* to reach 5-log inactivation under irradiation of 222 nm KrCl excimer lamp while only 2.4 mJ/cm^2 was required for *E. coli* (Tsenter et al., 2022). Therefore, there are wide variations in UVC resistance of different bacteria (Huang et al., 2016). Under the same UVC-LED irradiation conditions, the inactivation rate of *A. salmonicida* was higher than that of *E. coli*. *A. salmonicida* showed a high sensitivity and poor tolerance to UVC-LED. In standard protocols, only 2.7 mJ/cm^2 was required for *A. salmonicida* to reach 2-log inactivation under irradiation of 254 nm LP lamp while 6.4 mJ/cm^2 and 5.6 mJ/cm^2 was required for *E. coli* by 275 nm and 265 nm UV-LED (Masjoudi et al., 2021). Differences in UVC sterilization effects were associated with UVC wavelength, microorganisms, initial bacterial concentration and other conditions. UVC radiation directly damaged to bacterial DNA. However, the commonly used evaluation method, gel electrophoresis, which can only detect the extent of double-strand breaks in bacterial DNA, and it cannot be well detected other types of DNA damage such as single-strand break. UVC irradiation is usually used in the disinfection process of source water, wastewater or recirculating water in aquaculture systems, while reactive oxygen species residues may be present in the water and could potentially cause oxidative damage to aquatic animals (Lushchak, 2011). Especially, if UVC irradiation is used for breeding disinfection, it is necessary to evaluate its safety.

4.2 Comparisons of photoreactivation and dark repair

When bacteria are not completely inactivated by UVC irradiation, some of them remain in a sublethal state of "viable-but-nonculturable", which may be restored to the culturable state under certain conditions (Arvaniti et al., 2021). Although the inactivation rate of low-dose UVC treatment on bacteria reached 99% and their growth activities were significantly inhibited, they were still in a culturable state. Therefore, in this study, photoreactivation rates of *A. salmonicida* and *E. coli* at low-dose UVC-LED treatment were significantly higher than those at high-dose UVC treatments. In a previous study, the photoreactivation rates of *E. coli* were 28.73% after 5 mJ/cm^2 UVC irradiation and 0.042% after 20 mJ/cm^2 UVC irradiation using 254 nm low-pressure mercury lamp (Guo et al., 2009a). Besides, high doses of UVC irradiation may aggravate the DNA damage of bacteria and require a longer time to repair, thereby reducing the bacterial photoreactivation rate (Guo et al., 2011; Shafaei et al., 2017). Photoreactivation delay was observed in the high-dose UVC-LED treated group, the highest photoreactivation rate of *A. salmonicida* appeared at 48 h after 12 mJ/cm^2 UVC-LED irradiation, and appeared at 72 h after 24 mJ/cm^2 UVC-LED irradiation. Similarly, the highest photoreactivation rates of *E. coli* treated with 20 mJ/cm^2 and 36 mJ/cm^2 UVC-LED irradiation were established at 48 h and 72 h, respectively. The photoreactivation rate was also associated with light intensity. Increasing the reactivation intensity improved the photoreactivation rate of *E. coli* to a certain extent. The recovered *E. coli* concentration under light intensity of 2920 lux was higher than that of 296 lux (Lamont et al., 2004).

Compared with photoreactivation, the efficiency of dark reactivation of both bacteria was significantly lower, suggesting that light can provide energy for *A. salmonicida* and *E. coli* reactivations. Photolyase can convert this energy into chemical energy and generate free radicals to act on cyclobutane pyrimidine dimers (CPDs), promoting bacterial reactivation (Cadet and Davies, 2017). Moreover, photoreactivation, which is light-dependent, requires less energy and is more efficient. Photoreactivation of *E. coli* was significantly higher than that of dark repair, and increased with prolongation of time (Chen et al., 1994). After UVC exposure of 5 mJ/cm^2, photoreactivation rate of *E. coli* reached 10.5%, while the dark repair rate was only 1.98% after reactivation for 24 h (Xu et al., 2015). Li et al. (Li et al., 2017a) also confirmed the lower reactivation rate of *E. coli* under dark conditions. Therefore, a sufficient high dose of UVC irradiation should be used to inhibit bacterial reactivation during aquaculture wastewater treatment. Moreover, bacterial reactivation can be inhibited to a certain extent by reducing the time and intensity of visible light exposure after sterilization.

4.3 Effects of temperature on photoreactivation

The activity of bacteria may be inhibited by various factors, including temperature, which may directly affect the rate of the intracellular enzymatic reaction or affects the mobility of the cell membrane (Wan et al., 2022). Considering the practical applications of UVC inactivation in aquaculture, it is important to investigate bacterial photoreactivations at different temperatures. In this study, the two gram-negative bacteria exhibited different reactivation effects under the same temperature and reactivation durations. The optimal culture temperatures for *A. salmonicida* and

E. coli were 28°C and 37°C, respectively. The photoreactivation rates for bacteria were not consistent with optimal culture temperatures, indicating that bacterial photoactivation did not depend on their optimal culture temperatures. In a previous study, differences in photoreactivation kinetics of *E. coli* cultured at 15-30°C were insignificant while photoreactivation efficiencies of bacteria significantly decreased when the temperature exceeded 37°C (Xu et al., 2015). Besides the significant reduction in photoactivation efficiencies of *E. coli*, the intracellular photolysis protein levels also decreased when *E. coli* was cultured in this temperature range. Photolyase of *E. coli* may be a cryogenic enzyme that exerts better photoreactivation abilities at lower temperatures. Differences in structure, metabolism, and photolyase numbers result in differences in bacterial photoreactivation responses (Quek and Hu, 2008; Cadet and Davies, 2017). Temperature directly affects the rate of the intracellular enzymatic reaction, which leads to differences in the growth and metabolic behavior of bacteria under different temperature conditions. It influences the contents of unsaturated fatty acids in microbial cells, thus affecting the mobility of the cell membrane, the absorption of nutrients and the secretion of metabolites (Wan et al., 2022). Maximum photoreactivations of *A. salmonicida* and *E. coli* appeared at 72 h and 48 h, which might be associated with bacterial reproduction rates. *A. salmonicida* grows slowly and should be cultured at 28°C for 48 h, while *E. coli* is cultured at 37°C for 24 h. Studies on reactivation of *A. salmonicida* are very few and photoactivation as well as its influencing factors should be investigated further. In summary, elucidation of inactivation and reactivation of *A. salmonicida* by UVC-LED will inform on application potential of UVC-LED in aquaculture.

5 Conclusions

UVC-LED effectively disinfects the common pathogenic bacteria (*A. salmonicida* and *E. coli*) in aquaculture. However, there were variations in bacterial resistance to UVC-LED, and *A. salmonicida* being more sensitive to UVC-LED than *E. coli*. Compared to dark repair, photoreactivation was the best reactivation mechanism for irradiated bacteria, as light provides energy to promote the reactivation of bacteria. With the increase of UVC-LED irradiation dose, it may increase the damage degree of bacteria and reduce the regeneration potential, leading to delayed reactivation. The intensity of reactivation light also affected bacterial reactivation. In addition, temperature affected the bacterial photoreactivation rate. Photoreactivation rates of *A. salmonicida* and *E. coli* exhibited different variation trends with temperature elevations, and their optimal reactivation temperatures were 25°C and 15°C, respectively. Therefore, photoreactivation mechanisms of the two bacteria differed. In present study, we did not focus on the sterilization in the breeding process. When UVC irradiation applied during breeding, more attention needs to be given to the potential harm on the cultured organisms. This study shows the feasibility of UVC-LED to effectively inactivate bacteria in aquaculture wastewater and elucidates on the reactivation mechanisms of *A. salmonicida* and *E. coli* after inactivation by UVC-LED. Our findings provide a reference point for optimal design and operations of ultraviolet sterilization devices in aquaculture. The results of present study are important reference for large-scale aquaculture wastewater treatment and provide insights into the treatment of aquaculture source water.

Data availability statement

The raw data supporting the conclusions of this article will be made available by the authors, without undue reservation.

Author contributions

WZ conducted the sample collection, data curation and draft writing. RH performed the molecular work. TZ, BW, NL and YS performed the data visualization. HM and JZ contributed to the concept and design of the study. YL and QZ conducted the writing-review and editing. All authors contributed to the article and approved the submitted version.

Funding

This study was funded by Modern Agro-industry Technology Research System (CARS-49), Innovation Support Program for High-level Talents of Dalian City (2019RD12), Basic scientific research project of Education Department of Liaoning province (LJKMZ20221107), The Overseas Training Program for Innovation Team of Liaoning Province (201818), Innovation and Entrepreneurship Project for High-Level Talents of Dalian (2020RQ109).

Acknowledgments

We would like to thank Foshan Electrical and Lighting Co., Ltd and Shenzhen Fluence Technology PLC for their assistance with light source design in our experiments.

Conflict of interest

The authors declare that the research was conducted in the absence of any commercial or financial relationships that could be construed as a potential conflict of interest.

Publisher's note

References

Arvaniti, M., Tsakanikas, P., Papadopoulou, V., Giannakopoulou, A., and Skandamis, P. (2021). *Listeria monocytogenes* sublethal injury and viable-but-Nonculturable state induced by acidic conditions and disinfectants. *Microbiol. Spectrum.* 9 (3), e01377–e01321. doi: 10.1128/Spectrum.01377-21

Beck, S. E., Ryu, H., Boczek, L. A., Cashdollar, J. L., Jeanis, K. M., Rosenblum, J. S., et al. (2017). Evaluating UV-c LED disinfection performance and investigating potential dual-wavelength synergy. *Water Res.* 109, 207–216. doi: 10.1016/j.watres.2016.11.024

Bowker, C., Sain, A., Shatalov, M., and Ducoste, J. (2011). Microbial UV fluence-response assessment using a novel UV-LED collimated beam system. *Water Res.* 45 (5), 2011–2019. doi: 10.1016/j.watres.2010.12.005

Cadet, J., and Davies, K. J. A. (2017). Oxidative DNA damage & repair: an introduction. *Free Radical Biol. Med.* 107, 2–12. doi: 10.1016/j.freeradbiomed.2017.03.030

Chatterley, C., and Linden, K. (2010). Demonstration and evaluation of germicidal UV-LEDs for point-of-use water disinfection. *J. Water Health* 8 (3), 479–486. doi: 10.2166/wh.2010.124

Chen, J., Mitchell, D. L., and Britt, A. B. (1994). A light-dependent pathway for the elimination of UV-induced pyrimidine (6-4) pyrimidinone photoproducts in arabidopsis. *Plant Cell.* 6 (9), 1311–1317. doi: 10.1105/tpc.6.9.1311

China Fisher Statistical Yearbook (2022) (Beijing).

Coscelli, G. A., Bermúdez, R., Losada, A. P., Santos, Y., and Quiroga, M. I. (2015). Vaccination against *Aeromonas salmonicida* in turbot (*Scophthalmus maximus* l.): study of the efficacy, morphological changes and antigen distribution. *Aquacult.* 445, 22–32. doi: 10.1016/j.aquaculture.2015.04.011

Deborde, M., and Von Gunten, U. (2008). Reactions of chlorine with inorganic and organic compounds during water treatment–kinetics and mechanisms: a critical review. *Water Res.* 42 (1-2), 13–51. doi: 10.1016/j.watres.2007.07.025

Green, A., Popović, V., Pierscianowski, J., Biancaniello, M., Warriner, K., and Koutchma, T. (2018). Inactivation of *Escherichia coli*, *Listeria* and *Salmonella* by single and multiple wavelength ultraviolet-light emitting diodes. *Innovative Food Sci. Emerging Technologies.* 47, 353–361. doi: 10.1016/j.ifset.2018.03.019

Guo, M., Hu, H., Bolton, J. R., and El-Din, M. G. (2009a). Comparison of low- and medium-pressure ultraviolet lamps: photoreactivation of *Escherichia coli* and total coliforms in secondary effluents of municipal wastewater treatment plants. *Water Res.* 43 (3), 815–821. doi: 10.1016/j.watres.2008.11.028

Guo, M., Hu, H., and Liu, W. (2009b). Preliminary investigation on safety of post-UV disinfection of wastewater: bio-stability in laboratory-scale simulated reuse water pipelines. *Desalination.* 239 (1-3), 22–28. doi: 10.1016/j.desal.2008.03.003

Guo, M., Huang, J., Hu, H., and Liu, W. (2011). Growth and repair potential of three species of bacteria in reclaimed wastewater after UV disinfection. *Biomed. Environ. Sci.* 24 (4), 400–407. doi: 10.3967/0895-3988.2011.04.011

Hijnen, W. A. M., Beerendonk, E. F., and Medema, G. J. (2006). Inactivation credit of UV radiation for viruses, bacteria and protozoan (oo)cysts in water: a review. *Water Res.* 40 (1), 3–22. doi: 10.1016/j.watres.2005.10.030

Hu, X., Cao, Y., Lu, M., Xu, Y., Su, H., Xu, W., et al. (2019). Research progress of microalgae in treatment of nitrogen and phosphorus in tail water from aquaculture. *Open J. Fisheries Res.* 6 (4), 172–178. doi: 10.12677/OJFR.2019.64023

Huang, J., Xi, J., Hu, H., Li, Y., Lu, S., Tang, F., et al. (2016). UV Light tolerance and reactivation potential of tetracycline-resistant bacteria from secondary effluents of a wastewater treatment plant. *J. Environ. Sci.* 41, 146–153. doi: 10.1016/j.jes.2015.04.034

Jeong, Y., and Ha, J. (2019). Simultaneous effects of UV-a and UV-b irradiation on the survival of *Escherichia coli* O157:H7, *Salmonella* typhimurium, and *Listeria monocytogenes* in buffer solution and apple juice. *J. Food Protection.* 82 (12), 2065–2070. doi: 10.4315/0362-028x.Jfp-19-131

Kashimada, K., Kamiko, N., Yamamoto, K., and Ohgaki, S. (1996). Assessment of photoreactivation following ultraviolet light disinfection. *Water Sci. Technol.* 33(10), 261–269. doi: 10.1016/0273-1223(96)00428-3

Kelner, A. (1949). Effect of visible light on the recovery of streptomyces griseus conidia from ultraviolet irradiation injury. *Proc. Natl. Acad. Sci.* 35(2), 73–79. doi: 10.1073/pnas.35.2.73

Kim, S., Kim, D., and Kang, D. (2016). Using UVC light-emitting diodes at wavelengths of 266 to 279 nanometers to inactivate foodborne pathogens and pasteurize sliced cheese. *Appl. Environ. Microbiol.* 82(1), 11–17. doi: 10.1128/AEM.02092-15

Kollu, K., and Ormeci, B. (2015). UV-Induced self-aggregation of *E. coli* after low and medium pressure ultraviolet irradiation. *J. Photochem. Photobiol. B: Biol.* 148, 310–321. doi: 10.1016/j.jphotobiol.2015.04.013

Lamont, Y., MacGregor, S., Anderson, J., and Fouracre, R. (2004). "Effect of visible light exposure on *E. coli* treated with pulsed UV-rich light," in *Conference Record of the Twenty-Sixth International Power Modulator Symposium, 2004 and 2004 High-Voltage Workshop.* San Francisco, CA, USA pp. 619–622. doi: 10.1109/MODSYM.2004.1433653

Lee, Y., and Von Gunten, U. (2016). Advances in predicting organic contaminant abatement during ozonation of municipal wastewater effluent: reaction kinetics, transformation products, and changes of biological effects. *Environ. Science: Water Res. Technol.* 2 (3), 421–442. doi: 10.1039/C6EW00025H

Li, H., Osman, H. B., Kang, C., and Ba, T. (2017b). Numerical and experimental investigation of UV disinfection for water treatment. *Appl. Thermal Engineering.* 111, 280–291. doi: 10.1016/j.applthermaleng.2016.09.106

Li, G., Wang, W., Huo, Z., Lu, Y., and Hu, H. (2017a). Comparison of UV-LED and low pressure UV for water disinfection: photoreactivation and dark repair of *Escherichia coli*. *Water Res.* 126, 134–143. doi: 10.1016/j.watres.2017.09.030

Lindenauer, K. G., and Darby, J. L. (1994). Ultraviolet disinfection of wastewater: effect of dose on subsequent photoreactivation. *Water Res.* 28 (4), 805–817. doi: 10.1016/0043-1354(94)90087-6

Locas, A., Demers, J., and Payment, P. (2008). Evaluation of photoreactivation of escherichia coli and enterococci after UV disinfection of municipal wastewater. *Can. J. Microbiol.* 54 (11), 971–975. doi: 10.1139/w08-088%m18997854

Lu, Y., Yang, B., Zhang, H., and Lai, A. C.-K. (2021). Inactivation of foodborne pathogenic and spoilage bacteria by single and dual wavelength UV-LEDs: synergistic effect and pulsed operation. *Food Control.* 125, 107999. doi: 10.1016/j.foodcont.2021.107999

Lushchak, V. I. (2011). Environmentally induced oxidative stress in aquatic animals. *Aquat. Toxicol.* 101 (1), 13–30. doi: 10.1016/j.aquatox.2010.10.006

Mamane-Gravetz, H., and Linden, K. G. (2005). Relationship between physiochemical properties, aggregation and uv inactivation of isolated indigenous spores in water. *J. Appl. Microbiol.* 98 (2), 351–363. doi: 10.1111/j.1365-2672.2004.02455.x

Masjoudi, M., Mohseni, M., and Bolton, J. R. (2021). Sensitivity of bacteria, protozoa, viruses, and other microorganisms to ultraviolet radiation. *J. Res. Natl. Inst Standards Technol.* 126, 1–77. doi: 10.6028/jres.126.021

Moreno-Andrés, J., Rueda-Márquez, J. J., Homola, T., Vielma, J., Moríñigo, M.Á., Mikola, A., et al. (2020). A comparison of photolytic, photochemical and photocatalytic processes for disinfection of recirculation aquaculture systems (RAS) streams. *Water Res.* 181, 115928. doi: 10.1016/j.watres.2020.115928

Nebot Sanz, E., Salcedo Dávila, I., Andrade Balao, J. A., and Quiroga Alonso, J. M. (2007). Modelling of reactivation after UV disinfection: effect of UV-c dose on subsequent photoreactivation and dark repair. *Water Res.* 41 (14), 3141–3151. doi: 10.1016/j.watres.2007.04.008

Nyangaresi, P. O., Qin, Y., Chen, G., Zhang, B., Lu, Y., and Shen, L. (2018). Effects of single and combined UV-LEDs on inactivation and subsequent reactivation of *E. coli* in water disinfection. *Water Res.* 147, 331–341. doi: 10.1016/j.watres.2018.10.014

Nyhan, L., Przyjalgowski, M., Lewis, L., Begley, M., and Callanan, M. (2021). Investigating the use of ultraviolet light emitting diodes (UV-LEDs) for the inactivation of bacteria in powdered food ingredients. *Foods.* 10 (4), 797. doi: 10.3390/foods10040797

Oguma, K., Katayama, H., and Ohgaki, S. (2004). Photoreactivation of *Legionella pneumophila* after inactivation by low- or medium-pressure ultraviolet lamp. *Water Res.* 38 (11), 2757–2763. doi: 10.1016/j.watres.2004.03.024

Okeke, B. C., Thomson, M. S., and Moss, E. M. (2011). Occurrence, molecular characterization and antibiogram of water quality indicator bacteria in river water serving a water treatment plant. *Sci. Total Environment.* 409 (23), 4979–4985. doi: 10.1016/j.scitotenv.2011.07.029

Quek, P. H., and Hu, J. (2008). Influence of photoreactivating light intensity and incubation temperature on photoreactivation of *Escherichia coli* following LP and MP UV disinfection. *J. Appl. Microbiol.* 105 (1), 124–133. doi: 10.1111/j.1365-2672.2008.03723.x

Ramírez, N., Serey, M., Illanes, A., Piumetti, M., and Ottone, C. (2021). Immobilization strategies of photolyases: challenges and perspectives for DNA repairing application. *J. Photochem. Photobiol. B: Biol.* 215, 112113. doi: 10.1016/j.jphotobiol.2020.112113

Rohde, M. (2019). The gram-positive bacterial cell wall. *Microbiol. Spectrum.* 7 (3), 7.3.10. doi: 10.1128/microbiolspec.GPP3-0044-2018

Serna-Galvis, E. A., Troyon, J. A., Giannakis, S., Torres-Palma, R. A., Carena, L., Vione, D., et al. (2019). Kinetic modeling of lag times during photo-induced inactivation of *E. coli* in sunlit surface waters: unraveling the pathways of exogenous action. *Water Res.* 163, 114894. doi: 10.1016/j.watres.2019.114894

Shafaei, S., Klamerth, N., Zhang, Y., McPhedran, K., Bolton, J. R., and El-Din, M. G. (2017). Impact of environmental conditions on bacterial photoreactivation in wastewater effluents. *Environ. Science: Processes Impacts.* 19 (1), 31–37. doi: 10.1039/C6EM00501B

Shen, L., Griffith, T. M., Nyangaresi, P. O., Qin, Y., Pang, X., Chen, G., et al. (2020). Efficacy of UVC-LED in water disinfection on bacillus species with consideration of antibiotic resistance issue. *J. Hazardous Materials.* 386, 121968. doi: 10.1016/j.jhazmat.2019.121968

Shu, H., Sun, H., Huang, W., Zhao, Y., Ma, Y., Chen, W., et al. (2022). Nitrogen removal characteristics and potential application of the heterotrophic nitrifying-aerobic

denitrifying bacteria *Pseudomonas mendocina* S16 and *Enterobacter cloacae* DS'5 isolated from aquaculture wastewater ponds. *Bioresource Technol.* 345, 126541. doi: 10.1016/j.biortech.2021.126541

Song, K., Mohseni, M., and Taghipour, F. (2019). Mechanisms investigation on bacterial inactivation through combinations of UV wavelengths. *Water Res.* 163, 114875. doi: 10.1016/j.watres.2019.114875

Tsenter, I., Garkusheva, N., Matafonova, G., and Batoev, V. (2022). A novel water disinfection method based on dual-wavelength UV radiation of KrCl (222 nm) and XeBr (282 nm) excilamps. *J. Environ. Chem. Engineering.* 10 (3), 107537. doi: 10.1016/j.jece.2022.107537

Wan, C., Fu, L., Li, Z., Liu, X., Lin, L., and Wu, C. (2022). Formation, application, and storage-reactivation of aerobic granular sludge: a review. *J. Environ. Management.* 323, 116302. doi: 10.1016/j.jenvman.2022.116302

Wang, Y., Zheng, Y., Qian, X., Yang, X., Chen, J., and Wu, W. (2022). Aquaculture wastewater pollution and purification technology in China: research progress. *J. Agricult.* 12 (3), 65–70. doi: 10.11923/j.issn.2095-4050.cjas20200300088

Xu, L., Tian, C., Lu, X., Ling, L., Lv, J., Wu, M., et al. (2015). Photoreactivation of *Escherichia coli* is impaired at high growth temperatures. *J. Photochem. Photobiol. B: Biol.* 147, 37–46. doi: 10.1016/j.jphotobiol.2015.03.012

Zheng, R., Xiang, K., and Zhu, S. (2011). Bacterial inactivation effect of UV in aquaculture recirculating water. *Trans. Chin. Soc. Agric. Engineering.* 27 (11), 257–262. doi: 10.3969/j.issn.1002-6819.2011.11.049

Zhou, X., Li, Z., Lan, J., Yan, Y., and Zhu, N. (2017). Kinetics of inactivation and photoreactivation of *Escherichia coli* using ultrasound-enhanced UV-c light-emitting diodes disinfection. *Ultrason Sonochem.* 35 (Pt A), 471–477. doi: 10.1016/j.ultsonch.2016.10.028

Frontiers in Marine Science

Explores ocean-based solutions for emerging global challenges

The third most-cited marine and freshwater biology journal, advancing our understanding of marine systems and addressing global challenges including overfishing, pollution, and climate change.

Discover the latest Research Topics

See more →

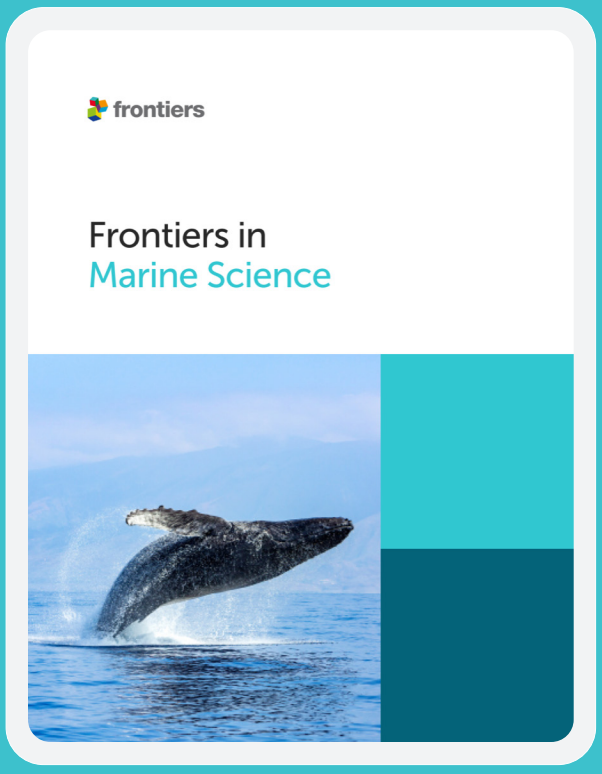

Frontiers

Avenue du Tribunal-Fédéral 34
1005 Lausanne, Switzerland
frontiersin.org

Contact us

+41 (0)21 510 17 00
frontiersin.org/about/contact